CHAPTER ONE

INTRODUCTION

1.1 Background of Study

By 1995, the value of wheat and wheat flour imports in Nigeria exceeded US$293 million (FAO, 1997). In order to reduce the import bill on wheat, the Federal Government of Nigeria institutionalized a policy in 2004 which compelled flour mills to include 10% cassava flour in all flour produced in Nigeria. Implementation of this policy would require 200,000 tonne of cassava flour out of which only about 10,000 tonne can be supplied. These efforts fuelled by the comparative advantage of the country as a major cassava producer gave birth to the Integrated Cassava Project of the International Institute of Tropical Agriculture (IITA) and sponsored by the Federal Government of Nigeria(FGN), the Niger Delta Development Commission (NDDC), Shell Petroleum Development Company of Nigeria (SPDC), the Nigerian National Petroleum Corporation (NNPC), and its joint venture partners, the United States Agency for International Development (USAID), and the State governments in Nigeria provided support.

The project was meant for economic development of Nigerians through value addition and commercialisation of all cassava products. Their efforts led to the development of many cassava processing equipment for the production of various products from cassava root. It also nurtured the emergence of cassava flash driers as the most economical equipment for the production of cassava flour.

Pneumatic conveying dryer design has been mostly done by trial-and-error or experimentation and to that extent its design has been described as an ‘art’ or ‘soft science’. This is due mostly to the lack of information that will help the designer to understand its workings and make informed decisions during design. The very little

work done on the flash dryer was mostly experimental and by commercial manufacturers of pneumatic conveying drying equipment, and consequently, did not make the results available to the public as it is considered a trade secret. Yet the problems arising from improper design of this equipment are very evident and have generated a lot of outcry. In Nigeria, this problem contributed to the Flour Millers refusing to take the product of these poorly-designed pneumatic conveying dryers, in spite of Federal Government directives for 10% cassava flour inclusion into wheat flour. A detailed list of cassava pneumatic drying equipment with rejected stock and (or) no local purchase order (LPO) from flour millers with the installed capacity of their pneumatic dryers is attached in appendix 1-1.

International Institute of Tropical Agriculture (IITA) in a bid to tackle the increase demand for efficient flash dryer for cassava flour in Nigeria, assembled a team of engineers drawn from academia, research institutes and private sector as well as fabricators who have worked on cassava flour dryers with the mandate to:

- Understudy the existing flash dryer in Nigeria
- Understudy the flash dryers from other regions
- Identify the Gap
- Develop appropriate framework for local fabrication of efficient cassava flour flash dryer

These objectives tally with those of the Raw Materials Research and Development Council who had earlier embarked on the promotion of design and fabrication of cassava processing equipment.

To achieve these objectives the design team for the flash dryer was set up. The Flash Dryer Design Team designed, fabricated, installed, as well as test-ran an improved flash drier and published the report in a book (Kuye et al, 2009).

1.2 Background Information on Cassava

Cassava, also called Manioc, Mandioc, or Yuca, is the staple food of about 500 million people worldwide. It is a mainstay of over 200 million and a major food crop in the developing countries of the sub-Saharan Africa (Onabolu et al, 2001). Presently Nigeria is the largest producer of this important staple food worldwide (Kolawale et al, 2007).

It tolerates drought and low fertility and is primarily grown and eaten by small-scale farmers in areas with poor soils or unfavourable climates. It requires minimal fertilizer, pesticides and water. Also, because cassava can be harvested anytime from 8 to 24 months after planting, it can be left in the ground as a safeguard against unexpected food shortages. This makes it a reliable food security crop (Onabolu, 2001). Cassava belongs to the family ***Euphorbiaceae***. Both bitter and sweet is classified as ***Manihot esculenta*** or *Manihot utilissima* or *Manihot Aipi* (http://www.starch.dk/isi/starch/cassava.asp, accessed 18/06/10).

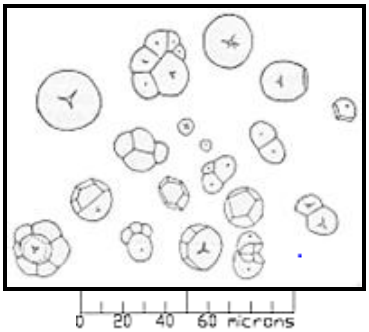

Fig1.1:Tapiocastarch (Amylum manihot)

Its starchy roots produce more calories per unit of land than any other crop in the world, except perhaps sugar cane. The leaves of the plants provide vitamins and proteins when eaten as a vegetable - a common practice in Africa. The leaves are often fed to livestock too. Two varieties of the cassava are of economic value: the bitter, or poisonous; and the sweet, or non-poisonous. Because the volatile poison can be destroyed by heat in the process of preparation, both varieties yield a wholesome food. Cassava is the chief source of tapioca, and in South America a sauce and an intoxicating beverage are prepared from the juice.

The root in powder form is used to prepare farinha, a meal used to make thin cakes sometimes called cassava bread. The starch of cassava yields a product called Brazilian arrowroot. In Florida, where sweet cassava is grown, the roots are eaten as food, fed to stock, or used in the manufacture of starch and glucose. In Africa Gari is a popular food preparation. Tapioca easily digested starchy foodstuff is extracted from the root of the cassava plant. Tapioca is often used in pudding. The term "tapioca" is used to designate products made from cassava like starch, dried chips etc. Tapioca is also replacing mung bean starch - the prime material for making clear starch noodles, however, tapioca starch needs modification to produce a gel with the same strength as mung bean starch, which is very high in amylase.

An extremely variable species, cassava probably is a hybrid. It is perennial with conspicuous, almost palmate (fan-shaped) leaves resembling those of the castor bean but more deeply parted into five to nine lobes. The fleshy roots are reminiscent of dahlia tubers. Different varieties range from low herbs through many-branched, 1-metre- tall shrubs to slender, unbranched 5-m trees. Some are adapted to dry areas of alkaline soil and others to acid mudbanks along rivers.

Presently, Nigeria is regarded as the world's largest producer of Cassava and in an effort to take advantage of this situation; Nigerian government and indeed governments in the developing countries have promoted the development of value added products for human consumption, industrial uses and export from this crop. The increased production and associated processing to improved market value are set to fight hunger and poverty (Onyeka et al, 2005)

1.2.1 Cassava Moisture Content

Fresh cassava roots cannot be stored for long because they rot within 72 hours of harvest mainly because of its high moisture content (http://www.fiiro-ng.org/cassava-flour.htm, accessed 18/06/10). They are bulky with about 70% moisture content, and therefore transportation of the tubers to urban markets is difficult and expensive. The moisture content of cassava roots averages about 63% (Bradbury and Holloway, 1988), though the moisture content of cassava roots depend on a lot of factors which includes, age, cultivar, and even climatic conditions.

Therefore, cassava must be processed into various forms in order to increase the shelf life of the products, facilitate transportation and marketing, reduce cyanide content and improve palatability.

1.2.2 Cassava Toxicity

The starchy root of cassava (Manihot esculenta Crantz) is a staple food for millions of people and this number would have increased tremendously but for the fear generated by the mishandling of the issue of the crop's toxicity.

The cassava plant carries two cyanogenic glucosides, linamarin and lotaustralin, in its edible roots and leaves. The amounts of these potentially toxic compounds vary considerably, according to cultivar and growing conditions. "Sweet" varieties usually have such small amounts as to be innocuous, whereas "bitter" varieties have sufficiently high levels to require domestic processing to remove most of the toxins (Padmaja G, 1995).

In situations where famine or extreme poverty may force a population to eat poorly processed cassava in a diet that is also deficient in nutrients such as protein, the plant's cyanogenic glucosides can lead to poisoning. A classic case was the infantile kwashiorkor epidemic in famine-stricken Biafra in 1968, but there have also been recent examples of spastic paraparesis, or konzo, in drought-stricken regions of Mozambique and Tanzania.

Farming populations who cultivate cassava have developed many methods of detoxifying cassava. Boiling and drying are sufficient to make low-cyanogen cultivars safe for consumption, but more rigorous procedures such as grating, fermenting, and sun-drying, are necessary to effectively remove cyanogens from cultivars of higher toxicity (Padmaja G, 1995). At a workshop in Nampula City (Ernesto et al, 2002), it was reported that a strategy was developed to reduce daily cyanide intake as follows:

1. Introduce other staples, vegetables, pulses and fruits to decrease the daily cyanide intake and broaden the diet.
2. Improve processing of cassava roots giving products with less residual cyanide.
3. Introduce low cyanide, high yielding and well-adapted varieties of cassava.

4. Improve early warning systems using picrate kits (Egan et al, 1984); to monitor cyanide levels in cassava products and urinary thiocyanate concentrations in the population (Bradbury et al, 1999).

1.3 Cassava Flash Drying

Since its moisture content is responsible for the short shelf-life of cassava root, efforts are then geared towards removal of moisture by drying to convert the cassava roots to a more stable form and also for economic value addition to the product. Cassava root is processed into many products and the end product essentially determines the process route. One of the major products, cassava flour could be produced by two main methods, either by milling dried cassava chips or by milling dewatered and dried cassava mash. The selection of appropriate production method is necessary to ensure good quality product and elongation of the shelf life of the products as well as lower the cost of production/Kg to the barest minimum while keeping the throughput as high as possible.

Flash dryers have been reported to be one of the most economical choices for drying mash and solids that have between 30 – 40% moisture content. The name flash dryer originates from the fact that drying is carried out in a short span of time usually 0.5 to 3 seconds. The principle of flash drying is to evaporate surface moisture instantaneously. Wet particulate material is entrained in hot gas or steam flowing through an insulated duct. The particles are dried and the gas or steam temperature decreases (Saastamoinen J, 1992). In most systems air is used as the gas. It is a well-known fact that the surface area of wet lump increases as the size of lump decreases. The wet cake is disintegrated into fines to increase the surface area. The drying is instantaneous and the material remains at wet bulb temperature of air, hence it is also

called as "wet bulb drying". The air velocities are similar to that of pneumatic conveying with the powder remains suspended in air and gets conveyed while drying. It is therefore called a pneumatic conveying dryer.

Flash driers consist mainly of a hot air generator, a feeder unit, a flash column and a cyclone separator. The hot air generator could be a heat exchanger fired by a burner or any other heat source. The feeder unit meters the wet mash and introduces it into the hot air stream while the flash column is the section of the drier where the drying occurs as the hot air transports the wet mash through it. The column could be oriented in different ways; vertical upwards, vertical downwards, horizontal and the column could still be operated in an inclined position. Certainly the choice of the orientation of the flash column must be based on certain criteria which overall aims at improving the efficiency of drying or as a trade off to a functional requirement imposed on the drier by the system to which it belongs. However, in the absence of external constraints, the vertical upward configuration has the major advantage of using the least floor space of all the other configurations. Downstream of the flash column, a cyclone separator is always used to separate the dried mash from the hot air stream. A bag filter could still be installed to collect fines because of environmental concerns.

Irrespective of the orientation of the flash column, flash dryers can be classified as positive-pressure type, negative-pressure type or mixed depending on the position of the blower with respect to the feed point. When the blower is placed upstream of the feed point, the dryer is regarded as positive-pressure type as shown in fig 1.2 because the air that conveys and dries the feed material “blows” the material through the system. Conversely, when the blower is placed downstream of the feed point, the dryer is regarded as negative pressure type because the air that conveys and dries the

feed material "sucks" the material through the system as shown in fig 1.3. The dryer is termed mixed type if blowers are installed both upstream and downstream of the feed point as shown in fig 1.4.

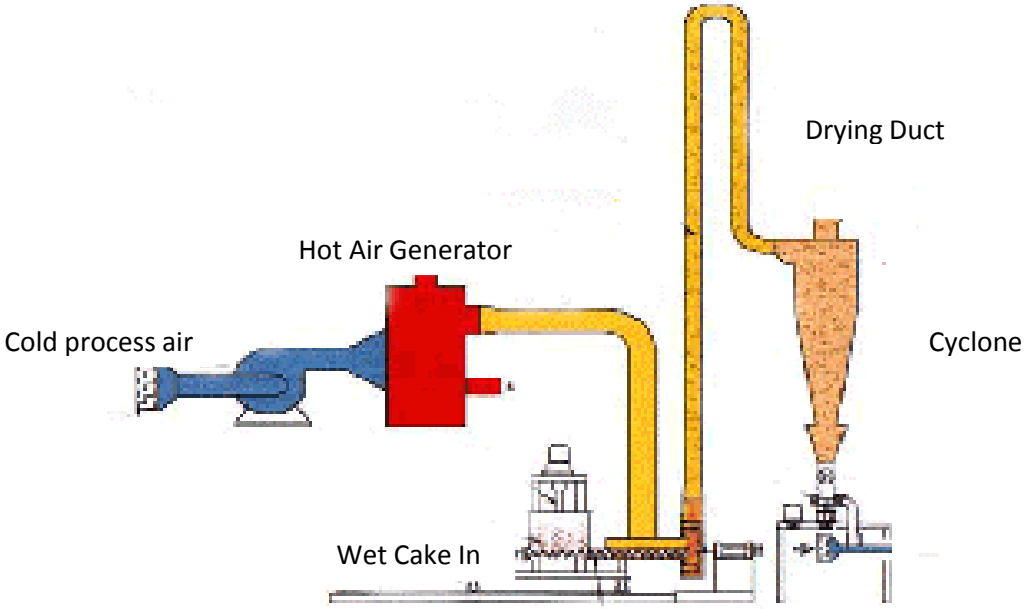

Fig. 1.2: Positive-Type Pneumatic Conveying Dryer (http://www.ecokleen.com/FLASH%20DRYER%20%20LITERATURE.pdf, accessed 26/06.2010)

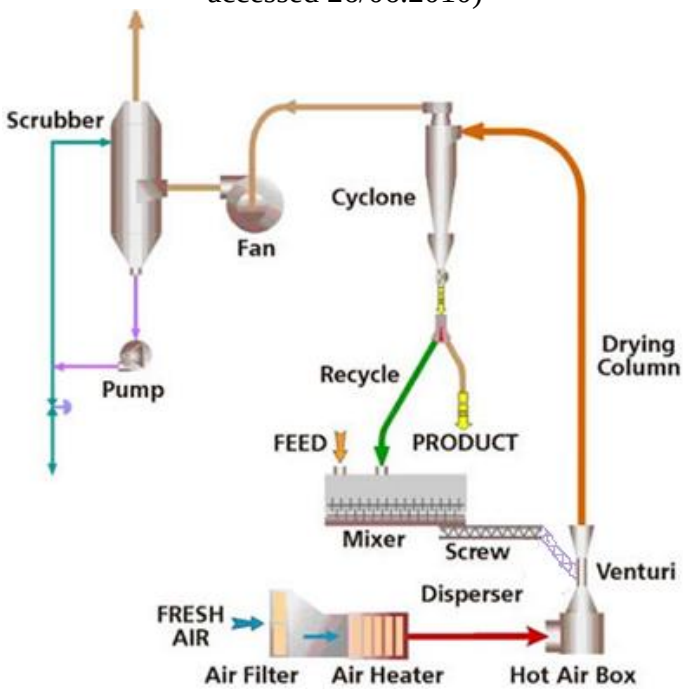

Fig. 1.3: Negative-Type Pneumatic Conveying Dryer (http://www.barr-rosin.com/images/products/open-circuit-flash-dryer.jpg, accessed 26/06.2010)

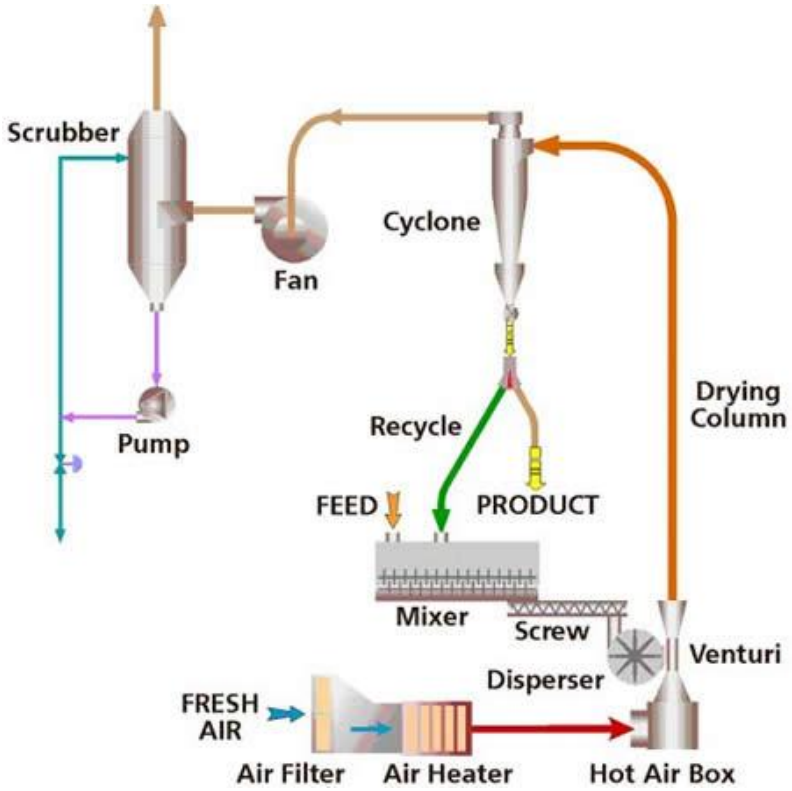

Fig. 1.4: Mixed Type Pneumatic conveying Dryer (http://www.barr-rosin.com/images/products/open-circuit-flash-dryer.jpg, accessed 26/06.2010).

Whether a dryer is positive, negative or mixed type, dryers could be classified as vertically upward, vertically downward or horizontal depending on the orientation and direction of flow of air through the flash tube or drying column. A vertical upward dryer is such that the air conveys the feed material upwards as it dries it, while a vertical downward dryer conveys the feed material downwards as it is dried. A horizontal dryer as the name implies involves the conveyance of feed material horizontally as it is dried. The vertical upward, vertical downward and horizontal drier could be positive, negative or mixed as explained above.

The area of interest of the work is the vertical flash tube only, this means that I intend to shed some light on what happens when the material is introduced into the air stream, regardless of the feeder type, till it exits the flash tube or column prior to its entry into the solid separator.

1.4 Statement of Problem

The effort of the Flash Dryer Design Team, on the Conceptual Design of a Flash Dryer, produced an improved flash dryer in terms of energy efficiency, product quality and throughput. However, it was observed that though the work shed some light on flash drying but there are still some areas that need more study for us to fully understand its nature and the variables affecting them.

One of such areas is the solid-air interaction that occurs within the flash tube, and so there is a need to study the effect of dryer variables on drying rate so that drying rate could be optimised. When determining the length of the flash tube, the procedures assumed that the particles were travelling at a steady velocity close to the gas velocity. In their work, Baeyens et al (1995) pointed out that these methods can over-predict the required dryer length by between 200% to 400%.

Therefore there is a need to better understand the variables that affect drying in a vertical upward pneumatic conveying drier, by modelling using Finite Element Analysis method. This is with a view to optimizing the drying of cassava mash for flour production, with the attendant savings in production cost.

1.5 Aim and Objectives of Study

The aim of this study is to develop a finite element model of cassava (TME 419) flash drying in a vertical upwards pneumatic conveying dryer.

To achieve the above aim, this study has the following objectives:

1. Develop a mathematical model for the gas phase, implemented on Comsol Script platform, to determine the change in the state of the gas phase as pneumatic conveying drying occurs on cassava particle.
2. Couple the data from the gas phase to a finite element model of the particle, on Comsol Multiphysics platform, to determine the state of moisture concentration as drying progresses.
3. Determine the effect of dryer variables on the particle moisture concentration.
4. Determine the effect of dryer variables on each other as variables like air inlet velocity, temperature and pressure drop across will be required in the selection of an appropriate blower and heat exchanger rating.
5. Determine the moisture content of cassava particle along the flash tube and in effect the optimal height of the flash tube.
6. Provide a tool for the design of flash drying plants and in the selection and specification of components.
7. Provide a tool for studying an existing flash drying plant with a view to upgrading it.

1.6 Significance of Study

The failure of the Integrated Cassava Project of the Federal Government, which was aimed at improving the socio-economic status of Nigerians by creating employment and generating revenue from value addition to the entire cassava value chain, is still fresh in our mind. The project failed mostly because the equipment deployed in processing cassava into different product were in efficient and not cost effective. The inefficiency affected the quality of the product which lead to rejections and this situation was aggravated by cost ineffectiveness of the operations. Processing cassava into cassava flour by the use of flash dryers was determined as most economically viable value chain but unfortunately it was hit by rejection by flour miller because of low product quality and hence this work. The physical, thermal and aerodynamic properties of Tme 419 were determined and will be available for use by other researches and design engineers. The implementation of the models provides insight into the interaction between the cassava particle and hot air as pneumatic conveying drying occurs. By predicting the pressure drop across the flash tube, error in the selection of blower (over rated /under rate) for a flash drying plant. The implementation of the model using data from an existing plant will help in predicting the performance of the plant when alterations are made. This allows the performance assessment/audit of a flash drying plant and upgrading of such facilities at near zero cost. The application of the data and tool provided will lead to the design and fabrication of efficient and cost effective dryer that will help in deriving the socio economic benefits envisaged in the setting up of the Integrated Cassava Project of the Federal Government or any other Cassava Initiative.

1.7 Scope and Limitations of the Study

It is important to note that the properties of cassava, physical and thermal depends on specie and age and so the study is limited to a cultivar of cassava, TMe 419. The roots used for the study was acquired from National Root Crop Research Institute, Umudike and they were harvested at the age of 10 months. This implies that the formulation cannot be applied to other specie or even the same specie of widely varied age without determining the properties of the new sample and making the necessary substitutions to the model data before implementation.

The limitations to this work were mostly related to the simplifying assumptions made in formulating the model. First is the assumption that the interaction between the solid phase and the gas phase happens on a particulate level. This implies that individual particles interact with the air stream without interacting with the adjacent particle. This of course is a simplifying assumption and so has to be managed properly in order not to introduce erroneous errors into the model results. The second limitation arises in trying to model the representative sample of the grated cassava particle as a sphere where it is actually very irregular and no single particle is a true representative of the bulk. The shape modification factor varies with particle and that brings arbitrariness into the determination of the surface modification factor.

CHAPTER 2

REVIEW OF RELATED WORK

2.1 Kuye Et Al Model

Many research works have been done in pneumatic conveying, convective drying and pneumatic conveying drying with the focus on mineral processing, food processing and other areas. Attempt was made to review these works and to provide a firm foundation based on the body of knowledge available presently. For the flash drying system which is of the vertical pneumatic conveying type, Kuye et al (1995) used the energy balance equation as a model of the system.

$$\frac{Q}{M_s} = C_s(T_p - T_f) + X_f C_{p,l}(T_v - T_f) + (X_t - X_p)\lambda + X_p C_{p,l}(T_p - T_v) + (X_t - X_p)\, C_{p,v}(T_{v,b} - T_v) \quad (2.1)$$

Kuye et al (1995) used Equation (2.1) to determine the total quantity of heat that was required to raise the temperature of 492 kg of pressed cassava mash to a level that would allow the moisture content to be reduced from initial moisture content of 45% to a final moisture content of 10%. Since that quantity of pressed mash was the required throughput (wet basis) per hour, the heat load per hour was determined. The air inlet temperature was taken from the value of temperature from existing flash dryers. The enthalpy at these temperatures was read-off charts and used to calculate the total mass of air and subsequently volume of air at 180°C required to carry the amount of energy determined with equation (2.1). This air volume/hour was used as the volumetric flow rate requirement for the blower. The model used by Kuye et al (1995) is a modified form of the equation for rate of energy accumulation;

2.2 El-Behery Et Al Model

In their work, El Behery et al, (2009) developed a model based on steady two-phase flow for drying porous materials in a vertical upward pneumatic conveyor. The model which was used by Hamed M. H (2005) and modified by El Behery et al (2009) are as summarised below:

- The mass balance equation for the gas phase was written as:

$$\frac{d}{dx}\left[\alpha_g \rho_g u_g A\right] = S_{mass} \tag{2.3}$$

-The momentum equation for the gas phase was expressed as:

$$\frac{d}{dx}\left(\alpha_g \rho_g u_g^2 A\right) = -A\frac{dP}{dx} - \alpha_g \rho_g g A - F_{wg} + S_{mom} + S_{mass}\, u_d \tag{2.4}$$

-The total energy equation for the gas phase was written as:

$$\frac{d}{dx}\left[\alpha_g \rho_g u_g A\left(H_g + \frac{u_g^2}{2}\right)\right] = Q_{wall} - \alpha_g \rho_g u_g A g + S_{mass}\left(H_{wv} + \frac{u_g^2}{2}\right) + S_{energy} \tag{2.5}$$

-The equation of motion of a particle in a gas was given as:

$$\frac{du_d^2}{dx} = \frac{3\rho_g C_d}{2\rho_d d_p}\left(u_g - u_d\right)\left|u_g - u_d\right| - 2g\left(1 - \frac{\rho_g}{\rho_d}\right) - f_p\,\frac{u_d|u_d|}{d} \tag{2.6}$$

-The equation for particle temperature assuming temperature is uniform throughout the particle was written as:

$$u_d m_p C_{pd}\,\frac{dT_d}{dx} = \chi \pi d_p^2 h\left(T_g - T_d\right) - \dot{m}_d H_{fg} \tag{2.7}$$

-The residence time of the particles at the gas phase was given as:

$$\frac{dt_d}{dx} = \frac{1}{u_d} \tag{2.8}$$

The analysis was based on the two-phase gas-solid flows and the mutual effect between the two phases was considered. The systems of equations (2.3) – (2.8) in addition to other complementary equations were solved numerically to predict the

effects of some variables on pneumatic conveying dryer using conservative variable formulation and fourth order Rounge-Kutta method.

2.3 Levy and Borde Model

A steady- state one-dimensional model for pneumatic drying of wet particle was presented by Levy and Borde (1999). They assumed a two-stage drying process, with mass transfer controlled by evaporation from a saturated outer particle surface in the first stage and by diffusion within the particle in the second stage. The model predictions were compared with the experimental data obtained in large scale and pilot scale pneumatic dryers and a good agreement was obtained. It should be pointed out here that based on the assumption that the two dimensional vertical flow is non rotational and axis-symmetrical, both phases velocities have only one component, which is in the Z direction and they are a function of both the axial and the radial location in the pipe. The conservation equations of the gas and the solid phases were written as.

-Mass balance of the gas phase:

$$\frac{\partial(\rho_g u_g \emptyset_g)}{\partial z} = S_m \tag{2.9}$$

-Momentum balance of the gas phase

$$\frac{\partial(\rho_g u_g^2 \emptyset_g)}{\partial z} = -\frac{\partial P}{\partial z} + \left[\frac{1}{r}\frac{\partial}{\partial r}\left(r\emptyset_g \mu_g \frac{\partial u_g}{\partial_r}\right)\right] + F_g + S_m u_d + \frac{\partial}{\partial z}\left(\emptyset_g \mu_g \frac{\partial u_g}{\partial z}\right) \tag{2.10}$$

-Energy balance equation for the gas phase

$$\frac{\partial}{\partial z}\left[\emptyset_g \rho_g u_g \left(H_g + \frac{u_g^2}{2}\right)\right] = \frac{1}{r}\frac{\partial}{\partial r}\left(\emptyset_g k_g \frac{\partial T_g}{\partial r}\right) + Q_g - W_g + S_m \left(H_{gd} + \frac{u_d^2}{2}\right) \tag{2.11}$$

-Mass balance of the dispersed phase

$$\frac{\partial(\rho_d u_d \emptyset_d)}{\partial z} = -S_m \tag{2.12}$$

-Momentum balance equation of the dispersed phase

$$\frac{\partial(\rho_d u_d^2 \emptyset_d)}{\partial z} = -\rho_d g \emptyset_d + F_d - S_d u_d \tag{2.13}$$

-Energy balance equation for the dispersed phase

$$\frac{\partial}{\partial z}\left[\emptyset_d \rho_d u_d \left(H_d + \frac{u_d^2}{2}\right)\right] = Q_d - W_d - \rho_d u_d \emptyset_d g - S_m \left(H_{gd} + \frac{u_d^2}{2}\right) \tag{2.14}$$

The predictions of the model were compared to the same experimental data used in Levy and Borde (1999). The predictions of the two-dimensional model did not present any significant difference as compared to those provided in Levy and Borde (1999) .

2.4 Pelegrina and Crapiste Model

In their work, Pelegrina and Crapiste (2001) presented a one-dimensional model for drying of food particles. The model took into account the particle shrinkage during the drying process and the non spherical shape of the particle was considered in drag and heat transfer coefficients. They assumed that the internal resistance does not control the mass and energy transfer between solid particles and air. They found that, in the low range of air flow rates; the pressure drop under drying conditions is higher than that under transport conditions. An opposite effect was observed at higher velocities. However, the model was not verified with experimental results.

The models proposed by Pelegrina and Crapiste (2001) is shown below

$$v\frac{dv}{dz} = \frac{A_p}{2V_p} C_d \frac{\rho_g}{\rho_s}(u-v)|u-v| - \left(1 - \frac{\rho_g}{\rho_s}\right) g - \frac{1}{2D_t} f_p v^2 \tag{2.15}$$

$$u\frac{du}{dz} = -\frac{1}{\rho_g}\frac{dP}{dz} - g - \frac{2}{D_t} u^2 f_f - \frac{A_p}{2V_p}\frac{(1-\varepsilon)}{\varepsilon} C_d (u-v)|u-v| - \frac{fS}{\rho_g}\frac{(1-\varepsilon)}{\varepsilon}(u-v) \tag{2.16}$$

$$\frac{dX}{dz} = \frac{1}{W_s}\frac{d}{dz}\left[\rho_s v(1-\varepsilon)A_p\right] = -\frac{Sf(1-X)}{\rho_s v} \tag{2.17}$$

$$\frac{dY}{dz} = \frac{1}{W_g}\frac{d}{dz}\left[\rho_g u \varepsilon A_p\right] = -\frac{Sf(1-X)}{\rho_s v}\frac{W_s}{W_g} \tag{2.18}$$

$$\frac{dT_s}{dz} = \frac{S}{C_{ps}\rho_s v}\left[Q - fH_s\right] \tag{2.19}$$

$$\frac{dT_g}{dz} = \frac{a}{C_{pg}\rho_g u}\frac{(1-\varepsilon)}{\varepsilon}(-Q) - \frac{Q_p}{W_g C_{pg}(1+Y)} - \frac{fa C_{pv}}{\rho_g u C_{pg}}\frac{(1-\varepsilon)}{\varepsilon}\left(T_g - T_s\right) \tag{2.20}$$

2.5 Narimatsu Et Al Model

In their work, Narimatsu et al (2007) investigated numerically and experimentally the drying process of porous alumina and solid glass particles in a vertical dryer using the models developed by Rocha S.C.S (1988) and Pelegrina & Crapiste (2001). The model was for one dimensional incompressible flow and the internal resistance did not control the heat and mass transfer. Dry solids were used in heat transfer experiments, and the measurements of heat transfer coefficient indicted that the maximum value of heat transfer coefficient occurred at the velocity of minimum pressure drop. Furthermore, it was noticed that the morphology of particles (porous or non porous) did not influence the air temperature profiles.

The model proposed by Rocha S.C.S (1988) based on two phase flow is summarised below:

$$\frac{d\varepsilon}{dz} = \left[\frac{g}{w(u-v)} - \frac{F_D}{w\rho_s(u-v)}\right] \tag{2.21}$$

$$\frac{dp}{dz} = -\left[\frac{g}{w(u-v)} - \frac{F_D}{w\rho_s(u-v)}\right]\left(\rho_s v^2 - \rho_g u^2\right) - F_f - \left[\rho_s(1-\varepsilon) + \rho_g \varepsilon\right]g \tag{2.22}$$

$$\frac{dv}{dz} = \frac{v}{(1-\varepsilon)}\left[\frac{g}{w(u-v)} - \frac{F_D}{w\rho_s(u-v)}\right] \tag{2.23}$$

$$\frac{du}{dz} = -\frac{u}{\varepsilon}\left[\frac{g}{w(u-v)} - \frac{F_D}{w\rho_s(u-v)}\right] \tag{2.24}$$

$$\frac{dX}{dz} = -\frac{6A_t}{W_s d_p}\frac{v(1-\varepsilon)}{u\varepsilon}k_y(Y_s - Y) \tag{2.25}$$

$$\frac{dY}{dz} = \frac{6A_t}{W_g d_p}\frac{v(1-\varepsilon)}{u\varepsilon}k_y(Y_s - Y) \tag{2.26}$$

$$\frac{dT_s}{dz} = \frac{6A_t}{W_s d_p}\frac{v(1-\varepsilon)}{u\varepsilon}\left[\frac{h(T_g - T_s) - k_y(Y_s - Y)(H_v + C_{pv}T_s)}{(C_{ps} + C_{pa}X)}\right] - \frac{C_{pa}T_s}{(C_{ps} + C_{pa}X)}\frac{dX}{dz} \tag{2.27}$$

$$\frac{dT_g}{dz} = \frac{6A_t}{W_g d_p}\frac{v(1-\varepsilon)}{u\varepsilon}\left[\frac{k_y(Y_s - Y)(H_v + C_{pv}T_s) - h(T_g - T_s)}{C_{pg}}\right] - \frac{C_{pv}T_g + H_v}{C_{pv}}\frac{dY}{dz} - \frac{a_t A_t U_{TC}(T_g - T\infty)}{W_g C_{pg}} \tag{2.28}$$

2.6 Hamed Model

Hamed M. H. (2005) presented a model for the subsonic gas particle two phase flow with the assumptions that:

- The flow is one dimensional and steady
- The particles are spherical in shape
- The radiative properties of gas and particle are gray
- The heat transfer between duct wall and the particle is negligible
- The particle density is constant

Continuity equation

$$\frac{1}{A}\frac{\partial}{\partial x}(\alpha_c \rho_c U A) = S_{mass} \tag{2.29}$$

Momentum equation

$$\frac{1}{A}\frac{\partial}{\partial x}(\alpha_c \rho_c U^2 A) = -\alpha_c \frac{\partial P}{\partial x} + \alpha_c \rho_c g - \frac{1}{R_h}\tau_w + S_{mass}.V + S_{mom} \tag{2.30}$$

Energy equation

$$\frac{1}{A}\frac{\partial}{\partial x}\left[\alpha_c \rho_c U A\left(h_c + \frac{U^2}{2}\right)\right] = -\frac{q_w'}{R_h} - \frac{1}{A}\frac{\partial}{\partial x}(A q_c') + \alpha_c \rho_c g U - \frac{P}{A}\frac{\partial}{\partial x}(\alpha_p V A) +$$

$$S_{mass}.\left(h_s + \frac{V^2}{2}\right) + S_{energy\ p} \tag{2.31}$$

Aside from the work discussed so far, Kilfoil M. (2003) developed a numerical simulation of simultaneous drying and pneumatic conveying of small metallic filter cake particles by dedicated program generated on Matlab. He used the model developed by Littman et al. (2000) for the evaporation of water from large glass particles in pneumatic transport. The work is relevant for estimating the coating solution feed rate and the length of the draft tube in Wurster-type particle coaters. Specifically, the rate of evaporation of water from 1 mm glass particles in a 28.45 mm

tube was calculated from the model. The rate increased with solids mass flow rate, inlet air temperature and inlet particle temperature. The heat was more rapidly removed from the particle phase than from the air phase and high inlet air temperatures are tolerated. The model presupposes that the gas and particle velocities and voidage are known and that the water film on a particle is thin and uniformly distributed. Hydrodynamic considerations that impact on the calculations were discussed.

This model by Kilfoil M. (2003) generated steady state pressure drop and required heat input during simultaneous drying and pneumatic conveying of mineral product. However the program consists of loops that contain series of equations which are evaluated sequentially with the variables changed one at a time, for each iteration. Since several variables change simultaneously in pneumatic conveying drying, the results will have limited practical application because the mechanism is that of coupled parameters changing simultaneously.

By employing a volumetric heat transfer concept, as used for rotary dryers, simple estimation procedures have been suggested by Moyers and Baldwin (1997). These procedures assumed that the particles were travelling at a steady velocity close to the gas velocity. It was pointed out (Baeyens et al, 1995) that these methods can over-predict the required dryer length by 200% to 400%. This also is reasonable considering that the dominant mode of heat transfer between hot air and the dispersed medium is convective. This means that it relies mostly on difference in velocity between the hot air stream and the particle to be dried. Therefore to assume that the velocity of the particle is close to the velocity of the air for this analysis is not appropriate.

To model the acceleration zone accurately, a stepwise procedure has been suggested by many workers (Hamed M. H, 2005; Han et al, 2000). Although these procedures are considerable improvements on the steady-state, Kemp et al (1994), reported that they can still give errors of 50-100% in the tube length prediction. Baeyens et al (1995) and Radford R. D. (1997) neglected the effect of acceleration zone near the feed point in their stepwise procedure.

A more complex model for a pneumatic dryer considering a distribution of particle sizes for steam drying of wood chips has been developed (Fyhr and Rasmuson, 1997a; Fyhr and Rasmusom, 1997). The model includes a comprehensive two-dimensional model for single particle drying of single wood chip and one-dimensional plug flow was assumed. The irregular movement and the non spherical shape of the wood chips were accounted for by measuring drag and heat transfer coefficients. To validate the model, measurements of the temperature and pressure profiles as well as the final moisture content were carried out, and the predictions agreed well with the experimental results. Unlike the above studies, which were performed in a vertical upward pneumatic dryer, Alvarez et al, (2005) have studied numerically and experimentally the drying process in a vertical downward pneumatic dryer. The model was for non shrinkage spherical particle and steady state one-dimensional flow. Some experimental works on the pneumatic dryer were given (NamKung and Cho, 2004; Kaensup et al, 2006a; Kaensup et al, 2006b).

2.7 Review of Multiphase Flow Formulation

The vertically upward pneumatic conveying dryer that is to be modelled is essentially a moving body of hot air with particles of cassava mash entrained in the flow stream. The moving air is regarded as the continuous phase while the entrained solid particle is regarded as the dispersed phase. The solid loading ratio, which is the ratio of the mass of the dispersed phase in the continuous phase, will determine the conveying mode that is possible with the material in question. David Mills (2004) identified three major conveying modes possible:

- dilute phase (non-suspension flow)
- dilute phase (suspension flow)
- and the dense phase conveying mode (plug /bed flow)

There is no clear distinction between the dilute phase and the dense phase. However, the dilute phase is characterised with high speed material flow while dense phase conveying is characterised by a lower material flow velocity. Dilute phase (suspension flow) is however distinct in that the dispersed phase is completely suspended in the continuous phase. The right formulation method has to be adopted to be able to accurately describe the situation at hand. Consequently a review of multiphase models is necessary.

2.7.1 Homogenous Equilibrium Model

In the homogeneous equilibrium model (HEM) one assumes that the velocity, temperature and pressure between the phases are equal (http://wins.engr.wisc.edu/teaching/mpfBook/node12.html). This assumption is based on the belief that differences in these three potential variables (and chemical potential if chemical reactions are considered) will promote momentum, energy, and mass

transfer between the phases rapidly enough so that equilibrium is reached instantaneously. For example, when one phase is finely dispersed in another phase generating large interfacial area, under certain circumstances this assumption can be made; for example, bubbly flow of air in water or steam in water at high pressures. The resulting equations resemble those for a pseudo-fluid with mixture properties and an equation of state which links the phases to obtain these mixture thermodynamic properties. Whenever the HEM model is used it is advisable to check the validity of the equilibrium assumptions by using more accurate theoretical models for comparison. For example, rapid acceleration or pressure changes cannot be always accurately modelled with the HEM model; that is, discharge of flashing vapour-liquid mixtures, or shock wave propagation through a multiphase medium. This is especially true when the pressure change is large when compared to the ambient pressure, or any of the driving potentials are large relative to their reference values. Such a 'rule-of-thumb' is very crude and one must carefully consider the timescales for equilibration of these driving potentials with allowable characteristic times for the problem of interest. The governing equations for the Homogenous Equilibrium Model are:

Mass:

$$\frac{\partial}{\partial z}(\rho A) = -\frac{\partial}{\partial z}(\rho A v) \tag{2.32}$$

Energy:

$$\frac{\partial(\rho A c)}{\partial z} = -\frac{\partial}{\partial z}\big(\rho A v(e + Pv)\big) + q_w^{''} Per + v\tau_w + \frac{\partial}{\partial z}\left(kA\frac{\partial T}{\partial z}\right) \tag{2.33}$$

Momentum

$$\frac{\partial A v}{\partial z} = -\frac{\partial(\rho A v^2)}{\partial z} - \rho g A sin(\theta) - \tau_w Per - \frac{\partial PA}{\partial z} \tag{2.34}$$

For the formulation above, the geometry has been chosen to be a one-dimensional channel inclined from the horizontal by a known angle, θ ,

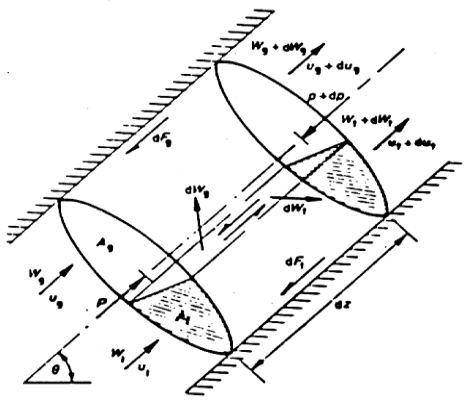

Fig. 2.1: Inclined one dimensional channel

(http://wins.engr.wisc.edu/teaching/mpfBook/node13.html).

The microscopic equations have been averaged over the channel cross-sectional area using the techniques first proposed by Ishii M (1974) , leaving a partial differential equation in time, *t*, and the axial space dimension, *z*. The definitions of the mixture thermodynamic properties (for example, ρ, u, v) consider only two-phases but can be simply extended to more phases or components.

The multiphase transport properties of viscosity and thermal conductivity (μ, k) are another matter, because it is not clear how one should average their effect in an area-average, mass average or volume-average sense. In many situations such as for pressure drop calculations the mixture transport properties have been arbitrarily averaged on a volume average or mass average basis, for example,

$$\mu = X_1\mu_1 + X_2\mu_2 \text{ or } \mu = \alpha_1\mu_1 + \alpha_2\mu_2 \qquad (2.35)$$

However, these averaging schemes are not exact and are usually empirically corrected by fitting coefficients to a set of experimental data. In other situations the effect of multiphases are neglected and the liquid or gas property values for viscosity on the

thermal conductivity are used, for example, when the amount of liquid in the channel is large (low quality or void fraction), the viscosity can be taken to be that of the liquid.

2.7.2 Separated Flow Model

In the separated flow model the restriction on equal phase velocities is relaxed and one now models the momentum exchange between the phases and the channel separately with different velocities, for example, vapour and liquid velocities (Rodolfo et al, 2006). The relaxation of equal velocities is most important when the densities between the phases are quite different in the presence of a gravitational potential field or large pressure gradients. Given a density difference, buoyancy effects tend to induce a drift velocity of the lighter phase in the heavier phase. One measure of this density ratio is the Atwood ratio and is defined as:

$$\frac{\rho_2-\rho_1}{\rho_2+\rho_1} \tag{2.36}$$

Where ρ_1 and ρ_2 are the densities of the different interacting phases.

One notices that as this density ratio approaches zero the HEM model would become more valid because the drift velocity would be reduced as the buoyancy of the lighter phase diminishes. The remaining assumptions of equal temperatures and pressures between the phases are usually retained in most applications. This is because it is usually felt the rates of mass and energy exchange are large enough to promote equilibrium. The governing equations for the separated flow model are given as:

Mass:

$$\frac{\partial}{\partial z}(\rho A) = -\frac{\partial}{\partial z}(\rho_1\alpha_1 v_1 A + \rho_2\alpha_2 v_2 A) \tag{2.37}$$

Energy:

$$\frac{\partial(\rho Ac)}{\partial z} = -\frac{\partial}{\partial z}(\rho_1\alpha_1 v_1 A(e_1 + Pv_1) + \rho_2\alpha_2 v_2 A(e_2 + Pv_2)) + q_w'' Per \quad (2.38)$$

Momentum (phase 1)

$$\frac{\partial}{\partial z}(\rho_1 A\alpha_1 v_1) = -\frac{\partial}{\partial z}(\rho_1 A\alpha_1 v_1^2) - \rho_1\alpha_1 gAsin(\theta) - \alpha_1\tau_w Per - \frac{\tau_1 A_1}{L_1} - \alpha_1 \frac{\partial PA}{\partial z} \quad (2.39)$$

Momentum (phase 2)

$$\frac{\partial}{\partial z}(\rho_2 A\alpha_2 v_2) = -\frac{\partial}{\partial z}(\rho_2 A\alpha_2 v_2^2) - \rho_2\alpha_2 gAsin(\theta) - \alpha_2\tau_w Per - \frac{\tau_2 A_2}{L_2} - \alpha_2 \frac{\partial PA}{\partial z} \quad (2.40)$$

In the formulation just presented, a one-dimensional area averaged formulation for two phases was used. There are two important differences in the equations that one should notice. First, there are now two momentum equations. In each equation there appears a term which represents the friction force at the phase interface caused by the relative velocity between the phases. If the equations are solved separately then one must develop a constitutive relation model for this momentum transfer term. Second, the properties are not averaged exclusively using the void fraction and density of the phases, but require a separate constitutive relation that relates the volume fraction to the flowing mass fraction. Traditionally the separated flow model has been used primarily for calculating the pressure drop in a flow channel. In this application the usual method of solution is to add the phase momentum equations and eliminate the need to model the interfacial shear stress, τ_i. Then one empirically correlates to obtain a model for the frictional pressure drop for the channel, τ_w , and for the slip ratio, v_2/v_1, or velocity differences$(v_2 - v_1)$ between the phases as a function of volume fraction and properties. The model for τ_w is substituted back in the combined momentum equation and the algebraic correlation for v_2/v_1 or $(v_2 - v_1)$is used as a substitute for the second balance equation. These types of models are described in more detail when one considers multiphase pressure drop. The drift flux model is a

special case of such models, because it is physically based as it predicts void fractions given velocity difference.

2.7.3 Two Fluid Model

The final type of multiphase model formulation is the multiple fluid model (better known as the two-fluid model, designating two phases). This model treats the general case of modelling each phase or component as a separate fluid with its own set of governing balance equations (Ishii M, 1974). In general each phase has its own velocity, temperature and pressure. The velocity difference as in the separated flow is induced by density differences. The temperature differences between the phases are fundamentally induced by the time lag of energy transfer between the phases at the interface as thermal equilibrium is reached. If the multiphase system involves rapidly changing flow conditions due to area changes in steady flow or transient conditions then the time lag for reaching thermal equilibrium between the phases may become significant in comparison to the characteristic time it takes for flow conditions to change. One may estimate this condition by computing a characteristic Fourier number the system under expected flow conditions given as:

$$\text{Fourier No.} \quad = \frac{az}{L^2} \tag{2.41}$$

Therefore, thermal nonequilibrium becomes important and one must include the possibility of a temperature difference by separate energy balances in a multiphase model for two or more separate fluids.

The modelling of pressure nonequilibrium is much more complex. The pressure difference between two phases is caused by three main effects:

(1) pressure differences due to surface energy of a curved interface,

(2) pressure differences due to mass transfer,

(3) pressure differences due to dynamic effects.

In the first case the simple existence of an interface (probably curved) requires from overall mechanical equilibrium that some pressure difference exist between the phases. This pressure difference is proportional to the interfacial surface tension and inversely proportional to the radius of curvature$(\sim 2\sigma/r)$ and is usually quite small in most applications $(r > 100\mu m)$. The second effect is noticeable when the mass flux due to phase change is large at the interface between the phases; for example, large evaporation or condensation rates. The final effect is caused by dynamics where one phase has a larger pressure relative to the other phase due to very rapid energy deposition or pressurization effects. A common example of an induced dynamic pressure difference is the flow of a mixture of air bubbles and water through a converging-diverging nozzle. If the rate of flow is high and the area change dramatic enough the liquid will depressurize quickly as it passes through the nozzle leaving the vapour bubbles at a higher pressure. This dynamic pressure difference will cause the vapour bubbles to grow, over expand and then oscillate around a new mean pressure. This example takes on the second effect if the situation were steam bubbles in water since mass transfer would also be present. The importance of pressure non equilibrium between the phases is inversely proportional to the time scale of the rate of phase change or external pressure oscillations. For most applications of two-fluid modelling this pressure non equilibrium is usually neglected; i.e., only when the rate of phase change and pressure oscillation become of equal time scales does this non equilibrium effect become important. One way to estimate this is to compare the flow velocity to the speed of sound in the multiphase system. Only when the flow velocity

approaches or exceeds the multiphase sound speed would the pressure non-equilibrium be important. The two-fluid model equations are given as:

Mass:

$$\frac{\partial}{\partial_z}(\rho_1\alpha_1 A) = -\frac{\partial}{\partial_z}(\rho_1\alpha_1 v_1 A) + \Gamma_1 \tag{2.42}$$

Energy:

$$\frac{\partial}{\partial z}(\rho_1\alpha_1 A e_1) = +q_i^{''}\frac{A_i}{L_i} + \Gamma_1(e_i) - P_i\frac{\partial a_i A}{\partial z} \tag{2.43}$$

Momentum:

$$\frac{\partial}{\partial z}(\rho_1 A\alpha_1 v_1) = -\frac{\partial}{\partial z}(\rho_1 A\alpha_1 v_1^2) - \rho_1\alpha_1 gAsin(\theta) - \tau_w Pe\tau - \frac{\tau_i A_i}{L_i} + \Gamma_1(v_2) - \alpha_1\frac{\partial PA}{\partial z} \tag{2.44}$$

One should note that when a two-fluid model is used, a number of interfacial transport coefficients $(\gamma_i, \tau_i, q_i^{''}, P_i,)$ are defined and require constitutive relation models to complete the overall model. This approach has an advantage in that the actual transport processes can be rigorously defined; however, the disadvantage is that one is required to model these kinetic processes in detail, which implies a much greater depth of experimental data and insight.

The usual method of modelling pressure differences between the fluids is to assume that the pressure is equal in both phases. If, as previously discussed, one finds that pressure non equilibrium between the phases is important one must introduce a local constitutive relation which accounts for this pressure difference due to dynamic and interfacial effects. For example, in research done with explosive boiling a local momentum equation (for example, Rayleigh momentum equation) is used to model this difference in the pressure of the two fluids; this allows for dynamic pressure differences as well as the effect of surface tension and mass transfer.

The other required constitutive relations for interfacial transfer $(\gamma_i, \tau_i, q_i^{''})$ are complicated functions of the fluid velocities and their local properties. These kinetic models are also a strong function of the multiphase flow pattern. The model one would develop for the interfacial shear stress or heat flux is significantly different for a dispersed flow pattern in contrast to a stratified flow pattern. In fact, the interfacial models would be different if one had gas bubbles in a liquid versus liquid droplets in a gas.

The final point to make about all the multiphase models is how turbulence is included in the analysis. The first point one should notice is that the multiphase governing equations do not seem to directly include the time-averaging due to local turbulent velocity fluctuations. This is somewhat misleading because when one looks into the complete derivation (Ishii M, 1974) one finds that constitutive relations for τ_w and τ_i inherently include turbulence effects. The important question then is: how is turbulence modelled in these relations? At the present time turbulence modelling is rather phenomenological when compared to the detailed formulations for single phase flow. The inherent assumption in modelling τ_w and τ_i is that one can use simple turbulence models (for example, empirical friction factors, mixing length scales) developed for single phase applications at the local level of the multiphase system and then correct for effects of multiple phases by a combination of phenomenological models averaging techniques for the bulk flow, and using empirical correlations from specific data. The following sections considering pressure drop and critical flow models are good examples of these techniques.

2.8 Summary

This dissertation shall adopt a more accurate method of analysis, the finite element method, in implementing a steady state 1D model for drying of cassava mash in a vertical upward pneumatic conveying dryer. Also unlike all previous work, the model shall be developed specifically for drying pressed cassava mash variety, TMe 419. The particles shall be modelled as non porous and variation in particle velocity in flash tube and the irregular shape of the particles shall be accounted for. Consistent with the model formulation method of some of the works discussed, the review of pneumatic conveyance and multiphase flow formulation indicated clearly that the situation being modelled in this work can best be described as dilute phase flow and shall be modelled based on the two-fluid theory.

CHAPTER 3

MATERIALS AND METHODS

3.1 Model Development Approach

Several modelling approaches have been developed, ranging from discrete, particle-based methods to macroscopic (continuum), semi-empirical, and two-phase descriptions. Particle-based methods are suitable when there is a limited number of a solid particle, which may be determined by the mode of the particular pneumatic conveyance. When on the other hand, there are many particles, the particle-based approach is deficient and it is then better to use a macroscopic, or averaged, model that tracks the volume fractions.

The situation being modelled is based on the two fluid theory and this work shall combine two different approaches in describing the different phases of the two phase flow model being analysed. The continuous phase shall be modelled with the continuum modelling approach while the dispersed phase shall be modelled using the particulate approach. This approach is consistent with the nature of the phases and considering that the pneumatic conveying drying being modelled has earlier been characterized as dilute phase flow. This means that the dispersed media interacts with the continuous phase on a particulate level and hence justified the Particulate approach being used for the dispersed phase. In modelling the continuum physical system the steps suggested in Rodolfo et al, (2006) shall be adopted for the continuous phase as outlined below.

- Identify appropriate conservation laws (for example mass, momentum, energy) and their corresponding densities and fluxes.
- Write the corresponding equations using conservation laws.

- Close the system of equations by proposing appropriate (constitutive) relationships between the fluxes and the densities.
- Analysis/Solution and Validation of model

3.2 Conservation Laws and their Fluxes

In order to study the drying of cassava mash under pneumatic conveyance in the flash tube, which is usually a cylindrical pipe, a quasi-one dimensional situation has been considered as shown in the Fig 3.1.

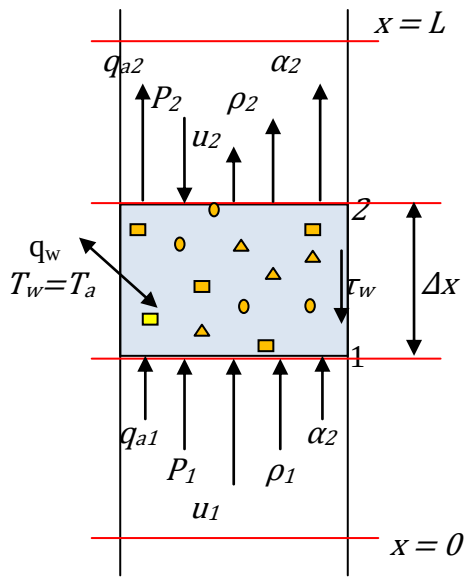

Fig. 3.1: Flash tube and control volume

3.3 Continuous Phase Formulation

Considering the control volume shown in fig 3.1, the conservation laws for the gas phase are: conservation of mass, conservation of linear momentum and conservation of energy. In this formulation, the variation of flow properties along the x axis (along the length of the vertical flash tube) was considered as important while the variation of flow properties along the other axis are regarded as cross-sectional average values.

3.3.1 Continuity Equation

Considering the control volume between boundaries 1 and 2 in fig. 3.1, the governing equations for the continuous phase (air) are derived according to the basic laws of fluid mechanics as follows:

The mass flow of the gas component (g) through the boundary (1) of the control volume per unit area is given by $\rho_g \alpha_g u_g$ and therefore the net outflow of mass of the gas component for the control volume is given by the divergence of $\rho_g \alpha_g u_g$ or

$$\frac{\partial(\rho_g \alpha_g u_g)}{\partial x} \tag{3.1}$$

The rate of increase of mass of the gas component stored in the control volume is as given in equation (3.1) and hence conservation of mass of the gas component demands that;

Rate of increase of stored mass (rate of accumulation) + rate of mass outflow = rate of transfer of mass from other components (rate of inflow) per unit volume

$$\frac{\partial}{\partial t}(\rho_g \alpha_g) + \frac{\partial(\rho_g \alpha_g u_g)}{\partial x} = S_{mass} \tag{3.2}$$

The S_{mass} term (mass transfer to the phase/unit volume) was added to the right side of the equation instead of zero (0) as in the Navier Stokes equation because there is mass transferred from the particles as drying progresses in the form of water vapour and the term accounts for it. So equation (3.2) is just the one dimensional Navier Stokes equation but with a mass interaction term.

$$\frac{\partial}{\partial t}(\rho_g \alpha_g) + \nabla(\rho_g \alpha_g u_g) = S_{mass} \tag{3.3}$$

It is important to note that Navier Stokes equation can only be used to model single phase flow situation, one component flow only and is grossly inadequate for two phase flow and hence shall not be use in this formulation.

For a duct of cross sectional area, A the continuity equation for the gas component becomes:

$$\frac{\partial}{\partial t}(\rho_g \alpha_g) + \frac{\partial}{\partial x}(A\rho_g \alpha_g u_g) = S_{mass} \quad (3.4)$$

The first term in equation 3.3 represents the accumulated mass in the control volume, and since the control volume is open equation (3.4) becomes

$$\frac{\partial}{\partial x}\left(A\rho_g \alpha_g u_g\right) = S_{mass} \quad (3.5)$$

expanding LHS of (3.5) implicitly,

$$\frac{d}{dx}\left(A\rho_g \alpha_g u_g\right) = \rho_g \alpha_g u_g \frac{dA}{dx} + A\alpha_g u_g \frac{d\rho_g}{dx} + A\rho_g u_g \frac{d\alpha_g}{dx} + A\rho_g \alpha_g \frac{du_g}{dx} = S_{mass} \quad (3.6)$$

To simplify equation (3.6) the following are considered:

First, the cross sectional area of the flash tube is uniform, this implies that the first term on the RHS becomes zero because

$$\frac{dA}{dx} = 0$$

Secondly, in pneumatic drying, it is critical that the mass fraction of the solid is kept constant throughout the drying period. This is to prevent the alteration of the thermodynamic balance established between the gas phase and the dispersed phase and ensure that the same exit conditions, like moisture concentration or moisture content are constant. If the moisture concentration varies due to varied mass fraction then inconsistent product quality will occur, a situation that must be avoided at all cost because it is one of the important functional requirements for pneumatic conveying drying. Since

$$\alpha_s + \alpha_g = 1$$

then at constant α_s,

$$\frac{d\alpha_g}{dx} = 0$$

Finally, if it is assumed that the change in the density of the gas phase is negligible then,

$$\frac{d\rho_g}{dx} = 0$$

Equation (3.6) becomes:

$$A\rho_g \alpha_g \ \frac{du_g}{dx} = S_{mass}$$

rearranging,

$$\frac{du_g}{dx} = s_{mass} / A\rho_g \alpha_g \qquad (3.7)$$

Integrating equation (3.7) yields

$$\int \frac{du_g}{dx} dx = \frac{1}{A\rho_g \alpha_g} S_{mass} \int dx$$

$$u_g = \frac{1}{A\rho_g \alpha_g} S_{mass}\, x + c \qquad (3.8)$$

Using the initial boundary conditions

$$x = 0 \qquad u_g = u_{g1}$$

then $c = u_{g,1}$ (minimum carrying velocity)

the solution to the continuity equation becomes

$$u_{g2} = \frac{1}{A\rho_g \alpha_g} S_{mass}\, x + u_{g,1} \qquad (3.9)$$

3.3.2 Constitutive Relationships (Continuity)

The number of particles per unit length, N_p, can be expressed as:

$$N_p = \frac{6\alpha_s}{\pi d_p^3 \ A} \tag{3.10}$$

The mass transfer source term per unit length can be obtained by multiplying the evaporation rate from a single particle $\dot{m}_s$ by the number of particles in the control volume per unit length (Levy and Borde, 1999)

$$S_{mass} = N_p \dot{m}_s \tag{3.11}$$

The mass transfer in the present model is based on a single stage drying process. In this stage, the solid surface can be considered to be fully wetted and the resistance to the mass transfer is located in the gas side. Drying starts when the particle surface receives heat from the moving air stream and evaporation commences on the surface and this is referred to as the constant-rate drying period.

At this point the transport of the water in the solid into the gas phase is driven by concentration difference and it is enhanced by convection, and it is evident that the mass flux of the water component will be higher than would occur in molecular diffusion. Convective mass transfer will occur in liquids and gases and within the structures of a porous solid. The relative contribution of molecular diffusion and convective mass transfer will depend on the magnitude of the convective currents within the gas phase. The convective mass transfer coefficient h_m is defined as rate of mass transfer per unit area per concentration difference. Thus

$$h_m = \frac{\dot{m}_s}{A(c_{s1} - c_{s2})} \tag{3.12}$$

Where $\dot{m}_s$ is the mass flux (kg/s); c is concentration of the water component, mass per unit volume (kg/m^3); A is area (m^2). The units of h_m is W/m^{2}K and the coefficient

represents the volume (m^3) of the water component transported across a boundary of one square metre per second

By using the relationship presented in equation (3.12), the mass transport due to convection becomes:

$$\dot{m}_s = \frac{h_m A M_w}{\Re T_g}(p_{s1} - p_{s2}) \tag{3.13}$$

The expression is used to estimate the mass flux based on the vapour pressure gradient in the region of mass transport. The humidity ratio, W (sometimes called the moisture content or the specific humidity) is defined as the mass of water vapour per unit mass of dry air and is defined by the following equation

$$W = 0.622\frac{p_{vo}}{p_{vg} - p_{vo}} = \frac{M_s}{M_a} \tag{3.14}$$

p_{vo} = partial pressure exerted by water vapour and p_{vg} = total pressure of moist air

When the specific application of mass transport is water vapour in air, Equation (3.14) can be incorporated into (3.13) to obtain:

$$\dot{m}_s = \frac{h_m A M_w P}{0.622\Re T_A}(W_1 - W_2) \tag{3.15}$$

The evaporation rate from individual spherical particle submerged in a stream of drying air can also be expressed as given in Welty J. R et al (1984) as:

$$\dot{m}_s = h_m \chi \pi d_p^2 \left(\frac{M_w p_{vo}}{\Re T_s} - \frac{M_w p_{vg}}{\Re T_g}\right) \tag{3.16}$$

It is assumed that the solid particles are true spheres but with vastly increased surface area to account for the roughness and protuberances. The sphericity, χ can be defined as the ratio of the true surface area and the spherical surface area as given in (Radford R. D., 1997) as:

$$\chi = \frac{A_{so}\rho_{sa} d_p}{6} \tag{3.17}$$

When computing the convective transport of water vapour in air, Equations (3.15) or (3.16) can be used, and the gradient is in the form of a humidity ratio gradient in the region of convective mass transport.

For a situation that involves molecular diffusion and mass transfer due to forced convection, the following variables are important: mass diffusivity $D_{wv,g}$, from water vapour component to the gas phase, the velocity of the fluid, u_g, the density of the fluid, ρ_g, the viscosity of the fluid, μ_g, the characteristic dimension d_p, which for the present work corresponds to the particle diameter, and the convective mass transfer coefficient h_m.

The variables are grouped into the following dimensionless numbers:

Sherwood number

$$Sh = \frac{h_m d_p}{D_{wv,g}} \tag{3.18}$$

Schmidt's number

$$Sc = \frac{\mu_g}{\rho D_{wv,g}} \tag{3.19}$$

Reynolds number

$$Re_p = \rho_g d_p |u_g - u_s| / \mu_g \tag{3.20}$$

Lewis number

$$L_e = \frac{h}{\rho C_p D_{wv,g}} \tag{3.21}$$

The functional relationship that correlated these dimensionless numbers for forced convection are:

$$Sh = f(Re_p, Sc) \tag{3.22}$$

The convective mass transfer coefficient for evaluating mass transfer for flow over a spherical object is obtained from an expression similar to the Froessling correlation for heat transfer as suggested by Singh and Heldman (2001):

$$Sh = 2.0 + \left(0.4Re_p^{\frac{1}{2}} + 0.06Re_p^{\frac{2}{3}}\right)Sc^{0.4} \qquad (3.23)$$

After evaluating the correlation above the Sherwood number is substituted into equation (3.18) and h_m can then be solved for.

If the drying occurs in two stages then the second drying stage period starts when the particulate surface becomes no longer wetted and evaporation must occur from within the pores. At this point corresponding to the critical moisture content, evaporation must drive moisture from inside the particle outwards to be evaporated while heat transfer progresses towards the centre of the particle. This is the falling rate period.

This was assumed to occur at solid water content, *X*, less than the critical solid water content, *Xcr*. Radford R. D. (1997) mentioned that there are five possible mechanisms of evaporation during this period (the falling-rate period). The predominant mechanism at any time will depend upon the pressure, temperature and the diameter of pore from which evaporation is occurring.

The critical moisture content of solids, X_{cr}, can be determined experimentally or estimated from the following equation;

$$X_{cr} = \rho_w \left(\frac{1}{\rho_{sa}} - \frac{1}{\rho_s}\right) \qquad (3.24)$$

The density of the dispersed phase, which is composed of liquid water and solid material can be expressed as;

$$\rho_s = \rho_{sa}(1 + X) \qquad (3.25)$$

The five mechanisms describe the evaporation rate during the second drying stage (falling-rate period). The appropriate evaporation mechanism through any specific pore will depend upon the prevailing condition at the time under consideration. The selection of the drying mechanism must be established for each pore at the prevailing conditions.

The drying curve for TMe 419 was determined experimentally. The curve showed that the drying rate was constant up to the desired final moisture content of 10%. This result was further collaborated by Nwabanne J.T., (2009) who produced the drying curves for three cassava species, TMS 30572, NR 8082 and a native cultivar. This work revealed that the three cultivars exhibited constant drying rate down to a moisture content of 10% which is the expected final moisture content from cassava flash drying (Sanni L.O. et al, 2005). These indicates that the evaporation rate for cassava pneumatic conveying drying of TMe 419 can be appropriately represented by the constant-rate drying equation only as in equation (3.15) or (3.16)

3.3.3 Momentum Equation

For the momentum balance it is assumed that the flow across the control volume is laminar and steady. The formulation for the gas momentum balance assumes for simplicity that there are no particles of the dispersed phase within the control volume. The assumption also implies that the cross-section of the particle is small and therefore the influence of the pressure gradient on the inertia of the solid particle is negligible when compared to that of the drag force. Hence the pressure gradient contributes only to the momentum of the gas.

The flux of momentum of the gas component in the k direction through the side perpendicular to the i direction is $\rho_g \alpha_g u_{gi} u_{gk}$ and hence the net flux of momentum

(in the k direction) out of the control volume is given by the divergence of $\rho_g \alpha_g u_{gi} u_{gk}$ or

$$\frac{\partial\,(\rho_g \alpha_g u_{gi} u_{gk}\,)}{\partial xi} \tag{3.36}$$

The rate of increase in momentum of gas component in the k direction

$$= \frac{\partial\,(\rho_g \alpha_g u_{gk}\,)}{\partial t} \tag{3.27}$$

Thus the momentum conservation principle demands that the net force in the k direction acting on the gas component in the control volume (of unit volume), S_{mom} is given by:

Net rate of momentum inflow = rate of momentum accumulation + Net rate of momentum outflow

or

$$F_{gk} = \frac{\partial\,(\rho_g \alpha_g u_{gk}\,)}{\partial t} + \frac{\partial\,(\rho_g \alpha_g u_{gi} u_{gk}\,)}{\partial xi} \tag{3.28}$$

It is more difficult to construct the forces F_{gk} in order to complete the equation of motion. Body forces acting within the control volume must be included:

-the force due to pressure

-the viscous stresses on the exterior of the control volume

-and most particularly, the force that each component imposes on the other component within the control volume.

The first contribution to F_{gk} is due to an external field on the gas component within the control volume, in the case of gravitational forces this is given by

$$\alpha_g \rho_g g_k \tag{3.29}$$

Where g_k is the component of the gravitational acceleration in the k direction (the direction of g is considered vertically downwards).

The second contribution to F_{gk} namely, that due to traction on the control volume, differ for the two phases. It is zero for the disperse phase but for the continuous phase stress tensor, σ_{gki}, is defined so that the contribution from the surface traction to the force on the phase is

$$\frac{\partial \sigma_{gki}}{\partial x_i} \tag{3.30}$$

σ_{gki} can be decomposed into

$$\sigma_{gki} = -P_g \delta_{ki} + \sigma^s_{gki} \tag{3.31}$$

Equation (3.30) becomes

$$\frac{\partial\left(-P_g \delta_{ki} + \sigma^s_{gki}\right)}{\partial x_i}$$

$$-\frac{\partial\left(P_g \delta_{ki}\right)}{\partial x_i} + \frac{\partial \sigma^s_{gki}}{\partial x_i}$$

But δ_{ki} is the Kronecker delta such that δ_{ki} = 1 for $k = i$

Therefore,

$$-\frac{\partial P_g}{\partial x_i} + \frac{\partial \sigma^s_{gki}}{\partial x_i} \tag{3.32}$$

The third contribution to F_{gk} is as a result of the force (per unit volume) imposed on the gas component by the solid component within the control volume. This can be written as:

Force (imposed on gas component by solid component) = S_{mom} (3.33)

Now rewriting equation (3.28) considering the contributions of (3.29), (3.32) and (3.33)

$$\frac{\partial\,(\rho_g \alpha_g u_{gk})}{\partial t} + \frac{\partial\,(\rho_g \alpha_g u_{gi} u_{gk})}{\partial xi} = -\alpha_g \rho_g g_k + S_{mom} - \frac{\partial P_g}{\partial x_i} + \frac{\partial \sigma^s_{gki}}{\partial x_i} \tag{3.34}$$

Assuming that the contribution from the surface traction to the force on the phase is negligible then equation (3.34) becomes

$$\frac{\partial\ (\rho_g \alpha_g u_{gk}\ )}{\partial t} + \frac{\partial\ (\rho_g \alpha_g u_{gi} u_{gk}\ )}{\partial xi} \quad = \quad -\alpha_g \rho_g g_k + S_{mom} \ - \frac{\partial P_g}{\partial x_i} \qquad (3.35)$$

The use of continuity equation results in the appearance of the mass interaction, S_{mass} and one obtains:

$$\rho_g \alpha_g \left\{\frac{\partial u_{gk}}{\partial t} + u_{gi} \frac{\partial u_{gk}}{\partial_{xi}}\right\} = -\alpha_g \rho_g g_k + S_{mom} \ + S_{mass}\, u_{gk} - \frac{\partial P_g}{\partial x_i} + \frac{\partial \sigma^{s}_{gki}}{\partial x_i} \qquad (3.36)$$

The left side of the equation is the normal rate of increase of momentum of the gas component; the term $S_{mass}\, u_{gk}$ is the rate of increase of momentum in the gas component due to the gain of the mass by that phase.

`For one dimensional duct flow the equation becomes

$$\frac{\partial}{\partial t}\left(\rho_g \alpha_g u_g\right) + \frac{\partial}{\partial x}\left(A \rho_g \alpha_g u_g^2\right) = -\frac{\partial P_g}{\partial x_{ig}} - \frac{\acute{P} \tau_w}{A} - \alpha_g \rho_g g_x + S_{mom} \ + S_{mass}\, u_g \quad (3.37)$$

Where $\acute{P}$ is the perimeter of the cross section and τ_w is the wall shear stress.

Considering that momentum accumulation is zero for the situation being modelled, the one dimensional duct flow equation becomes:

$$\frac{d}{dx}\left(A \rho_g \alpha_g u_g^2\right) = -\frac{dP_g}{dx} - \frac{\acute{P} \tau_w}{A} - \alpha_g \rho_g g_x + S_{mom} \ + S_{mass}\, u_g$$

Rewriting the equation above in terms of unit length gives:

$$\frac{d}{dx}\left(A \rho_g \alpha_g u_g^2\right) = -A \frac{dP_g}{dx} - \acute{P} \tau_w - A \alpha_g \rho_g g_x + S_{mom} \ + S_{mass}\, u_g \qquad (3.38)$$

Simplifying the LHS

$$\frac{d}{dx}\left(A \rho_g \alpha_g u_g^2\right) = \rho_g \alpha_g u_g^2 \frac{dA}{dx} + A \alpha_g u_g^2 \frac{d\rho_g}{dx} + A \rho_g u_g^2 \frac{d\alpha_g}{dx} + A \rho_g \alpha_g \frac{du_g^2}{dx}$$

Applying the conditions and simplifying assumptions that were made in solving the continuity equation:

$$\frac{dA}{dx} = 0, \qquad \frac{d\alpha_g}{dx} = 0 \qquad and \qquad \frac{d\rho_g}{dx} = 0$$

then equation (3.38) now becomes

$$\rho_g \alpha_g \frac{du_g^2}{dx} = -A \frac{dP_g}{dx} - \acute{P} \tau_w - A \alpha_g \rho_g g_x + S_{mom} \ + S_{mass}\, u_g$$

and

$$\frac{dP_g}{dx} = -\frac{\rho_g \alpha_g}{A}\frac{du_g^2}{dx} - \frac{\acute{P}\tau_w}{A} - \alpha_g \rho_g g_x + \frac{S_{mom}}{A} + \frac{S_{mass}\, u_g}{A} \qquad (3.39)$$

but,

$$\frac{du_g^2}{dx} = 2u_g \frac{du_g}{dx}$$

Equation (3.39) becomes

$$\frac{dP_g}{dx} = -\frac{\rho_g \alpha_g}{A} 2u_g \frac{du_g}{dx} - \frac{\acute{P}\tau_w}{A} - \alpha_g \rho_g g_x + \frac{S_{mom}}{A} + \frac{S_{mass}\, u_g}{A} \qquad (3.40)$$

But from equation (3.7)

$$\frac{du_g}{dx} = s_{mass} / A\rho_g \alpha_g$$

Rewriting (3.7) in terms of unit volume, yields

$$\frac{du_g}{dx} = s_{mass} / \rho_g \alpha_g$$

Therefore equation (3.40) becomes

$$\frac{dP_g}{dx} = -\frac{\rho_g \alpha_g}{A} 2u_g \frac{s_{mass}}{\rho_g \alpha_g} - \frac{\acute{P}\tau_w}{A} - \alpha_g \rho_g g_x + \frac{S_{mom}}{A} + \frac{S_{mass}\, u_g}{A}$$

$$\frac{dP_g}{dx} = -\frac{2u_g s_{mass}}{A} + \frac{S_{mass}\, u_g}{A} - \frac{\acute{P}\tau_w}{A} - \alpha_g \rho_g g_x + \frac{S_{mom}}{A}$$

$$\frac{dP_g}{dx} = -\frac{u_g s_{mass}}{A} - \frac{\acute{P}\tau_w}{A} - \alpha_g \rho_g g_x + \frac{S_{mom}}{A}$$

Integrating,

$$\int \frac{dP_g}{dx} = -\frac{u_g s_{mass}}{A}\int dx - \frac{\acute{P}\tau_w}{A}\int dx - \alpha_g \rho_g g_x \int dx + \frac{S_{mom}}{A}\int dx$$

$$P = -\frac{u_g S_{mass}\, x}{A} - \frac{\acute{P}\tau_w}{A} x - \alpha_g \rho_g g_x x + \frac{S_{mom}\, x}{A} + C \qquad (3.41)$$

Using initial conditions

$x = 0,$ and $P = P_1$ then, $C = P_1$

then equation (3.41) becomes

$$P_2 = P_1 - \frac{u_g S_{mass}}{A} x - \frac{\acute{P}\tau_w}{A} x - \alpha_g \rho_g g_x x + \frac{S_{mom}}{A} x \qquad (3.42)$$

3.3.4 Constitutive Relationships (Momentum)

The frictional force per unit length between the pipe wall and the gas phase was estimated by,

$$\tau_{wg} = \pi d_{pipe} \frac{f}{2} \rho_g \left(\alpha_g u_g\right)^2 \qquad (3.43)$$

The friction factor, f, can be calculated from Blasius formulation. In addition the friction factor between particles and the wall of the pipe can be calculated as in Debrand S. (1974).

$$f_p = 1.0503 Fr_p^{-1.831} \qquad (3.44)$$

Where,

Particle Froude number, $Fr_p = u_s / \left(g d_p\right)^{0.5}$ (3.45)

For dilute phase pneumatic conveying a relatively high conveying air velocity must be maintained. This is typically in the region of 12 m/s for a fine powder, to 16 m/s for a fine granular material, and beyond for larger particles and higher density materials. For dense phase conveying, air velocities can be down to 3 m/s, and lower in certain circumstances. However a pneumatic conveying experiment shall be set up to determine the various conveying variables and as such be the basis for the validation of the result generated by the analytical approach.

Equation (3.36) will provide the pressure at discrete points along the flash tube and this can be used to predict the flow velocity profile of the continuous phase and using the basic thermodynamic equation;

$$\frac{P_1\dot{V}_1}{T_1} = \frac{P_2\dot{V}_2}{T_2} \tag{3.46}$$

where , $\dot{V}$ and T are pressure, volumetric flow rate, and temperature and for a pipe section with uniform cross sectional area:

$$u_{g2} = \frac{P_1 u_{g1} T_2}{P_2 T_1} \tag{3.47}$$

Where, $\dot{V} = Au_g$ (A = pipe cross sectional area).

It should be emphasized that absolute values of both pressure and temperature must always be used in these equations. Most data for these values, such as that for minimum conveying air velocity are generally determined experimentally or from operating experience. It is for the purposes of this work, important to take the presence of the particles into account because in accelerating the material at zero velocity at the feed point to some value along the flow line requires momentum exchange between the particles and the continuous phase.

In dilute phase conveying, with particles in suspension in the air, the mechanism of conveying is one of drag force. The velocity of the particles, therefore, will be lower than that of the conveying air. It is a difficult and complex process to measure particle velocity, and apart from research purposes, particle velocity is rarely measured. Once again it is generally only the velocity of the air that is ever referred to in pneumatic conveying.

In a horizontal pipeline the velocity of the particles will typically be about 80% of that of the air. This is usually expressed in terms of a slip ratio, defined in terms of the

velocity of the particles divided by the velocity of the air transporting the particles, and in this case it would be 0.8. The value depends upon the particle size, shape and density, and so the value can vary over an extremely wide range. In vertically upward flow in a pipeline a typical value of the slip ratio will be about 0.7.

These values relate to steady flow conditions in pipelines remote from the point at which the material is fed into the pipeline, bends in the pipeline and other possible flow disturbances and shall be used as a ball pack check on the result of analytical methods. At the point at which the material is fed into the pipeline, the material will essentially have zero velocity. The material will then be accelerated by the conveying air to its slip velocity value. This process will require a significant pipeline length and this is referred to as the acceleration length. The actual distance will depend once again on particle size, shape and density.

There is a pressure drop associated with acceleration of the particles in the air stream and it has to be taken into account by some means. It is not only at the material feed point that there is an acceleration pressure drop. It is likely to occur at all bends in the pipeline. In traversing a bend the particles will generally make impact with the bend wall and so be retarded. The slip velocity at exit from a bend will be lower than that at inlet and so the particles will have to be re-accelerated back to their steady-state value. This additional element of the pressure drop is usually incorporated in the overall loss associated with a bend.

The momentum coupling source term (per unit volume) due to the reverse effect of particles can be expressed as suggested by Hamed M. H (2005):

$$S_{mom} = -N_p \frac{1}{2} C_D \frac{\pi d_p^2}{4} \rho_p x \left(u_g - u_s\right) \left|u_g - u_s\right| \qquad (3.48)$$

3.3.5 Energy Equation

In writing the energy equations for a multi phase flow, it is necessary to construct an energy equation for each of the phases or components. First total energy density (per unit mass) e_N^* is defined for each component such that

$$e_N^* = e_N + \frac{1}{2} u_{Ni} u_{Ni} + gx \tag{3.49}$$

Then the appropriate statement of the first law of thermodynamics for each phase becomes:

Rate of heat addition to N from outside control volume, Q_N

+ Rate of work done to N by the exterior surroundings, WA_N

+ Heat transfer to N within the control volume, QI_N

+ Rate of work done to N by the other component in the control volume, WI_N

= Rate of increase of total kinetic energy of N in control volume

+ Net flux of internal energy of N out of the control volume (3.50)

The second term on the RHS of equation (3.50) contains two contributions: (i) minus the rate of work done by the stress acting on the component of N on the surface of the control volume and (ii) the rate of external shaft work, W_N, done on the component N. In evaluating the first of these, the same modifications to the control volume as we did for the momentum equation are made; specifically small deformations is made to the control volume so that its boundaries lie wholly within the continuous phase.

Then using continuous phase stress tensor,σ_{gij} , as defined earlier the expression for WA_N becomes:

$$WA_g = W_g + \frac{\partial}{\partial x_j}\left(u_{gi}\sigma_{gij}\right) \tag{3.51}$$

And

$$WA_s = W_N \tag{3.52}$$

Also the last two terms of equation (3.3.60) can be written as

$$\frac{\partial}{\partial t}\left(\rho_g \alpha_g e_{Ng}^*\right) + \frac{\partial}{\partial x_i}\left(\rho_g \alpha_g e_g^* u_{gi}\right) \tag{3.53}$$

Then the energy equation can be written as:

$$\frac{\partial}{\partial t}\left(\rho_g \alpha_g e_g^*\right) + \frac{\partial}{\partial x_i}\left(\rho_g \alpha_g e_g^* u_{gi}\right) = Q_g - W_g + QI_g + WI_g + \delta_g \frac{\partial}{\partial x_j}\left(u_{gi}\sigma_{gij}\right) \tag{3.54}$$

Note that the two terms involving internal exchange of energy between the phases may be combined into an energy interaction term given by

$$S_{energy\ ,T} = QI_g + WI_g \tag{3.55}$$

It then follows that

$$\sum_N QI_g = 0$$

and

$$\sum_N WI_g = 0$$

and

$$\sum_N S_{energy\ ,T} = 0$$

Moreover, the work done terms, WI_N, may clearly be related to the interaction forces, S_{mom} . In a two phase flow with one dispersed phase:

$$QI_g = -QI_s \ , \ WI_g = -WI_s = -u_{si}F_{si} \ , \qquad S_{energy\ ,g} = -S_{energy\ ,s} \tag{3.56}$$

When the left hand side of equation (3.54) are expanded and use is made of continuity equations and momentum equation , it results in the thermodynamic form of the energy equation. Using expression (3.54) and the relation

$$e_g = c_{Vg}T_g + constant \tag{3.57}$$

Between the internal energy, e_g , the specific heat capacity at constant volume, c_{Vg}, and the temperature, T_g, of the continuous phase, the energy equation can be written as

$$\rho_g \alpha_g C_{vg} \left\{\frac{\partial T_g}{\partial t} + u_g \frac{\partial T_g}{\partial x_i}\right\} = \delta_N \sigma_{gij} \frac{\partial u_{gi}}{\partial x_j} + Q_g + W_g + QI_g + S_{mom}\left(u_s - u_g\right) - \left(e_g^* - u_g^2\right) S_{mass} \quad (3.58)$$

In equation (3.58) it has been assumed that the specific heat,c_{vN}, is constant and uniform. Finally the one –dimensional duct flow equation for energy balance is:

$$\frac{\partial}{\partial t}\left(\rho_g \alpha_g e_g^*\right) + \frac{1}{A}\frac{\partial}{\partial x}\left(A\rho_g \alpha_g e_g^* u_g\right) = Q_g + W_g + QI_g + WI_g + \delta_g \frac{\partial}{\partial x}\left(pu_g\right) \quad (3.59)$$

In simplifying the last term on the RHS of equation (3.59) notice that for continuous phase, $\delta_N = 1$ while for the dispersed phase, $\delta_N = 0$. And that for the flow situation under consideration, there no shaft work done on the gas component therefore

$$\frac{\partial}{\partial t}\left(\rho_g \alpha_g e_g^*\right) + \frac{1}{A}\frac{\partial}{\partial x}\left(A\rho_g \alpha_g e_g^* u_g\right) = Q_g + QI_g + WI_g + \frac{\partial}{\partial x}\left(pu_g\right)$$

Since there is no energy accumulation on the control volume, this further simplifies to

$$\frac{1}{A}\frac{\partial}{\partial x}\left(A\rho_g \alpha_g e_g^* u_g\right) = Q_g + QI_g + WI_g + \frac{\partial}{\partial x}\left(pu_g\right) \quad (3.60)$$

Now

$$\frac{\partial}{\partial x}\left(A\rho_g \alpha_g e_g^* u_g\right)$$

$$= \frac{\partial A}{\partial x}\left(\rho_g \alpha_g e_g^* u_g\right) + \frac{\partial \rho_g}{\partial x}\left(A\alpha_g e_g^* u_g\right) + \frac{\partial \alpha_g}{\partial x}\left(A\rho_g e_g^* u_g\right)$$

$$+ \frac{\partial e_g^*}{\partial x}\left(A\rho_g \alpha_g u_g\right) + \frac{\partial u_g}{\partial x}\left(A\rho_g \alpha_g e_g^*\right)$$

but

$$\frac{\partial A}{\partial x} = 0 \qquad \frac{\partial \rho_g}{\partial x} = 0 \qquad \frac{\partial \alpha_g}{\partial x} = 0$$

So LHS of equation (3.60)

$$\frac{1}{A}\frac{\partial}{\partial x}\left(A\rho_g\alpha_g e_g^* u_g\right) = \frac{\partial e_g^*}{\partial x}\left(\rho_g\alpha_g u_g\right) + \frac{\partial u_g}{\partial x}\left(\rho_g\alpha_g e_g^*\right)$$

equation (3.60) becomes:

$$\rho_g\alpha_g\left(u_g\frac{\partial e_g^*}{\partial x} + e_g^*\frac{\partial u_g}{\partial x}\right) = Q_g + QI_g + WI_g + \frac{\partial}{\partial x}\left(pu_g\right) \qquad (3.61)$$

$$\frac{\partial}{\partial x}\left(pu_g\right) = u_g\frac{\partial p}{\partial x} + p\frac{\partial u_g}{\partial x}$$

let

$$\frac{du_g}{dx} = S_{mass}/\rho_g\alpha_g = a$$

$$\frac{dp_g}{dx} = -\alpha_g\rho_g g_x - \frac{\acute{P}\tau_w}{A} + \frac{S_{mom}}{A} - u_g S_{mass} = b$$

Since the values of $\frac{du_g}{dx}$ and $\frac{dp_g}{dx}$ are coefficients their values can be replaced with a and b for convenience

$$\frac{\partial}{\partial x}\left(pu_g\right) = \left(u_g b + pa\right)$$

Equation (3.61) can be rewritten as

$$\rho_g\alpha_g\left(u_g\frac{\partial e_g^*}{\partial x} + e_g^*\frac{S_{mass}}{\rho_g\alpha_g}\right) = Q_g + QI_g + WI_g + \left(u_g b + pa\right)$$

rearranging

$$\rho_g\alpha_g u_g\frac{\partial e_g^*}{\partial x} + e_g^* S_{mass} = Q_g + QI_g + WI_g + \left(u_g b + pa\right)$$

and

$$\frac{\partial e_g^*}{\partial x} + e_g^*\frac{S_{mass}}{\rho_g\alpha_g u_g} = \frac{1}{\rho_g\alpha_g u_g}\left(Q_g + QI_g + WI_g + \left(u_g b + pa\right)\right) \qquad (3.62)$$

Again, since the entire LHS is a constant, it is denoted with m for convenience

$$\frac{1}{\rho_g\alpha_g u_g}\left(Q_g + S_{energy} + \left(u_g b + pa\right)\right) = m$$

Equation (3.62) becomes

$$\frac{\partial e_g^*}{\partial x} + e_g^* \frac{S_{mass}}{\rho_g \alpha_g u_g} = m$$

$$\frac{\partial e_g^*}{\partial x} = m - e_g^* \frac{S_{mass}}{\rho_g \alpha_g u_g}$$

$$\frac{\partial e_g^*}{\partial x} = \left(-\frac{m\rho_g \alpha_g u_g}{S_{mass}} + e_g^*\right) - \frac{S_{mass}}{\rho_g \alpha_g u_g}$$

$$\frac{\partial e_g^* / \partial_x}{e_g^* - \frac{m\rho_g \alpha_g u_g}{S_{mass}}} = -\frac{S_{mass}}{\rho_g \alpha_g u_g} \tag{3.63}$$

Equation (3.63) is variable separable and integrating gives

$$ln\left|e_g^* - \frac{m\rho_g \alpha_g u_g}{S_{mass}}\right| = -\frac{S_{mass}}{\rho_g \alpha_g u_g} x + C$$

$$e_g^* = \left(\frac{m\rho_g \alpha_g u_g}{S_{mass}}\right) + Ce^{-\frac{S_{mass}}{\rho_g \alpha_g u_g} x} \tag{3.64}$$

Using the following initial conditions

$$x = 0 \;\; ; \qquad e_g^* = e_{g1}^*$$

Then

$$C = e_{g1}^* - \frac{m\rho_g \alpha_g u_g}{S_{mass}}$$

$$e_g^* = \left(\frac{m\rho_g \alpha_g u_g}{S_{mass}}\right) + \left(e_{g1}^* - \frac{m\rho_g \alpha_g u_g}{S_{mass}}\right) e^{-\frac{S_{mass}}{\rho_g \alpha_g u_g} x}$$

$$e_g^* = c_{Vg} T_g + \frac{u_g^2}{2} + gx$$

$$T_{g2} = \left(\left(\left(\frac{m\rho_g \alpha_g u_g}{S_{mass}}\right) + \left(e_{g1}^* - \frac{m\rho_g \alpha_g u_g}{S_{mass}}\right) e^{-\frac{S_{mass}}{\rho_g \alpha_g u_g} x}\right) - \frac{u_g^2}{2} - gx\right) \Big/ c_{Vg}$$

$$T_{g2} = \left(\left(\left(\frac{m\rho_g \alpha_g u_g}{S_{mass}}\right) + \left(\left(c_{Vg} T_{g1} + \frac{u_{g1}^2}{2} + gx\right) - \frac{m\rho_g \alpha_g u_g}{S_{mass}}\right) e^{-\frac{S_{mass}}{\rho_g \alpha_g u_g} x}\right) - \frac{u_g^2}{2} - gx\right) \Big/ c_{Vg} \tag{3.65}$$

3.3.6 Constitutive Relationships (Energy)

The energy coupling source term for the total energy equation involves convective heat transfer and the work due to particle drag as suggested by Hamed M. H (2005) is expressed as:

$$S_{energy} = -N_p hA\chi\pi d_p^2 (T_g - T_s) + S_{mom}\, u_s \tag{3.66}$$

The dispersed phase is introduced into the dispersing phase at a point along the flow path; the feed point which is always upstream of the flash tube. At this point the dispersed phase temperature is much smaller than the dispersing phase temperature.

Heat transfer between the phases tends to reduce the difference in temperature. Therefore it is necessary to characterize the rate of equilibration of the particle and fluid temperatures by defining a temperature relaxation time, t_T. This temperature relaxation time can be obtained by equating the rate of heat transfer from the continuous phase to the particle with the rate of increase of heat stored in the particle. The heat transfer to the particle can occur as a result of conduction, convection or radiation and there are practical flows in which each of these mechanisms are important but for the situation at hand the radiation component shall be neglected.

If the relative motion between the particles and the fluid is sufficiently small, the only contributing mechanism is conduction and it is limited by the thermal conductivity, k_g of the gas since the thermal conductivity of the particle is usually much higher. Then the rate of heat transfer to the particle of radius, R will be given approximately by

$$2\pi R k_g (T_g - T_s) \tag{3.67}$$

where T_g and T_s are respectively temperatures of the gas phase and the particle.

Since the situation being modelled involves conveyance and drying, the relative motion that is slip velocity can only be low to the extent that it guarantees conveyance

and in this situation conveyance takes precedence over heat transfer which drives drying.

In determining the convective heat transfer coefficient the empirical approach was used. The usual drawback of using the empirical approach is that it requires a large number of experiments to obtain the required data. This challenge is overcome by the use of dimensionless numbers. To formulate this approach, first the required dimensionless numbers are identified: Reynolds number, Re, Nusselt number, Nu, and Prantl number, Pr

To add the component of heat transfer by convection caused by relative motion is done by defining the Nusselt number, Nu, as twice the ratio of the rate of heat transfer with convection to that without convection. Then the rate of heat transfer becomes Nu times the above result for conduction.

The convective heat transfer coefficient, h, was calculated from Nusselt number, Nu, which is expressed as a function of Reynold number, Re_p and Prantl number, Pr, which are defined as:

$$Re = 2\left(u_s - u_g\right)R/v_g \tag{3.68}$$

$$Pr = \frac{\rho_g\, v_g\, C_{pg}}{k_g} \tag{3.69}$$

Various empirical correlations that can be used to calculate the heat transfer coefficient has been proposed and are listed below.

- Frantz correlation (Radford R. D., 1997)

The correlation was used by Radford to calculate the heat transfer coefficient in pneumatic conveying dryer.

$$Nu = 0.015 Re_p^{1.6} Pr^{0.667} \tag{3.70}$$

- De Brandt correlation (Fyhr C. and Rasmuson A., 1997)

The correlation was developed for pneumatic drier,

$$Nu = 0.16Re_p^{1.6}Pr^{0.667} \tag{3.71}$$

- De Brand correlation (Debrand S., 1974)

The correlation was developed for a pneumatic dryer,

$$Nu = 0.035Re_p^{1.15}Pr^{0.333} \tag{3.72}$$

- Bayeans et al. Correlation (Baeyens et al, 1995)

The correlation was developed for large scale pneumatic conveyor

$$Nu = 0.15Re_p \tag{3.73}$$

- Modified Ranz-Marshall correlation (Levy and Borde, 1999)

The correlation was developed for simple droplet/wet particle and it takes into account the resistance of the liquid vapour around the particle to the heat transfer by Spalding number, B.

$$Nu = \frac{2+0.6Re_p^{0.5}Pr^{0.333}}{(1+B)^{0.7}} \tag{3.74}$$

$$B = \frac{C_{pwv}\left(T_g - T_s\right)}{H_{fg}} \tag{3.75}$$

- Modified Weber correlation (Kemp et al, 1994)

An additional term proportional to $Re_p^{0.8}$ was added to Ranz-Marshall correlation to account for turbulent flow.

$$Nu = 2 + \left(0.5Re_p^{0.5} + 0.06Re_p^{0.8}\right)Pr^{0.333} \tag{3.76}$$

- Ranz and Marshall correlation

$$Nu = 2 + 0.6Re^{1/2}Pr^{1/3} \tag{3.77}$$

The correlation above reduces to pure conduction result, Nu = 2, when the second term on the right hand is small. Assuming that the particle temperature has a roughly uniform value of T_s, it follows that

$$QI_s = 2\pi Rk_g Nu\left(T_g - T_s\right)n_s = \rho_s \alpha_s c_s \frac{DT_s}{Dt} \tag{3.78}$$

where the material derivative D/Dt, follows the particle. This provides the equation that must be solved for T_s, namely

$$\frac{DT_s}{Dt} = \frac{Nu}{2}\frac{(T_g - T_s)}{t_T} \tag{3.79}$$

where,

$$t_T = c_s \rho_s R^2 / 3k_g \tag{3.80}$$

- Singh and Heldman correlation (Singh and Heldman, 2001)

For a flow past a single sphere, when the single sphere may be heated or cooled, the following equation will apply:

$$Nu = 2 + 0.60 Re^{\frac{1}{2}} Pr^{\frac{1}{3}} \qquad \text{for } 1 < Re < 70000 \text{ and } 0.6 < Pr < 400 \tag{3.81}$$

where the characteristic dimension, d_p, is the outside diameter of the sphere.

The correlation suggested by Singh and Heldman (2001) shall be used for this work.

3.4 Solid Phase Formulation

Haven determined the conservation laws applicable to the continuous phase attempt shall now be made to get similar formulations for the dispersed phase. In doing this, it is important to note that, based on the dilute phase assumption, the particle is completely dispersed in the gas and so the interaction between the fluid and the dispersed particle happens on the particle scale. This means that the fluid interacts with each and every particle of the fluid and the analysis of this interaction could be described by the effect and influence of the fluid on the particle of the dispersed phase. Therefore it is important to derive the equations of motion for the individual particle. The analysis is implicitly confined to those circumstances in which the interaction between neighbouring particles are negligible.

It should also be noted that, for the situation being modelled, the dispersed phase is introduced into the dispersing phase at a point along the flow path, usually the feed point which is upstream of the flash tube. At the point of introduction the particle velocity is zero but that of the fluid is not. Drag will tend to reduce the difference. Therefore it becomes necessary to characterize the rate of equilibration of particle and fluid velocities by defining a velocity relaxation time, t_u .

It is common in dealing with gas flow laden with small particles to assume that the equation of motion can be approximated by just two terms; particle inertia and Stokes drag, which for spherical particles is (Singh and Heldman, 2001):

$$F_{Drag} = \frac{C_D A_p \rho_g \bar{u}^2}{2} \tag{3.82}$$

Where,

F_{Drag} = drag force

C_D = drag coefficient

A_p = projected particle area in the direction of motion

ρ_g = density of surrounding fluid

$\bar{u}$ = relative velocity between particle and fluid

The relative velocity decays exponentially with a time constant t_u, given by

$$t_u = m_p / 6\pi R\mu c \qquad (3.83)$$

The model assumes that the dispersed (solid) phase is moved as discrete particles and it is as discrete particles that heat is transferred to it. With that in mind, the following equations can then be written:

-The equation of motion of a particle in a gas was given as:

$$\frac{du_s^2}{dx} = \frac{3\rho_g C_D}{2\rho_s d_p}(u_g - u_s)|u_g - u_s| - 2g\left(1 - \frac{\rho_g}{\rho_s}\right) - f_p \frac{u_s|u_s|}{d_{pipe}} \qquad (3.84)$$

$$\frac{du_s^2}{dx} = 2u_s \frac{du_s}{dx}$$

Then equation (3.84) can be rewritten as:

$$2u_s \frac{du_s}{dx} = \frac{3\rho_g C_D}{2\rho_s d_p}(u_g - u_s)|u_g - u_s| - 2g\left(1 - \frac{\rho_g}{\rho_s}\right) - f_p \frac{u_s|u_s|}{d_{pipe}}$$

and

$$\frac{du_s}{dx} = \frac{3\rho_g C_D}{4u_s\rho_s d_p}(u_g - u_s)|u_g - u_s| - \frac{g}{u_s}\left(1 - \frac{\rho_g}{\rho_s}\right) - f_p \frac{|u_s|}{2d_{pipe}}$$

-The equation for particle temperature assuming temperature is uniform throughout the particle was written as:

$$u_s m_p C_{ps} \frac{dT_s}{dx} = \chi\pi d_p^2 h(T_g - T_s) - \dot{m}_s H_{fg} \qquad (3.85)$$

equation (3.85) can be rewritten as

$$\frac{dT_s}{dx} = \frac{\chi\pi\, d_p^2 h(T_g - T_s) - \dot{m}_s H_{fg}}{u_s m_p C_{ps}} \qquad (3.86)$$

The residence time of the particle at the gas phase was calculated as suggested by ref (9) as

$$-\frac{dt_s}{dx} = \frac{1}{u_s} \tag{3.87}$$

3.5 Summary

The solved model or discretized equations for upward vertical pneumatic conveying drying are stated below:

$$u_{g2} = \frac{1}{A\rho_g\alpha_g} x S_{mass} + u_{g,1} \tag{3.9}$$

$$P_2 = P_1 - \frac{u_g S_{mass}}{A} x - \frac{\acute{P}\tau_w}{A} x - \alpha_g \rho_g g_x x + \frac{S_{mom}}{A} x \tag{3.42}$$

$$T_{g2} = \left(\left(\left(\frac{m\rho_g\alpha_g u_g}{S_{mass}}\right) + \left(\left(c_{Vg}T_{g1} + \frac{u_{g1}^2}{2} + gx\right) - \frac{m\rho_g\alpha_g u_g}{S_{mass}}\right) e^{-\frac{S_{mass}}{\rho_g\alpha_g u_g}x}\right) - \frac{u_g^2}{2} - gx\right) \Big/ c_{Vg} \tag{3.65}$$

$$\frac{du_s^2}{dx} = \frac{3\rho_g C_D}{2\rho_s d_p}(u_g - u_s)|u_g - u_s| - 2g\left(1 - \frac{\rho_g}{\rho_s}\right) - f_p \frac{u_s|u_s|}{d_{pipe}} \tag{3.84}$$

$$\frac{dT_s}{dx} = \frac{\chi\pi\, d_p^2 h T_g - \chi\pi\, d_p^2 h T_s - \dot{m}_s H_{fg}}{u_s m_p C_{ps}} \tag{3.86}$$

$$t_s = \frac{x}{u_s} \tag{3.87}$$

The model for both the continuous phase and solid phase has been established and discretized. The Finite Element Analysis approach shall subsequently be applied to the solution domain, governed by the just derived and discretized equations to determine more accurately the effect of dryer variables for TMe 419.

3.6 Experimental Determination of TMe 419 Properties

Researchers and design engineers are excited by cassava's potentials as an income-generator as well as food; new industrial uses are constantly being developed from it (Halos-Kim, L. 1998). But the techniques used by farmers are still very crude which largely account for inefficiency in the process, and so developing appropriate tools and equipment to address the constraint in processing cassava into different products is a task for design engineers (Otuu Obinna et al, 2009).

It is a fact that locally fabricated process equipment has failed in the past due to various reasons all of which are somehow linked to the lack of machine design / machine building infrastructure (Otuu Obinna et al, 2009). It is also obvious that the design of equipment for handling and processing cassava requires a thorough understanding of the engineering properties of cassava tuber and this is very evident from the task at hand which is the modelling of a vertical upward cassava flash dryer.

The bending strength of cassava tuber was reported by Agbetoye, L.A.S (1999) while Oladele P. K (2007) reported the tensile strength, the compressive strength and elasticity of a cassava cultivar, TMS 4(2) 1425 released by IITA. Presently there are no reports in open literature on the physical, mechanical and transport properties of

the cultivar, TMe 419 and these data are needed to implement the model. The properties of interest to this work are to be determined experimentally.

Some of the properties that are reported vary with specie, maturity and moisture content. The intention on one hand is to generate data on the specie of interest, TMe 419, so as to be able to solve the model proposed in subsequent chapter. While on the other hand TMe 419 data that are required in the design of Pneumatic conveying dryer shall be generated.

a. Properties required for the identification of the material
    i. Particle shape
    ii. Particle size
    iii. Size distribution
    iv. Particle density
b. Properties required for pneumatic transport design
    i. Particle hardness
    ii. Friability
    iii. Particle weight and geometry
c. Properties required to determine conveying capability
    i. Terminal Velocity
    ii. Drag coefficient

iii. Mass transfer coefficient

d. Properties required to describe thermal behaviour

i. specific heat capacity

ii. thermal conductivity

iii. thermal diffusivity

iv. heat transfer coefficient

v. evaporation rate from a single particle

vi. drying curve

3.6.1 Particle Shape

The shape of the particles of some material are similar to each other while in some other material the particle shape is unique to each particle. The most established approach is to describe shape by quantitative terms that give an indication as to the shape of the particles as observed with the naked eye or through a microscope. In some cases it might be necessary to ascribe a numerical value to particle shape. For this purpose a sphere is generally taken as the reference shape.

Shape is clearly difficult to define with one meaningful parameter, the significance of which can be understood universally. For this reason quantitative terms are used to give some indication of the general nature of shape, and standards exist that attempt to define the terms. A British Standard defines the terminology of particle shape for powders, defined as particles with a maximum dimension of less than 1000 micron, as follows (David Mills, 2004):

Descriptive Classification of Particle Shape

Term	Definition
Acicular	Needle-shaped
Angular	Sharp-edged or having roughly polyhedral shape
Crystalline	Of geometric shape, freely developed in a fluid medium
Dendritic	Having a branched crystalline shape
Fibrous	Regularly or irregularly thread-like
Flaky	Plate-like
Granular	Having an approximately equidimensional but irregular shape
Irregular	Lacking any symmetry
Nodular	Having a rounded irregular shape
Spherical	Globule shaped

The problem with descriptive terms is that they are relative and, despite attempts to define the terminology, everyone has his own ideas regarding the meaning of the terms such as angular, irregular, nodular, and so on. Efforts have been made by researchers, therefore, to define shape on a more quantitative basis and many shape factors have been proposed. These are generally based on different measured characteristics of the particles.

One characteristic that has a physical significance is sphericity, ϕ, which is defined as the ratio of the surface area of a sphere having the same volume as the particle to the surface area of the particle. In mathematical terms this is given by David Mills (2004) as:

$$\phi = \frac{\pi\left(\frac{6V}{\pi}\right)^{2/3}}{S} \qquad (3.88)$$

where V is the particle volume (m^3) and S, the particle surface area (m^2).

The significance of this is that it gives an indication of the departure of the particle shape from that of a sphere of the same volume. Thus, for a sphere $\phi = 1$, but for any other shape ϕ will have a value less than unity (for example for a cube $\phi = 0.8$).

Unfortunately the problem with using this apparently useful parameter is purely a practical one, in that it is not easy to measure the volume V and surface area A of a single irregular particle. There is then the additional problem of specifying a single representative value for the bulk that could contain particles of varying shape.

Sample Collection and Preparation.

The cultivar was peeled, washed, grated and bagged for pressing. The sample was dewatered in a press by subjecting it to pressure that reduced the moisture content of the consolidated mass to 45%. The consolidated cake was subsequently broken down by passing it through a grater. The dewatered cassava mash was then sieved to-go on mesh of 4mm and no-go on 3mm mesh and particles viewed under an Axiom computer interfaced microscope

3.6.2 Particle Size

Particle size is a property that can relate to both individual particles and to the bulk, while shape is principally a particle property. Most bulk solids consist of many particles of different sizes, randomly grouped together to form a bulk. For some purposes a single linear dimension, as a representative value of particle size, may be all that is required to specify a material. In other cases some form of distribution may also be necessary in order to give some indication of the size range of the particles constituting the bulk material.

A spherical particle is clearly defined by its diameter and this is a meaningful parameter. The general definition of particle size, however, is neither straightforward nor unique. Irregular particles may have a diameter defined in terms of a three-dimensional equivalence, such as:

• the diameter of a sphere having the same surface area,

• the diameter of a sphere having the same volume or mass,

• the size of a hole (circular or square) through which the particle will just pass.

Alternatively the equivalent diameter could be defined in terms of a two-dimensional equivalence, such as:

• the diameter of an inscribed circle,

• the diameter of a circumscribed circle,

• the diameter of a circle with the same perimeter.

There are also statistical diameters, such as:

• Feret's diameter, which is the distance between the tangents to extremities of the particle, measured in a fixed direction;

• Martin's diameter, which is the length of the line, in a fixed direction, that divides the particle seen in three dimensions into two equal areas.

A size distribution can be obtained by submitting a representative sample of a bulk solid to a particle size analysis. This relates the distribution of the particle size fractions that comprise the bulk. Two methods of presenting the data are commonly used. One is a cumulative plot and the other is a fractional plot. Both linear and logarithmic plots are also used for the particle size axis.

Materials and Method:

The feedstock for cassava flash drying is dewatered cassava mash. This requires size reduction from the tuber to the mash and this is usually done by grating. The size reduction of cassava tubers by grating is affected by a lot of parameters which includes the height of the rasp above the rasp sheet, the number of rasps per unit area, and the clearance between the rasp sheet and the backing plate. Other parameters like the grating drum diameter, length, speed and feed pressure affects the throughput of the grating process (Otuu Obinna et al, 2009). This brings to the fore the problem of varied particle size as there is indeed no attempt at standardising these parameters. This is important because large variations in the size distribution of the feedstock will alter the thermodynamic balance of the drying process and definitely the expected final product moisture content. If the distribution shifts to a predominantly lower particle size than the designed size, there will be over reduction of the moisture content which translates to a waste of energy and if the converse is the case the expected moisture reduction will not be achieved. In the light of the above, this paper shall determine the particle size of grated and dewatered mash by sieving.

After the material was rasped, it was then dewatered as a pre-drying operation, to reduce the moisture content from about 70% to between 30 - 40% before flash drying. Cassava mash dewatering parameters were identified and the work evaluated the influence of cassava age on these parameters. They reported that the moisture content was reduced as the cultivar ages because of the presence of fibre which offers resistance to compression. Cassava cultivar TMS 4(2) 1425 has the best garification properties based on an IITA report (IITA, 1987). Cassava was pressed at a pressure of 48.3 kN/m^2 over a platen area of 0.0707 m^2 to arrive at a moisture content of 43.3%. Garification process requires some level of moisture but in the case of flour the

intention is to reduce the moisture so that drying can be more efficient. The dewatering should be carried as far as is possible and economically viable to reduce the moisture content as low as possible. This will reduce the moisture-load that the needs to be removed during flash drying. This also brings to the fore the arbitrariness in the design of dewatering presses. There is no information on the force per area required to reduce mechanically the moisture content of cassava (TMe 419) from values A% to B%. However, for the purpose of this work the mash was pressed to a pressure that enabled a change of the initial moisture content of the mash from 61% to 45% moisture content.

The pressed cake is consolidated by the pressure used in dewatering, and for the material to be fed into the sieve, the cake must be broken. This is achieved by passing the cake through the same grater that was used for size reduction. It is at this point that the particle size analysis was then carried out.

Sample Collection and Preparation.

The selected cultivar, TMe 419 was obtained from National Root Crop Research Institute, (NRCRI) Umudike, Abia state. This was for the accurate determination of the cultivar and its age. The cultivar was peeled, washed, grated and bagged for pressing. The sample was dewatered in a press by subjecting it to a pressure that reduced the moisture content of the consolidated cake from 61% to 45% moisture content. The consolidated cake was subsequently broken down by passing it through a grater. A particle size distribution was determined using the sieve method.

3.6.3 Particle Density

Particle density relates to the individual particles in a bulk solid. Particle density is the mass of an individual particle of a bulk solid, divided by the volume of the particle. The dimensions used for both particle and bulk density are kg/m^3.

The volume may be measured inclusive or exclusive of any open and closed pores that may exist. Closed pores are defined as being cavities not communicating with the surface of the particle. As a result, particle density can be expressed in a number of different ways (David Mills, 2004):

• *True particle density*: This is the mass of the particle divided by the volume of the particle, excluding open and closed pores.

• *Apparent particle density*: This is the mass of the particle divided by the volume of the particle, excluding open pores but including closed pores.

• *Effective particle density*: This is the mass of the particle divided by the volume of the particle, including both open and closed pores.

Materials and Method

The sample collection and preparation procedure is same as for the determination of particle size. It is a fact that the density of particle extracted from different parts of the cassava tuber exhibit slightly different density due basically to the variation of pore diameters and fibre content in those areas. This work assumes that the density of cassava tuber is uniform on any part of the tuber. This implies that the density of the tuber is same as that of the particle as the size only has been changed. In determining the particle density, an analytical balance is used to determine the precise weight of the sample and subsequently of the volume of the tuber was determined by displacement method. This method involved immersing the tuber into a partially filled measuring cylinder and the difference taken as the volume of the tuber.

Fig 3.2: Weight measurement

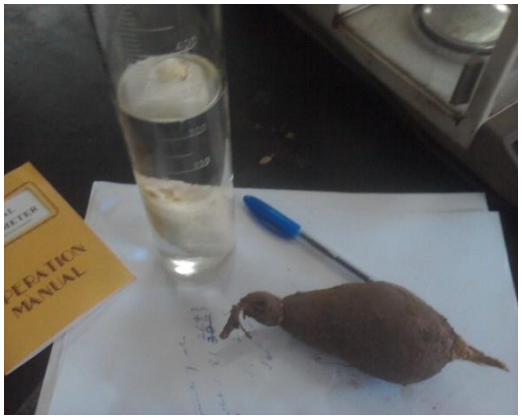

Fig 3.3: Volume measurement

3.7 Properties for Pneumatic Design

3.7.1 Particle Hardness

The value of the particle hardness of the material being conveyed is the major indicator of the potential erosiveness of the material. The influence of particle hardness on erosive wear was investigated by Goodwin J.E et al (1969) with a rig in which abrasive particles were impacted against test plates. Wall erosion is related to particle hardness by the expression suggested by David Mills (2004):

$$Erosion = constant \times H_p^{2.4} \qquad (3.89)$$

where H_p is the particle hardness (kg/mm^2).

It is generally considered, however, that there is a threshold value of particle hardness beyond which erosion remains essentially constant. This occurs at a particle hardness of about 800 kg/mm^2, and so materials with hardness values much greater than this would not be substantially more erosive than sand particles.

Materials and Methods

The cultivar, Tme 419 was peeled and washed and tested with a GY-4 of Penetrometer (Sclerometer) at the Food Science laboratory of Kaduna Polytechnic, Kaduna State. The penetrometer has a load limit of 20kg, a resolution of 0.01kg and an accuracy of $\pm$ 0.5%. Figure 3.4 shows the equipment used for the test;

Fig 3.4: Hardness Penetrometer

The 3.5mm diameter probe was used to pierce different parts of the sample and the peak values of the force recorded.

3.7.2 Friability

Particle friability is similarly important in terms of material degradation. A friable substance is any substance that can be reduced to fibres or finer particles by the action of a small pressure or friction on its mass, such as inadvertently brushing up against the substance. The term could also apply to any material that exhibits these properties. The resistivity to breakage can be measured by using the 'ROCHE' test, which subjects the tablets to mechanical shock, in order to establish a friability factor based on the loss in tablet weight due to breakage caused by induced mechanical stress. Though "ROCHE" test could not be carried out, the fact that drying is immediately followed by size reduction makes friability of no adverse effect if it exists.

3.7.3 Particle Weight

In determining the aerodynamic properties of irregular particulate material, the accurate determination of the particle weight is important and necessary in the calculation of the diameter of equivalent sphere. For material that is grated and sieved (extremely irregular) it is important to note passing the bulk through a series of sieves

narrows the size distribution within the bulk, in fact the closer the sieve sizes are together, the narrower the particle size distribution. It is for this reason that attempt was made, in determining the weight, to deliberately select (within material sieved to go on a mesh) the large sized particles in preference for the smaller sized particles. Also underestimating of the particle weight will lead to non-conveyance of the particles and blocking of the pneumatic conveying system

Materials and Method

The cultivar was peeled, washed, grated and pressed to a moisture content of 45%. The consolidated cake was subsequently broken down by passing it through a grater. The dewatered cassava mash was then sieved to-go on appropriate sieves and particles were isolated on a colony counter in groups of 50 particles before they were weighed on a Mettler AE163 precision weighing scale of accuracy 0.0001g. This was done in order to achieve a more accurate result in addition to the fact that the weight of a particle that was sieved undersize on Ø0.582 mm sieve was too small to be measured by the weighing scale.

3.7.4 Terminal velocity (Experimental)

Information on the physical and aerodynamic properties of cassava mash is important in the design and adjustment of cassava pneumatic conveying dryers. Terminal velocity could be determined experimentally by free-fall, vertical air tunnel and elutriator method. The value of aerodynamic drag coefficient, which is used for determining the aerodynamic drag force (F_d), acting upon a particle moving through air depends upon particle characteristics (mass, projected area, shape and terminal velocity) as well as the conditions of airflow. These properties must be known but unfortunately, the highly irregular shape of the particle makes experimentation one of the ways of determining these properties reliably.

Materials and Method

Fresh tubers of TMe 419 were acquired from National Root Crop Research Institute (NRCRI) Umudike, Abia State Nigeria to ensure proper identification of cultivar and determination of age. The sample was later peeled, washed, grated and dewatered mechanically to a moisture content of 42%. The consolidated lump was broken down again by passing it through a grater and subsequently graded by the use of sieves. The samples of a given particle size range, were subsequently placed in the experimental apparatus for measurement, vertical air tunnel.

The experimental setup used to determine the terminal velocity is shown in figure 3.5.

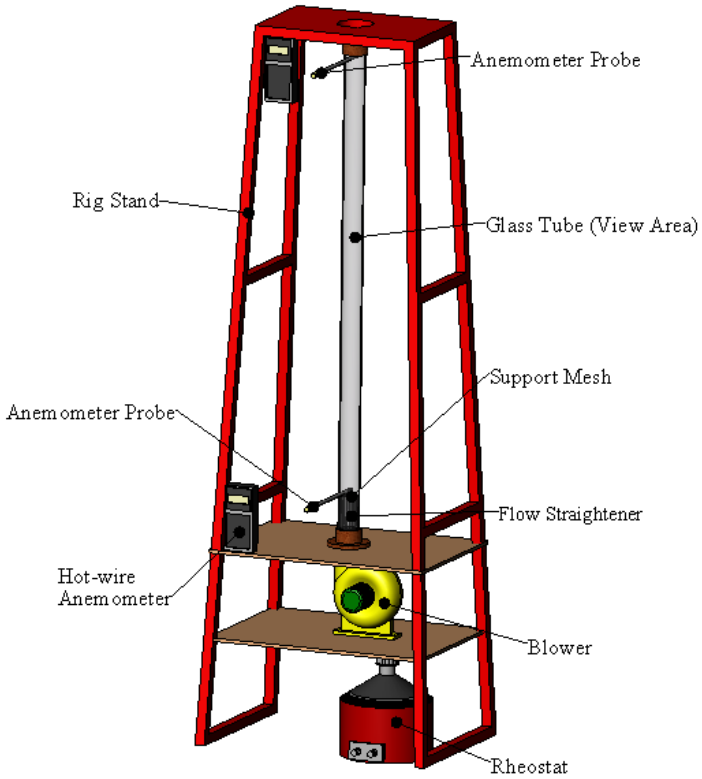

Fig 3.5: Experimental set-up for determination of terminal velocity

It consists of a blower fitted with a speed regulator, electric motor, air flow straighteners, vertical transparent tube with a diameter of 64.3 mm. The air flow velocity is changed steplessly by the use of the speed regulator while hot wire anemometers having a least count of 0.1 m/s and a vane type anemometer were used

for the measurement of air velocity in the tube. Because of the impracticability of measuring the particle size given its irregularity, the dimensions of the particles were approximated by the use of sieves. A batch of grated and dewatered mash was sieved through sieves of size diameters 0.150 mm to 6.350 mm successively. This way the fines are removed first and the size distribution of the particles that goes though the next sieve are tightly bound around the mean particle size to the extent that the mesh size becomes a good approximation of the size/geometric mean diameter of the equivalent sphere.

3.7.5 Drag Coefficient

The drag coefficient was calculated using equation:

$$C_d = \frac{2m_p g}{\rho_a (V_{et})^2 A_p} \tag{3.90}$$

C_d = drag coefficient

m_p = mass of cassava particle (kg)

V_{et} = experimental terminal velocity (m/s)

A_p = projected area of cassava particle (m^2)

3.8 Thermal Properties

It is evident that a basic understanding of the mechanism of heat transfer, both in the food and the material used in the construction of food processing equipment, is necessary before any heat transfer equipment can be designed or evaluated. Properties such as specific heat, thermal conductivity, and thermal diffusivity of food play an important role in determining the heat transfer rate which is at the heart of this analysis. The task is to develop a quantitative description of the thermal properties of TMe 419. For this purpose, the use of empirical models developed in previous works

including that of Nwabanne J. T. (2009) will be adopted. All these relationships rely solely on data generated by the proximate analysis of the food product. Proximate analysis of a food sample determines the total protein, fat, carbohydrate, ash, and moisture reported as the percentage composition of the product.

3.8.1 Proximate Analysis

Materials and Methods

Fresh samples of TME 419 were used all through during the analysis. Efforts were made in making sure that the samples used remained fresh during the analysis, by making sure that fresh samples from the farm were used on harvesting.

The analysis was carried out at the Zonal Laboratory of the National Agency of Food, Drugs, Administration and Control, Agulu, Anambra State. For each experiment, a total of four repeated experiment was carried out and the average used for the final calculations.

3.8.2 Determination Of Moisture Content

Method: Oven Drying at 105^0C.

Principle: This method is based on loss on drying at an oven temperature of 105^0C. Besides water, loss will include other volatile matter at 105^0C.

Procedure: a clean, dry flat dish made of silica was used, the dish which was cool at the onset was weighed and tagged (W_1) . 5g of the sample was introduced into the dish and the weight taken as (W_2). The dish and its content were placed into the air oven operating at 105^0C for 3 hours. A pair of tongs was used to transfer the dish into the desiccator, it was allowed to cool and the final weight of the sample was taken. The dish together with its content were returned to the oven for 30 minutes and subsequently cooled in the desiccator. The same was repeated till a constant weight was attained which was tagged (W_3).

The relation below was used to calculate the percentage moisture content.

$$\% \text{ moisture} = \frac{(W_2 - W_3)}{(W_2 - W_1)} \times \frac{100}{1}. \qquad (3.91)$$

W_1 =Weight of the cooled dish

W_2 = Weight of the dish + Sample before heating

W_3 = Weight of the dish + Sample in the oven after 30 minutes.

3.8.3 Determination of Ash Content

Principle: The organic component of food is burnt off in air. The residue is ash which consists of the inorganic components in the form of oxides.

Apparatus: Silica Dish

Procedure: A clean, silica dish was washed and cleaned, it was subsequently weight and tagged (W_1), 5g of the sample was placed into the dish, the dish with the sample was weighed and tagged (W_2).

The sample with the dish were placed into the muffle furnace, the sample was allowed to burn out at 500^oC, for 8 hours. Subsequently, the burnt sample was removed from the muffle furnace with a tong and place into a dessicator, the sample was moisten

with distilled water, dried on boiling water bath and returned into the furnace. It was later removed, cooled, the ash was washed, and the difference in weight from the initial and the final was taken and recorded. The ash content was deducted as a percentage by using the correlation below:

$$\% \, Ash = \frac{(W_3 - W_1)}{(W_2 - W_1)} \times \frac{100}{1} \qquad (3.92)$$

3.8.4 Determination of Lipid / Fat Content

Method: Rose Gottlieb

Principle: the protein is precipitated by alcohol and dissolved by ammonia. The freed fat is then extracted with either and petroleum ether.

Apparatus: Gottlieb tubes with siphons

Procedure: 5g of the sample (W) was placed into the Gottlieb tubes. The sample was well disperse with 10 ml of water. 2 ml of 0.88 ammonia solution and mixed. 10 ml of alcohol (95%) was added and mixed well, subsequently; 25 ml of diethyl ether was added. The tube was corked and shaken vigorously for 1 minute. After which 25 ml of light petroleum ether was added and shaken for 30 seconds. Around bottom flask was weighed as W_1. The extraction was repeated twice again using 25 ml portion of a mixture (1:1) of diethyl ether and petroleum ether and the ether of fat was collected as fat layer in the same weighed flask. The ether was distilled off, the residue was oven dry at $100^o C$, cooled and then the weight was taken as W_2.

Calculations:

The percentage fat/lipid content was obtained using the correlation below

$$\% \, fat \ or \ lipid = \frac{W_2 - W_1}{W} \times \frac{100}{1} \qquad (3.93)$$

Where

W_1 = Weight of the empty flat bottom flask

W_2 = Weight of the empty flat bottom flask + Sample after heating

W = Weight of the Sample taken

3.8.5 Determination of Nitrogen/Crude Protein Content

Method: the Macro Kjeldahl Method

Fig. 3.6: Kjeldahl apparatus

Principle: this method will not include nitrogen from nitrites and nitrates but will include nitrogen from proteins, alkaloids and nucleic acids. The organic matter is oxidized by concentrated sulphuric acid in the presence of catalyst and the nitrogen converted to ammonium sulphate. This is then made alkaline, and the librated ammonia is distilled and estimated. As a very large part of the nitrogen present in foods is derived from proteins, the crude protein is estimated by multiplying the percentage of nitrogen by an appropriate factor.

Reagents Used:

a. Concentrated sulphuric acid- Nitrogen free
b. 50% solution of NaOH containing 5% Sodium Thiosulphate.
c. 2% Boric acid Solution.
d. 0.1N Sulphuric acid.
e. Screen Methyl red indicator 0.016% methyl red and 0.083% Bromocresol green in alcohol.
f. Kjeldahl catalyst tablets containing:

1. 1 gram of Na_2SO_4 and 0.1 gram of Copper Sulphate or
2. 1 gram of Na_2SO_4 and 0.1 gram Mercury or
3. 1 gram of Na_2SO_4 and 0.5 gram of Selenium.

Apparatus:

Kjeldahl digestion and distillation apparatus

Procedure: a part of the sample was weighed that is equivalent to 0.2 g protein and transferred into the Kjeldahl flask, a filter paper was used to transfer the sample into the apparatus. Using a measuring cylinder, 25 ml concentrated sulphuric acid was added. 2 tablets of mercury catalyst were also added.

The flask was heated gently in a fume cupboard, using a fume mantle. The flask was inclined at a position, the flask was swirled occasionally, after the initial rigorous reaction has dried down, the heat was increased and the digestion continued until the liquid is clear and free from the black or brown colour. The essence of the swirling from time to time to wash down charred particles from the sides of the flask.

The flask with the content was allowed to cool off; it was then diluted with about 200 ml of distilled water. The distillation apparatus consisting of 500 ml flask capacity was connected, the stopper of the apparatus consisting of dropping funnel and splash head adopter, a vertical condenser as shown in fig 3.7, which is attached to a straight delivery tube.

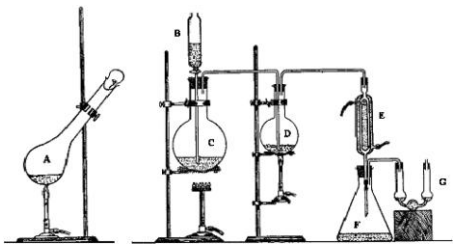

Fig 3.7: Kjeldahl digestion and distillation apparatus

50 ml of boric acid solution was added into the conical flask, a few drops of screened methyl red indicator was also added and placed on the receiver so that the end of the delivery tube dips below the level of the boric acid.

A few pieces of granulated zinc and some anti-bumping granules to the distillation flask. The apparatus was closed, 85 ml of the Sodium hydroxide solution through the dropping funnel to make the liquid in the flask distinctly alkaline. 50 ml water was added through the dropping funnel, the tap was closed with some water remaining in the funnel. The apparatus was shaken gently to ensure that the mixing of the content was thorough. It was boiled vigorously until about 250 ml had distilled over. The receiver was removed with the delivery tube; the dropping funnel was opened to remove the source of the heat.

The delivery tube was washed down with standard solution acid to a dull slate coloured end point.

Calculations:

The percentage Nitrogen was computed for three different samples and the average taken using the correlation below:

$$\% \, Nitrogen = \frac{V \times 0.0014}{W} \times \frac{100}{1} \qquad (3.94)$$

where

W is weight of the sample taken

% protein = *NxF* where F is a factor equal to 5.70 for wheat, 6.38 for milk, 5.55 for gelatine and 6.25 for other foods.

3.8.6 Determination of Carbohydrate Content

The carbohydrate content is the difference between the other analytes out of 100%

Thus, percentage carbohydrate content in TME 419 is

= 100 – (% protein + % fat/lipid+ % ash+ % moisture) (3.95)

3.8.8 Specific Heat Capacity

Specific heat is the quantity of heat that is lost or gained by a unit mass of product to accomplish a unit change in temperature without change in state:

$$C_p = \frac{Q}{m(\Delta T)} \quad (3.96)$$

Where Q is the heat gained or lost (kJ), m is mass (kg), ΔT is temperature change in material (°C).

Specific heat is an essential part of thermal analysis in food processing or of the equipment used in heating or cooling of foods. With food material, this property is a function of various components that constitute food, its moisture content, temperature and pressure. The specific heat of food generally increases as the moisture content increases.

In order to solve the model numerical values of the specific heat of TMe 419 are needed and there are two ways to obtain such values. Published data may be used if available or the use of predictive equations. The predictive equations are empirical expressions, obtained by fitting experimental data to mathematical models. One of the earliest models to calculate specific heat was proposed by Siebel J. E. (1892) as

$$C_p = 0.837 + 3.349X_w \quad (3.97)$$

Where X_w is the water content expressed as fraction. This model does not show the effect of temperature or other components of the food product. The influence of product components was expressed in empirical equation proposed by Charm S. E. (1978) as

$$C_p = 2.093X_f + 1.256X_s + 4.187X_w \quad (3.98)$$

X is the mass fraction; and subscript f is fat, s is non fat solid and w is water. It is worthy of note that the coefficient of each fraction of the components is the specific heat values of the respective components.

The following expression based on the components of food product was proposed by Heldmam D. R. and Singh R. P. (1981)

$$C_p = 1.424X_c + 1.549X_p + 1.675X_f + 0.837X_a + 4.187X_w \qquad (3.99)$$

Where X is the mass fraction; and the subscripts are c, carbohydrate; p, protein; f, fat; a, ash; and w, moisture. Note again that this expression does not include the dependence on temperature.

However for the purposes of this analysis which has considerable temperature change, the predictive model of Choi Y. and Okos M. R. (1986) which presented a comprehensive model based on composition and temperature shall be adopted.

The model is as follows:

$$C_p = \sum_{i=1}^{n} C_{pi} X_i \qquad (3.100)$$

Where X_i is the fraction of the ith component, n is the total number of components in a food and C_{pi} is the specific heat of the ith component. The correlations for the coefficients of the various components are given in the table 3.0:

Table 3.0: Coefficients to Estimate Food Properties

Property	Component	Temperature function
k (W/[m°C])	Protein	$k = 1.7881 \times 10^{-1} + 1.1958 \times 10^{-3}T - 2.7178 \times 10^{-6}T^2$
	Fat	$k = 1.8071 \times 10^{-1} - 2.7604 \times 10^{-3}T - 1.7749 \times 10^{-7}T^2$
	Carbohydrate	$k = 2.0141 \times 10^{-1} + 1.3874 \times 10^{-3}T - 4.3312 \times 10^{-6}T^2$
	Fibre	$k = 1.8331 \times 10^{-1} + 1.2497 \times 10^{-3}T - 3.1683 \times 10^{-6}T^2$
	Ash	$k = 3.2962 \times 10^{-1} + 1.4011 \times 10^{-3}T - 2.9069 \times 10^{-6}T^2$
	Water	$k = 5.7109 \times 10^{-1} + 1.7625 \times 10^{-3}T - 6.7036 \times 10^{-6}T^2$
	Ice	$k = 2.2196 - 6.2489 \times 10^{-3}T + 1.0154 \times 10^{-4}T^2$

α (m^2/s)	Protein	$\alpha = 6.8714 \times 10^{-2} + 4.7578 \times 10^{-4}T - 1.4646 \times 10^{-6}T^2$
	Fat	$\alpha = 9.8777 \times 10^{-2} - 1.2569 \times 10^{-4}T - 3.8286 \times 10^{-8}T^2$
	Carbohydrate	$\alpha = 8.0842 \times 10^{-2} + 5.3052 \times 10^{-4}T - 2.3218 \times 10^{-6}T^2$
	Fibre	$\alpha = 7.3976 \times 10^{-2} + 5.1902 \times 10^{-4}T - 2.2202 \times 10^{-6}T^2$
	Ash	$\alpha = 1.2461 \times 10^{-1} + 3.7321 \times 10^{-4}T - 1.2244 \times 10^{-6}T^2$
	Water	$\alpha = 1.3168 \times 10^{-1} + 6.2477 \times 10^{-4}T - 2.4022 \times 10^{-6}T^2$
	Ice	$\alpha = 1.1756 - 6.0833 \times 10^{-3}T + 9.5037 \times 10^{-5}T^2$
ρ (kg/m^3)	Protein	$\rho = 1.3299 \times 10^{3} - 5.1840 \times 10^{-1}T$
	Fat	$\rho = 9.2559 \times 10^{2} - 4.1757 \times 10^{-1}T$
	Carbohydrate	$\rho = 1.5991 \times 10^{3} - 3.1046 \times 10^{-1}T$
	Fibre	$\rho = 1.3115 \times 10^{3} - 3.6589 \times 10^{-1}T$
	Ash	$\rho = 2.4238 \times 10^{3} - 2.8063 \times 10^{-1}T$
	Water	$\rho = 9.9718 \times 10^{2} - 3.1439 \times 10^{-3}T - 3.7574 \times 10^{-3}T^2$
	Ice	$\rho = 9.1689 \times 10^{2} - 1.3071 \times 10^{-1}T$
C_p (kJ/[Kg °C])	Protein	$C_p = 2.0082 + 1.2089 \times 10^{-3}T - 1.3129 \times 10^{-6}T^2$
	Fat	$C_p = 1.9842 + 1.4733 \times 10^{-3}T - 4.8008 \times 10^{-6}T^2$
	Carbohydrate	$C_p = 1.5488 + 1.9625 \times 10^{-3}T - 5.9399 \times 10^{-6}T^2$
	Fibre	$C_p = 1.8459 + 1.8306 \times 10^{-3}T - 4.6509 \times 10^{-6}T^2$
	Ash	$C_p = 1.0926 + 1.8896 \times 10^{-3}T - 3.6817 \times 10^{-6}T^2$
	Water[a]	$C_p = 4.0817 - 5.3062 \times 10^{-3}T + 9.99516 \times 10^{-4}T^2$
	Water[b]	$C_p = 4.1762 - 9.0864 \times 10^{-5}T - 5.4731 \times 10^{-6}T^2$
	Ice	$C_p = 2.0623 + 6.0769 \times 10^{-3}T$

Source: Choi and Okos (1986)
[a]For the temperature range of -40 to 0°C
[b]For the temperature range of 0 to 150°C

3.8.9 Thermal Conductivity

The thermal conductivity is employed in the model for calculations involving rate of heat transfer. In quantitative terms, it gives the amount of heat that will be conducted per unit time through a unit thickness of the material if a unit temperature gradient exists across the thickness. Thermal conductivity is

$$k = \frac{J}{s\,m\,°\mathrm{C}} = \frac{W}{m\,°\mathrm{C}}$$

Note that W/(m °C) is same as W/(m K).

Empirical predictive equations are however useful in process calculations where temperature changes occur as in this situation. For fruits and vegetables with a water content greater than 60%, the following equation has been proposed (Almendingen et al, 2000)

$$k = 0.148 + 0.493X_w \qquad (3.101)$$

Where k is thermal conductivity, W/(m °C) and X_w is water content expressed as a fraction. For meat and fish at temperature 0 - 60°C, water content 60- 80%, wet basis Siebel J. E. (1892) proposed the following equation

$$k = 0.008 + 0.52X_w \qquad (3.102)$$

Another empirical equation developed by Charm S. E. (1978) in fitting a set of 430 data points for solid and liquid foods as follows:

$$k = 0.25X_c + 0.155X_p + 0.16X_f + 0.135X_a + 0.58X_w \qquad (3.103)$$

Where X is the mass fraction, and subscript c is for carbohydrate, p is protein, f is fat, a is ash and w is water.

While the equations discussed above are simple expressions for calculating thermal conductivity of foods, they do not include the effect of temperature. The following expression that includes the effect of product composition and temperature was given by Choi Y. and Okos M. R. (1986) as

$$k = \sum_{i=1}^{n} k_i Y_i \quad (3.104)$$

Where a food material has n components, k_i is the thermal conductivity of the ith component, Y_i is the volume fraction of the ith component, obtained as follows:

$$Y_i = \frac{X_i/\rho_i}{\sum_{i=1}^{n}(X_i/\rho_i)} \quad (3.105)$$

Where X_i is the weight fraction and ρ_i is the density (kg/m^3) of the ith component

3.8.10 Thermal Diffusivity

Thermal diffusivity is a ratio involving thermal conductivity, density and specific heat and is given as:

$$\alpha = \frac{k}{\rho c_p} \left(\frac{m^2}{s}\right) \quad (3.106)$$

Choi Y. and Okos M. R. (1986) suggested the following predictive equation for determining thermal diffusivity

$$\alpha = \sum_{i=1}^{n} \alpha_i X_i \quad (3.107)$$

Where n is the number of components, α_i is the thermal diffusivity of the ith component, and X_i is the mass fraction of each component.

3.8.12 Heat Transfer Coefficient (Gas Phase-Pipe Inner Wall)

Determination of the rate of heat transfer due to convection is complicated because of the presence of fluid motion. However there is a useful procedure called the empirical approach which shall be adopted in this work in the determination of the rate of convective heat transfer. The only drawback of this approach is that it requires large experimental data input. However that could be avoided by the use of appropriate dimensionless numbers as suggested by Singh and Heldman (2001) and adopted in

this work. The relevant dimensionless numbers are Reynold Number, Nusselt Number and Prantl number.

The Reynolds number provides an indication of the inertial and viscous forces present in a fluid. Reynolds Number is calculated as follows:

$$N_{Re} = \frac{\rho \bar{u} D}{\mu} = \frac{4\dot{m}}{\mu \pi D} \tag{3.108}$$

where ρ = fluid density; $\bar{u}$ = fluid velocity; D = pipe diameter; μ =fluid viscosity and $\dot{m}$ = fluid mass flowrate.

The second required dimensionless number is the Nusselt number which is the dimensionless form of convective heat transfer coefficient, h. Nusselt number may be considered as the enhancement in the rate of heat transfer caused by convection over the conduction mode. The Nusselt number is calculated as follows:

$$N_{Nu} \equiv \frac{h d_c}{k} \tag{3.109}$$

where h = convective heat transfer coefficient, d_c= inside diameter of the pipe and k = thermal conductivity

The third required dimensionless number for this analysis is the Prantl number which describes the thickness of the hydrodynamic boundary layer compared with the thermal boundary layer. It is essentially the ratio between molecular diffusivity of momentum to the molecular diffusivity of heat. Prantl number is calculated with the following expression:

$$N_{Pr} = \frac{\mu C_p}{k} \tag{3.110}$$

The basis of this analysis using the dimensionless numbers is the relationship established between the dimensionless numbers and given as:

$$N_{Nu} = CN_{Re}^{m} N_{Pr}^{n} \tag{3.111}$$

where C, m and n are constants.

By substituting experimentally obtained constants into the equation above, we obtain empirical correlation specific to a given condition. Previous works have determined the experimental correlations for a variety of operating conditions such as flow in a pipe, flow over a pipe or over a sphere. Different relations are obtained depending on whether the flow is laminar or turbulent.

In all, this work will adopt the steps outlined in Singh and Heldman (2001) in the determination of convective heat transfer coefficient using empirical correlations as follows;

- Identify flow geometry
- Identify fluid and determine its properties
- Calculate Reynolds number
- Select an appropriate empirical correlation
- Calculate Nusselt number
- Calculate convective heat transfer coefficient

Step 1: Identify flow geometry

The flow situation for this work is that heated air is pumped through a pipe and particles are introduced into the air stream. The point of focus is the heat transfer between the particles introduced into the air stream and the body of fluid flowing through the pipe. Essentially we have flow over a spherical body (the particles of TMe 419)

Step 2: Identify fluid and determine its properties

Air is a mixture of several constituent gases. The composition of air varies slightly depending on the geographical location and altitude. For scientific purposes, the commonly acceptable composition is referred to as standard air. The composition of standard air as used in this work and as suggested in http://www.grc.nasa.gov/WWW/K-12/airplane/airprop.html is given in table 3.1.

Table 3.1: Composition of Standard Air

Constituents	Percentage by Volume
Nitrogen	78.084000
Oxygen	20.947600
Argon	0.934000
Carbon dioxide	0.031400
Neon	0.001818
Helium	0.000524
Other gases	0.000658
	100.000000

In addition to the physical composition of air, the thermodynamic properties have to be determined for drying air fed into the flash tube. It has also been emphasised that the properties of air varies over time and so some form of average has to be used for the purposes of this analysis. The air properties are taken as suggested by http://www.jazminesmeralda.ifunnyblog.com/averageweatherfornigeria for the yearly average conditions for Nigeria:

Dry bulb temperature	= 25.8°C = 298.95K
Wet bulb temperature	= 24.351°C = 297.501K
Dew point:	= 23.854°C = 297.004K
Humidity	= 50%
Air moisture concentration (c0_air)	= 0.0135*rho_air (appendix 4-3)
Specific moisture capacity (C_m_air)	=

The air is driven through the heat exchanger where it is heated up. Heating or cooling of air is accomplished without addition or removal of moisture (Singh and Heldman,

2001). Thus the humidity ratio remains constant. Consequently the air properties as it exits the heat exchanger and enters the flash tube will be as follows:

Dry bulb temperature	= 160°C = 433.15K
Wet bulb temperature	= 134.041 °C = 407.191K (appendix 4-4)
Dew point:	= 133.433°C = 406.583K
Humidity:	= 50%
Air moisture concentration	= 0.0135*rho_air (appendix 4-3)

The phenomenon of adiabatic saturation of air is applicable to convective drying of food materials. The adiabatic saturation process can be visualised by considering a well-insulated chamber with an inlet and an outlet. The chamber prevents the gain or loss of heat to the surrounding (adiabatic conditions). Air enters the chamber and blows over water inside the chamber and exits through the outlet. In the process, part of the sensible heat of the entering air is transformed into latent heat.

For the condition described above, the process of evaporating water into the air results in saturation by converting part of the sensible heat of the air into latent heat in the process referred to as adiabatic saturation.

When heated air is forced through a bed of moist granular food, the drying process can be described on the psychrometric chart as an adiabatic saturation process. The heat of evaporation required to dry the product is supplied only by the drying air; no transfer of heat occurs due to conduction or radiation from the surroundings. As air passes through the granular mass, a major part of the sensible heat is converted to latent heat, as water is held in the air as vapour.

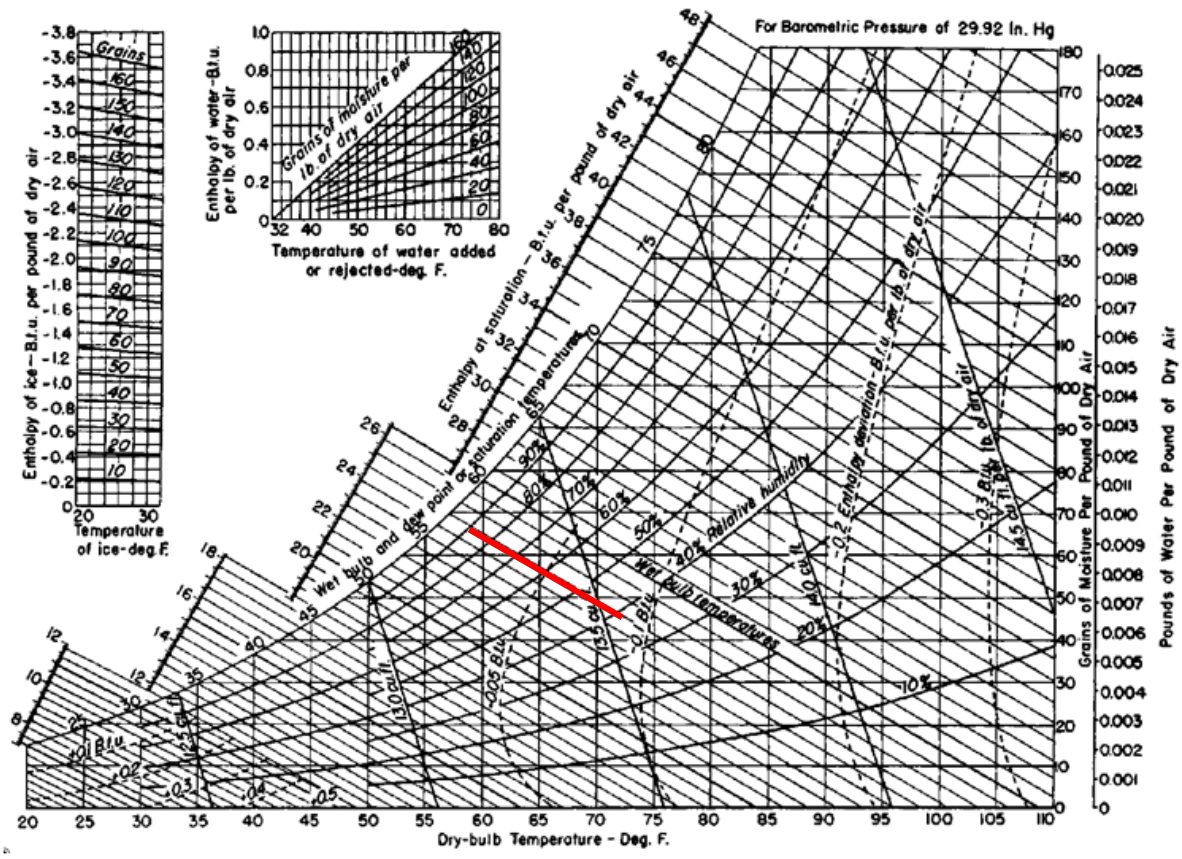

(Source: http://www.f150forum.com/f70/ecoboost-condensate-drain-hole-post-your-results-here-223824/index26/)

Fig. 3.8: Psychrometric Chart

The drying process happens at constant enthalpy and the two points on the red line shows the state of the drying air at the beginning and at the end of the convective drying. The use of psychrometric chart though simple shall not be adopted for this work, but the relevant correlations shall be used to suit the modelling process.

Step 3: Calculate Reynolds number

In pneumatic conveying drying, the air is driven by a blower through a heat exchanger, so that it is heated up and has improved capacity to retain moisture, before it is then introduced into the flash tube. To understand the nature and properties of the

air that is entering the flash tube through the heat exchanger the air data have to be provided.

It should be noted that air inlet velocity shall be varied to determine its effect on the drying rate of cassava mash but the inlet velocity must be such that it is above the minimum carrying velocity determined experimentally. It is also important to note that nature of the flow, laminar or turbulent, for our situation is for a material that is being conveyed as it is dried. At entry the velocity of the solid particle is zero and the nature of the flow is determined based on the velocity of the gas phase only. But an instant later the flowing stream imparts momentum on the particle to cause it to move by transferring momentum to it; at that point the nature of the flow is determined by the difference in the velocity between the gas phase and the solid dispersed phase. The program shall be designed to monitor the nature of flow and apply the appropriate correlations for determining the variable.

$$Re = \frac{VD_H}{\nu} = \frac{\rho_a V d_p}{\mu_a} = Rep \quad = \quad \rho_g d_p \left| u_g - u_s \right| / \mu_g \qquad (3.112)$$

The drag coefficient is calculated by the relation suggested by Han T. et al (2000)

$$C_D = \frac{24}{Re_p} \qquad \mathrm{Re_p} \leq 1 \qquad (3.113)$$

$$C_D = \frac{24}{Re_p^{0.646}} \qquad 1 < \mathrm{Rep} \leq 400 \qquad (3.114)$$

$$C_D = 0.5 \qquad 400 < \mathrm{Re_p} < 3 \times 10^5 \qquad (3.115)$$

$$C_D = 0.5 \qquad (3.116)$$

Diffusivity of water vapour in air, $D_{wv,a} = 0.26 \times 10^{-4}$

Step 4: Select the appropriate correlation

$$Sc = \frac{\nu}{D_{wv,a}} \qquad (3.117)$$

` For $Re < 5 \times 10^5$- (laminar flow)

Step5: Calculate Nusselt Number:

For flow past a single sphere, when th single sphere may be heated or cooled, the Nusselt number is evaluated as follows:

$$N_{Nu} = 2 + 0.60Re^{0.5}Pr^{1/3}$$

For 1<Re<70000 ; 0.6<Pr<400

$$Sh = \frac{h_m L}{D_{wv,a}} = L = d_p \quad (3.118)$$

$$h_m = \frac{0.664 Re^{1/2} Sc^{1/3} D_{wv,a}}{L} \quad (3.119)$$

$$\chi = \text{sphericity} = \frac{A_{so}\rho_{sa} d_p}{6} \quad (3.120)$$

During constant-rate drying period, the product surface temperature remains at the wet bulb temperature of the heated air. The magnitude of water vapour transfer $\dot{m}$, during constant-rate drying is described by the following mass transfer expression (Singh and Heldman, 2001):

$$\dot{m} = \frac{h_m \chi \pi d_p^2 M_w P}{0.622 R T_g}\left(W_s - W_g\right) \quad (3.121)$$

R_g = gas constant = 8.314 m^3 KPa/(kg mol)

M_w = molecular weight of water vapour =18 kg/kg mol

P = atmospheric pressure (kPa) = 101.325

W_1= humidity ratio at product surface (kg water/kg dry air)

= humidity ratio for saturated air at T_s.

The maximum amount of water vapour in the air is achieved when $p_w = p_{ws}$ the saturation pressure of water vapour. At the actual temperature the following expression can be used:

$$W_1 = 0.62198 p_{ws}/(p_a - p_{ws}) \quad (3.122)$$

where

W_1 = specific humidity at saturation (kg_{water}/kg_{air})

p_{ws} = saturation pressure of water vapour

p_a= atmospheric pressure of moist air

W_2 = humidity ratio for air (kg water/kg dry air) = humidity ratio at T_g and at air relative humidity
Alternatively, $\dot{m}$ can be determined by the method of partial pressures

e = Euler number = 2.718281828459

p_{vo} = saturated H_2O vapour pressure at $T_s(K)$ = e $^{(77.3450+0.0057T-7235/T)}$/T$^{8.2}$ = 3.13030 kPa

$$p_w = p_{wb} - \frac{(p_B - p_{wb})(T_{db} - T_{wb})}{1555.56 - 0.722T_s} \quad (3.123)$$

p_{wb} = p_{vo} water vapour saturation pressure at T_s (kPa)
p_B = barometric pressure (kPa) =
T_{db} = dry bulb temperature (°C)
T_{wb} = wet bulb temperature (°C)
M_w = molecular weight of water vapour =18 kg/kg mol
$\Re$ = universal gas constant = 8.314 m^3 kPa/(kg mol K)
$p_{vg} = p_w$ = partial pressure of water at T_{db} (kPa)
$\dot{m}_s = h_m \chi \pi d_p^2 \left(\frac{M_w p_{vo}}{\Re T_s} - \frac{M_w p_{vg}}{\Re T_g} \right)$ (kg/s)

3.8.13 Drying Curve

The removal of moisture from a food product will follow a series of drying curves. Usually the initial removal of moisture occurs as the product and the water inside experience a slight temperature increase. Subsequently the product experiences a period of constant moisture removal termed Constant-Rate Drying Period. At this stage the product is at the wet bulb temperature of air. The constant rate drying period continues until the moisture content is reduced to the critical moisture content. This is the beginning of the falling-rate drying period. At this point forward, the rate of moisture removal decreases over time.

It is obvious that the formulation and analysis method for drying within the constant-rate period varies widely with that may be employed for the falling-rate period of drying. However, it is important to see the behaviour of TMe 419 during drying through the drying curve and also to determine the appropriate form of analysis required to model the drying process.

Sample Collection and Preparation.

The selected cultivar, TMe 419 was peeled, washed, and tagged for drying.

Method

The experimental drying kinetics of TMe 419 were investigated, and the experiments were carried out under isothermal conditions, using Heraeus thermicon P, heated batch drier at 40, 45, 50, 55 and 60 ºC. The moisture ratio data obtained from change of moisture content with the drying time of 240 minutes, at an interval of 30 minutes, the sample was weighed and the difference recorded to get the moisture ratio at each temperature.

3.9 Modelling Approach

This work models the convection drying of a representative sample of cassava cultivar TMe 419 in a vertically upward pneumatic conveying dryer. There are several reasons for studying pneumatic conveying drying through a combination of mathematical modelling and experiments. First, the energy efficiency of already designed equipment desperately needs improvement. The throughput and product quality from existing equipment are inadequate and there is little understanding of the

interplay of several parameters that are manifested during pneumatic conveying drying that it seems that designers are working in the dark. This is primarily as a result of lack of information on the subject matter and more so the particular case of cassava pneumatic conveying drying. It is common to hear people say that the design of pneumatic conveying dryer is an 'art' or a 'soft science'. This underlines the import of this effort.

This work builds a time-dependent model of the convection drying of TMe 419 and it shows the temperature rise over time in the feedstock. This simulation also models the moisture concentration in the feedstock, which is defined as the mass of water per volume of feedstock. From the viewpoint of product quality, it is of interest to reduce the moisture content of the feedstock to a maximum of 10%. In this regard, moisture concentration is a quantity that measures how much moisture, in percent, remains in the cassava particle after the drying process. Furthermore, the moisture concentration also influences the temperature field by heat loss due to vapourization and also by changing the feed stock's thermal conductivity.

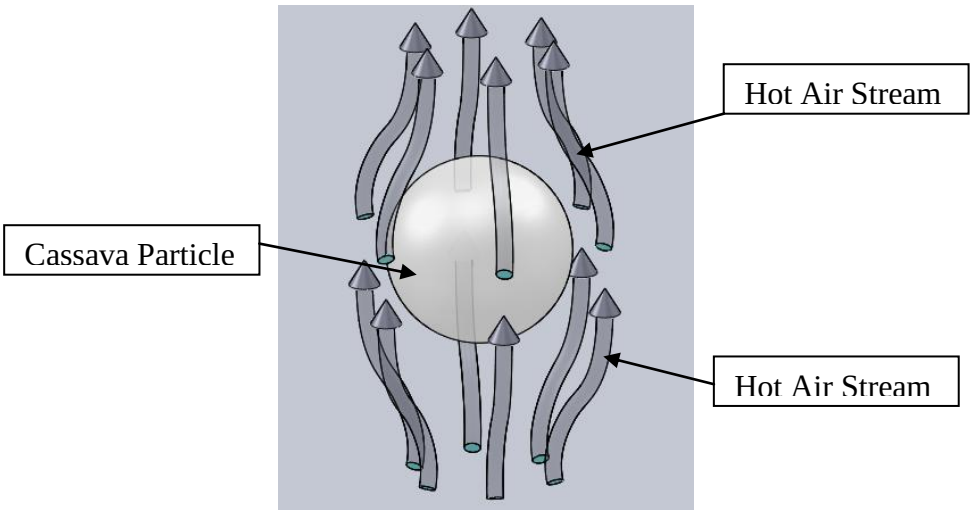

Fig 3.9: Convective Drying of TMe 419

This work couples two time-dependent application modes coded in comsol script and implemented in Comsol Multiphysics platform, describing the temperature and the moisture concentration, respectively. In order to reduce the complexity of the coding, the finite element analysis simulation set up in this work does not model the convective velocity field outside the cassava particle. However, the values for the coefficients for convective heat and moisture transfer to the surrounding air have been derived by the application of time-stepping algorithm on the continuous phase and the result obtained shall be applied here directly.

The system of model equations (3.9, 3.42, 3.65, 3.84 and 3.86) derived earlier together with the help of supplementary equations was solved numerically using one-step method (conservative variable formulation) for the gas p hase while fourth order Runge Kutta method is used for the solid phase. The one-step method is a cell by cell iterative approach where the gas phase variables are specified upstream and the downstream variables are sought. The average values of the gas phase variables are used to calculate the solid phase velocity and temperature. The source terms for mass, momentum and energy are re-evaluated based on the downstream variables of the initial cell and based on them the variables of the continuous phase for the next cell is calculated. This means that once the solution is obtained for one cell, the exit conditions are taken as the starting conditions for the adjacent cell and the procedure is repeated. The procedure is continued until the solid phase moisture content becomes less than 10%.

3.10 One Step Method with Comsol Script

Once the model is developed, it is them coded into a computer program for implementation. Although the form of the model will depend to some extent on the

feature of the simulation language, the basic design of the model should be produced before commencement of programming.

It is important to prepare a good flowchart or a suitable algorithm for the model as most of the problems of logic is solved before coding. The model is coded using a programming language and the choice must be made between a general-purpose language and a specialized simulation language.

One argument sometimes made against simulation languages, especially by experienced programmers, is that they lack flexibility. Clearly the high-level language with very powerful commands allows the user to modify the model extensively with few instructions. But if one needs a language with the ability to make highly selective and detailed modification to the model, a high-level language may not be sufficiently flexible. However since this work is an academic exercise and the ramifications of the model proposed has not been handled in any known process simulation software, the program will be developed on Comsol Script and run on Comsol Multiphysics together with some established Comsol Multiphysics algorithms for efficiency.

Input parameters: It is known that simulation requires a large body of data and following are the input variables for the determination of output variables:

Particle density, particle diameter, modification factor for particle irregular surface area, initial particle velocity, initial particle temperature, particle specific heat capacity, dispersion, pipe diameter, initial air velocity, initial air temperature, relative humidity, wet bulb temperature, air density, air specific heat capacity, air thermal conductivity, air kinematic viscosity, air dynamic viscosity

Derived variables: The input variables are required to calculate other derived variables and subsequently the variables that indicate the downstream state of the cell.

The conservative equations for both the continuous phase and the dispersed phase has been formulated and solved. The solutions summarised above will then be employed to determine the state of the variables along the pipe length. The equations above lend themselves to spatial discretisation based on an appropriate step size. Because the variables to be handled are many and the step must be small to improve accuracy, the data generation shall be handled by a computer program. The program is written using Comsol script to generate the variables along the flash tube. The Program shall for each spatial step determine the continuous phase variables which will in turn be used to determine the dispersed phase variables and all the variables determined shall be used as initial values for evaluating the variables at the next spatial point.

Fig. 3.10: Comsolscript Program Flowchart

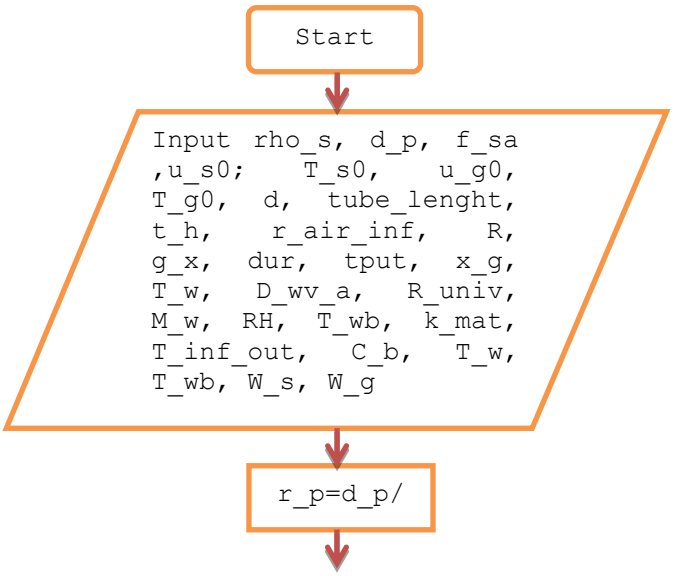

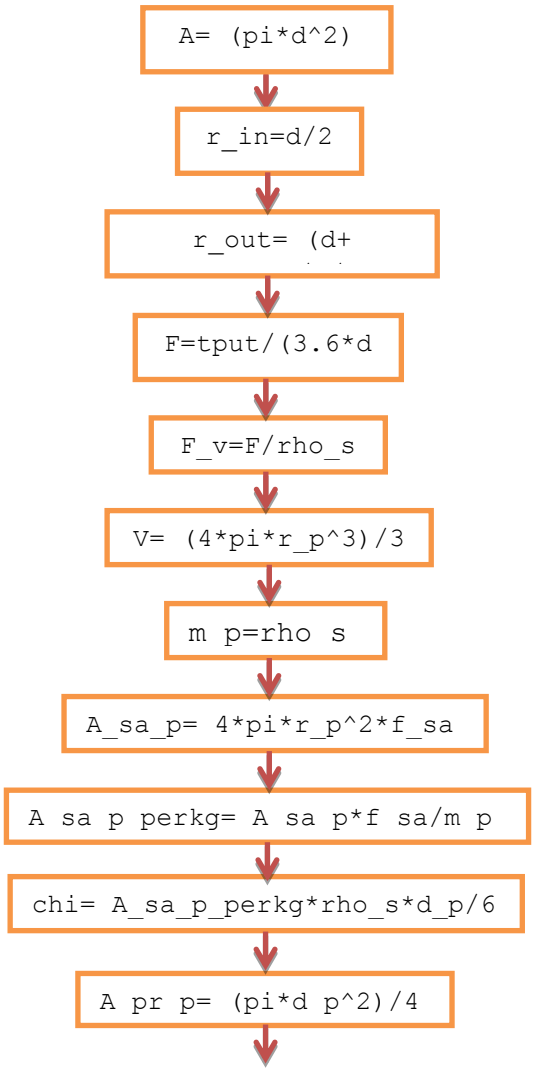

Fig. 3.10: Comsolscript Program Flowchart

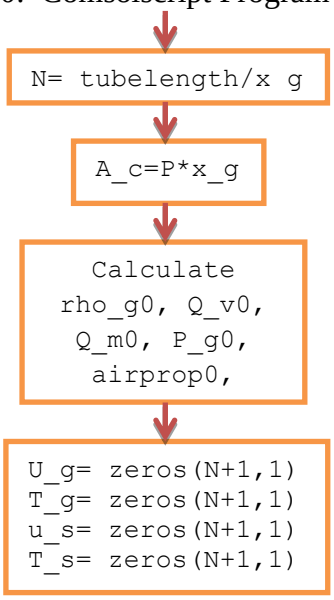

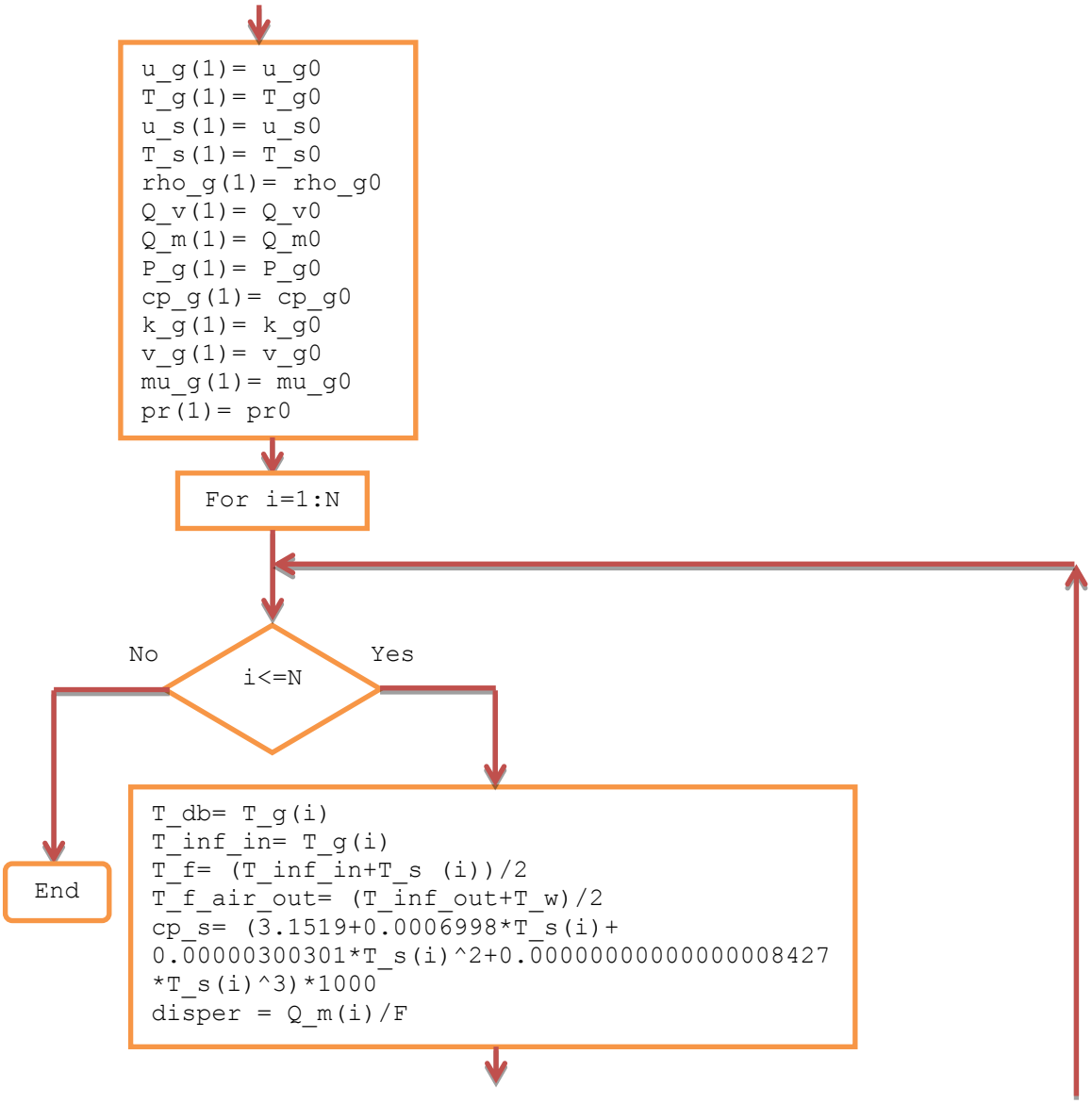

Fig. 3.10: Comsolscript Program Flowchart

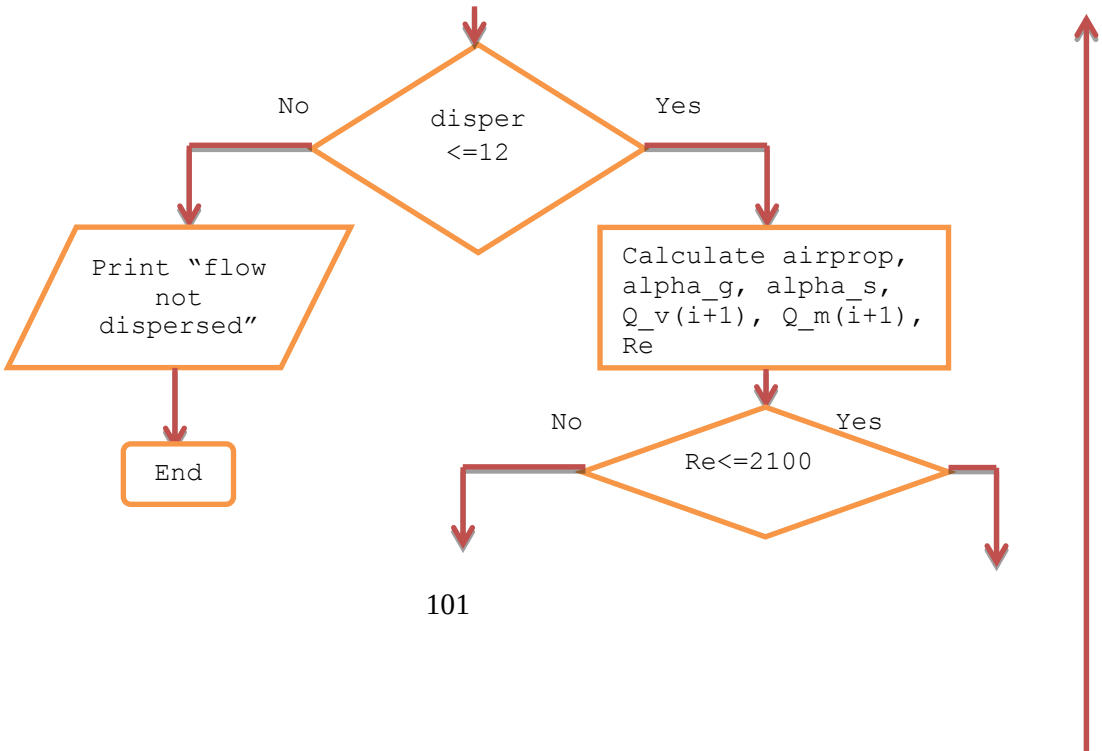

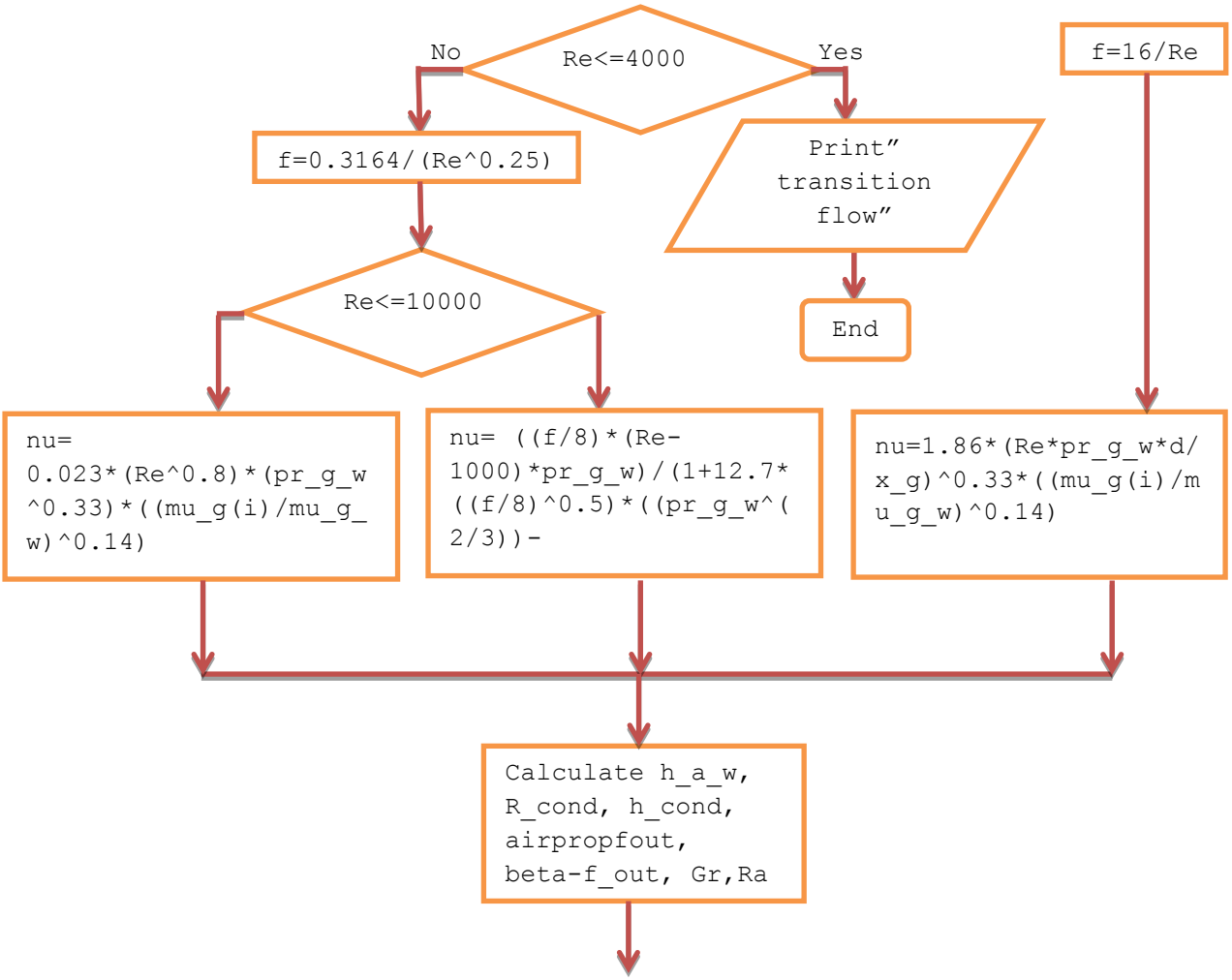

Fig. 3.10: Comsolscript Program Flowchart

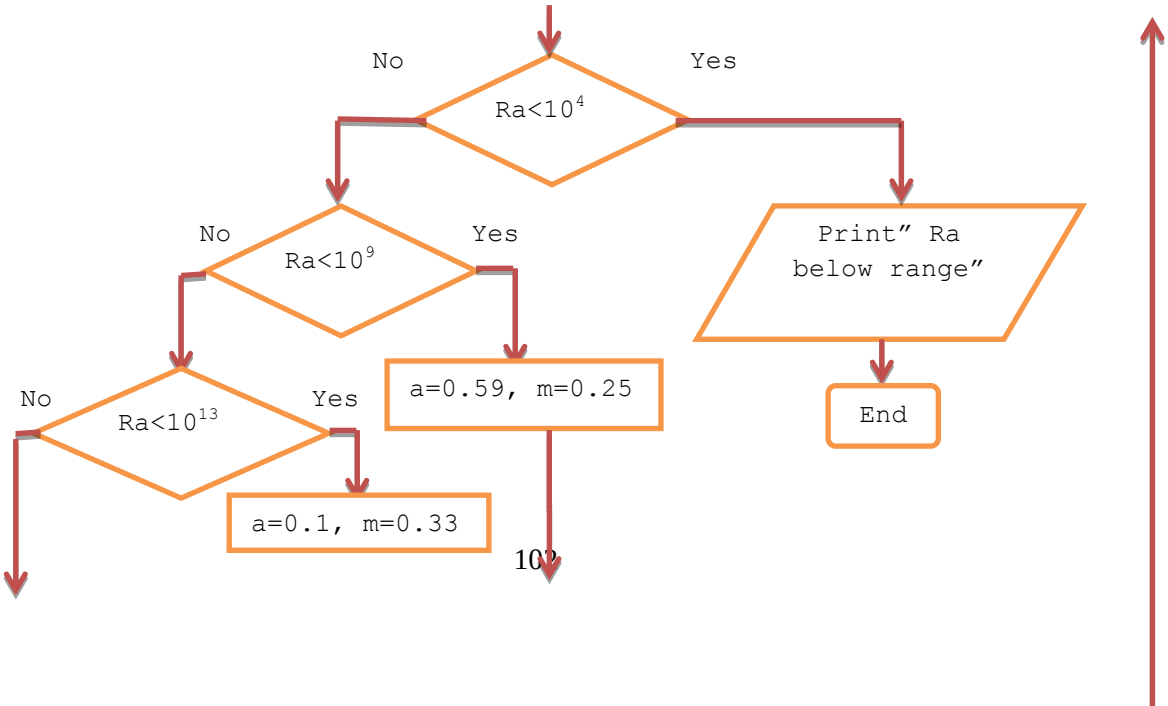

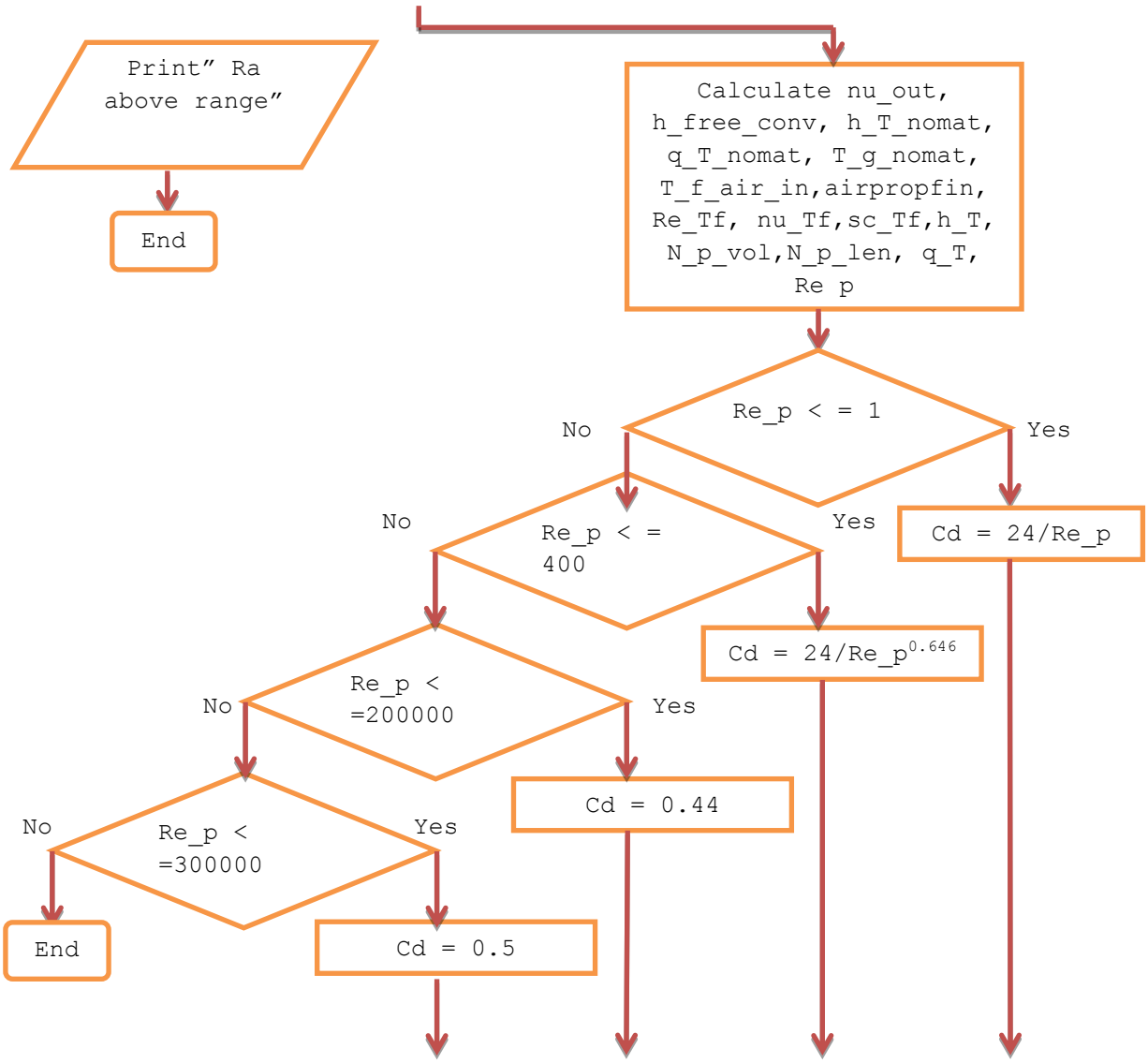

Fig. 3.10: Comsolscript Program Flowchart

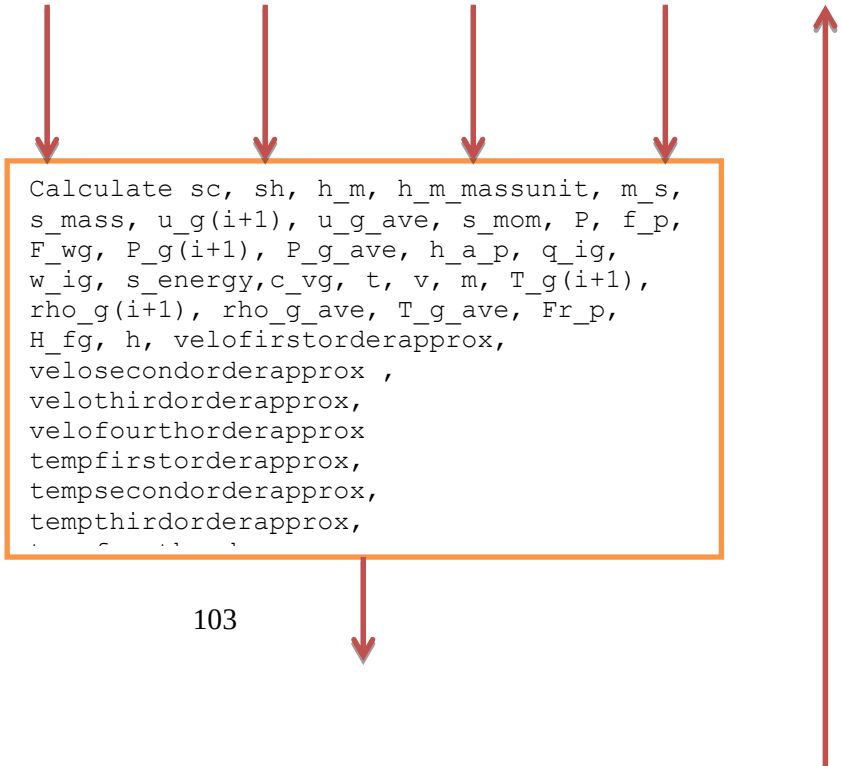

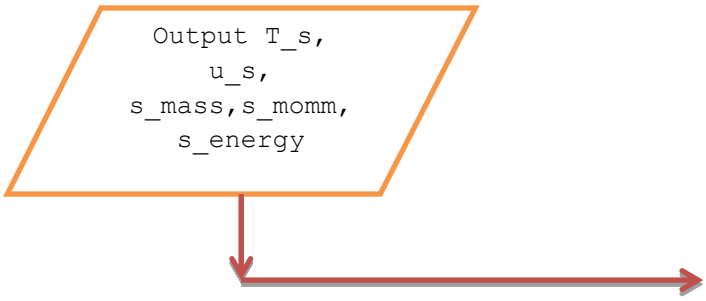

3.11 FEA Modelling

Haven determined through the Comsol Script program the condition of the air stream as it interacts with the particle along the tube length. It is necessary to determine, by the use of Finite Element Analysis method, what happens within the cassava particle under these external conditions especially to its moisture content.

3.11.1 FEA Modelling Equations

The fundamental law governing all heat transfer is the first law of thermodynamics, commonly referred to as the principle of conservation of energy. However, internal energy, *U*, is a rather inconvenient quantity to measure and use in simulations. Therefore, the basic law is usually rewritten in terms of temperature, *T*. For a fluid, the resulting *heat equation* is:

$$\rho C_p \left(\frac{\partial T}{\partial t} + (u \cdot \nabla)T\right) = -(\nabla \cdot q) + \tau : S - \frac{T}{\rho}\frac{\partial p}{\partial T}\bigg|_p \left(\frac{\partial p}{\partial t} + (u \cdot \nabla)p\right) + Q \qquad (3.124)$$

where

- •ρ is the density (kg/m^3)
- •C_p is the specific heat capacity at constant pressure (J/(kg·K))
- •*T* is absolute temperature (K)
- •**u** is the velocity vector (m/s)
- •**q** is the heat flux by conduction (W/m^2)
- •*p* is pressure (Pa)
- •τ is the viscous stress tensor (Pa)
- •**S** is the strain rate tensor (1/s): $S = \frac{1}{2}(\nabla u + (\nabla u)^T)$
- •*Q* contains heat sources other than viscous heating (W/m^3)

In deriving equation (3.124), a number of thermodynamic relations have been used. The equation also assumes that mass is always conserved, which means that density and velocity must be related through:

$$\frac{\partial \rho}{\partial t} + \nabla \cdot (\rho v) = 0$$

The Fourier's law of conduction which states that the conductive heat flux, **q**, is proportional to the temperature gradient:

$$q_i = -k\frac{\partial T}{\partial x_i} \qquad (3.125)$$

where k is the thermal conductivity (W/(m·K)). In a solid, the thermal conductivity can be different in different directions. Then k becomes a tensor

$$k = \begin{bmatrix} k_{xx} & k_{xy} & k_{xz} \\ k_{yx} & k_{yy} & k_{yz} \\ k_{zx} & k_{zy} & k_{zz} \end{bmatrix}$$

and the conductive heat flux is given by

$$q_i = -\sum_j k_{ij} \frac{\partial T}{\partial x_j}$$

The second term on the right of equation (3.124) represents viscous heating of a fluid. An analogous term arises from the internal viscous damping of a solid. The operation ":" is a contraction and can in this case be written on the following form:

$$a : b = \sum_n \sum_m a_{nm} b_{nm} \tag{3.126}$$

The third term represents pressure work and is responsible for the heating of a fluid under adiabatic compression and for some thermo-acoustic effects. It is generally small for low Mach number flows. A similar term can be included to account for thermo-elastic effects in solids.

Inserting equation (3.125) into equation (3.124), reordering the terms and ignoring viscous heating and pressure work puts the heat equation on a perhaps more familiar form:

$$\rho C_p \frac{\partial T}{\partial t} + \nabla \cdot (-k \nabla T) = Q - \rho C_p u \cdot \nabla T \tag{3.127}$$

The General Heat Transfer application mode solves this equation for the temperature, T. When convective heat transfer is active, you can provide the velocity **u** as a mathematical expression of the independent variables or calculate it within COMSOL Multiphysics by a coupling to a momentum-transfer application mode such as

Incompressible Navier-Stokes or Weakly Compressible Flow application mode. If the velocity is set to zero, you finally get the equation governing pure conductive heat transfer in a solid:

$$\rho C_p \frac{\partial T}{\partial t} + \nabla.(-k\nabla T) = 0 \tag{3.128}$$

This work determined that the specific heat capacity varies with temperature according to the expression:

$$C_p = 3151.9 + 0.6998\Delta T + 0.00300301\Delta T^2 \tag{3.129}$$

C_p : unit in (J/kg.K)

where $\Delta T = (T - 0\ °C)$ and the dimensions of the numerical coefficients are such that the dimension of C_p is as stated.

For the moisture concentration, apply the diffusion equation

$$\frac{\partial c}{\partial t} + \nabla.(-D\nabla c) = 0$$

where c is the moisture concentration (kg/m^3), and D is the diffusion coefficient (m^2/s).

3.11.2 Model Geometry / Solution Domain

The figure 3.11 depicts a particle of TMe 419 undergoing pneumatic conveying drying. The particle geometry is represented by an equivalent sphere as determined earlier. In applying symmetry as a modelling technique, it is easy to see that the 3 dimensional model could indeed be modelled as a 2 dimensional axisymmetric model (2d quadrant) while capturing all the details of the sphere thus simplifying the modelling effort and reducing simulation time considerably. Consequently this particle shall be modelled as a two dimensional quadrant as shown in fig 3.11.

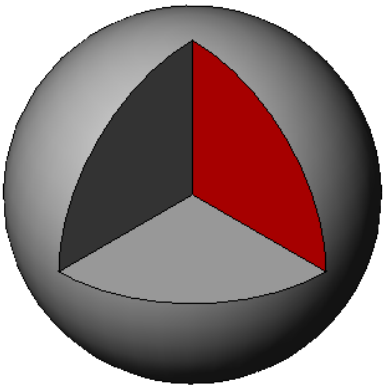

Fig. 3.11: Model geometry of TMe 419 particle

The model geometry is replicated in comsol multiphysics platform and is as shown in figure 3.12:

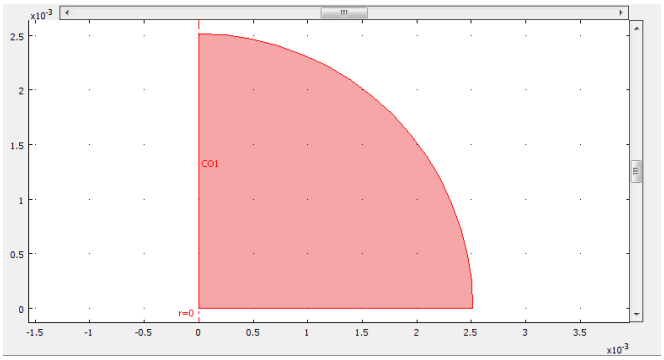

Fig 3.12: TMe 419 model geometry

3.11.3 Boundary Numbering / Boundary Condition

These simplifications result in a simple domain with diameter of 5.027 mm and a radius of 2.5135 mm (or radius of equivalent sphere). The figure 3.13 describes the boundary numbering used when specifying the boundary conditions.

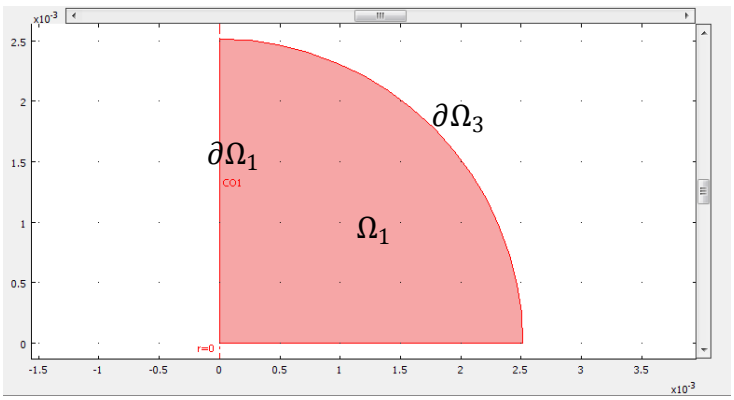

$\partial\Omega_2$

Fig 3.13: TMe 419 model boundary conditions

The heat equation accepts two basic types of boundary conditions: specified temperature and specified heat flux. The former is of Dirichlet type and prescribes the temperature at a boundary:

$$T = T_0 \text{ on } \partial\Omega$$

while the latter specifies the inward heat flux

$$-n \cdot \boldsymbol{q} = q_0 \text{ on } \partial\Omega$$

where:

· $\boldsymbol{q}$ is the total heat flux vector (W/m^2)

$$\boldsymbol{q} = -k\nabla T + \rho C_p \boldsymbol{u} T$$

· n is the normal vector of the boundary

· q_0 is the inward heat flux (W/m^2)

However, when convective heat transfer is active, heat flux boundary condition is a mixed, or Robin type boundary condition rather than a pure Neumann boundary condition

The special case $q_0 = 0$ is called *thermal insulation.* Another special case is $q_0 = \rho C_p \boldsymbol{u} T$, or equivalently$-n \cdot (-k\nabla T)$, which is known as convective flux. This is usually the appropriate condition on an outflow boundary in a model with convection. If the velocities are zero, thermal insulation and convective flux are equivalent conditions.

The inward heat flux q_0 is normally a sum of contributions from different heat transfer processes. It is often convenient to split the heat flux boundary condition as

$$-\boldsymbol{n} \cdot \boldsymbol{q} = q_0 + q_r + q_s + h(T_{inf} - T) \text{ on } \partial\Omega$$

where q_r represents incoming radiation and q_s is a contribution from a thin but highly conducting shell in contact with the boundary. The last term is a product of a heat

transfer coefficient, h, and the difference between the surface temperature T and a reference temperature T_{inf}. It can be used to model a thin shell with low thermal conductivity or, more commonly, the convective cooling of a surface exposed to a flowing fluid with bulk temperature T_{inf}.

The equations describing moisture diffusion are coupled to the heat equation in the following two ways:

The thermal conductivity, k, increases with moisture concentration according to $k = 0.2559 + 0.009757(c/\rho) + 0.0001497(c/\rho)^2 + 0.0000009110(c/\rho)^3$

Where concentration, c, and the density, ρ, must be expressed in the previously stated units.

The vapourization of water at the cassava particle outer boundaries generates a heat flux out of the particle. This heat flux is represented with the term $D_m \lambda \nabla c$ in the boundary condition for boundary 3.

Where D_m is the moisture diffusion coefficient (m^2/s) from the particle to the surrounding air and λ is the latent heat of vapourisation (J/kg)

Assume symmetry for the temperature field on Boundaries 1 and 2. Air convection adds heat on Boundaries 3 and 4. According to the assumptions made earlier, add a term for the heat flux out of the cassava particle due to moisture vapourization on Boundaries 3 and 4.

Summarizing, the boundary conditions for the general heat transfer application mode are:

$\boldsymbol{n} \cdot (-k\nabla T) = 0$ at $\partial\Omega_1$ and $\partial\Omega_2$

$\boldsymbol{n} \cdot (k\nabla T) = h_T\left(T_{inf} - T\right) + \boldsymbol{n} \cdot (D_m \lambda \nabla c)$ at $\partial\Omega_3$

Where h_T is the heat transfer coefficient (W/(m^2.K)), and T_{inf} is the conveying air temperature.

The boundary conditions for the diffusion application mode are

$\boldsymbol{n} \cdot (-D\nabla \mathrm{c}) = 0$ at $\partial\Omega_1$ and $\partial\Omega_2$

$\boldsymbol{n} \cdot (D\nabla \mathrm{c}) = k_c(c_b - c)$ at $\partial\Omega_3$

where D is the moisture diffusion coefficient in the cassava particle (m^2/s), k_c refers to the mass transfer coefficient (m/s), and c_b denotes the outside air (bulk) moisture concentration (kg/m^3). The diffusion coefficient and the mass transfer coefficient are given, respectively, by

$$D = \frac{k_m}{\rho C_m}, \quad k_c = \frac{h_m}{\rho C_m}$$

where C_m equals the specific moisture capacity (kg moisture/kg dry air), k_m refers to the moisture conductivity (kg/(m·s)), and h_m denotes the mass transfer coefficient in mass units (kg/(m^2·s)).

3.11.4 Summary of Data for FEA

It is a known fact that the Finite Element Method requires a lot of data for the solution to be implemented and so an attempt was made to collect the data from various sources that are required for the implementation of the Finite Element Analysis.

Air Properties
T_g = air temperature [°C] = 160°C – selected based on heat exchanger output
rho_g = air density [kg/m^3] = 0.815kg/m^3 – Table 4.24
c_b = air moisture concentration = 0.015x *rho_g*
C_m = air specific moisture capacity = 0.003767
(http://www.engineeringtoolbox.com/humidity-ratio-air-d_686.html)

Cassava Properties: heat diffusion
T = Cassava initial temperature [K] = 22° C = measurement of mash temperature
ΔT = (T - 0° C)
ρ = Cassava particle density [kg/m^3] = 1083.53 kg/m^3 (chap.4, pp 78)
c_p = Specific heat capacity [J/(kg.k)] 3.1712 $kJ/(kg°C)$ (chap.4, pp115)
c_p = 3151.9 + 0.6998 ΔT + 0.00300301(ΔT)^2 + 0.00000000000008427(ΔT)^3 [J/(kg.k)]
(equ.4.22, pp117)
h_T= heat transfer coefficient = 70.5 [W/m^2*K]
k = thermal conductivity [W/ (m*K)] = 0.500298347 W/ (m*K) (chap.4, pp.120)
k_m = moisture conductivity [kg/(m*s)] = s_mass = (comsol script)
h_m = mass transfer coefficient (in mass units)= 3.75 x 10^{-4} - comsolscript
h_T = heat transfer coefficient [W/ (m^2*K)] = 257.9075 W/ (m^2*K) - Comsolscript
Cassava Properties: moisture diffusion
$c0$ = initial moisture concentration [kg/m^3] = 0.40*rho_s [kg/m^3]
D = diffusion coefficient [m^2/s] =2.39 x 10^{-9}(cassava to surrounding)
(Ranges from 1.12x10^{-9} -3.64x10^{-9} m^{2}s^{-1})
[W.J.N. Fernando, HuaChin Low, and A. L. Ahmad, 'The Effect of Infrared o Diffusion Coefficient and activation energies in Convectional Drying: Astudy on Banana, Cassava and Pumpkin', 2001, Journal of Applied Sciences 11(21): 3635-3639]

D_m= surface moisture diffusivity = 2.14 x 10^{-7}
(www.kytl.com/upload/tech/20067201347244420.pdf)

Relationship between thermal conductivity and moisture concentration:

$$k_T = 0.2559 + 0.0009c0 - 0.000001c0^2 + 0.0000000007c0^3$$

Volume integral of a sphere = $\frac{4\pi R^3}{3}$ = 6.652 x 10^{-8}

CHAPTER 4

RESULTS AND DISCUSSIONS

4.1 Particle Shape

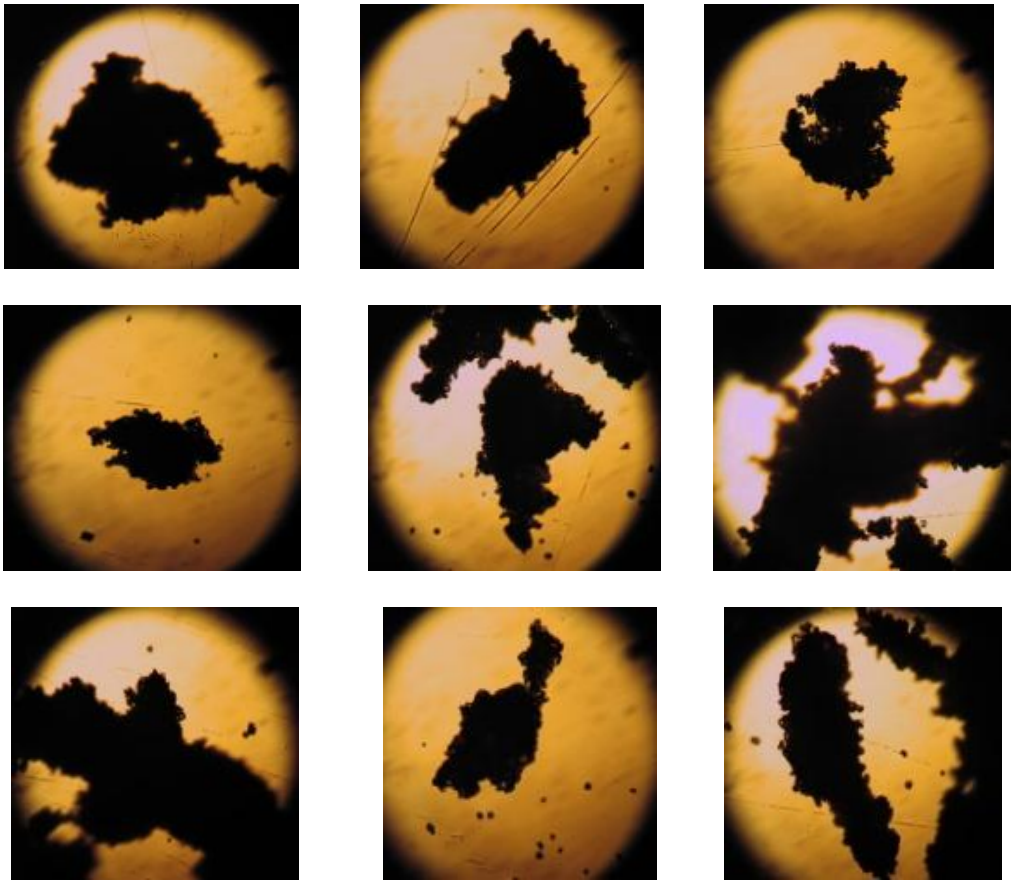

Fig 4.0: Shapes of TMe 419 Particles

The images from the computer interfaced microscope, shown in fig.4.3 confirm that the shape of grated cassava particles is very irregular and no particle shape can be a true or even approximate representation of the shape of the next particle. For the purpose of this work, the diameter of the cassava particle shall be taken as the diameter of the sieve opening trough which the bulk passed with some surface area modification factor to account for the irregular shape.

4.2 Particle Size:

A particle size distribution was determined for the material, using the sieve method and the results are presented in fig.4-1, 4.2 and 4.3 with the table in appendix 4-1.

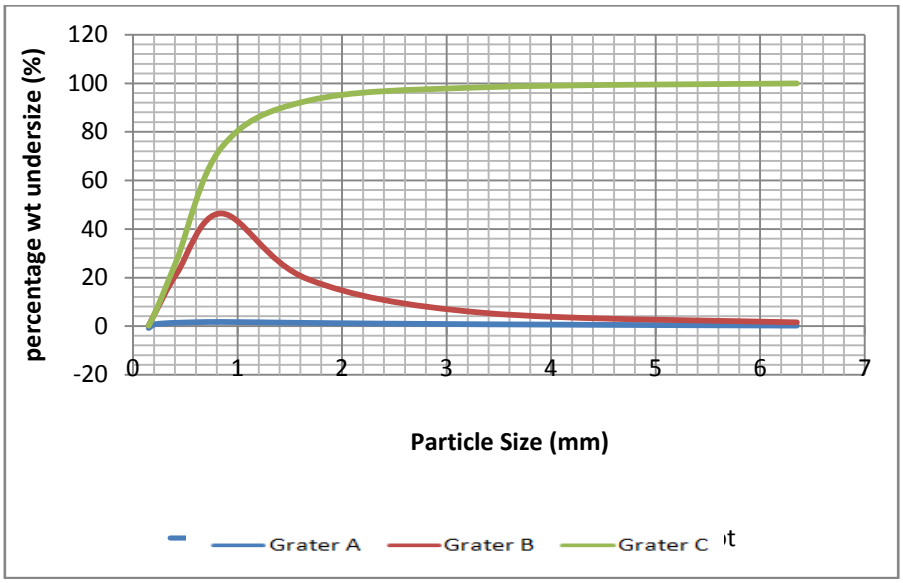

Fig 4.1: Fractional Particle Size Distribution Plot

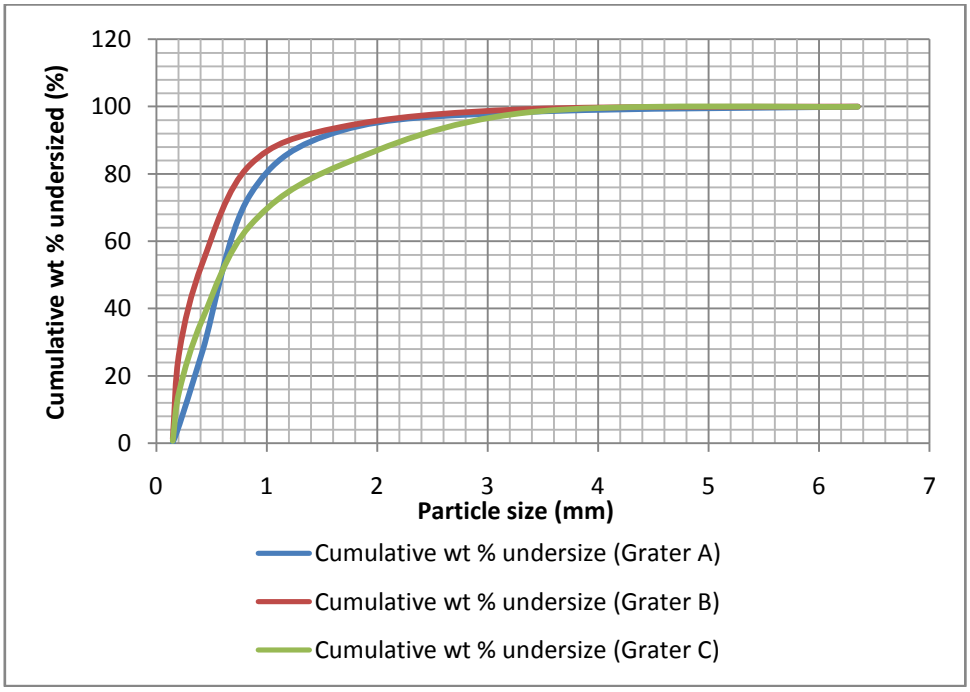

Fig 4.2: Cumulative Particle Size Distribution Plot

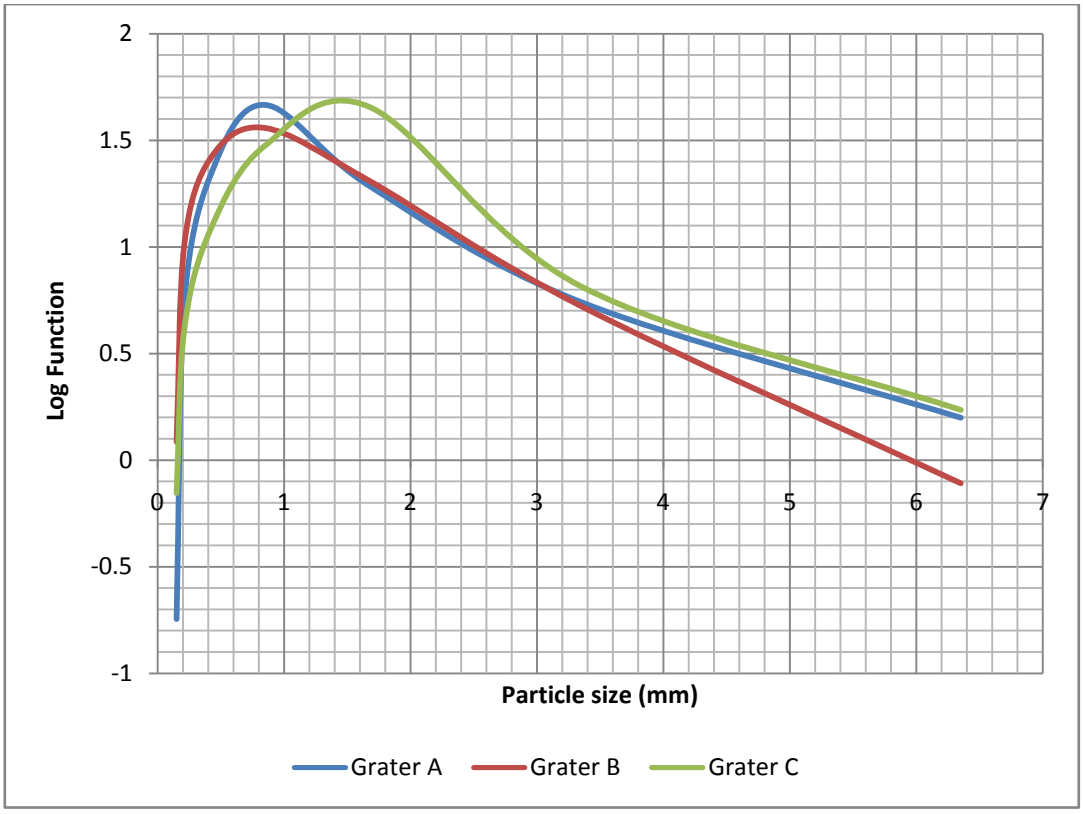

Fig. 4.3: Particle Size Log Function Plot.

The result indicated that the particle size distribution and cumulative particle size distribution of the material is unique to each grater suggesting that there is a distinctive difference in this distributions obtained for each grater. This underlines the importance of grater characterisation and / or standardization. This will help the designers of equipment that uses grating as a pre-processing operation to predict the size distribution that will be obtained from a grater. In addition the mean particle size determined from the cumulative size distribution plot is as summarized:

Grater	Mean Particle Size (mm)
A	0.6
B	0.4
C	0.6

4.3 Particle Density

Result:

Mass of sample=81.2647g = 0.0812647Kg

Table 4.1: Data from Volume Displacement Experiment

Initial volume (ml)	245	200	350	380
Final volume (ml)	320	275	425	455
Sample volume (ml)	75	75	75	75

True Density, ρ_t = 1083.53 kg/m^3

The value obtained is consistent with that published by Sopa Cansee et al (2008) which was 1010 kg/m^3 for cassava tuber considering that the value depends on age, cultivar and moisture content.

However, what goes into the flash drier is dewatered cassava mashes which have had its moisture content reduced from 60% to between 40%-45%. Therefore it follows that if one assumes that there is no change in volume as a result of dewatering, the density of dewatered mash can be determined considering the mass of water lost to dewatering.

Therefore, density of dewatered mash is given by: change in mass per volume (assuming shrinkage due to moisture loss to be negligible). That is

(0.0812647 - 0.0812647 x 0.2)/0.000075 =866.8235 kg/m^3

4.4 Particle Hardness

The use of Penetrometer or Sclerometer on representative sample of TMe 419 tuber gave the results shown below.

Table 4.2: Penetration Test Result

GY-4 Penetrometer Probe Size: Ø3.5mm Probe area: 9.625mm^2			
Penetrations	Peak Force (N)	Peak Mass (kg)	Hardness (kg/mm^2)
1	74.2	7.56	0.786
2	67.3	6.86	0.713
3	67.4	6.87	0.714
4	77.2	7.87	0.818
5	75.3	7.68	0.798
6	73.5	7.49	0.778
7	72.1	7.35	0.764
8	78.5	8.00	0.831
9	70.4	7.18	0.746
10	72.5	7.39	0.768
11	72.6	7.40	0.769
12	70.6	7.20	0.748
		Average	0.769

The result indicates that the hardness of cassava cultivar, TMe 419 is 0.769 kg/mm^2. This result compared to the threshold value of 800kg/mm2 suggested by Goodwin J.E et al (1969) indicates that for the purposes of design, the abrasiveness of cassava mash particles under pneumatic conveyance is insignificant and can for all intents and purposes be ignored.

4.5 Particle Weight

The weight of 10 groups of 50 randomly selected particles were determined and the average calculated and summarized in the table 4.3

Table 4.3: Particle weight

Opening Size (mm)	Weight – 50 particles (g)	Weight – 1Particle (g)	Particle weight (kg)
6.350	8.3770	0.16754	0.00016754
5.027	1.5612	0.031224	0.000031224
1.438	0.0888	0.001776	0.000001776
1.226	0.0272	0.000544	0.000000544
0.874	0.0077	0.000150	0.000000150
0.582	0.0021	0.000042	0.000000042
0.150	-		

4.6 Experimental Terminal Velocity

The grated and dewatered sample was sieved starting with the smallest and the same sample sieved progressively till the largest sieve. The sieved sample is subsequently fed into the bottom support mesh on the rig and air velocity increased gradually until the particle is lifted through the tube. The result is summarized and presented in table 4.4.

Table 4.4: Particle Terminal Velocity

Opening Size (mm)	Terminal Velocity, V_{et} (m/s)
6.350	13.38
5.027	8.92
1.438	3.60
1.226	3.20
0.874	2.40
0.582	2.00
0.150	-

A plot of the data in table 4.4 is given in fig 4.4.

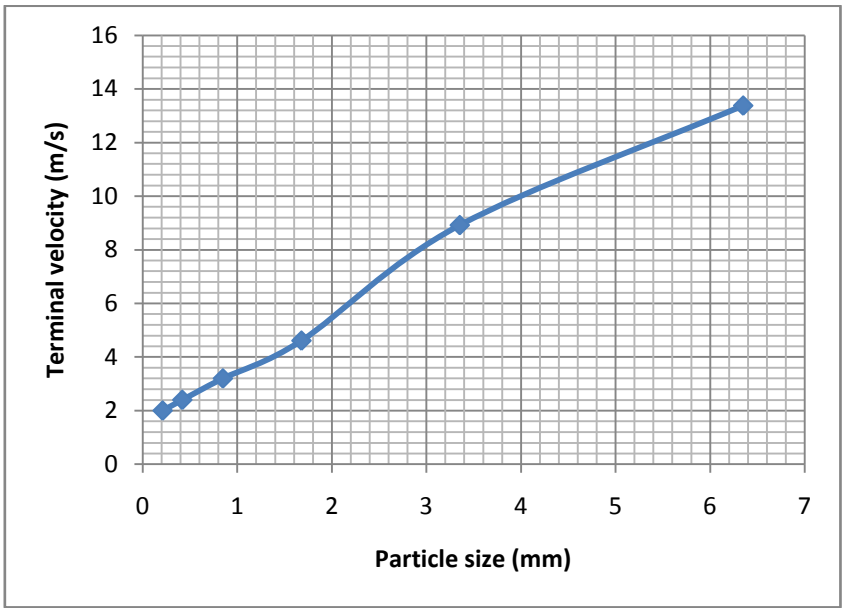

Fig 4.4: Plot of Terminal velocity against Particle size

The plot is necessary as it would be used to generate a correlation that will be coded into the program to predict the terminal velocities at different diameters. Consequently it will no longer be necessary to determine experimentally the terminal velocity of TMe 419 with every diameter change of the program input value.

4.7 Drag Coefficient

The coefficient of discharge is calculated based on the minimum projected area of the cassava particle whose diameter is equal to the sieve opening.

Table 4.5: Particle Coefficient of Discharge

Opening Size (mm)	Projected area (m^2)	Coefficient of discharge, C_D
6.350	0.0000316692	0.04733
5.027	0.0000198476	0.31668
1.438	0.00000162408	1.35143
1.226	0.00000118051	0.72076
0.874	0.000000599947	0.69522
0.582	0.000000266033	0.63214
0.150	-	-

4.8 Moisture Content

Using equation (3.91) and recorded data, the moisture contents were calculated and repeated in table 4.6.

Table 4.6: Moisture content determination (mass basis)

Test	W_1(g)	W_2(g)	W_3(g)	Moisture content (%)
A	2.5968	12.5996	6.46	61.38
B	2.5777	12.5770	6.49	60.87
C	2.5724	12.584	6.56	60.17
D	2.5648	12.5875	6.49	60.84
			Average	60.82

Initial moisture concentration = 0.60815 kg/kg

Initial moisture concentration = 658.9477 kg/m^3 or

Initial moisture concentration (c0_s) = 0.60815*rho_s [kg/m^3] (4.1)

4.9 Ash Content

Using equation (3.92) and recorded data, the ash contents were calculated and repeated in table 4.7.

Table 4.7: Ash content determination

Test	W_1(g)	W_2(g)	W_3(g)	Ash (%)
A	37.61	47.61	37.75	1.4
B	30.65	40.78	30.78	1.3
C	31.20	41.20	31.33	1.3
			Average	1.3

4.10 Lipid / Fat Content

Using equation (3.93) and recorded data, the fat/lipid contents were calculated and repeated in table 4.8.

Table 4.8: Lipid/ Fat content determination

Test	W (g)	W_1(g)	W_2(g)	Ash (%)
A	10	98.36	98.49	1.3
B	10	98.70	68.85	1.5
C	10	87.42	87.54	1.3
			Average	1.3

Specific Moisture Capacity (C_m_s) of TMe 419 expressed as (kg-water/kg-dry mash) is given as:

$$C\_m\_s = 1.552305 \text{ kg/kg} \qquad (4.12)$$

4.11 Nitrogen / Crude Protein Content

The percentage Nitrogen was computed for three different samples and the average taken using the correlation below:

$$\%\, Nitrogen = \frac{V \times 0.0014}{W} \times \frac{100}{1} \qquad (3.94)$$

where

W is weight of the sample taken

% protein = *NxF* where F is a factor equal to 5.70 for wheat, 6.38 for milk, 5.55 for gelatine and 6.25 for other foods.

Weight of sample A taken = 10.19 g

Weight of sample B taken = 10.25 g

Weight of sample C taken = 10.38 g

Table 4.9: *Titration Tabulations*

S/N	Weight (g)	Initial (ml)	Final (ml)	End Point (ml)	Nitrogen (%)
1	10.19	0.00	6.75	6.75	0.58
2	10.25	6.75	13.75	7.00	0.60
3	10.38	0.00	6.85	6.85	0.58
				Average	0.59

W= weight of the sample

V ml = end point value for each weight

N= Nitrogen percentage present in the sample

F= factor equal to 6.25

4.12 Carbohydrate Content

Thus, percentage carbohydrate content in TME 419 is

$$= 100 - (\%\ protein + \%\ fat/lipid + \%\ ash + \%\ moisture) \qquad (3.95)$$

On substituting the values obtained

It implies that,

% carbohydrate= 100- (0.59+1.3+1.3+60.92) = 35.89

Thus, the percentage carbohydrate content of TME 419 is 35.89%

4.13 Proximate Analysis Summary

The summary of the result of the proximate analysis of TMe 419 is as presented below:

Table 4.10: Result of Proximate analysis of TMe 419

Cultivar	% Ash	% Fat	% Protein	%Moisture	% Carbohydrate
TMe 419	1.3	1.3	0.59	60.92	35.89

4.14 Specific Heat Capacity

The specific heat based on the predictive equations, can be coded into a program such that as temperature changes, the routine recalculates the value of the specific heat at the new condition. The algorithm shall be set out on excel and later coded into ComsolScript.

Table 4.10b: Proximate analysis expressed as Mass fraction

Cultivar	% Ash	% Fat	% Protein	%Moisture	%Fibre	% Carbohydrate
TMe 419	1.3	1.3	0.59	60.92	0	35.89
Component C_p	1.1289	2.0117	2.0082	4.1762	1.8807	1.5857
%Mass	X_a	X_f	X_p	X_w	X_{fibre}	X_c
	0.013	0.013	0.0059	0.6092	0	0.3589

Result:

$$C_p = 3.1422\ kJ/(kg°C)$$

The value obtained agrees with that of Njie, D.N et al (1998) which ranged from 1.636 to 3.26 kJ for moisture content ranging between 10-68%.

4.15 Thermal Conductivity

The thermal conductivity based on the predictive equation is be coded into a program such that as temperature changes, the routine recalculates the value of the specific heat at the new condition. The algorithm is set out on excel and later coded into ComsolScript for FEA implementation.

$$k = 0.4634\ \frac{W}{m\ °C}$$

The value obtained agrees with that determined by Njie, D.N et al (1998) which ranged from 0.16 to 0.57 $\frac{W}{m\ °C}$ for cassava at moisture content range of 18–70%.

4.16 Thermal Diffusivity

The thermal diffusivity based on the predictive equation is coded into a program such that as temperature changes, the routine recalculates the value of the thermal diffusivity at the new condition. The algorithm is set out on excel and coded into ComsolScript for FEA implementation.

$$\alpha = 0.1164\ (\frac{m^2}{s})$$

4.17 Thermal Properties Summary

The summary of the thermal properties of TMe 419 determined by the predictive equations are presented below:

Table 4.11: Summary of thermal properties of TMe 419

s/no	property	symbol	value	unit
1	specific heat capacity	C_p	3.1422	$kJ/(kg°C)$or $kJ/(kg°K)$
2	thermal conductivity	k	0.4634	$W/m°C$ or $W/m°K$
3	thermal diffusivity	α	0.1164	m^2/s
4	density	ρ	620.7987	kg/m^3
	heat transfer coefficient	h_m	$varies$	$W/m^2°C$ or $W/m^2°K$
5	Mass transfer coefficient	k_m	$varies$	m/s
6	Evaporation rate from one particle	$\dot{m}$	$varies$	kg/s

4.18 Drying Curve

The data obtained from the drying experiments are presented in fig. 4.5-4.10 and their tables in appendix 4-12 to 4-16.

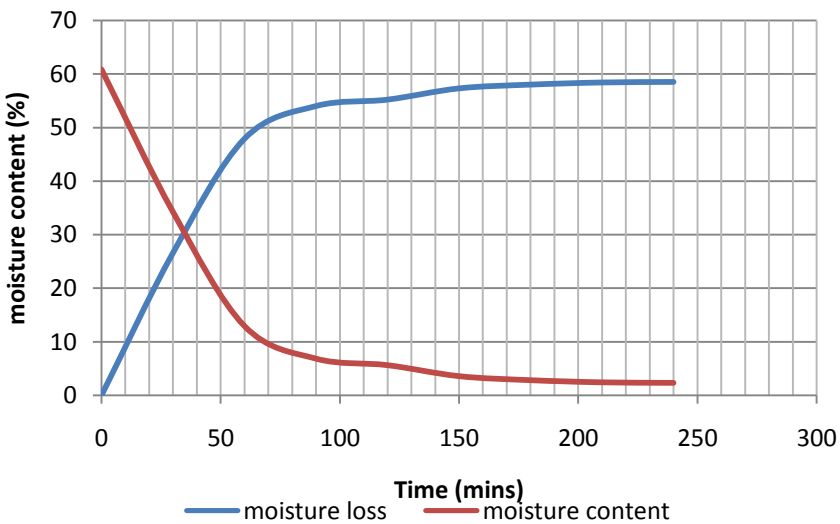

Fig 4.5: Drying curve at 40°C

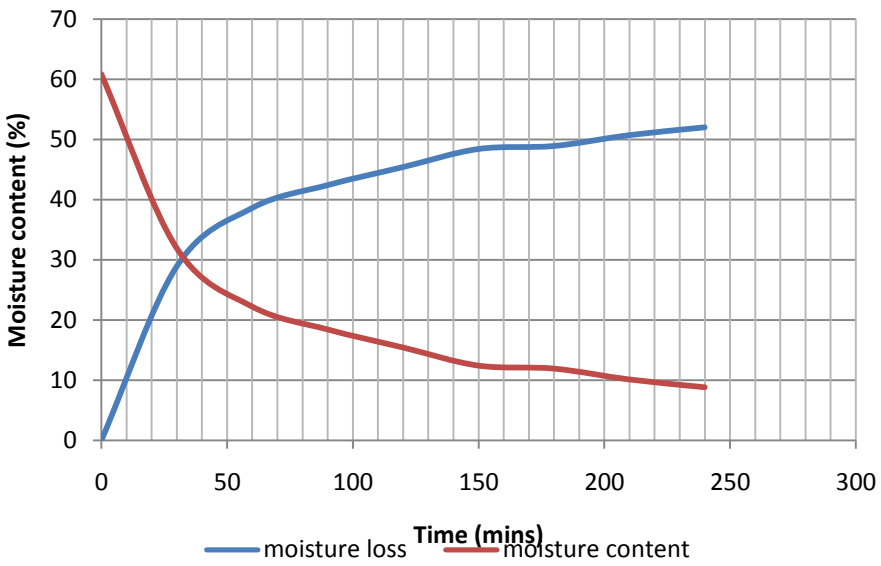

Fig 4.6: Drying curve at 45°C

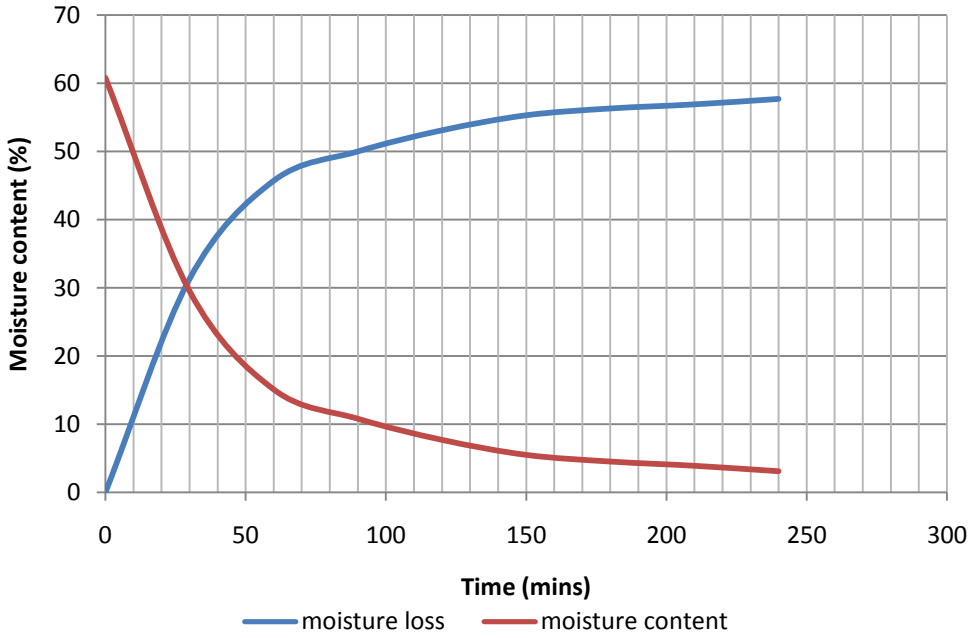

Fig 4.7: Drying curve at 50°C

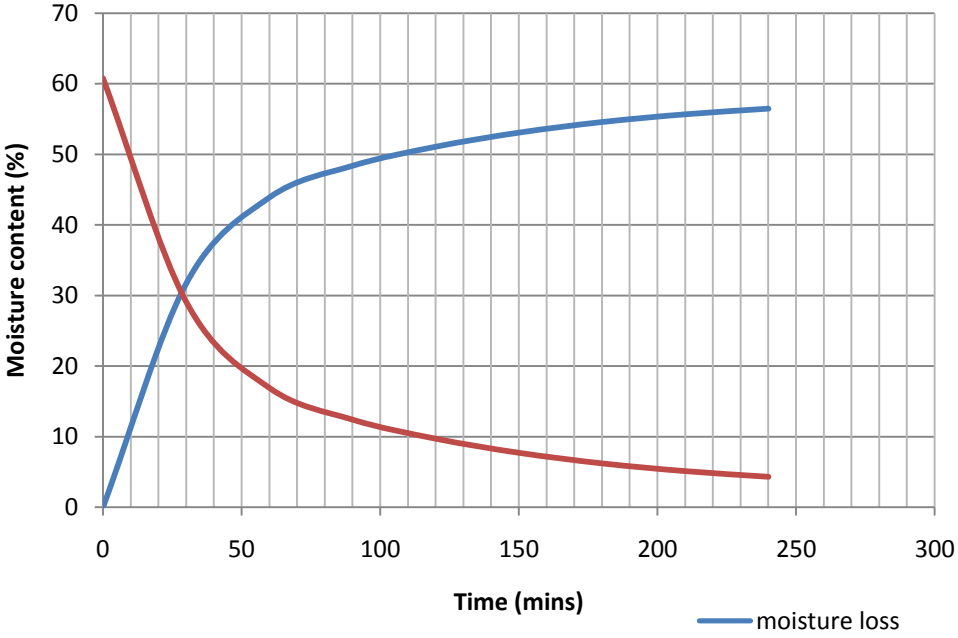

Fig 4.8: Drying curve at 55°C

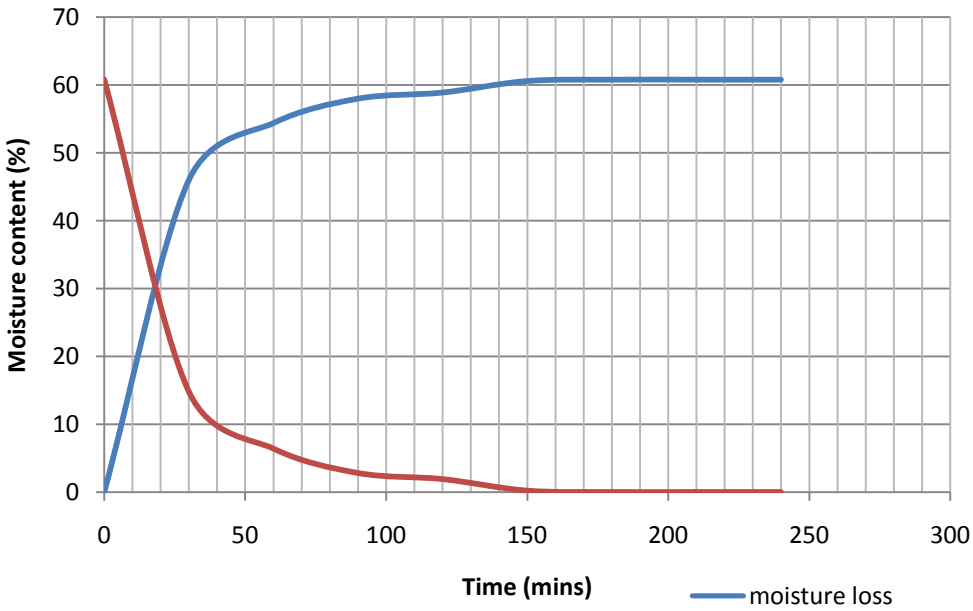

Fig 4.9: Drying curve at 60°C

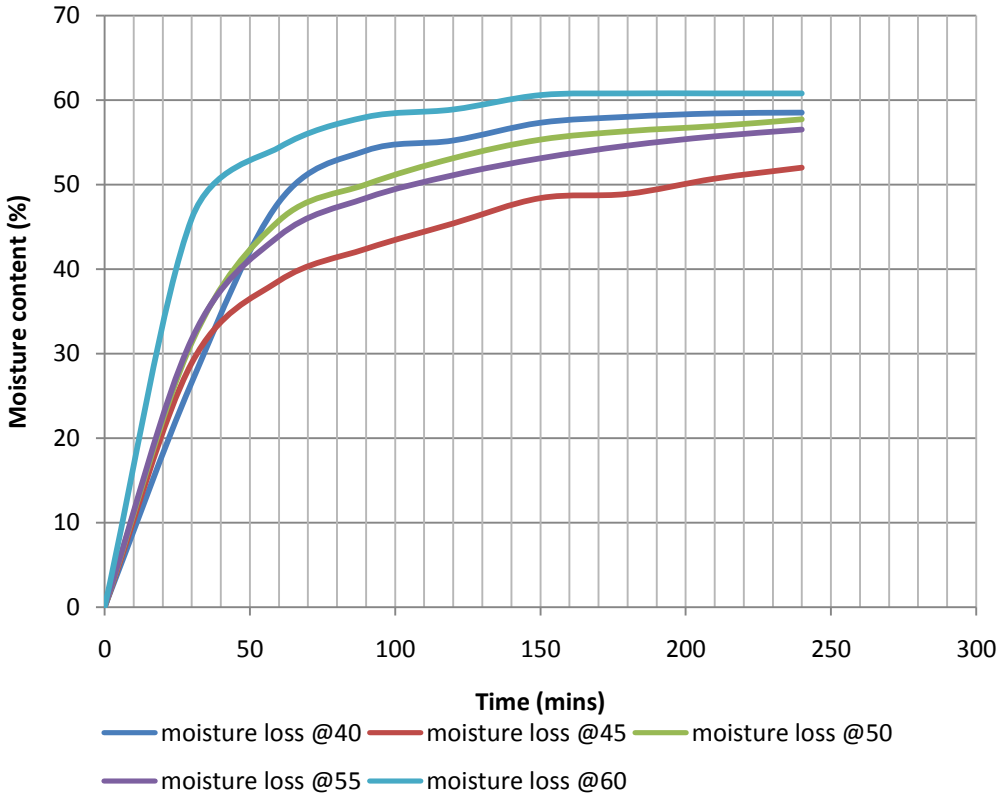

Fig 4.10: Drying curves at various adiabatic conditions

Discussion

There is no record of the thermal properties of unfermented TMe 419 as determined in this work; the drying curve showed clearly the dynamics expected of tubers as reported in previous work by IITA (1987). Nwabanne J. T (2009) worked on different specie which was also fermented before the experimental determination of its thermal properties.

At the start of heating, the rate of moisture removal will be at a constant rate (ie constant rate period) but the rate will gradually fall as drying progresses usually referred to as the falling rate region of the curve. The transition between the constant drying rate regime and the falling rate regime usually happens at the attainment of critical moisture content. It is easy to glen from the graphs that the critical moisture

content which represents the beginning of the constant rate drying period, is below the required product moisture content.

The significance of this is that the appropriate formulation for the analysis of the pneumatic conveying drying of TMe 419 is based on the constant-rate drying conditions.

4.18.1 Standard Air Correlations.

The use of psychrometric chart though simple could not be used in this work for predicting the condition of standard air at various conditions, but the relevant correlations shall be used to suit the modelling process. Since the properties of air will be changing, the correlations for how these properties vary with temperature are generated. For this the table of properties of air in appendix 4-6 will be used to generate the correlations to make for easy read-in by a program.

Fig 4.11: Variation of air density with temperature

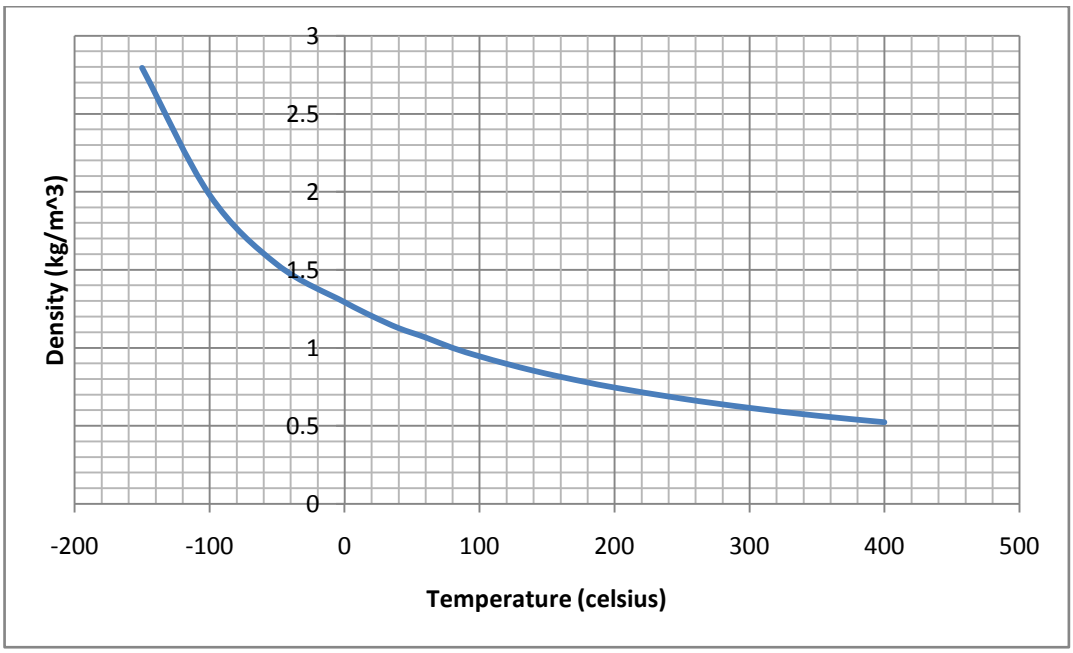


```
rho_g=1.287841156-0.004250962*T_g+0.00000944905*T_g^2-
0.00000000903741*T_g^3
```

Fig 4.12: Variation of air specific heat with temperature

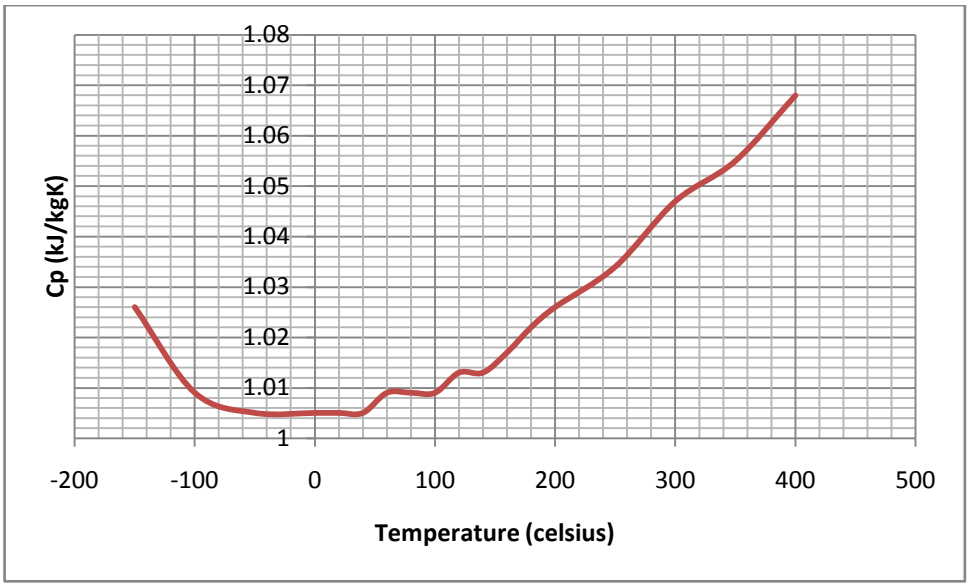


```
cp_g=1.005256941-0.0000147268*T_g+0.00000070019*T_g^2-
0.000000000684638*T_g^3
```

Fig 4.13: Variation of air thermal conductivity with temperature

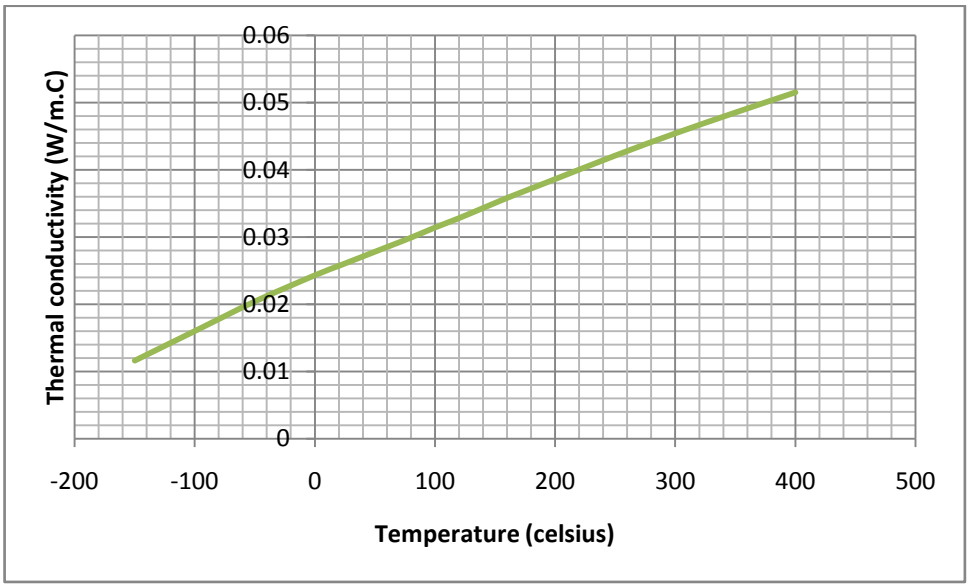


```
k_g=0.024283313+0.0000693881*T_g+0.0000000251525*T_g^2-
0.00000000007194*T_g^3
```

Fig 4.14: Variation of air kinematic viscosity with temperature

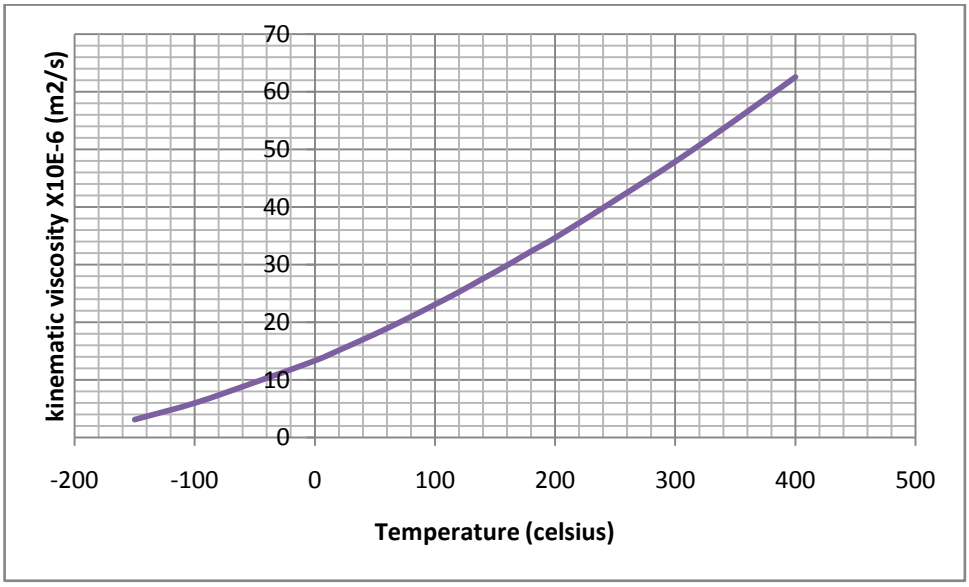


```
v_g=(13.29152006+0.087903505*T_g+0.000102887*T_g^2-
0.0000000374881*T_g^3)*0.000001
```

Fig 4.15: Variation of air Prantl number

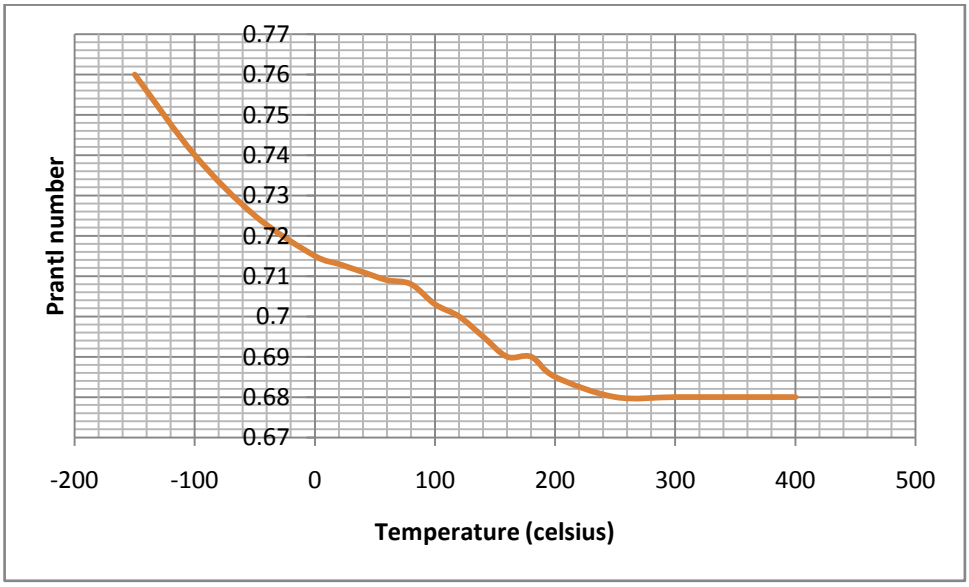


```
pr= 0.716049954-0.000110828*T_g-
0.000000406781*T_g^2+0.0000000017347*T_g^3
```

4.18.2 Summary of Standard Air Correlations.

$$\rho = 1.287841156 - 0.004250962T + 0.00000944905T^2 - 0.00000000903741T^3$$

$$Cp = 1.005256914 - 0.0000147268T + 0.00000070019T^2 - 0.0000000006846 38T^3$$

$$k = 0.02483313 + 0.0000693881T + 0.0000000251525T^2 - 0.00000000007194T^3$$

$$v = (13.291520006 + 0.87903505T + 0.000102887T^2 - 0.0000000374881T^3)0.000001$$

4.19 Results (Comsol Script implementation on Gas Phase)

The implementation of the program allows us to study the effect or state of variables when one of the variables is altered. This is important because in the design of pneumatic conveying dryers, a lot of variables are at play and there is need to understand how these variables affect the system and hence use the capability to optimise the system by altering the variables.

The selection of a fan, blower or compressor is probably one of the most important decisions to be made in the design of a pneumatic conveying system. It is often the largest single item of capital expenditure and the potential conveying capacity of the plant is dependent upon the correct choice being made. The rating of the fan, blower or compressor is expressed in terms of the supply pressure required and the volumetric flow to be delivered . Any error in this specification will result in a system that is either over-rated, is not capable of achieving the desired material flow rate, or will cause a pipeline blockage and convey nothing. This makes the determination of the state of pressure across the flash tube very important. The model developed as applied in the investigation of the state of pressure across the flash tube at various air inlet velocities and material feed rate.

4.19.1: Investigation of the change in pressure drop across flash tube of a specified length under various air inlet velocities

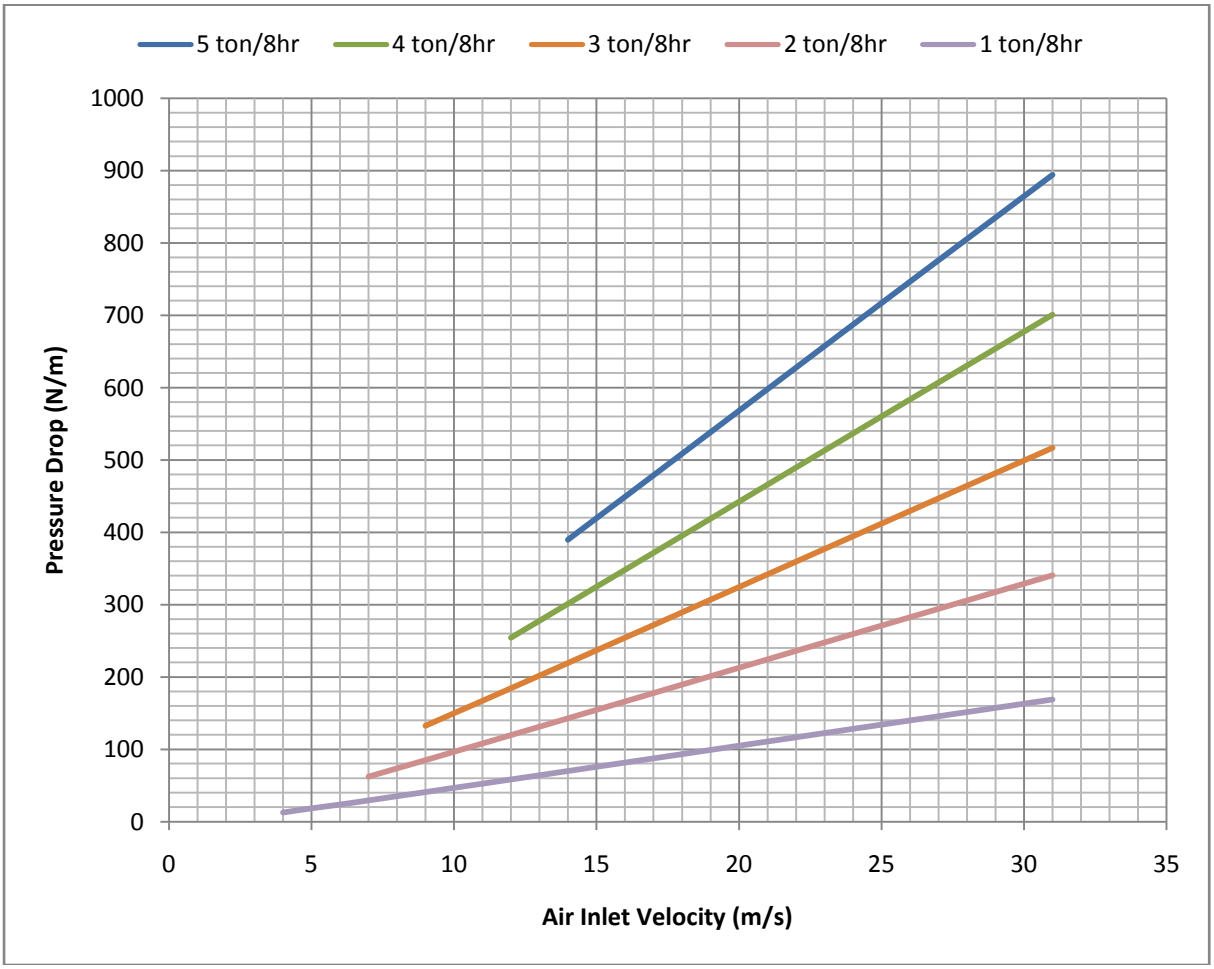

Fig. 4.16: Pressure Drop at various Inlet Velocities

Figure 4.11 generated from the implementation of the gas phase model can be described as 'Design Curves for Vertical Upwards Pneumatic Conveyance of Cassava Particles'. It is similar to those employed by David Mills (2004) in the determination of the interplay of variables during pneumatic conveyor design.

One of the objects of this work is to provide a means of investigating the state of the very many variables that are at work during pneumatic drying. Given that there are too many variables for a simple universal relationship to be applicable. And since only three variables can be represented on a single graph, a complete family of graphs is needed in order to represent a fourth variable. The family of graphs are simply generated by the model developed and coded in Comsol Script by simply altering the variables. The data or design curve generated will determine the state of all the variables involved and hence allow the designer of the system to make informed decisions.

In the first set of curves flash tube pressure drop is plotted against air inlet velocity and lines of constant material feed rate are superimposed. Material flow rate is represented as the fourth variable in this set of curves and five values ranging from 1 to 5 tonne / 8 hr are considered. All five graphs are drawn for each material flow rate and the graphs are discontinuous in areas where the subsisting air inlet velocity and pressure could not support the material flow rate under dispersed flow situation.

4.19.2: Investigation of gas phase and solid phase temperature along the flash tube length

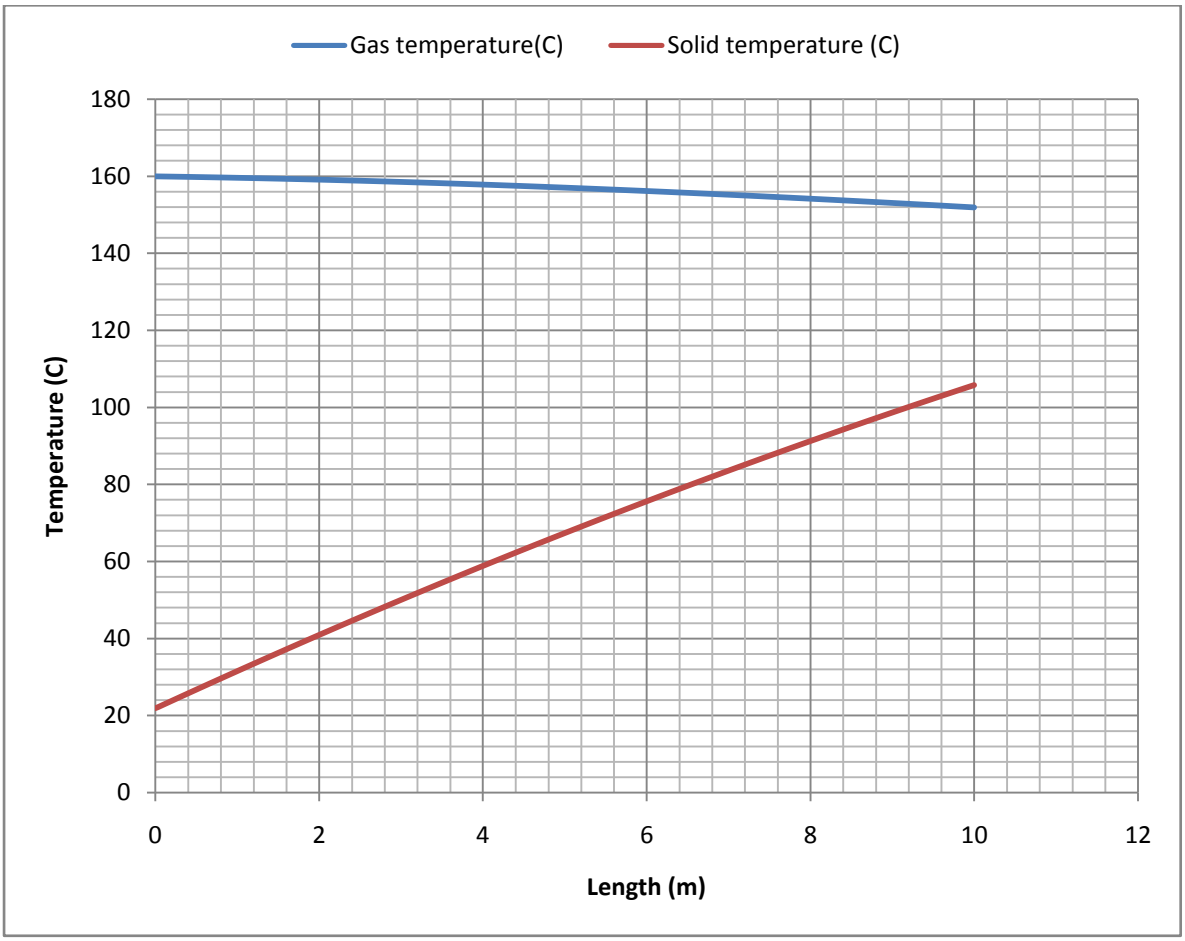

Fig. 4.17: Variation of Gas/Solid Temperatures along the Flash Tube

The effects of inlet gas temperature, air mass flow rate, solid mass flow rate, on the axial distribution of gas temperature, solid Temperature can be studied as shown in Fig. 4.12. The data was generated for a given inlet gas temperature, air inlet velocity, which has a relationship to air mass flow rate and solid flow rate to investigate the

state of gas and solid phase temperatures. Under a different set of input conditions the output conditions can de predicted.

In general, it can be seen from figure 4.12 that the gas temperature continuously decreases along the dryer, while the solid phase temperature increases continuously until, if the residence time allows, it attains the wet bulb temperature (adiabatic saturation resulting in constant enthalpy/ temperature).

4.19.3: Investigation of the gas phase and solid phase velocities along the flash tube length.

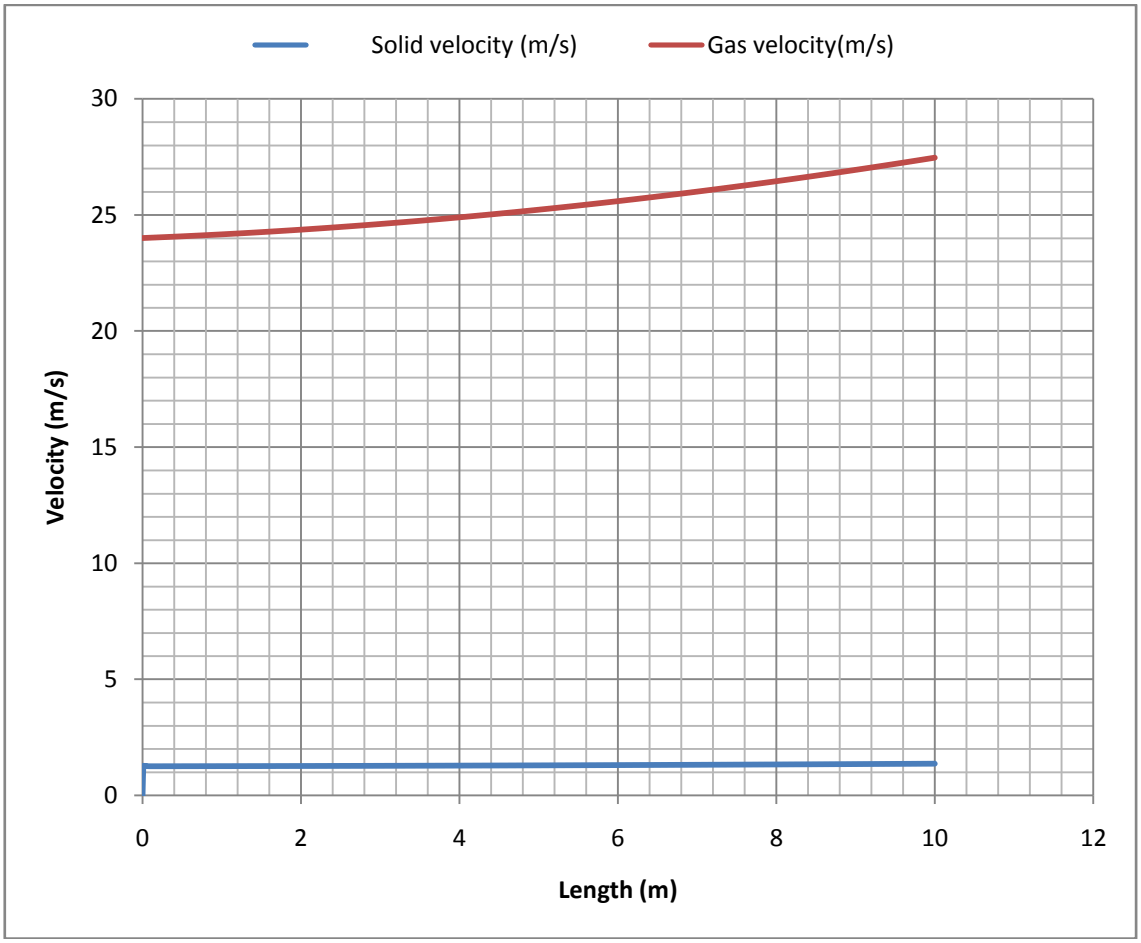

Fig. 4.18: Gas and Solid Phase Velocity along the Flash tube

The increase in the velocity of the gas phase is as a result of the continuous influx of material into the flash tube. The velocity of

the particle increases from zero or near zero at the point of introduction accelerates for a while, and attains and maintains the terminal velocity for the rest of its journey through the flash tube. This explains why some of the models reviewed in Chapter 2 assumes that the particle travels at a uniform velocity across the flash tube and do not account for the initial particle acceleration. This assumption may be valid for pneumatic conveying because it happens over a considerable distance and the residence time is much more when compared to pneumatic conveying drying or flash drying which happens within a very short interval of time. The very short resident time makes that initial interaction significant because it is at that point that the value of slip velocity and of course heat transfer between the air stream and the particle are at a maximum.

4.20 Results (Comsol Multiphysics implementation on the solid phase)

The most interesting result from this simulation is the time dependent state of the properties of the cassava particle as it is dried. The simulation is able to predict the surface and centre temperature of the cassava particle over time and also the moisture concentration over the same period of time. The snapshots of the simulation of moisture concentration and temperature within the

particle, at 0.5s intervals for the duration of the simulation (3s) is shown below and summarised in table 4.12.

Fig 4.19: Snapshots of moisture concentration distribution within the particle after 0.5s.

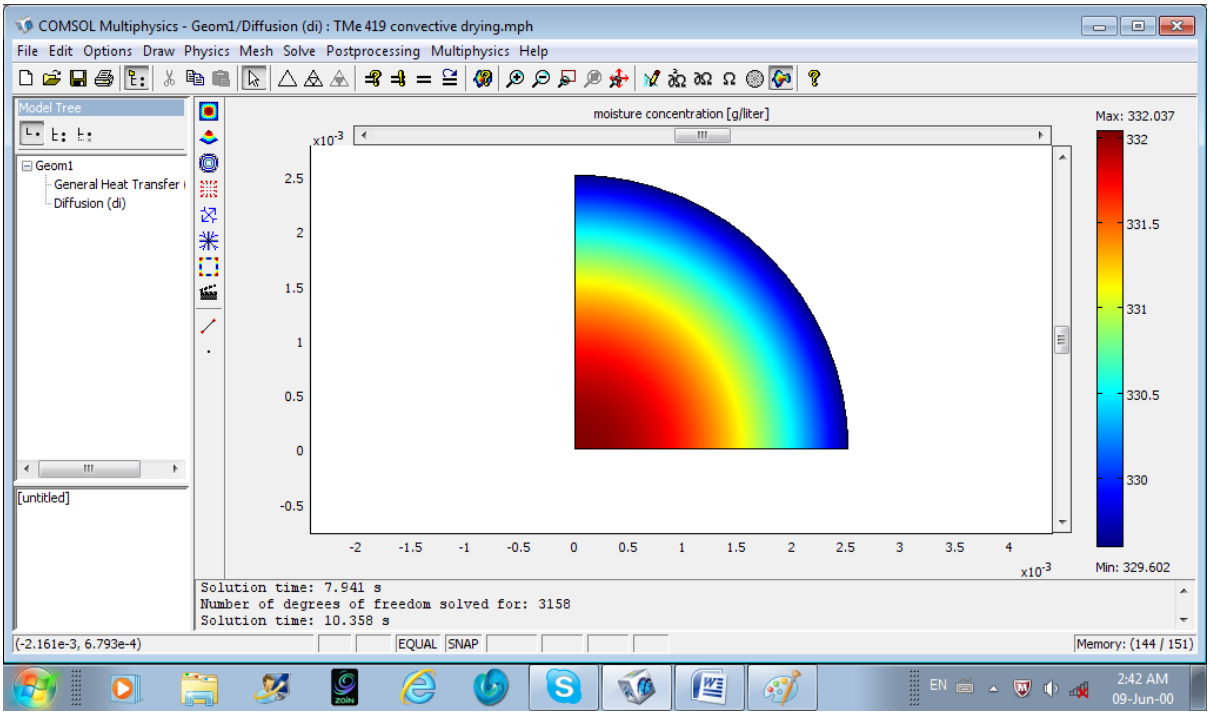

Fig 4.20: Snapshots of moisture concentration distribution within the particle after 1s.

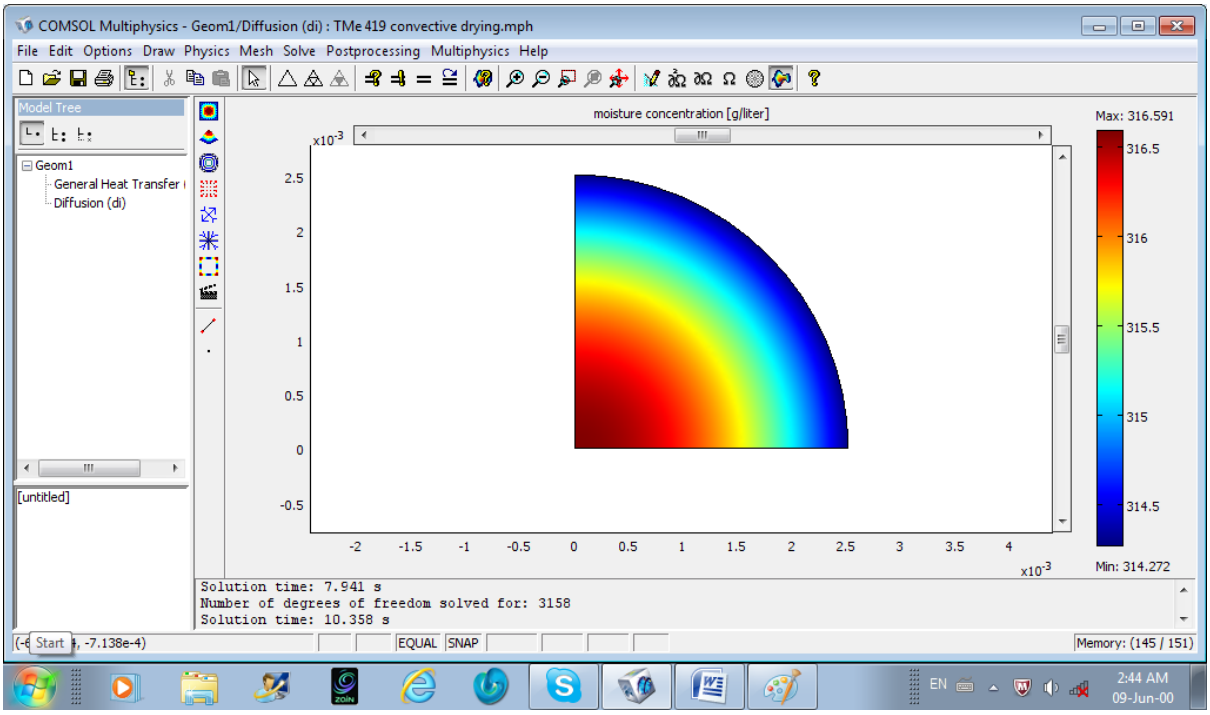

Fig 4.21: Snapshots of moisture concentration distribution within the particle after 1.5s.

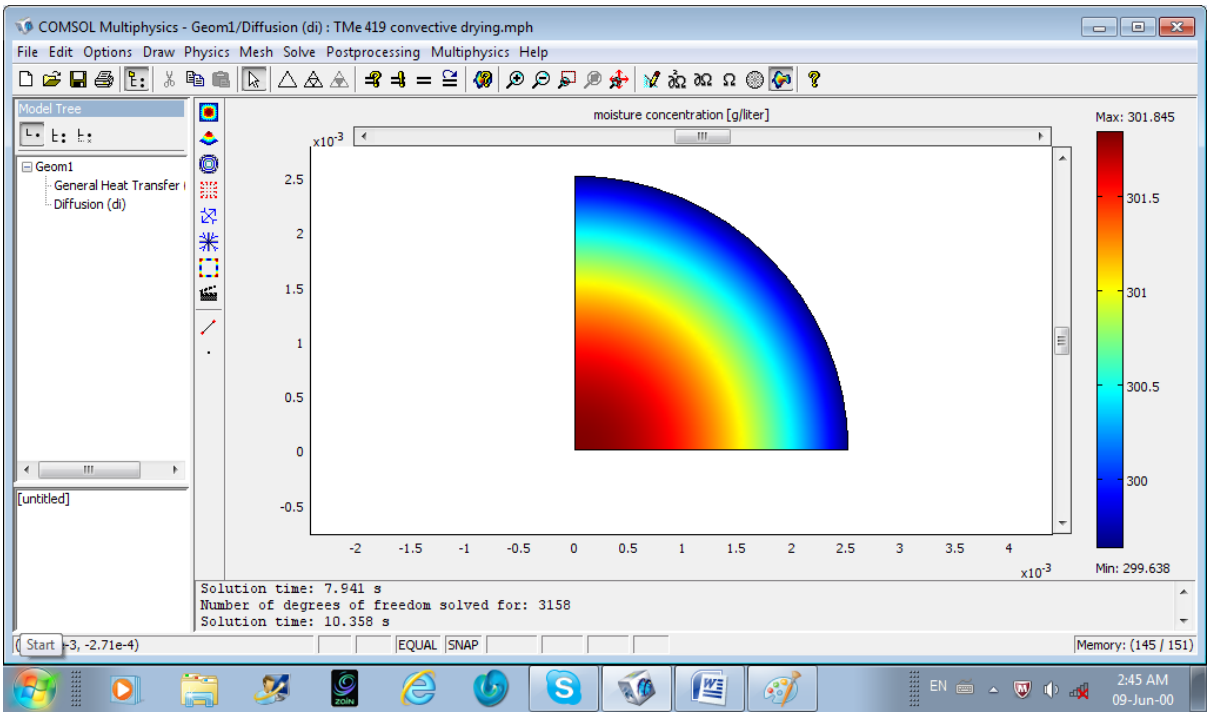

Fig 4.22: Snapshots of moisture concentration distribution within the particle after 2s.

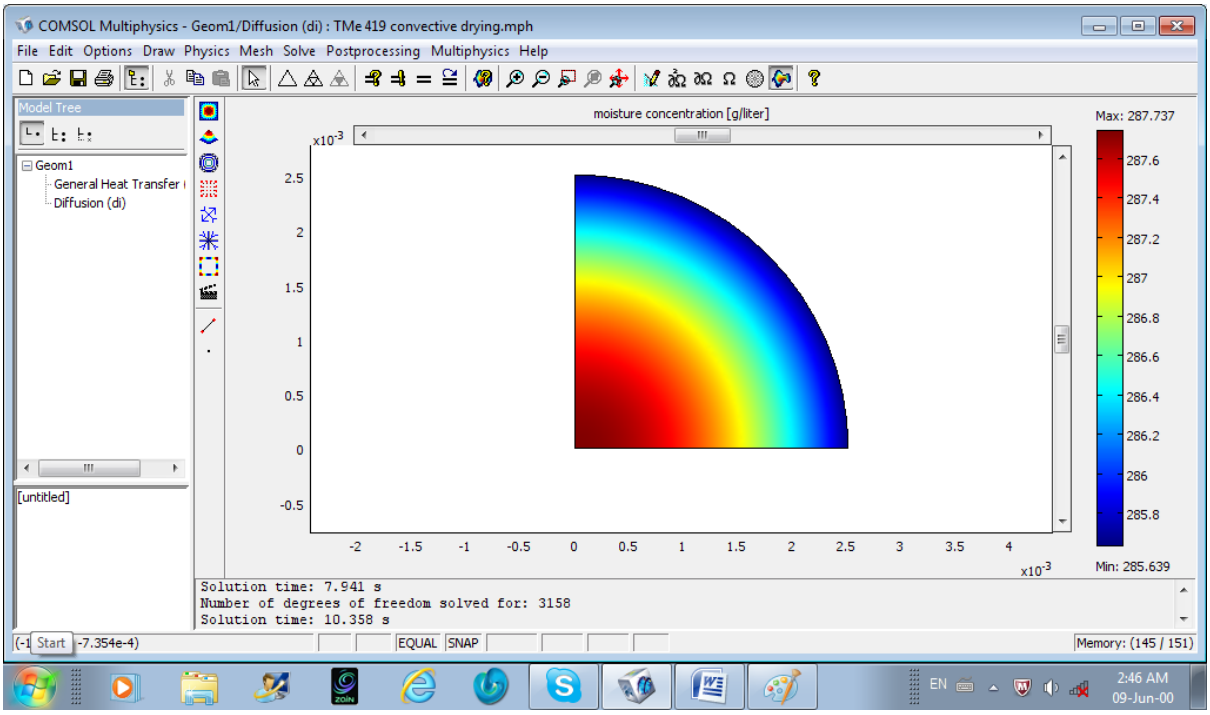

Fig 4.23: Snapshots of moisture concentration distribution within the particle after 2.5s.

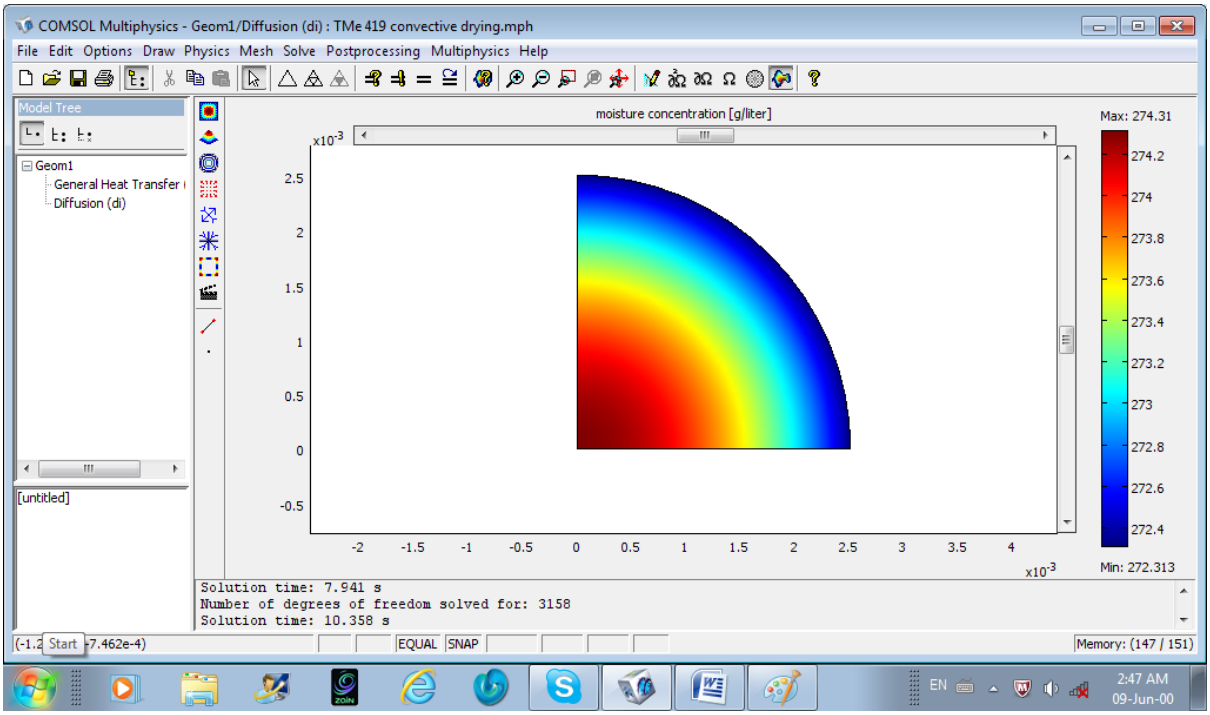

Fig 4.24: Snapshots of moisture concentration distribution within the particle after 3s.

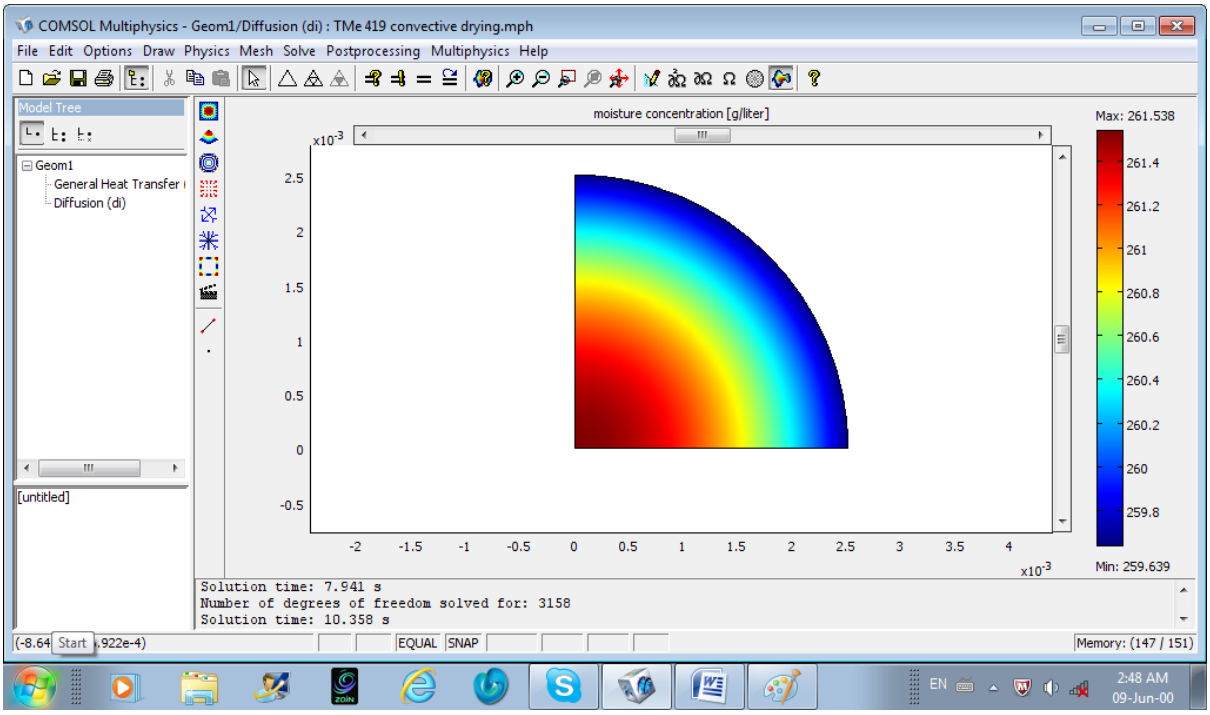

Fig 4.25: Snapshots of temperature distribution within the particle after 0.5s.

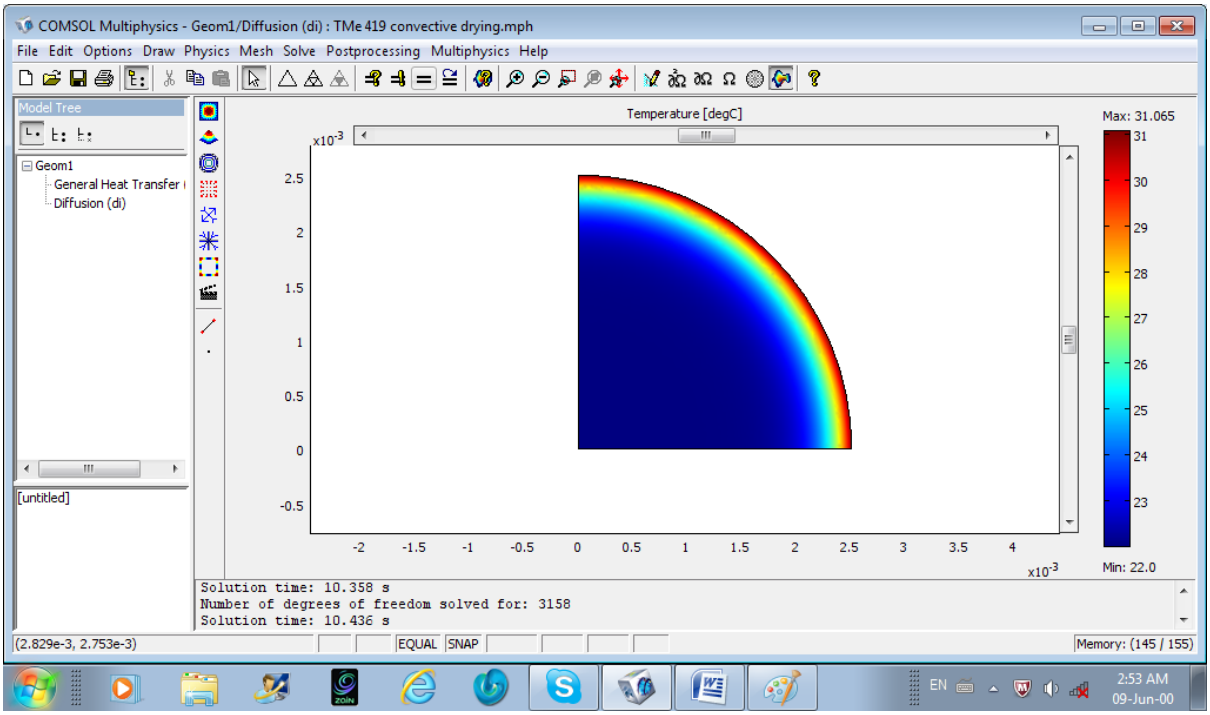

Fig 4.26: Snapshots of temperature distribution within the particle after 1s.

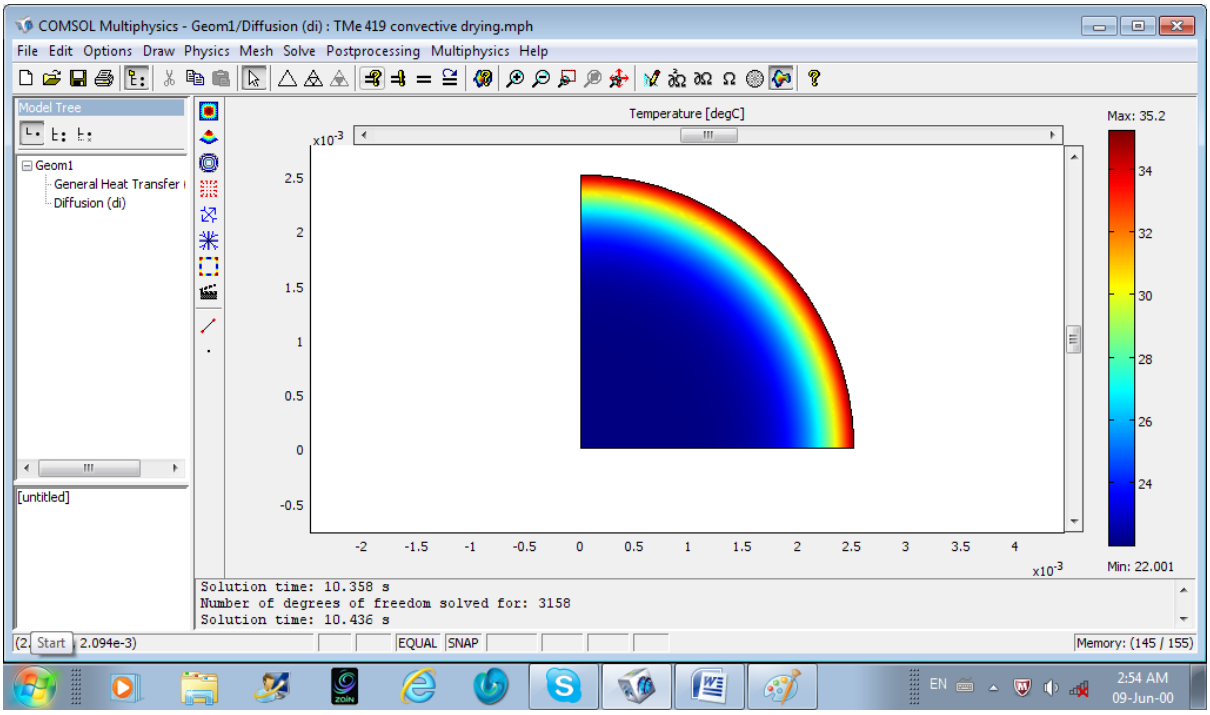

Fig 4.27: Snapshots of temperature distribution within the particle after 1.5s.

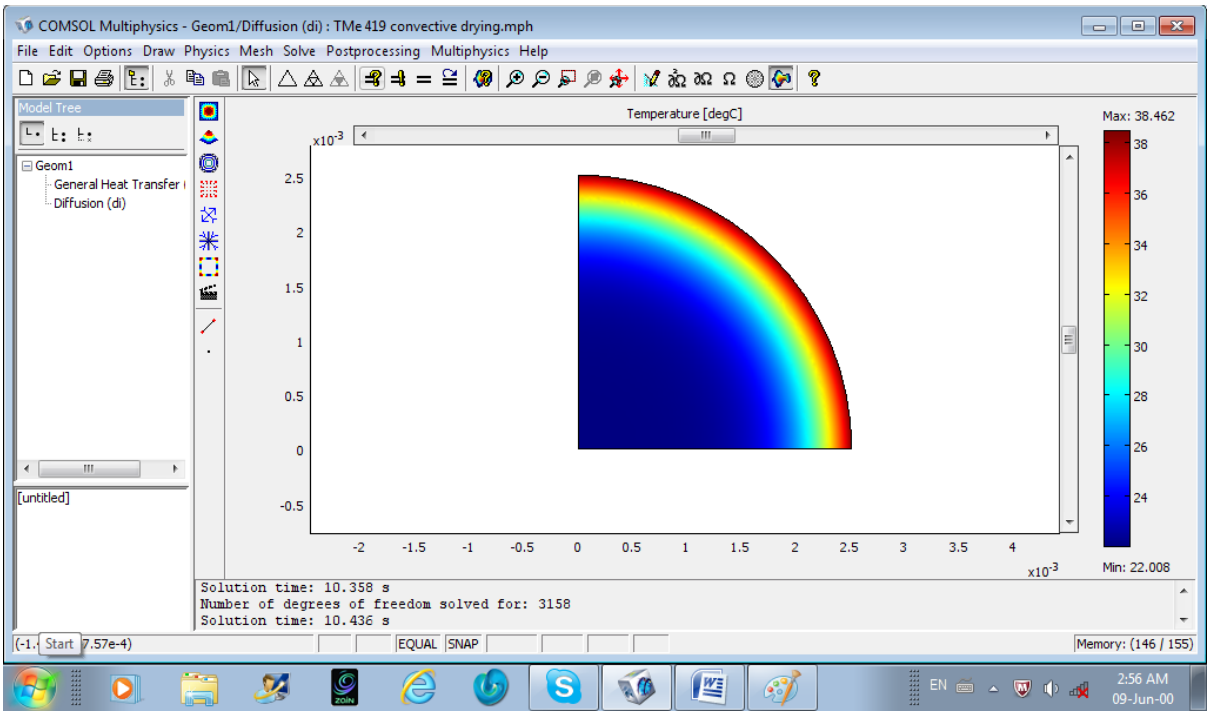

Fig 4.28: Snapshots of temperature distribution within the particle after 2s.

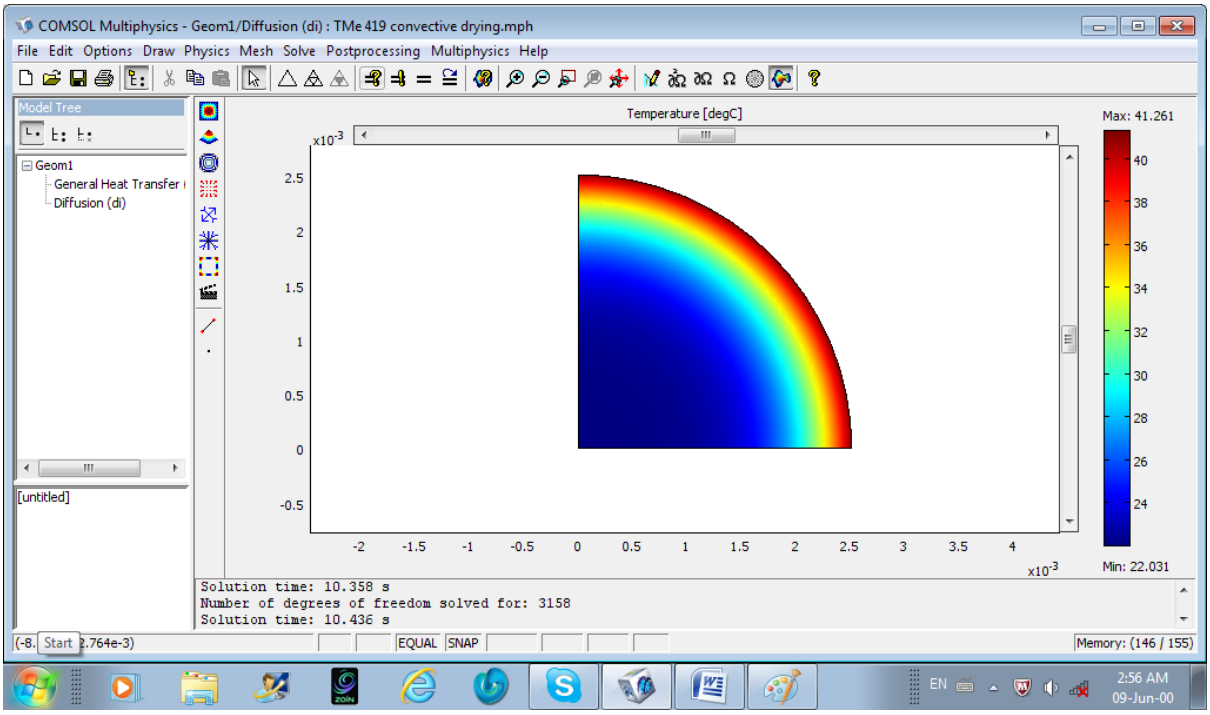

Fig 4.29: Snapshots of temperature distribution within the particle after 2.5s.

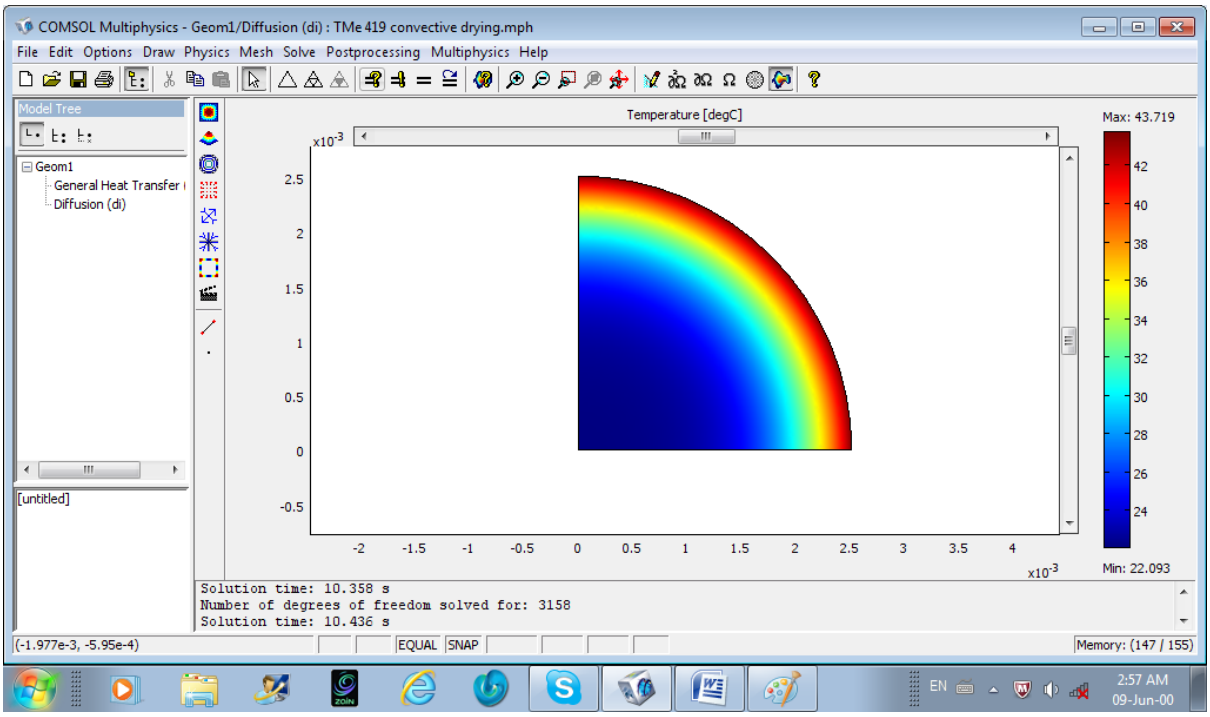

Fig 4.30: Snapshots of temperature distribution within the particle after 3s.

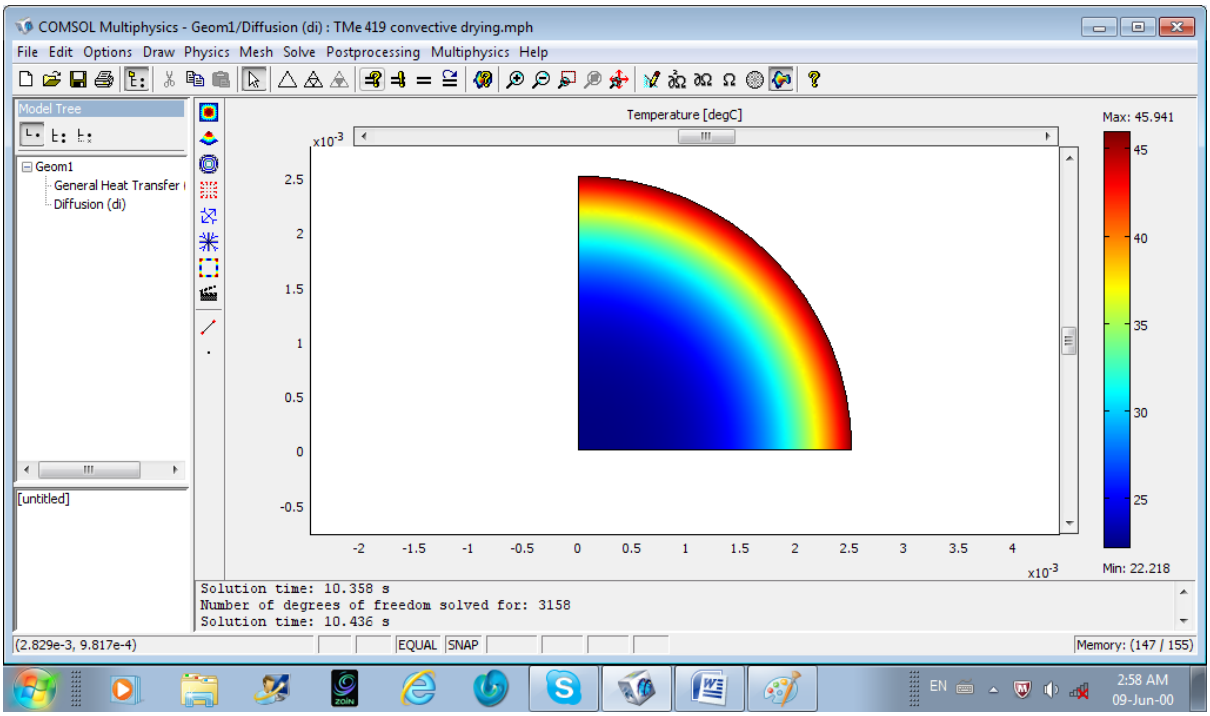

Table 4.12: Result of Convective drying simulation of TMe 419

Time (s)	Surface temp (°C)	Moisture Conc.	Volume Integral	Residual MC
0.5	31.065	332.0370	0.476676	0.1906704
1	35.200	316.5910	0.454504	0.1818016
1.5	38.462	301.8450	0.433336	0.1733344
2	41.261	287.7370	0.413088	0.1652652
2.5	43.719	274.3100	0.393814	0.1575256
3	45.941	261.5380	0.375483	0.1501932

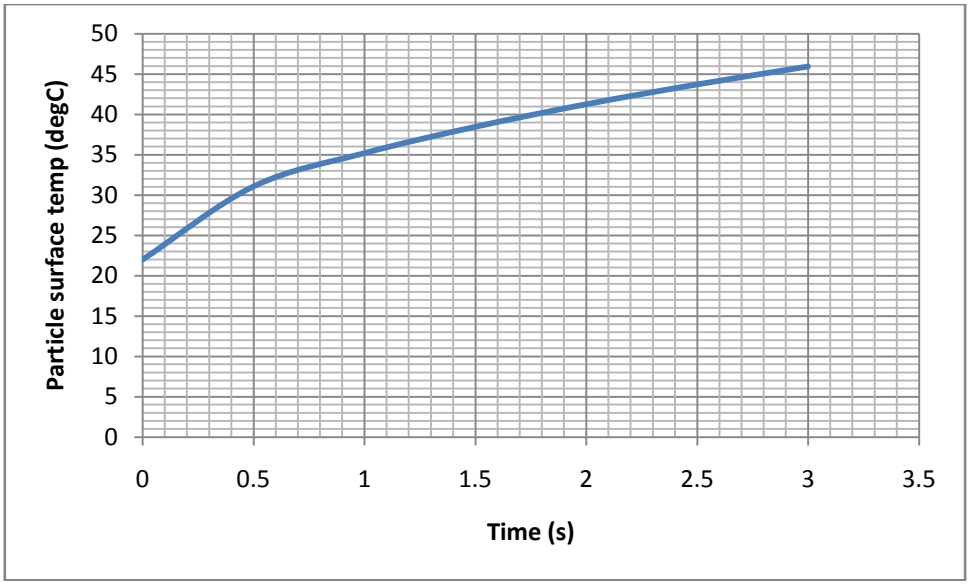

Fig 4.31: Plot of particle surface temperature over time

The plot in figure 4.31 shows the variation of particle surface temperature over time as it is introduced into the hot air stream. The plot shows an increase in surface temperature over the 3 s time interval but the rate of increase of temperature was relatively high between 0 s and 0.5 s then the rate of temperature increase gradually diminishes over time. This is as a result of the fact that the particle at 0 s is stationary and the slip velocity is equal to the velocity of the gas phase (maximum). A short while later the gas phase transfers momentum to the particles and it begins to accelerate. This period involves intense heat transfer between the particle and the gas phase. However as the particles gains speed, the slip velocity reduces together with the rate of heat transfer and increase of surface temperature.

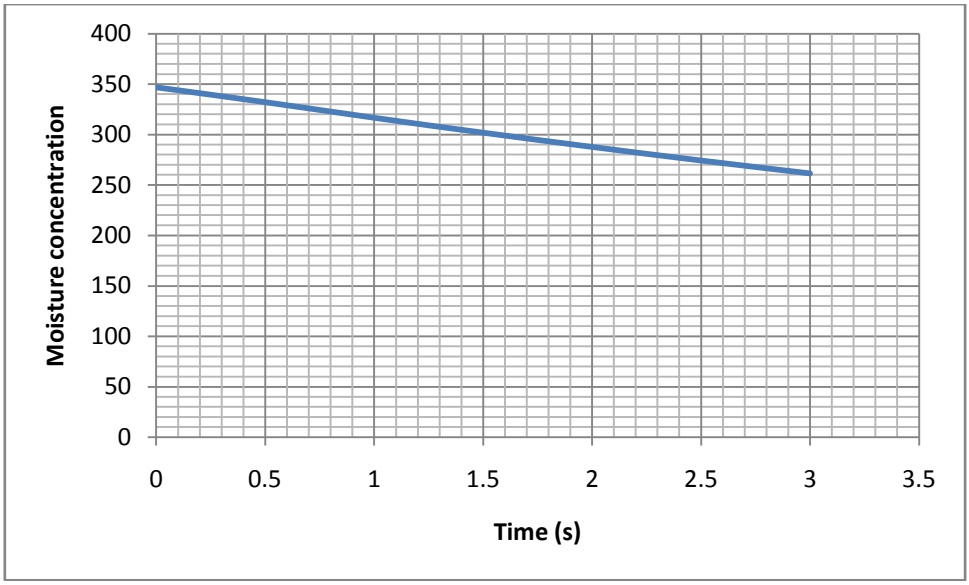

Fig 4.32: Plot of moisture concentration over time

The figure above shows the variation of moisture content over time and the plot shows that the rate of loss of moisture concentration is constant. This agrees perfectly with the drying curve for TMe 419, which indicated that the entire cassava flash drying occurs within the 'constant rate drying period'.

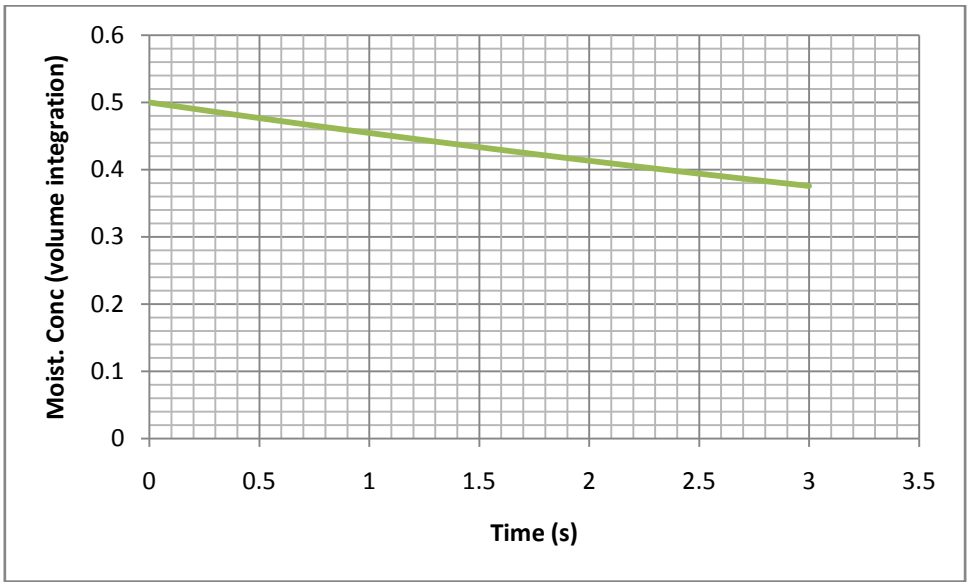

Fig 4.33: Plot of volume integration of moisture concentration over time

The plot shown in figure 4.33 is that of volume integration of the moisture concentration over time. This is important because the moisture concentration within the particle s not uniform as drying progresses and so to allow for the determination of residual moisture content, the volume integration of moisture content has to be determined. However the plot shows

constant rate of decrease like the moisture concentration plot because the process is at 'constant rate drying period'.

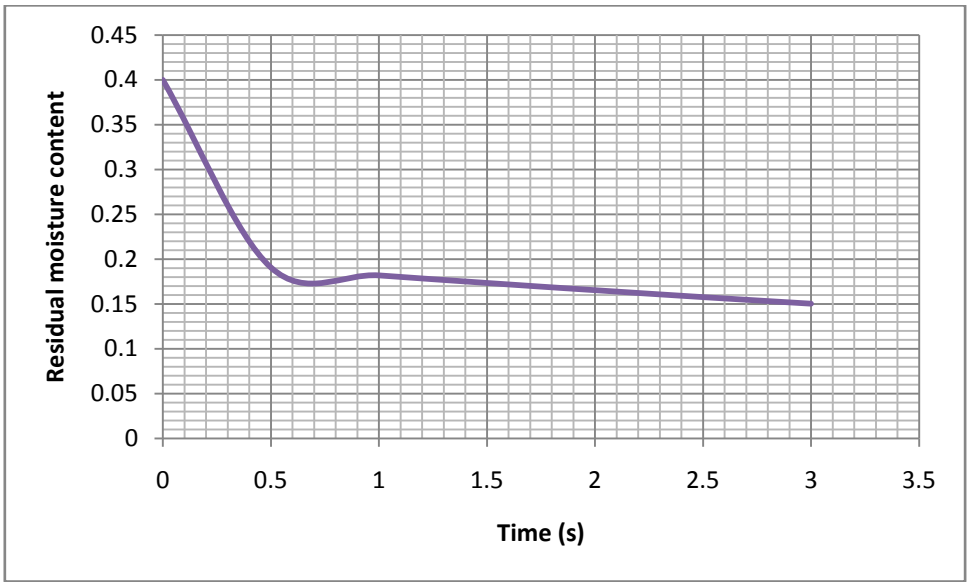

Fig 4.34: Plot of Residual moisture content over time

The plot of the simulation snapshot data shows an increase in the particle surface

The plot of the simulation snapshot for residual moisture content shows that the residual moisture content decreases rapidly and the rate of moisture loss diminishes. This is consistent with the fact the heat transfer to the particle is greatest immediately the particle is introduced into the hot air steam. It subsequently diminishes as the particle accelerates towards its 'terminal velocity' .Temperature (fig 4.32) and a decrease in the moisture concentration (fig. 4.33) and residual moisture concentration (fig. 4.34) over the duration of the simulation. The result is consistent with our expectations for particle drying.

4.21 Length of the Flash Tube

The length of the flash tube is calculated from the particle velocity determined by the ComsolScript Program. For the set of parameters investigated, the particle average velocity is 1.34921 m/s. The ComsolScript implementation predicts a residual moisture content value of 0.1501932 or 15% after convective drying for a period of 3s. The distance covered by the cassava particle during which the moisture content was reduced to the acceptable level will give an indication of the minimum length of the flash tube. For the conditions simulated, the minimum flash tube length is 4.04763m.

4.22 Validation

The model developed was validated against pneumatic transport data without heat or mass transfer. This is as a result of the cost of constructing a flash dryer rig and more so the cost of acquiring the instrumentation for required measurement. However, in chapter 3 section 3.7.4, a vertical air tunnel was used to determine the terminal velocity of cassava particles with different diameters. The same tube properties, same particle properties and same initial conditions were used to predict the particle terminal velocity of cassava particles of different diameters. The result of the simulation was matched against those obtained experimentally and the data is summarised in appendix 5:11 and presented in figure 4.18.

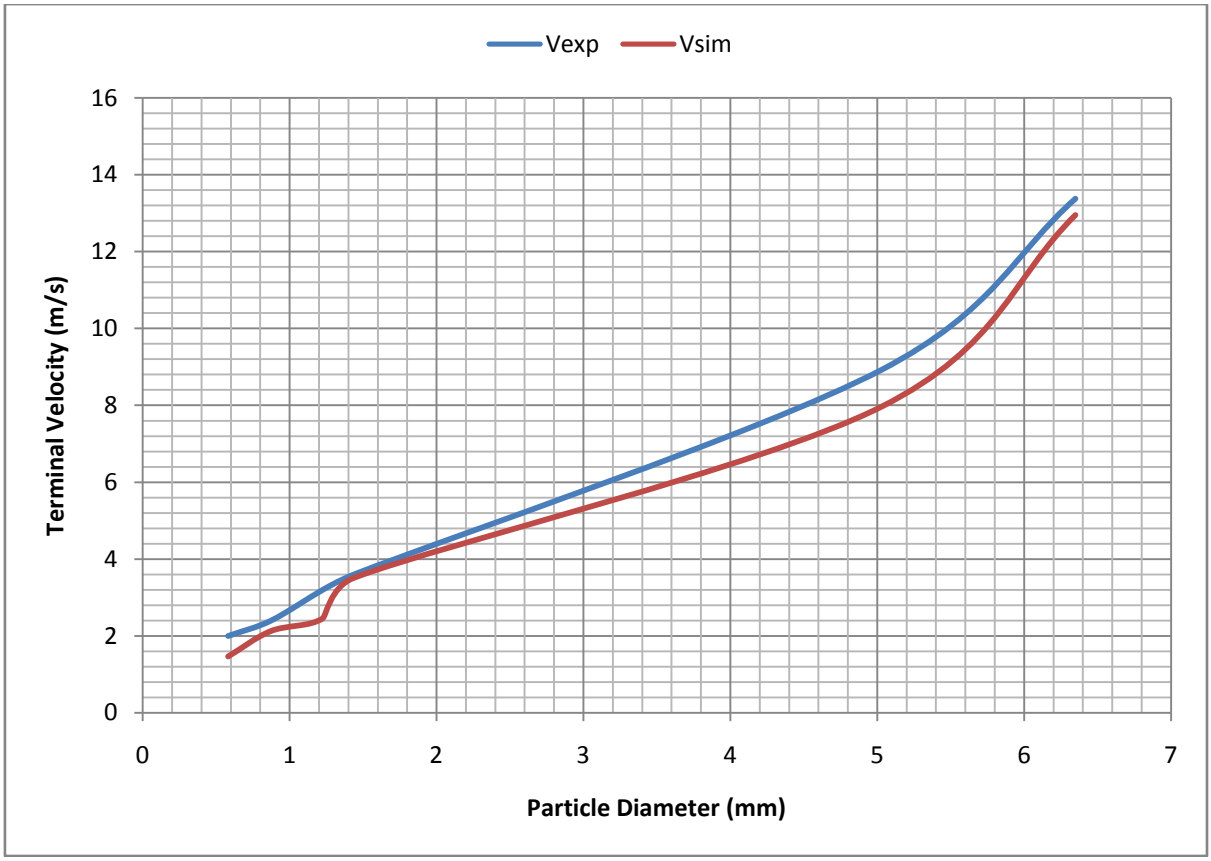

Fig 4.35: Plot of Terminal velocity against Particle size (Experimental/Simulated)

The simulated terminal velocity indicated an exponential dependence to particle diameter which has very good agreement with experimental results but with slightly lower values. This difference may be attributed to the assumption in the model that the particles are spherical while they are actually irregular. Though surface area modification factor was introduced to compensate for this variation but there is still the effect of rotation of the particle as it is conveyed.

CHAPTER 5
CONCLUSION AND RECOMMENDATION

5.1 Conclusion

One-dimensional steady-state non-equilibrium two-phase model has been developed to simulate the convective drying of cassava cultivar, TMe 419 in a vertical upward pneumatic conveying dryer. The model takes into account the momentum, heat and mass transfer between the continuous phase and the dispersed phase. The work determined the physical thermal and aerodynamic properties of cassava cultivar TMe 419. The results indicated that particles of grated cassava are irregular and their size distribution is grater-specific. The density of dewatered mash was determined to be 866.82 kg/m^3 while the particle hardness was 0.769 kg/mm^2, way below the abrasive threshold of 800 kg/mm^2. The terminal velocity of TMe 419 particle is correlated to the particle diameter by the expression $v_t = 0.0813d_p^3 - 0.6624d_p^2 + 2.9718d_p + 0.3967$. The specific heat capacity, thermal conductivity and thermal diffusivity of TMe 419 were determined to be $3.1422\ kJ/(kg°C)$, $0.4634\ \frac{W}{m\,°C}$ and $0.1164\ (\frac{m^2}{s})$ respectively. The drying curve for TMe 419 also showed that the expected moisture content is lower than the critical moisture content. This implies that flash drying is carried out within the constant-rate drying period and agrees with the assertion in literature that flash drying remove surface moisture. These data were inputted into the model which was solved numerically using fourth order Runge-Kutta implemented on

ComsolScript platform for the dispersed phase. The data generated from the solution of the gas phase was used to determine the state of the solid phase by simulation on ComsolMultiphysics platform based on finite element method of analysis. The implementation of the ComsolScript allowed the investigation of the effects of different variables on the operating conditions during pneumatic drying and also on each other. Dryer variables like air inlet velocity, temperature and pressure drop is required in the selection of an appropriate blower and heat exchanger rating. One of the significant results of the investigations is the 'Design Curve' for pneumatic conveyance of TMe 419. It involves the plot of the pressure drop at different air inlet velocities and material feed rate. It generated a family of curves and each curve drawn for each material flow rate. The graphs are discontinuous in areas where the subsisting air inlet velocity and pressure could not support the material flow rate under dispersed flow situation. It was also observed that gas temperature continuously decreases along the dryer, while the solid phase temperature increases continuously until (if the residence time allows) it attains the wet bulb temperature. The increase in the velocity of the gas phase is as a result of the continuous influx of material into the flash tube which far outweighs that of pressure drop due to non-slip boundary condition. The velocity of the particle increases from zero or near zero at the point of introduction accelerates for a while, and attains and maintains the terminal velocity for the rest of its journey through the flash tube. This explains why some of the models reviewed assumed that the particle travels at a uniform velocity across the flash tube and do not account for the initial particle acceleration. This assumption may be

valid for pneumatic conveying because it happens over a considerable distance and the residence time is much more when compared to pneumatic conveying drying or flash drying which happens within a very short interval of time. The very short resident time makes that initial interaction significant because it is at that point that the value of slip velocity and of course heat transfer between the air stream and the particle are at a maximum. Coupling the data from the gas phase to a finite element model of the particle, on Comsol Multiphysics platform predicted the moisture concentration as drying progresses and enables the prediction of optimal flash tube height.

Overall the work has provided a tool for gaining insight into the workings of pneumatic conveying drying of TMe 419 but could easily be adapted for other material or operating conditions by simply changing the relevant input data. Here a tool for the design and performance audit of existing pneumatic conveying dryers has been developed.

5.2 Contribution to Knowledge

This research work made the following contributions to knowledge:

- Generated data for the physical, thermal and aerodynamic properties of TMe 419.
- Adapted the formulation for two-fluid model in developing a model for convective drying of TMe 419.
- Generated a “Design Curve” for Flash drier design handling TMe 419.
- Provided a tool for designing new flash drying plants

- Provided a tool for performance assessment and upgrade of existing flash drier.

5.3 Recommendations

The validation of the model which ignored the mass and heat transfer needs to be revisited. Though good agreement was obtained when the model was modified for pneumatic conveyance only but the task was for pneumatic conveying drying and so the validation of the model must consider mass and heat transfer to obtain the needed assurances before the model is deployed for actual design or performance assessment of an existing plant. This can be done by designating an existing dryer for experimental purpose or constructing a small scale experimental flash dryer for the purpose with all the required instrumentation.

REFERENCES

A

Agbetoye, L.A.S (1999). The Bending Strength of Cassava Tuber, Journal of Science, Engineering and Technology, 6(2) 1800-1808

Almendingen K., Meltzer H.M., Pedersen J.I., Nilsen B.N. and Ellekjaer M.*Eur. J. Clin. Nutr.*, 2000, **54**, 20.

Alvarez P. I., Vega R. and Blasco R., 2005, "Cocurrent Downflow Fluidized Bed Dryer: Experimental Equipment and Modeling", Drying Tech., Vol. 23, pp. 1435-1449.

Ayo Kuye O., Lateef Sanni, Gbassey Tarawali, Ayo D. B,Raji A.O., Otuu Obinna O., Kwaya E.I, Kareem Babatunde, Asiru Bolanle, 2009, " Conceptual Design of Cassava Flash Drier", Technical Report.

B

Baeyens J., Gauwbergen D. V. and Vinckier I., 1995, "Pneumatic Drying: the Use of Large-Scale Data in a Design Procedure", PowderTech., Vol. 83, pp. 139-148.

Benedito J., Carcel J.A., Rossello C. and Mulet A.. *Meat Sci.*, 2001, **57**, 365.

Binaghi M.J., Baroni A., Greco C., Ronayne de Ferrer P.A. and Valencia M., *Arch. Latinoame. Nutr.*, 2002, **52** 43.

Bradbury, J.H. and D.W. Holloway, 1988. Chemical composition of tropical root crops from the south pacific: Significance for human nutrition. Canberra:Australian center of int. Agric. Res., pp: 103-104.

Bradbury, M.G., Egan, S.V., Bradbury, J.H., 1999. Determination of all forms of cyanogens in cassava roots and cassava products using picrate paper kits. Journal of the Science of Food and Agriculture 79, 593–601.

Bunyawanichakul P., Walker G. J., Sargison J. E. and Doe P. E., 2007,"Modelling and Simulation of Paddy Grain (Rice) Drying in a simple Pneumatic Dryer", Biosystems Eng., Vol. 96, pp. 335-344.

C

Charm S. E. (1978). "The Fundamentals of Food Engineering"' 3rd Edition, AVI Publ. Co., Westport, Connecticut.

Choi Y. and Okos M. R. (1986). "Effect of temperature and composition on the thermal properties of food". In "Food Engineering and Process Applications,"Vol 1, pp 93-101. Elsevier Applied Science Publishers, London.

Cotte J.F., Casabianca H., Chardon S., Lheritier J. and Grenier- Loustalot M.F., *J. Chromatogr. A*, 2003, **1021**, 145.

Coultate T.P., *Food: The Chemistry of its Components*, 4th edn., RSC Paperbacks, The Royal Society of Chemistry, Cambridge, 2002.

Cummings J.H. and Englyst H.N., *Trends Food Sci. Technol.*, 1991, **2**, 99.

D

David Mills, 2004,"Pneumatic Conveying Design Guide",2nd Edition,Elsevier Butterworth-Heinemann, pp. 236-257.

Debrand S., 1974, "Heat Transfer during a Flash Drying Process", Ind. Eng. Chem., Process Des. Develop., Vol. 13, pp. 396-404. International Journal of Mechanical Systems Science and Engineering 2:2 2010

Demirata B., Apak R., Afsar H. and Tor I., *J. AOAC Int.*, 2002, **85**, 971.

Doco T., O'Neill M.A. and Pellerin P., *Carbohydr. Polym.*, 2001, **46**, 249.

E

Egan SV, Yeoh HH & Bradbury JH (1998): Simple picrate paper kit for determination of the cyanogenic potential of cassava flour. J. Sci. Food Agric. 76, 39_/48. Ekpenyong TE (1984): Composition of some tropical

Englyst H., *Anim. Feed Sci. Technol.*, 1989, **23**, 27.

Ernesto, M., Cardoso, A.P., Nicala, D., Mirione, E., Massaza, F., Cliff, J., Haque, M.R., Bradbury, J.H., 2002a. Strategy for the elimination of konzo in Mozambique. Roots 8 (1), 8–11.

F

FAO, (1997). FAOSTAT, Statistical Data Base of the Food and Agricultural Organisation (FAO) Of The United Nations. Rome. Italy.

Fyhr C. and Rasmuson A., 1997, "Mathematical Model of Pneumatic Conveying Dryer", AICHE Journal, Vol. 43, pp. 2889-2902.

Fyhr C. and Rasmuson A., 1997, "Steam Drying of Wood Ships in Pneumatic Conveying Dryers", Drying Tech., Vol. 15, pp. 1775-1785.

G

Goñi I., Garcia-Alonso A. and Saura-Calixto F., *Nutr. Res.*, 1997, **17**, 427.

Goñi I., García-Diz L., Mañas E. and Saura-Calixto F., *Food Chem.*, 1996, **56**, 445.

Goodwin J.E, Sage W, Tilly G.P.(1969) "Study of Erosion by Solid Particles". Procedure of IMechE. Vol 183, Mo 15, pp 279-292.

Gorial B. Y, O'callaghan J.R. (1990). "Aerodynamic Properties of Grain/Straw Material". Journal of Agricultural Engineering Research. Volume 46, pp275-290.

Grift T.E., Walker J.T., Hofstee J.W. (1997). "Aerodynamic Properties of Individual Fertilizer Particles". Trans. ASAE, 40(1), pp 13-20.

Gursoy S., Guzel E. (2010). "Determination of Physical Properties of some Agricultural Grains", Research Journal of Applies Sciences, Engineering and Technology, Vol II, PP 492-498.

H

Halos-Kim, L.(1998). Cassava Research Benefit. Nigerian Weekly Newspaper
Concord Newspapers Nig. Ltd. July 14-July20

Hamed M. H., 2005," Choked Gas-Solid Two-Phase Flow in Pipes", J.Eng. Applied Science, Faculty of Engineering, Cairo University, Vol. 52, pp. 961-980.

Han, T., A. Levy, and Y. Peng, 2000, "Model for Dilute Gas-Particle Flow in Constant-Area Lance with Heating and Friction ", Powder Technology, Vol. 112, pp. 283-288.

Heldmam D. R. and Singh R. P. (1981). "Food Process Engineering" 2nd Edition, AVI Publ. Co., Westport, Connecticut.

Horwitz W., Albert R., Deutsch M.J. and Thompson J.N., *J. AOAC*, 1990, **73**, 661.

http://www.barr-rosin.com/images/products/open-circuit-flash-dryer.jpg, accessed 26/06.2010

http://www.barr-rosin.com/images/products/open-circuit-flash-dryer.jpg, accessed 26/06.2010

http://www.ecokleen.com/FLASH%20DRYER%20%20LITERATURE.pdf, accessed 26/06.2010

http://wins.engr.wisc.edu/teaching/mpfBook/node12.html#SECTION00610000000000 000000, accessed 24/01/2011

http://wins.engr.wisc.edu/teaching/mpfBook/node13.html#SECTION0062000000000 0000000, accessed 24/01/2011

http://www.fiiro-ng.org/cassava-flour.htm, accessed 18/06/10

http://www.grc.nasa.gov/WWW/K-12/airplane/airprop.html, accessed 12/02/11

http://www.jazminesmeralda.ifunnyblog.com/averageweatherfornigeria accessed 14/02/11

http://www.starch.dk/isi/starch/cassava.asp, accessed 18/06/10

I

IITA, (1987), Elite Cassava Clones Assessed for Gari Quality. IITA Annual Report &Research Highlights. Ibadan. Pp. 96-97

Isengard H-D., *Food Control*, 2001, **12**, 395.

Ishii M, 1974,"Thermo-Fluid Dynamic Theory of Two-Phase Flow, Eyrolles, France.

K

Kaensup W., Kulwong S. and Wongwises S., 2006, "A Small-Scale Pneumatic Conveying Dryer of Rough Rice", Drying Tech., Vol. 24, pp. 105-113.

Kaensup W., Kulwong S. and Wongwises S., 2006, "Comparison of Drying Kinetics of Paddy Using a Pneumatic Dryer with and without a Cyclone", Drying Tech., Vol. 24, pp. 1039-1045.

Kamerling J.P. and Vliegenthart J.F.G., in *Mass Spectrometry*, ed. Lawson A.M., Walter de Gruyter, Berlin, 1989, p. 176.

Kamizake N.K.K., Gonçalves M.M., Zaia C.T.B.V. and Zaia D.A.M., *J. Food Comp. Anal.*, 2003, **16**, 507.

Kemp I. C., Bahu R. E. and Pasley H. S., 1994, "Model Development and Experimental Studies of Vertical Pneumatic Conveying Dryers", Drying Tech., Vol. 12, pp. 1323-1340.

Kemp I. C and Oakley D. E., 1997, "Simulation and Scale-up of Pneumatic Conveying and Cascading Rotary Dryers", Drying Tech., Vol. 15, pp. 1699-1710.

Kilfoil M., 2003, "Numerical Simulation of Simultaneous Drying and Pneumatic Conveying: Small Metallic Filter Cake Particles", South African Institute of Mining and Metallurgy.

L

Lawrence J.F. and Iyengar J.R., *J. Chromatogr. A*, 1985, **350**, 237.

Levy A. and Borde I., 1999, "Steady State One Dimensional Flow Model for a Pneumatic Dryer", Chem. Eng. Processing, Vol. 38, pp. 121-130.

Littman, H., Day, J-Y and Morgan M.H., 2000, “A Model for the Evaporation of Water from Large Glass Particles in Pneumatic Transport”, *The Canadian Journal of Chemical Engineering*, vol. 78, part 1, Feb. 2000, pp. 124–131.

Lowry O.H., Rosebrough N.J., Farr A.L. and Randall R.J., *J. Biol. Chem.*, 1951, **193**, 265.

Lynch J.M.,. Barbano D.M, Healy P.A. and Fleming J.R., *J. AOAC Int.*, 1997, **80**, 1038.

M

Menezes E.W., De Melo A.T., Lima G.H. and Lajolo F.M., *J. Food Comp. Anal.*, 2004, **17**, 331.

Mkumbira, M. Patino, G. Ssemakula, and A. Dixon (2005). "Standards for cassava products and guidelines for export." IITA, Ibadan, Nigeria

Mohsenin, N.N.(1980). “Physical Properties of Plants and Animal Materials. Gordon and Breach science Publishers, New York.

Moyers C.G and Baldwin G.W., 1997, “Psychrometery, Evapourative Cooling, and Solid Drying,”Perry’s Chemical Engineer’s Handbook, 7th Ed., McGraw-Hill, Inc.

N

NamKung W. and Cho M., 2004, "Pneumatic Drying of Iron Ore particles in a Vertical tube", Drying Tech., Vol. 22, pp. 877-891.

Narimatsu C. P., Ferreira M. C. and Feire J. T., 2007, "Drying of Coarse Particles in a Vertical Pneumatic Conveyor", Drying Tech., Vol. 25, pp. 291-302.

Njie, D.N., Rumsey, T.R., Singh, R.P.,‘Thermal Properties of Cassava Yam and Plantain’, Journal of Food Engineering, June 1998. v. 37 (1)

Nwabanne J. T., 2009,”Drying Characteristics and Engineering Properties of Fermented Ground Cassava”, African Journal of Biotechnology, Vol. 8(5), pp. 873-876.

O

Obafemi, (1998). Cassava: African Today. June Pp 48.

Oladele Peter Kolawole, Leo A.S. Agbetoye, and A. S. Ogunlowo (2007) “Cassava Mash Dewatering Parameters”. International Journal of Food Engineering, Volume 3, issue 1, pp 1

Oladele P. K, Leo Ayodeji A, A. S. Ogunlowo, (2007), ‘Cassava Mash Dewatering Parameters’. International Journal of Food Engineering, Volume 3, issue 1.

Oladele P. K, Leo Ayodeji A, A. S. Ogunlowo, (2007), ‘Strength and Elastic Properties of Cassava Tuber’. International Journal of Food Engineering, Volume 3, issue 2.

Onabolu, A.O., Oluwole, O.S.A., Bokanga, M., Rosling, H., 2001. Ecological variation of intake of cassava food and dietary cyanide load in Nigerian communities. Public Health Nutrition 4, 871–876.

Onyeka T.J, Ekpo E.J, Dixon A.G.O (2005), "Virulence and host –pathogen Interaction of Botryodiplodia theobromae Isolates of Cassava Root Rot Disease". Journal of Phytopathology. Volume 153, issue 11-12, page 726-729.

Onyeike E. N. and Acheru G.N., *Food Chem.*, 2002, **77**, 431.

Otuu Obinna et al (2010), 'Characterisation of Cassava Graters'. Unpublished research paper.

Otuu Obinna et al (2009). 'Machine Building Infrastructure for Processing Equipment'. RMRDC Investors Forum

P

Paredes-López O., Guevara-Lara F., Schevenin-Pinedo M.L. and Montes-Rivera R., *Plant Foods Human Nutrit.* (Dordrecht, Netherlands), 1989, **39**, 137.

Padmaja, G., 1995. Cyanide detoxification in cassava for food and feed uses. Critical Reviews in Food Science and Nutrition 35, 299–339.

Paul Singh R., Dennis R. Heldman, 2001,"Introduction to Food Engineering"3rd Edition, Academic Press

Pelegrina A. H. and Crapiste G. H., 2001, "Modelling the Pneumatic Drying of Food Particles", J. Food Eng., Vol. 48, pp. 301-310.

Prosky L. and Mugford D., *Carbohydr. Polym.*, 2001, **44**, 81.

R

Radford R. D., 1997, "A Model of Particulate Drying in Pneumatic Conveying Systems", Powder Tech., Vol. 93, pp. 109-126.

Rocha, S.C.S. (1988), Contribution to study of vertical pneumatic drying: simulation and influence of the gas-solid heat transfer coefficient, PhD Thesis (in Portuguese), Escola Politécnica/USP, São Paulo, SP, 258 p.

Rodolfo R. Rosales, Adam Powell, Franz-Josef Ulm, Kenneth Beers, 2006,"Continuum Modelling Simulation", MIT.

Rosenthal I., Merin U., Popel G.and Bernstein S., *J. AOAC*, 1985, **68**, 1226.

S

Saastamoinen, J. (1992), *Model of flash drying*, Proceedings of the 8th International Drying Symposium (IDS'92), Montreal, Quebec, Canada, August 2-5, pp434 – 443

Samy M. El-Behery, W.A. El-Askary, K.A. Ibrahim and Mofreh H. Ahmed, 2009,"Porous Particle Drying in a Vertical Upward Pneumatic Conveying Dryer", World Academy of Science, Engineering and Technology, Vol 53.

Sanni, L.O., B. Maziya-Dixon, J. N. Akanya, C. I. Okoro, Y. Alaya, C. V. Egwuonwu, R. U. Okechukwu, C. Ezedinma, M. Akoroda, J. Lemchi, F. Ogbe, E. Okoro, G. Tarawali, J. Sebecicacute B., *Die Nahrung*, 1987, **31**, 817.

Siebel J. E. (1892). Specific heat of various products. Ice Refrigeration 2, pp 256

Singh P.C., Bhamidipati S., Singh R.K., Smith R.S. and Nelson P.E., *Food Control*, 1996, **7**, 141.

Skuratovsky I., Levy A. and Borde I., 2003, "Two-Fluid Two-Dimensional Model for Pneumatic Drying", Drying Tech., Vol. 21, pp. 1645-1668.

Skuratovsky I., Levy A. and Borde I., 2005, "Two-Dimensional Numerical Simulations of the Pneumatic Drying in Vertical pipes", Chem. Eng. Processing, Vol. 44, pp. 187-192.

Soral-Smietana M., Amarowicz R., Swigo A. and Sijtsma L., *Int. J. Food Sci. Nutr.*, 1999, **50**, 407.

Sopa Cansee[1], Cumnueng Watyotha[1], Thavachai Thivavarnvongs[1], Juntanee Uriyapongson[2], and Jatuphong Varith (2008). 'Effects of temperature and concentration thermal properties of cassava starch solution'. Songclanacarin Journal of science of technology. 30 (3), 405-411, May - Jun. 2008.

Sweat V. E. (1974). "Experimental values of thermal conductivity of selected fruits and vegetables," Journal of Food Science, vol 39. pp 1080

Sweat V. E (1975). "Modelling Thermal Conductivity of Meats. Trans American Society of Agric. Engrg. Vol 18 (1), pp 564-565, 567, 568.

Sweat V. E (1986). Thermal properties of foods. In "Engineering Properties of Foods," pp 49-87. Mercel Dekker Inc., New York. \

T

Takashi K., *Nutr. Res.*, 2001, **21**, 517.

Thorpe G.R., Wint A. and Coggan G.C., 1973, "The Mathematical Modelling of Industrial Pneumatic Driers", Transactions of the Institution of Chemical Engineers, Vol. 51, pp. 339–348.

W

Watkins K.L., Veum T.L. and Krause G.F., *J. AOAC*, 1987, **70**, 410.

Welty J. R., Wicks G. E. and Wilson R. E., 1984, "Fundamentals of Momentum, Heat, and Mass Transfer", 3rd Ed., John Wiley & Sons,

APPENDIX

Appendix 1-1: Cassava Pneumatic Drying Equipment Owners

S/N	Processors	Address	Installed Capacity (tonne)
1	PeakproductsLtd Abeokuta	Musada Complex Itaosin Abeokuta 08033342174	8
2	NextDoor Partners	Oyo (08051129296, 08059059192)	6
3	Vesa Farms Ltd, Benin City	62 Ugbor Rd Benin City (08039472587)	30
4	Jafee Nig Ltd,	Ogunsolu Village Obada Oko Abeokuta 08033488745	2.5
5	Jodek Ventures	Temidire, Eruwa, Oyo 08055280046	2.5
6	Blopamed Nig Ltd	Imuwen Ijebu Imusin 08023126236	2.5
7	Eltees Nig Ltd	Olomore Abeokuta 08033857463	6
8	Wahan Fds Ltd	Afon-Kwara State 08033016572	2.5
9	Elegance Farms & products	Wasimi Railway Station Abeokuta 08023145573	4
10	Opendoor systems Ltd	Otta-Ogun State (08067719487)	6
11	Human factor Engineers	Itori Abeokuta (08028491961)	3
12	Dele Solanke &	Olorunsogo village, Papalantor-Ifo,	3

	Assoc Ltd	Ogun State (08034222122)	
13	Agadu Farms Ltd	Gboko-Benue State (08082390495)	6
14	Don-Link Pharm Ltd	Iba Village (08034294292)	3
15	Adboi Farms Ltd	Km 10 Ondo-Ore Exp Road, Ondo (08065017253)	3
16	Bolfem Corporate Services	Jos (Pst Doye) 08059365036 or 08034649492	6
17	Fadett Farms Ltd	Ofada Town (08033156490)	3
18	Mic Makin Ind	Ondo Road Akure	6
19	Obasanjo farms	OFN Owiwi Abeokuta	3
20	Ijado Farm Project	Ilaro-Town, Ogun State 08028481127	3
21	Meridian Farms Ltd	Mowe Ofada	3
22	Twain Nig Ltd	157 Isolo Road Amazing Grace Shopping Complex, Isolo, Lagos	3
23	Matsol farms Ltd	Plot 1382 Block 62, Amuwo-Odofin Estate, Lagos (08037179296	3
24	Codas Resources Nig Ltd	606 Ikorodu road, kosofe Mile 12, Lagos 08034984602	6
25	Zubrab Global link Ltd	FF 77 Shy Shopping Plaza Hadan Kayo 08023727036	3
26	Dugba Farms	08033574542	3
27	Soko Tinjin Jion & Son Ent.	Mile 12 Ketu Lagos 08034085506	6
28	Aniplant & Company	Olusanya Comp. Ajegunle Junction Shagamu	2
29	Samdoab Nig Ltd	Betty Farms-Ifon Orolu, Osun State 08056993399	3
30	Kanawa Nig Ltd	Kano	4
31	Al-Janon Nig Ltd	Idiroko Ogun State (08055244042)	
32	Omooye Farms	Afin-Kwara State (08035101429)	3
33	Meridian Farms	Mowe-Ofada (08055321000)	3
34	Ginger Alla Vent.	Ibadan Plant (08037283944)	3
35	Sunab Tech Ltd	Kogi State (08023406529)	
36	Deladder Investment	Benin, Ugbor Road 0803384007	3
37	African World Services Ltd	Ibadan-Oyo	3
38	Zoo World Intl	Ilaro-Idogo Road (08054674467)	3
39	Morafel	Ogere-Ogun State	6

	Commodities		
40	A. G. Domie Int'L	J. S. Jarko Way Gboko(08034416171)	4
41	Lentus Ventures	Benin 08023014988	4
42	Grace & Gino Allied	Amuwo Odofin Estate	3
43	Ejilogwu Agro Allied	Ankpa Kogi	3
44	Godilogo farms	Obudu-Cross rivers 080378771410	7
45	Rose Endeavours	Ahoada, PortHarcourt, Rivers State	2.5
46	Jopat industries	Delta State	2.5
47	Jismac Farms	Ogoja - Cross Rivers state.	2.5

(Culled from *'Threat to Cassava Flour policy in Nigeria'* by Prof Lateef Sanni)

Appendix: 4-1: Cassava Particle Size Distribution

Table :Particle Size Distribution Test Results Summary

Sieve	Particle Size	Log	Grater A				Grater B				Grater C	
			Fractional plot (wt % undersize)	Cum. plot	Particle Size	Log	Fractional (wt % undersize)	Cum. (wt undersize)	Particle Size	Log	Fractional plot (wt % undersize)	Cum. plot
¼ in	6.35	0.199	1.58	100	6.35	-0.10791	0.78	100	6.35	0.2355	1.72	100
#6	3.353	0.74	5.5	98.42	3.353	0.72099	5.26	99.22	3.353	0.8129	6.5	98.28
#12	1.679	1.284	19.24	92.92	1.679	1.3084	20.34	93.96	1.679	1.6547	45.15	82.78
#20	0.848	1.666	46.39	73.68	0.848	1.5577	36.12	82.62	0.848	1.4736	29.76	64.63
#40	0.419	1.337	21.72	27.29	0.419	1.4161	26.07	53.5	0.419	1.0821	12.08	36.87
#70	0.211	0.732	5.39	5.57	0.211	1.0090	10.21	27.43	0.211	0.6117	4.09	15.79
#100	0.15	-0.745	0.18	0.18	0.15	0.0863	1.22	1.22	0.15	-0.1549	0.7	0.7

Appendix 4-2: Proximate

```
%program that calculates thermal properties based on Proximate
Analysis

T=25;%particle temperature in degrees celsius

x_a=0.013;%mass fraction of ash content
x_f=0.013;%mass fraction of fat content
```

```
x_p=0.0059;%mass fraction of protein content
x_w=0.6092;%mass fraction of water content
x_fib=0;%mass fraction of fibre content
x_c=0.3589;%mass fraction of carbohydrate content
x_all=x_a+x_f+x_p+x_w+x_fib+x_c

k_prot=0.17881+0.0011958*T-0.0000027178*T^2;%Temperature function
k01=x_p*k_prot;%property component contribution
k_fat=0.18071-0.0027604*T-0.00000017749*T^2;
k02=x_f*k_fat;
k_carb=0.20141+0.0013874*T-0.0000043312*T^2;
k03=x_c*k_carb;
k_fib=0.18331+0.0012497*T-0.0000031683*T^2;
k04=x_fib*k_fib;
k_ash=0.32962+0.0014011*T-0.0000029069*T^2;
k05=x_a*k_ash;
k_wat=0.57109+0.0017625*T-0.0000067036*T^2;
k06=x_w*k_wat;
k_ice=2.2196-0.0062489*T-0.00010154*T^2;
k07=0;
k=k01+k02+k03+k04+k05+k06+k07;%thermal conductivity

alpha_prot=0.068714+0.00047578*T-0.0000014646*T^2;
a01=x_p*alpha_prot;
alpha_fat=0.098777-0.00012569*T-0.000000038286*T^2;
a02=x_f*alpha_fat;
alpha_carb=0.080842+0.00053052*T-0.0000023218*T^2;
a03=x_c*alpha_carb;
alpha_fib=0.073976+0.00051902*T-0.0000022202*T^2;
a04=alpha_fib*x_fib;
alpha_ash=0.12461+0.00037321*T-0.0000012244*T^2;
a05=alpha_ash*x_a;
alpha_wat=0.13168+0.00062477-0.0000024022*T^2;
a06=alpha_wat*x_w;
alpha_ice=1.1756-0.0060833+0.000095037*T^2;
a07=0;
alpha=a01+a02+a03+a04+a05+a06+a07;%thermal diffussivity

rho_prot=1329.9-0.51840*T;
rho01=rho_prot*x_p;
rho_fat=925.59-0.41757*T;
rho02=rho_fat*x_f;
rho_carb=1599.1-0.31046*T;
rho03=rho_carb*x_c;
rho_fib=1311.5-0.36589*T;
rho04=rho_fib*x_fib;
rho_ash=2423.8-0.28063*T;
rho05=rho_ash*x_a;
rho_wat=0.099718-0.0031439*T-0.0037574*T^2;
rho06=rho_wat*x_w;
rho_ice=916.89-0.13071*T;
rho07=0;
rho=rho01+rho02+rho03+rho04+rho05+rho06+rho07;%density

cp_prot=2.0082+0.0012089*T-0.0000013129*T^2;
cp01=cp_prot*x_p;
cp_fat=1.9842+0.0014733*T-0.0000048008*T^2;
cp02=cp_fat*x_f;
cp_carb=1.5488+0.0019625-0.0000059399*T^2;
cp03=cp_carb*x_c;
cp_fib=1.8459+0.0018306*T-0.0000046509*T^2;
```

```
cp04=cp_fib*x_fib;
cp_ash=1.0926+0.0018896*T-0.000999516*T^2;
cp05=cp_ash*x_a;
cp_wat=4.1762-0.000090864-0.0000054731*T^2;
cp06=cp_wat*x_w;
cp_ice=2.0623+0.0060769*T;
cp07=0;
cp=cp01+cp02+cp03+cp04+cp05+cp06+cp07;%specific heat capacity
output=[cp,k,alpha,rho,x_all]
```

Appendix 4-3: reference for air moisture concentration.

www.engineeringtoolbox.com/moisture-holding-capacity-air-d_281.html

Appendix 4-4: reference for wet bulb temperature

www.sugartech.co.za/psychro/index.php

Appendix 4-5: reference for Dew point

www.sugartech.co.za/psychro/index.php

Appendix 4-6: Table of Air properties (www.engineeringtoolbox.com/air-properties-d_156html)

Temperature - t - (^oC)	Temperature - t - (K)	Density - - (kg/m^3)	Specific heat capacity - c_p - (kJ/kg.K)	Thermal conductivity - l - (W/m.K)	Kinematic viscosity - v - x 10^{-6} (m^2/s)	Expansion coefficient - b - x 10^{-3} (1/K)	Prandtl's number - P_r -
-150	123.15	2.793	1.026	0.0116	3.08	8.21	0.76
-100	173.15	1.98	1.009	0.016	5.95	5.82	0.74
-50	223.15	1.534	1.005	0.0204	9.55	4.51	0.725
0	273.15	1.293	1.005	0.0243	13.3	3.67	0.715
20	293.15	1.205	1.005	0.0257	15.11	3.43	0.713
40	313.15	1.127	1.005	0.0271	16.97	3.2	0.711

60	333.15	1.067	1.009	0.0285	18.9	3	0.709
80	353.15	1	1.009	0.0299	20.94	2.83	0.708
100	373.15	0.946	1.009	0.0314	23.06	2.68	0.703
120	393.15	0.898	1.013	0.0328	25.23	2.55	0.7
140	413.15	0.854	1.013	0.0343	27.55	2.43	0.695
160	433.15	0.815	1.017	0.0358	29.85	2.32	0.69
180	453.15	0.779	1.022	0.0372	32.29	2.21	0.69
200	473.15	0.746	1.026	0.0386	34.63	2.11	0.685
250	523.15	0.675	1.034	0.0421	41.17	1.91	0.68
300	573.15	0.616	1.047	0.0454	47.85	1.75	0.68
350	623.15	0.566	1.055	0.0485	55.05	1.61	0.68
400	673.15	0.524	1.068	0.0515	62.53	1.49	0.68

Appendix 4-12: Experimentation at 40°C

Initial moisture content = 60.82%			Time (mins)							
Crucible	Wgt of crucible(g)	Weight of sample (g)	30	60	90	120	150	180	210	240
A	2.57	10	7.73	5.34	4.77	4.62	4.31	4.30	4.25	4.20
B	2.56	10	6.03	4.73	4.23	4.24	4.16	4.11	4.07	4.02
C	2.57	10	7.70	5.37	4.67	4.51	4.28	4.17	4.13	4.02
D	2.56	10	7.88	5.41	4.74	4.55	4.34	4.21	4.17	4.12
	Average	10	7.34	5.21	4.60	4.48	4.27	4.20	4.16	4.15
Weight loss (moisture removed)			2.66	4.79	5.40	5.52	5.73	5.80	5.84	5.85
% weight loss(moisture removed)			26.6	47.9	54.0	55.2	57.3	58.0	58.4	58.5
% moisture content			34.22	12.92	6.84	5.62	3.57	2.82	2.42	2.32

Appendix 4-13: Experimentation at 45°C

Initial moisture content = 60.82			Time (mins)							
Crucible	Wgt of crucible(g)	Weight of sample (g)	30	60	90	120	150	180	210	240
A	2.55	10	7.18	6.22	5.85	5.56	5.25	5.11	5.02	4.88
B	2.56	10	6.82	5.89	5.55	5.28	5.00	4.86	4.78	4.66
C	2.57	10	7.52	6.42	5.92	5.56	5.22	5.05	4.96	4.83
D	2.58	10	6.95	6.04	5.71	5.45	5.18	5.04	4.96	4.85
	Average	10	7.11	6.14	5.76	5.46	5.16	5.11	4.93	4.80
Weight loss (moisture removed)			2.89	3.86	4.24	4.54	4.84	4.89	5.07	5.20
% weight loss(moisture removed)			28.9	38.6	42.4	45.4	48.4	48.9	50.7	52.0
% moisture content			31.92	22.22	18.42	15.42	12.42	11.92	10.12	8.82

Appendix 4-14: Experimentation at 50°C

Initial moisture content = 60.82			Time (mins)							
Crucible	Wgt of crucible(g)	Weight of sample (g)	30	60	90	120	150	180	210	240
A	2.57	10	6.62	5.09	4.67	4.41	4.25	4.21	4.18	4.16
B	2.56	10	6.68	5.91	5.46	5.06	4.79	4.61	4.48	4.38
C	2.56	10	7.50	5.47	5.03	4.71	4.50	4.39	4.31	4.19
D	2.57	10	6.66	5.24	4.84	4.57	4.32	4.27	4.25	4.19
	Average	10	6.87	5.43	5.00	4.69	4.47	4.37	4.31	4.23
Weight loss (moisture removed)			3.13	4.57	5.00	5.31	5.53	5.63	5.69	5.77
% weight loss(moisture removed)			31.3	45.7	50.0	53.1	55.3	56.3	56.9	57.7
% moisture content			29.54	15.12	10.82	7.72	5.52	4.54	3.92	3.12

Appendix 4-15: Experimentation at 55°C

Initial moisture content = 60.82			Time (mins)							
Crucible	Wgt of crucible(g)	Weight of sample (g)	30	60	90	120	150	180	210	240
A	2.59	10	7.00	5.53	5.04	4.77	4.55	4.40	4.31	4.26
B	2.56	10	7.34	5.99	5.51	5.21	4.97	4.81	4.65	4.53
C	2.57	10	6.90	5.81	5.34	5.05	4.84	4.67	4.53	4.41
D	2.55	10	6.06	5.09	4.73	4.52	4.38	4.29	4.24	4.19
	Average	10	6.83	5.61	5.16	4.89	4.69	4.54	4.43	4.35
Weight loss (moisture removed)			3.17	4.39	4.84	5.11	5.31	5.46	5.57	5.65
% weight loss(moisture removed)			31.7	43.9	48.4	51.1	53.1	54.6	55.7	56.5
% moisture content			29.12	16.92	12.42	9.72	7.72	6.22	5.12	4.32

Appendix 4-16: Experimentation at 60°C

Initial moisture content = 60.82			Time (mins)							
Crucible	Wgt of crucible(g)	Weight of sample (g)	30	60	90	120	150	180	210	240
A	2.56	10	5.58	4.68	4.31	4.20	4.04	3.95	3.85	3.75
B	2.57	10	5.21	4.39	4.07	3.95	3.76	3.63	3.51	3.42
C	2.56	10	5.39	4.53	4.21	4.09	3.93	3.83	3.74	3.66
D	2.58	10	5.43	4.62	4.32	4.21	4.04	3.95	3.85	3.78
	Average	10	5.40	4.56	4.20	4.11	3.94	3.92	3.92	3.92
Weight loss (moisture removed)			4.60	5.44	5.80	5.89	6.06	6.08	6.08	6.08
% weight loss(moisture removed)			46.0	54.4	58.0	58.9	60.6	60.8	60.8	60.8
% moisture content			14.82	6.42	2.82	1.92	0.22	0.02	0.02	0.02

Appendix 5-1: Comsol Script Program

```
%Program that evaluates gas and solid phase variables under
%Vertical Upwards Pneumatic Conveying Drying.
%format('long')
rho_s= 866.8235;%particle density
d=0.51;%pipe diameter in meters
d_p= 0.005027;%particle diameter in meters
r_p= d_p/2;%particle radius in meters
f_sa= 1.1;%surface area modification factor (sphericity)
A= (pi*d^2)/4;%tube cross-sectional area
D_wv_a= 0.000026;%diffusivity of water vapour in air
R_univ= 8314.4621;%universal gas constant
M_w= 18.015;%molecular weight of water
g= 9.81;% acceleration due to gravity
k_mat= 17;%thermal conductivity of tube material
t_h= 0.0015;%thickness of tube wall
r_in = d/2;%tube inner wall radius
r_out= (d+(2*t_h))/2;%tube outer wall radius
r_air_inf = 5; %estimated distance(m) away from the tube that the
temperature rise is not felt
R= 0.2871;%gas constant
g_x= 9.81;%acceleration due to gravity
dur= 8; %duration of feeding
tput= 3; %throughput (tonnes per dur)
F = tput/(3.6*dur); %feedrate in kg/s
F_v= F/rho_s;     %feedrate in m3/s
T_inf_out= 30;%temperature in the vicinity of the tube
V= (4*pi*r_p^3)/3;%volume of particle
m_p= rho_s*V;% mass of particle
P= pi*d;%tube perimeter

A_sa_p= 4*pi*r_p^2*f_sa;
A_sa_p_perkg= A_sa_p*f_sa/m_p;
chi= A_sa_p_perkg*rho_s*d_p/6;
A_pr_p= (pi*d_p^2)/4;

u_g0= 24;%inlet velocity must be high for dilute phase conveying
(stay above 10)
T_g0= 160;%air initial temperature
RH= 45;%relative humidity of air
C_b= 0.0135; %air moisture content, moisture concentration-
kgwater/kgdryair !!!read off psychrometric chart.
u_s0= 0.001;%initial particle velocity
T_s0= 25;%initial particle temperature
rho_g0= 1.287841156-0.004250962*T_g0+0.00000944905*T_g0^2-
0.00000000903741*T_g0^3;
Q_v0= A*u_g0;
Q_m0= rho_g0*Q_v0;
P_g0=0.365*Q_m0*(T_g0+273.15)/((d^2)*u_g0);%equ 9.19: David Mills
airprop0;%mfile that determines air properties at a initial
conditions
tube_length= 10;
x_g= 0.01;%discretisation size
N= tube_length/x_g;
A_c= P*x_g;
u_g= zeros(N+1,1);
T_g= zeros(N+1,1);
u_s= zeros(N+1,1);
T_s= zeros(N+1,1);
u_g(1)= u_g0;
T_g(1)= T_g0;
u_s(1)= u_s0;
```

```
T_s(1)= T_s0;
rho_g(1)= rho_g0;
Q_v(1)= Q_v0;
Q_m(1)= Q_m0;
P_g(1)= P_g0;
cp_g(1)= cp_g0;
k_g(1)= k_g0;
v_g(1)= v_g0;
mu_g(1)= mu_g0;
pr(1)= pr0;

for i = 1:N
  position=i*x_g;
  T_db= T_g(i);
T_w= 158;% tube wall temperature
T_wb= 134.041;
T_inf_in= T_g(i);
T_f= (T_inf_in+T_s(i))/2;
W_s= 0.0202;
W_g= 0.0101;
T_f_air_out= (T_inf_out+T_w)/2;
cp_s=
(3.1519+0.0006998*T_s(i)+0.00000300301*T_s(i)^2+0.0000000000000000842
7*T_s(i)^3)*1000;%is this verifiable visa vis proximate update
disper = Q_m(i)/F;
if disper<12 %the degree of dispersion of particles in the
air_stream.
  warning('The flow situation is no longer dispersed')
else
  %warning('The flow situation is dispersed')
end
airprop;%mfile that determines air properties at a given temperature
phi= F*dur/(F*3.6);% should be between 1 and 20 for valid model
analysis of dilute pneumatic conveyance
alpha_g= Q_m(i)/(Q_m(i)+F);
alpha_s= F/(F+Q_m(i));
Q_v(i+1)= A*u_g(i);
Q_m(i+1)= rho_g(i)*Q_v(i);
Re= (rho_g(i)*u_g(i)*d)/mu_g(i);
% the model assumes that all pipes are hydraulically smooth
if Re<2100
  f=16/Re;%Hagen-Poiseuille
  elseif Re<4000
    warning: 'reynold number is within transition flow range'
    elseif Re>4000;%Blasius
        f=0.3164/(Re^0.25);% Perry  pp.6-10
  end
% evaluating convective heat transfer between the gas phase and the
pipe inner wall
airpropw;%mfile that determines air properties at a the walls
if Re<2100
  nu=1.86*(Re*pr_g_w*d/x_g)^0.33*((mu_g(i)/mu_g_w)^0.14);
  warning:'flow is laminar'
  elseif Re<10000
    nu= ((f/8)*(Re-1000)*pr_g_w)/(1+12.7*((f/8)^0.5)*((pr_g_w^(2/3))-
1));
    warning:'flow is translational'
    elseif Re>10000
      nu= 0.023*(Re^0.8)*(pr_g_w^0.33)*((mu_g(i)/mu_g_w)^0.14);
      end
h_a_w = nu*k_g(i)/d;
```

```
%evaluates conductive heat transfer resistance between inner tube
wall and outer tube wall
R_cond =log(r_out/r_in)/(2*pi*x_g*k_mat);
h_cond = 1/R_cond; %conductive heat transfer between inner and outer
tube walls

%evaluation of natural convective heat transfer coefficient
airpropfout;%mfile that determines air property at the tube outside
film
beta_f_out= (3.655633-0.01216*T_f_air_out+0.0000274*T_f_air_out^2-
0.000000027*T_f_air_out^3)*0.001;
Gr= d^3*(rho_g_f_out^2)*g*beta_f_out*(T_w-T_inf_out)/mu_g_f_out^2;
if d<=35*x_g/Gr^0.25
  warning('the cylinder cannot be approximated to a flat plate')
else
  %warning('the cylinder approximates a flat plate')
end
Ra= Gr*pr_f_out;
if Ra<10^4
  warning('Rayliegh number is below range')
  elseif Ra<10^9
    a=0.59;
    m=0.25;
    elseif Ra<10^13
      a=0.1;
      m=0.33;
      else
        warning('Rayliegh number is above range')
        end
nu_out= a*Ra^m;
h_free_conv= nu_out*k_g_f_out/d ;
A_c= P*x_g;
h_T_nomat= 1/((1/h_a_w)+(t_h/(k_mat*A_c))+ (1/h_free_conv));%heat
transfer through the wall in the abscence of cassava particle
q_T_nomat= h_T_nomat*A_c*(T_g(i)-T_inf_out);

%SUMMARY OF AIR ONLY
PROPERTIES!!!!!!!!!!!!!!!!!!!!!!!!!!!!!!!!!!!!!!!!!!!!!!!!!!!!!!
T_g_nomat= T_g(i)-(q_T_nomat*0.001/(Q_m(i)*cp_g(i)));%(AIR ONLY
TEMPERATURE!!!)(T_g_(i+1))
%P_g(i+1) = P_g(i)-(4*f*x_g*rho_g(i)*u_g(i)^2/(2*d))*0.001; %(AIR
ONLY PRESSURE!!!)
%u_g(i+1)= P_g(i)*Q_v(i)*T_g(i+1)/(P_g(i+1)*T_g(i)*A);%(AIR ONLY FLOW
VELOCITY!!!)

%temperature with material
!!!!!!!!!!!!!!!!!!!!!!!!!!!!!!!!!!!!!!!!!!!!!!!!!!!!!!!!!!!!!!!!!!!!!!
!!!start

T_inf_air_in= T_g_nomat;

T_f_air_in= (T_s(i)+T_inf_air_in)/2;
airpropfin;
Re_Tf= rho_g_Tf*d_p*abs(u_g(i+1)-u_s(i))/mu_g_Tf;
nu_Tf= 2+(0.6*(Re_Tf^0.5)*(pr_Tf^(1/3))) ;
sc_Tf= mu_g_Tf/(rho_g_Tf*D_wv_a);
h_T = nu_Tf*k_g_Tf/d_p; %convective heat transfer coefficient between
air stream and particle
N_p_vol= 6*alpha_s/(pi*d_p^3);
N_p_len= 6*alpha_s*A/(pi*d_p^3);
q_T = N_p_vol*h_T*A_c*(T_inf_air_in-T_s(i));
```

```
Re_p= rho_g(i)*d_p*abs(u_g_mat-u_s(i))/mu_g(i);
if Re_p<=1
  cd= 24/Re_p;
  elseif Re_p<=400
    cd=24/Re_p^0.646;
    elseif Re_p<=200000
      cd= 0.44;
      elseif Re_p<300000
        cd= 0.5;
      elseif Re_p>300000
        warning('the particle Reynolds number is out of range')
       end

sc= mu_g(i)/(rho_g(i)*D_wv_a);
sh= 2+0.6*(Re_p^(1/2))*(sc^(1/3));
h_m= sh*D_wv_a/d_p; %mass transfer coefficient (k_c in m/s)
h_m_massunit = m_p/h_m; %mass transfer coefficient (mass units)
m_s= h_m*chi*pi*d_p^2*M_w*P_g(i)*(W_s-W_g)/(0.622*R_univ*T_wb);
%moisture loss per particle
s_mass= N_p_len*m_s;%mass transfer between phases
u_g(i+1)= (s_mass*x_g/(A*rho_g(i)*alpha_g))+ u_g_mat;%continuity
equation for gas phase - equation
3.9************************************************
u_g_ave = (u_g(i)+u_g(i+1))/2;
s_mom= -N_p_len*cd*pi*d_p^2*rho_s*(u_g(i+1)-u_s(i))*abs(u_g(i)-
u_s(i))/8;
P = pi*d;
f_p= 2*0.039*Re_p^(-0.26);
F_wg= pi*d*(f_p/2)*rho_g(i)*(alpha_g*u_g(i+1))^2;
%momentum equation for gas phase - equation
3.52*****************************************************************
*******************************
P_g(i+1)= P_g(i)-((-2*s_mass*A*u_g(i+1)*x_g)-
(F_wg*x_g/A)+(alpha_g*rho_g(i)*g*x_g)+ (s_mom*A*x_g))/1000;%(AIR
PRESSURE WITH MATERIAL INFLUENCE)
P_g_ave= (P_g(i)+P_g(i+1))/2;
%pressure with material!!!!!!!!!!!!stop
h_a_p = h_T;
q_ig= -N_p_vol*h_a_p*(d_p^2)*(T_g(i)-T_s(i));%rate of convective heat
transfer between air stream and particle
w_ig= s_mom*u_s(i);%rate of work done by the air stream to the
particle
s_energy= q_ig + w_ig;%rate of energy transfer between gas stream and
particle
c_vg= cp_g*1000-R_univ;
t= s_mass/(rho_g(i)*alpha_g);
v= (alpha_g*rho_g(i)*g)-(P*F_wg/A)+s_mom-(3*u_g(i)*s_mass);
m=1/(rho_g(i)*alpha_g*u_g(i)*(q_T+q_ig+w_ig+(u_g(i)*v+P_g(i+1)*1000*t
)));
%energy balance for gas phase - equation
3.75*****************************************************************
*********************************
T_g(i+1)= ((m*rho_g(i)*alpha_g*u_g(i)/s_mass)+
(((c_vg*T_g(i)+((u_g(i)^2)/2)+g*x_g)-
(m*rho_g(i)*alpha_g*u_g(i)/s_mass))*exp(-
s_mass*x_g/(rho_g(i)*alpha_g*u_g(i))))-((u_g(i)^2)/2)-(g*x_g))/c_vg;

rho_g(i+1)= 1.287841156-
0.004250962*T_g(i+1)+0.00000944905*T_g(i+1)^2-
0.00000000903741*T_g(i+1)^3;
rho_g_ave = (rho_g(i)+rho_g(i+1))/2;
```

```
T_g_ave= (T_g(i)+T_g(i+1))/2;
%Temperature with material !!!!stop
%SOLID PHASE PROPERTIES
Fr_p=u_s(i)/(g*d_p)^0.5;
f_p=1.0503*Fr_p^-1.831;
H_fg= 2.257;
h=x_g/4;
%Fourth order Runge kutta for particle velocity !!!!start
%momentum balance equation for solid phase - equation
3.94*****************************************************************
********************************
velofirstorderapprox; %mfile that calculates the first order
approximation of particle velocity
velosecondorderapprox;  %mfile that calculates the second order
approximation of particle velocity
velothirdorderapprox;%mfile that calculates the third order
approximation of particle velocity
velofourthorderapprox;%mfile that calculates the fourth order
approximation of particle velocity
t = position/u_s(i);
slip= u_g(i)-u_s(i);
%Fourth order Runge Kutta for particle temperature !!!!!!start
%energy balance equation for solid phase - equation
3.101****************************************************************
***************************
tempfirstorderapprox;
tempsecondorderapprox;
tempthirdorderapprox;
tempfourthorderapprox;
%Fourth Order Runge Kutta for particle temperature
!!!!!!!!!!!!!!!!!!!!!!!!!!!!!!!!!!!!!!!!!!!!!!!!!!!!!!!!stop
output = [u_g]
end
```

Appendix 5-2: Airprop0

```
%program that evaluates the properties of air at various temperature
%format('long')
rho_g0=1.287841156-0.004250962*T_g0+0.00000944905*T_g0^2-
0.00000000903741*T_g0^3;
cp_g0=1.005256941-0.0000147268*T_g0+0.00000070019*T_g0^2-
0.000000000684638*T_g0^3;
k_g0=0.024283313+0.0000693881*T_g0+0.0000000251525*T_g0^2-
0.00000000007194*T_g0^3;
v_g0=(13.29152006+0.087903505*T_g0+0.000102887*T_g0^2-
0.0000000374881*T_g0^3)*0.000001;
mu_g0= rho_g0*v_g0;
pr0= 0.716049954-0.000110828*T_g0-
0.000000406781*T_g0^2+0.0000000017347*T_g0^3;
```

Appendix 5-3: Airprop

```
%program that evaluates the properties of air at various temperature
%format('long')
%T_g= 160;%air initial temperature
rho_g(i)=1.287841156-0.004250962*T_g(i)+0.00000944905*T_g(i)^2-
0.00000000903741*T_g(i)^3;
```

```
cp_g(i)=1.005256941-0.0000147268*T_g(i)+0.00000070019*T_g(i)^2-
0.000000000684638*T_g(i)^3;
k_g(i)=0.024283313+0.0000693881*T_g(i)+0.0000000251525*T_g(i)^2-
0.00000000007194*T_g(i)^3;
v_g(i)=(13.29152006+0.087903505*T_g(i)+0.000102887*T_g(i)^2-
0.0000000374881*T_g(i)^3)*0.000001;
mu_g(i)= rho_g(i)*v_g(i);
pr(i)= 0.716049954-0.000110828*T_g(i)-
0.000000406781*T_g(i)^2+0.0000000017347*T_g(i)^3;
```

Appendix 5-4: Airpropw

```
%program that evaluates the properties of air at various temperature
%format('long')
rho_g_w= 1.287841156-0.004250962*T_w+0.00000944905*T_w^2-
0.00000000903741*T_w^3;
cp_g_w= 1.005256914-0.0000147268*T_w+0.00000070019*T_w^2-
0.000000000684638*T_w^3;
k_g_w= 0.02483313+0.0000693881*T_w+0.0000000251525*T_w^2-
0.00000000007194*T_w^3;
v_g_w=(13.291520006+0.087903505*T_w+0.000102887*T_w^2-
0.0000000374881*T_w^3)*0.000001;
mu_g_w= rho_g_w*v_g_w;
pr_g_w= 0.716049954-0.000110828*T_w-
0.000000406781*T_w^2+0.0000000017347*T_w^3;
```

Appendix 5-5: Airpropfout

```
program that evaluates the properties of air at various temperature
%format('long')
rho_g_f_out= 1.287841156-
0.004250962*T_f_air_out+0.00000944905*T_f_air_out^2-
0.00000000903741*T_f_air_out^3;
cp_g_f_out= 1.005256914-
0.0000147268*T_f_air_out+0.00000070019*T_f_air_out^2-
0.000000000684638*T_f_air_out^3;
k_g_f_out=
0.02483313+0.0000693881*T_f_air_out+0.0000000251525*T_f_air_out^2-
0.00000000007194*T_f_air_out^3;
v_g_f_out=
(13.291520006+0.087903505*T_f_air_out+0.000102887*T_f_air_out^2-
0.0000000374881*T_f_air_out^3)*0.000001;
mu_g_f_out= rho_g_f_out*v_g_f_out;
pr_f_out= 0.716049954-0.000110828*T_f_air_out-
0.000000406781*T_f_air_out^2+0.0000000017347*T_f_air_out^3;
```

Appendix 5-6: Airpropfin

```
%program that evaluates the properties of air at various temperature
%format('long')
rho_g_Tf= 1.287841156-
0.004250962*T_f_air_in+0.00000944905*T_f_air_in^2-
0.00000000903741*T_f_air_in^3;
```

```
cp_g_Tf= 1.005256914-
0.0000147268*T_f_air_in+0.00000070019*T_f_air_in^2-
0.000000000684638*T_f_air_in^3;
k_g_Tf=
0.02483313+0.0000693881*T_f_air_in+0.0000000251525*T_f_air_in^2-
0.00000000007194*T_f_air_in^3;
v_g_Tf=
(13.291520006+0.087903505*T_f_air_in+0.000102887*T_f_air_in^2-
0.0000000374881*T_f_air_in^3)*0.000001;
mu_g_Tf= rho_g_Tf*v_g_Tf;
cp_s_Tf=
3.1519+0.0006998*T_f_air_in+0.00000300301*T_f_air_in^2+0.000000000000
00008427*T_f_air_in^3;
pr_Tf= 0.716049954-0.000110828*T_f_air_in-
0.000000406781*T_f_air_in^2+0.0000000017347*T_f_air_in^3;
```

Appendix 5-7:Velofirstorderapprox

```
%program that calculates the first order approcimation of particle
velocity
k11=(3*rho_g_ave*cd*(u_g_ave-u_s(i))*abs(u_g_ave-
u_s(i))/(2*rho_s*d_p))-(2*g*(1-(rho_g_ave/rho_s)))-
(f_p*u_s(i)*abs(u_s(i))/d);
k12=(3*rho_g_ave*cd*(u_g_ave-(u_s(i)+0.5*h*k11))*abs(u_g_ave-
(u_s(i)+0.5*h*k11))/(2*rho_s*d_p))-(2*g*(1-(rho_g_ave/rho_s)))-
(f_p*(u_s(i)+0.5*h*k11)*abs(u_s(i)+0.5*h*k11)/d);
k13=(3*rho_g_ave*cd*(u_g_ave-(u_s(i)+0.5*h*k12))*abs(u_g_ave-
(u_s(i)+0.5*h*k12))/(2*rho_s*d_p))-(2*g*(1-(rho_g_ave/rho_s)))-
(f_p*(u_s(i)+0.5*h*k12)*abs(u_s(i)+0.5*h*k12)/d);
k14=(3*rho_g_ave*cd*(u_g_ave-(u_s(i)+h*k13))*abs(u_g_ave-
(u_s(i)+h*k13))/(2*rho_s*d_p))-(2*g*(1-(rho_g_ave/rho_s)))-
(f_p*(u_s(i)+h*k13)*abs(u_s(i)+h*k13)/d);
u_s_0025sqr =u_s(i)+h/6*(k11+2*k12+2*k13+k14);
u_s_0025= abs(u_s_0025sqr^0.5);

Fr_p= u_s_0025/(g*d_p)^0.5;
f_p= 1.0503*Fr_p^-1.831;
```

Appendix 5-8: Velosecondorderapprox

```
%program that calculates the second order approximation of particle
velocity
k21=(3*rho_g_ave*cd*(u_g_ave-u_s_0025)*abs(u_g_ave-
u_s_0025)/(4*u_s_0025*rho_s*d_p))-((g/u_s_0025)*(1-
(rho_g_ave/rho_s)))-(f_p*abs(u_s_0025)/2*d);
k22=(3*rho_g_ave*cd*(u_g_ave-(u_s_0025+0.5*h*k21))*abs(u_g_ave-
(u_s_0025+0.5*h*k21))/(4*u_s_0025*rho_s*d_p))-((g/u_s_0025)*(1-
(rho_g_ave/rho_s)))-(f_p*abs(u_s_0025+0.5*h*k21)/2*d);
k23=(3*rho_g_ave*cd*(u_g_ave-(u_s_0025+0.5*h*k22))*abs(u_g_ave-
(u_s_0025+0.5*h*k22))/(4*u_s_0025*rho_s*d_p))-((g/u_s_0025)*(1-
(rho_g_ave/rho_s)))-(f_p*abs(u_s_0025+0.5*h*k22)/2*d);
k24=(3*rho_g_ave*cd*(u_g_ave-(u_s_0025+h*k23))*abs(u_g_ave-
(u_s_0025+h*k23))/(4*u_s_0025*rho_s*d_p))-((g/u_s_0025)*(1-
(rho_g_ave/rho_s)))-(f_p*abs(u_s_0025+h*k23)/2*d);
u_s_005 =u_s_0025+h/6*(k21+2*k22+2*k23+k24);
```

```
Fr_p= u_s_005/(g*d_p)^0.5;
f_p= 1.0503*Fr_p^-1.831;
```

Appendix 5-9: Velothirdorderapprox

```
%program that calculates the second order approximation of particle
velocity
k31=(3*rho_g_ave*cd*(u_g_ave-u_s_005)*abs(u_g_ave-
u_s_005)/(4*u_s_005*rho_s*d_p))-((g/u_s_005)*(1-(rho_g_ave/rho_s)))-
(f_p*abs(u_s_005)/2*d);
k32=(3*rho_g_ave*cd*(u_g_ave-(u_s_005+0.5*h*k31))*abs(u_g_ave-
(u_s_005+0.5*h*k31))/(4*u_s_005*rho_s*d_p))-((g/u_s_005)*(1-
(rho_g_ave/rho_s)))-(f_p*abs(u_s_005+0.5*h*k31)/2*d);
k33=(3*rho_g_ave*cd*(u_g_ave-(u_s_005+0.5*h*k32))*abs(u_g_ave-
(u_s_005+0.5*h*k32))/(4*u_s_005*rho_s*d_p))-((g/u_s_005)*(1-
(rho_g_ave/rho_s)))-(f_p*abs(u_s_005+0.5*h*k32)/2*d);
k34=(3*rho_g_ave*cd*(u_g_ave-(u_s_005+h*k33))*abs(u_g_ave-
(u_s_005+h*k33))/(4*u_s_005*rho_s*d_p))-((g/u_s_005)*(1-
(rho_g_ave/rho_s)))-(f_p*abs(u_s_005+h*k33)/2*d);
u_s_0075=u_s_005+h/6*(k31+2*k32+2*k33+k34);

Fr_p= u_s_0075/(g*d_p)^0.5;
f_p= 1.0503*Fr_p^-1.831;
```

Appendix 5-10: Velofourthorderapprox

```
%program that calculates the second order approximation of particle
velocity
k41=(3*rho_g_ave*cd*(u_g_ave-u_s_0075)*abs(u_g_ave-
u_s_0075)/(4*u_s_0075*rho_s*d_p))-((g/u_s_0075)*(1-
(rho_g_ave/rho_s)))-(f_p*abs(u_s_0075)/2*d);
k42=(3*rho_g_ave*cd*(u_g_ave-(u_s_0075+0.5*h*k41))*abs(u_g_ave-
(u_s_0075+0.5*h*k41))/(4*u_s_0075*rho_s*d_p))-((g/u_s_0075)*(1-
(rho_g_ave/rho_s)))-(f_p*abs(u_s_0075+0.5*h*k41)/2*d);
k43=(3*rho_g_ave*cd*(u_g_ave-(u_s_0075+0.5*h*k42))*abs(u_g_ave-
(u_s_0075+0.5*h*k42))/(4*u_s_0075*rho_s*d_p))-((g/u_s_0075)*(1-
(rho_g_ave/rho_s)))-(f_p*abs(u_s_0075+0.5*h*k42)/2*d);
k44=(3*rho_g_ave*cd*(u_g_ave-(u_s_0075+h*k43))*abs(u_g_ave-
(u_s_0075+h*k43))/(4*u_s_0075*rho_s*d_p))-((g/u_s_0075)*(1-
(rho_g_ave/rho_s)))-(f_p*abs(u_s_0075+h*k43)/2*d);
u_s(i+1) =u_s_0075+h/6*(k41+2*k42+2*k43+k44);
```

Appendix 5-11: Particle Terminal Velocity- Experimental versus Simulated

Particle diameter (mm)	Experimental Terminal Velocity, V_{et} (m/s)	Simulated Terminal Velocity, V_{sim} (m/s)
6.350	13.38	12.954
5.027	8.92	7.958
1.438	3.60	3.508
1.226	3.20	2.452
0.874	2.40	2.124

0.582	2.00	1.461
0.150	-	-

Appendix 5-12: Pressure Drop at various Air Inlet Velocities.

inlet velocity (m/s)	5 ton/8hr pressure drop (N/m)	4 ton/8hr pressure drop (N/m)	3 ton/8hr pressure drop (N/m)	2 ton/8hr pressure drop (N/m)	1 ton/8hr pressure drop (N/m)
1					
2					
3					12.693
4					18.459
5					23.724
6				62.115	29.438
7				73.560	35.251
8			132.632	84.928	40.994
9			149.922	96.465	46.817
10			167.123	107.936	52.597
11		254.525	184.562	119.552	58.440
12		277.932	201.992	131.156	64.271
13	389.631	301.389	219.457	142.777	70.105
14	419.426	324.923	236.970	154.421	75.946
15	449.020	348.340	254.412	166.023	81.764
16	478.754	371.851	271.914	177.658	87.594
17	508.515	395.387	289.434	189.302	93.427
18	538.293	418.939	306.966	200.951	99.260
19	568.074	442.497	324.502	212.602	105.093
20	597.894	466.088	342.063	224.268	110.930
21	627.697	489.670	359.618	235.929	116.765
22	657.486	513.244	377.168	247.586	122.597
23	687.248	536.801	394.707	259.235	128.424

24	716.970	560.331	412.228	270.872	134.244
25	746.642	583.826	429.724	282.493	140.055
26	776.255	607.280	447.192	294.095	145.857
27	805.809	630.691	464.630	305.678	151.650
28	835.329	654.079	482.053	317.251	157.437
29	864.884	677.498	499.499	328.840	163.232
30	894.492	700.956	516.973	340.444	169.033

Appendix 5-13: Gas Phase and Solid Phase Temperatures during Conveyance.

Distance(m)	Gas temperature(C)	Solid temperature (C)
0	160	22
0.01	159.9968166	22.05540033
0.02	159.9937683	22.13023678
0.03	159.9906641	22.21842026
0.04	159.9875345	22.31249641
0.05	159.9843877	22.40896331
0.06	159.9812277	22.50636466
0.07	159.9780548	22.60410952
0.08	159.9748705	22.70197506
0.09	159.9716739	22.79986548
0.1	159.9684662	22.89775255
0.11	159.9652462	22.99561634
0.12	159.9620151	23.0934581
0.13	159.9587719	23.19126931
0.14	159.9555176	23.28905569
0.15	159.9522511	23.38681044
0.16	159.9489735	23.48453992
0.17	159.9456838	23.58223761
0.18	159.9423829	23.67990996
0.19	159.93907	23.7775505
0.2	159.9357459	23.87516569
0.21	159.9324097	23.97274906
0.22	159.9290624	24.07030707
0.23	159.925703	24.16783327
0.24	159.9223326	24.26533411
0.25	159.91895	24.36280312
0.26	159.9155563	24.46024677
0.27	159.9121506	24.55765861
0.28	159.9087337	24.65504508
0.29	159.9053048	24.75239972
0.3	159.9018648	24.849729
0.31	159.8984128	24.94702646
0.32	159.8949497	25.04429854
0.33	159.8914744	25.1415388

0.34	159.8879882	25.23875369
0.35	159.8844899	25.33593676
0.36	159.8809805	25.43309444
0.37	159.8774591	25.53022031
0.38	159.8739267	25.62732079
0.39	159.8703822	25.72438945
0.4	159.8668266	25.82143273
0.41	159.8632591	25.91844418
0.42	159.8596805	26.01543025
0.43	159.8560898	26.11238449
0.44	159.8524882	26.20931334
0.45	159.8488745	26.30621036
0.46	159.8452498	26.40308199
0.47	159.8416131	26.4999218
0.48	159.8379654	26.59673621
0.49	159.8343057	26.6935188
0.5	159.830635	26.79027599
0.51	159.8269523	26.88700135
0.52	159.8232586	26.9837013
0.53	159.8195529	27.08036944
0.54	159.8158363	27.17701217
0.55	159.8121076	27.27362307
0.56	159.808368	27.37020856
0.57	159.8046164	27.46676223
0.58	159.8008539	27.56329048
0.59	159.7970793	27.65978691
0.6	159.7932939	27.75625793
0.61	159.7894964	27.85269712
0.62	159.785688	27.94911088
0.63	159.7818676	28.04549283
0.64	159.7780364	28.14184935
0.65	159.7741931	28.23817405
0.66	159.770339	28.33447332
0.67	159.7664729	28.43074077
0.68	159.7625959	28.52698279
0.69	159.7587069	28.62319299
0.7	159.7548071	28.71937775
0.71	159.7508952	28.81553069
0.72	159.7469726	28.91165819
0.73	159.7430379	29.00775388
0.74	159.7390925	29.10382412
0.75	159.735135	29.19986254
0.76	159.7311668	29.29587552
0.77	159.7271865	29.39185667
0.78	159.7231955	29.48781238
0.79	159.7191925	29.58373627

0.8	159.7151787	29.67963471
0.81	159.7111529	29.77550133
0.82	159.7071164	29.87134249
0.83	159.7030679	29.96715184
0.84	159.6990086	30.06293573
0.85	159.6949374	30.1586878
0.86	159.6908555	30.25441441
0.87	159.6867615	30.3501092
0.88	159.6826569	30.44577853
0.89	159.6785402	30.54141604
0.9	159.6744129	30.63702809
0.91	159.6702736	30.73260832
0.92	159.6661237	30.82816308
0.93	159.6619617	30.92368602
0.94	159.6577891	31.01918349
0.95	159.6536045	31.11464915
0.96	159.6494093	31.21008933
0.97	159.6452021	31.30549769
0.98	159.6409842	31.40088058
0.99	159.6367544	31.49623165
1	159.632514	31.59155724
1.01	159.6282616	31.68685102
1.02	159.6239986	31.78211931
1.03	159.6197237	31.87735579
1.04	159.6154381	31.97256678
1.05	159.6111406	32.06774595
1.06	159.6068325	32.16289964
1.07	159.6025125	32.25802152
1.08	159.5981819	32.3531179
1.09	159.5938394	32.44818247
1.1	159.5894863	32.54322155
1.11	159.5851213	32.63822881
1.12	159.5807457	32.73321058
1.13	159.5763582	32.82816053
1.14	159.5719601	32.92308498
1.15	159.5675502	33.01797763
1.16	159.5631297	33.11284477
1.17	159.5586973	33.2076801
1.18	159.5542544	33.30248992
1.19	159.5497996	33.39726794
1.2	159.5453342	33.49202044
1.21	159.540857	33.58674114
1.22	159.5363693	33.68143633
1.23	159.5318697	33.77609971
1.24	159.5273596	33.87073757
1.25	159.5228377	33.96534363

1.26	159.5183052	34.05992417
1.27	159.5137609	34.1544729
1.28	159.5092061	34.24899612
1.29	159.5046395	34.34348753
1.3	159.5000624	34.43795342
1.31	159.4954735	34.5323875
1.32	159.4908741	34.62679606
1.33	159.4862628	34.72117282
1.34	159.4816412	34.81552404
1.35	159.4770077	34.90984347
1.36	159.4723637	35.00413736
1.37	159.467708	35.09839946
1.38	159.4630418	35.19263602
1.39	159.4583638	35.28684078
1.4	159.4536755	35.38102
1.41	159.4489752	35.47516743
1.42	159.4442647	35.56928932
1.43	159.4395423	35.66337941
1.44	159.4348095	35.75744396
1.45	159.4300649	35.85147671
1.46	159.42531	35.94548391
1.47	159.4205433	36.03945933
1.48	159.4157662	36.13340919
1.49	159.4109773	36.22732726
1.5	159.4061781	36.32121979
1.51	159.4013671	36.41508051
1.52	159.3965458	36.50891569
1.53	159.3917128	36.60271908
1.54	159.3868694	36.69649691
1.55	159.3820142	36.79024295
1.56	159.3771488	36.88396343
1.57	159.3722715	36.97765212
1.58	159.367384	37.07131526
1.59	159.3624848	37.16494661
1.6	159.3575753	37.25855239
1.61	159.352654	37.35212639
1.62	159.3477225	37.44567483
1.63	159.3427792	37.53919147
1.64	159.3378257	37.63268256
1.65	159.3328604	37.72614185
1.66	159.3278849	37.81957558
1.67	159.3228977	37.91297752
1.68	159.3179003	38.0063539
1.69	159.3128911	38.09969849
1.7	159.3078718	38.19301751
1.71	159.3028407	38.28630475

1.72	159.2977995	38.37956641
1.73	159.2927465	38.47279629
1.74	159.2876834	38.5660006
1.75	159.2826085	38.65917313
1.76	159.2775235	38.75232008
1.77	159.2724268	38.84543524
1.78	159.26732	38.93852483
1.79	159.2622014	39.03158264
1.8	159.2570728	39.12461488
1.81	159.2519324	39.21761533
1.82	159.2467819	39.3105902
1.83	159.2416198	39.40353329
1.84	159.2364475	39.4964508
1.85	159.2312636	39.58933653
1.86	159.2260696	39.68219668
1.87	159.2208639	39.77502505
1.88	159.2156482	39.86782783
1.89	159.2104208	39.96059885
1.9	159.2051833	40.05334427
1.91	159.1999342	40.14605792
1.92	159.194675	40.23874597
1.93	159.1894042	40.33140226
1.94	159.1841233	40.42403295
1.95	159.1788308	40.51663188
1.96	159.1735283	40.6092052
1.97	159.1682142	40.70174677
1.98	159.1628901	40.79426273
1.99	159.1575543	40.88674692
2	159.1522085	40.97920552
2.01	159.1468512	41.07163235
2.02	159.1414838	41.16403359
2.03	159.1361049	41.25640305
2.04	159.1307159	41.34874692
2.05	159.1253154	41.44105902
2.06	159.119905	41.53334552
2.07	159.1144829	41.62560026
2.08	159.1090509	41.71782939
2.09	159.1036073	41.81002676
2.1	159.0981538	41.90219853
2.11	159.0926887	41.99433854
2.12	159.0872138	42.08645293
2.13	159.0817272	42.17853558
2.14	159.0762308	42.27059261
2.15	159.0707227	42.36261788
2.16	159.0652048	42.45461755
2.17	159.0596754	42.54658546

2.18	159.0541361	42.63852775
2.19	159.0485852	42.7304383
2.2	159.0430245	42.82232323
2.21	159.0374523	42.91417641
2.22	159.0318702	43.00600397
2.23	159.0262766	43.09779978
2.24	159.0206731	43.18956998
2.25	159.0150582	43.28130842
2.26	159.0094334	43.37302125
2.27	159.0037971	43.46470233
2.28	158.998151	43.55635779
2.29	158.9924935	43.64798151
2.3	158.9868261	43.73957961
2.31	158.9811472	43.83114596
2.32	158.9754586	43.92268669
2.33	158.9697585	44.01419568
2.34	158.9640486	44.10567904
2.35	158.9583272	44.19713066
2.36	158.9525961	44.28855666
2.37	158.9468536	44.37995092
2.38	158.9411013	44.47131955
2.39	158.9353375	44.56265645
2.4	158.9295641	44.65396771
2.41	158.9237791	44.74524725
2.42	158.9179845	44.83650115
2.43	158.9121784	44.92772332
2.44	158.9063627	45.01891986
2.45	158.9005355	45.11008467
2.46	158.8946987	45.20122384
2.47	158.8888504	45.29233129
2.48	158.8829924	45.3834131
2.49	158.8771231	45.47446319
2.5	158.8712441	45.56548764
2.51	158.8653536	45.65648037
2.52	158.8594536	45.74744746
2.53	158.8535422	45.83838283
2.54	158.8476211	45.92929255
2.55	158.8416886	46.02017056
2.56	158.8357466	46.11102293
2.57	158.8297932	46.20184358
2.58	158.8238301	46.29263859
2.59	158.8178557	46.38340189
2.6	158.8118718	46.47413954
2.61	158.8058764	46.56484548
2.62	158.7998716	46.65552577
2.63	158.7938553	46.74617436

2.64	158.7878295	46.8367973
2.65	158.7817924	46.92738853
2.66	158.7757457	47.01795411
2.67	158.7696877	47.10848799
2.68	158.7636202	47.19899622
2.69	158.7575414	47.28947274
2.7	158.751453	47.37992362
2.71	158.7453533	47.47034279
2.72	158.7392442	47.56073632
2.73	158.7331237	47.65109814
2.74	158.7269938	47.74143431
2.75	158.7208525	47.83173879
2.76	158.7147019	47.92201761
2.77	158.7085399	48.01226474
2.78	158.7023684	48.10248622
2.79	158.6961857	48.192676
2.8	158.6899936	48.28284013
2.81	158.6837902	48.37297257
2.82	158.6775774	48.46307935
2.83	158.6713532	48.55315445
2.84	158.6651198	48.64320388
2.85	158.658875	48.73322164
2.86	158.6526209	48.82321373
2.87	158.6463555	48.91317414
2.88	158.6400808	49.0031089
2.89	158.6337948	49.09301197
2.9	158.6274995	49.18288939
2.91	158.6211929	49.27273512
2.92	158.614877	49.3625552
2.93	158.6085499	49.4523436
2.94	158.6022134	49.54210634
2.95	158.5958657	49.6318374
2.96	158.5895088	49.72154281
2.97	158.5831406	49.81121654
2.98	158.5767632	49.90086461
2.99	158.5703745	49.99048101
3	158.5639766	50.08007175
3.01	158.5575675	50.16963083
3.02	158.5511491	50.25916424
3.03	158.5447195	50.34866598
3.04	158.5382808	50.43814206
3.05	158.5318308	50.52758649
3.06	158.5253716	50.61700524
3.07	158.5189012	50.70639234
3.08	158.5124217	50.79575377
3.09	158.505931	50.88508354

3.1	158.4994311	50.97438765
3.11	158.49292	51.06366011
3.12	158.4863998	51.1529069
3.13	158.4798684	51.24212204
3.14	158.4733279	51.33131151
3.15	158.4667762	51.42046933
3.16	158.4602154	51.50960148
3.17	158.4536435	51.59870199
3.18	158.4470625	51.68777683
3.19	158.4404703	51.77682003
3.2	158.433869	51.86583756
3.21	158.4272567	51.95482345
3.22	158.4206352	52.04378367
3.23	158.4140026	52.13271225
3.24	158.407361	52.22161516
3.25	158.4007082	52.31048644
3.26	158.3940465	52.39933204
3.27	158.3873736	52.48814602
3.28	158.3806917	52.57693432
3.29	158.3739987	52.665691
3.3	158.3672967	52.754422
3.31	158.3605836	52.84312138
3.32	158.3538615	52.93179509
3.33	158.3471284	53.02043717
3.34	158.3403863	53.10905358
3.35	158.3336331	53.19763837
3.36	158.3268709	53.28619749
3.37	158.3200977	53.37472499
3.38	158.3133156	53.46322681
3.39	158.3065224	53.55169703
3.4	158.2997203	53.64014157
3.41	158.2929071	53.7285545
3.42	158.2860851	53.81694175
3.43	158.279252	53.9052974
3.44	158.27241	53.99362737
3.45	158.265557	54.08192574
3.46	158.2586951	54.17019843
3.47	158.2518223	54.25843952
3.48	158.2449405	54.34665494
3.49	158.2380478	54.43483875
3.5	158.2311462	54.5229969
3.51	158.2242336	54.61112344
3.52	158.2173122	54.69922431
3.53	158.2103798	54.78729359
3.54	158.2034386	54.8753372
3.55	158.1964865	54.96334921

3.56	158.1895255	55.05133555
3.57	158.1825536	55.1392903
3.58	158.1755728	55.22721938
3.59	158.1685812	55.31511687
3.6	158.1615808	55.40298869
3.61	158.1545694	55.49082892
3.62	158.1475493	55.57864348
3.63	158.1405183	55.66642647
3.64	158.1334785	55.75418378
3.65	158.1264278	55.84190951
3.66	158.1193684	55.92960957
3.67	158.1122981	56.01727806
3.68	158.105219	56.10492087
3.69	158.0981291	56.19253212
3.7	158.0910305	56.28011769
3.71	158.083921	56.3676717
3.72	158.0768028	56.45520003
3.73	158.0696738	56.5426968
3.74	158.0625361	56.63016789
3.75	158.0553875	56.71760743
3.76	158.0482303	56.80502129
3.77	158.0410623	56.89240359
3.78	158.0338856	56.97976023
3.79	158.026698	57.06708531
3.8	158.0195019	57.15438471
3.81	158.0122949	57.24165257
3.82	158.0050793	57.32889476
3.83	157.9978529	57.4161054
3.84	157.990618	57.50329036
3.85	157.9833722	57.59044379
3.86	157.9761178	57.67757154
3.87	157.9688527	57.76466775
3.88	157.961579	57.85173829
3.89	157.9542945	57.93877729
3.9	157.9470015	58.02579063
3.91	157.9396977	58.11277243
3.92	157.9323854	58.19972855
3.93	157.9250623	58.28665316
3.94	157.9177307	58.37355208
3.95	157.9103884	58.46041949
3.96	157.9030376	58.54726122
3.97	157.895676	58.63407143
3.98	157.888306	58.72085597
3.99	157.8809252	58.80760899
4	157.873536	58.89433635
4.01	157.866136	58.98103218

4.02	157.8587277	59.06770235
4.03	157.8513086	59.15434101
4.04	157.843881	59.240954
4.05	157.8364428	59.32753548
4.06	157.8289962	59.41409129
4.07	157.8215389	59.5006156
4.08	157.8140732	59.58711424
4.09	157.8065968	59.67358138
4.1	157.799112	59.76002285
4.11	157.7916166	59.84643283
4.12	157.7841128	59.93281714
4.13	157.7765984	60.01916996
4.14	157.7690756	60.1054971
4.15	157.7615421	60.19179277
4.16	157.7540004	60.27806276
4.17	157.746448	60.36430127
4.18	157.7388873	60.45051412
4.19	157.731316	60.53669548
4.2	157.7237363	60.62285118
4.21	157.7161461	60.7089754
4.22	157.7085476	60.79507396
4.23	157.7009385	60.88114104
4.24	157.6933211	60.96718246
4.25	157.6856931	61.05319241
4.26	157.6780569	61.1391767
4.27	157.6704101	61.22512952
4.28	157.6627551	61.31105668
4.29	157.6550895	61.39695238
4.3	157.6474157	61.48282242
4.31	157.6397314	61.568661
4.32	157.6320388	61.65447392
4.33	157.6243357	61.74025538
4.34	157.6166244	61.82601119
4.35	157.6089026	61.91173554
4.36	157.6011726	61.99743424
4.37	157.5934321	62.08310149
4.38	157.5856835	62.16874308
4.39	157.5779243	62.25435323
4.4	157.570157	62.33993772
4.41	157.5623792	62.42549078
4.42	157.5545933	62.51101817
4.43	157.5467969	62.59651414
4.44	157.5389924	62.68198445
4.45	157.5311774	62.76742333
4.46	157.5233544	62.85283655
4.47	157.5155208	62.93821835

4.48	157.5076793	63.02357449
4.49	157.4998272	63.10889922
4.5	157.4919671	63.19419829
4.51	157.4840966	63.27946594
4.52	157.476218	63.36470794
4.53	157.468329	63.44991853
4.54	157.4604319	63.53510347
4.55	157.4525245	63.620257
4.56	157.4446091	63.70538488
4.57	157.4366832	63.79048135
4.58	157.4287493	63.87555218
4.59	157.4208051	63.96059161
4.6	157.4128529	64.04560538
4.61	157.4048903	64.13058777
4.62	157.3969198	64.2155445
4.63	157.3889388	64.30046985
4.64	157.38095	64.38536954
4.65	157.3729507	64.47023786
4.66	157.3649436	64.55508052
4.67	157.3569261	64.63989181
4.68	157.3489007	64.72467745
4.69	157.340865	64.80943171
4.7	157.3328214	64.89416033
4.71	157.3247674	64.97885757
4.72	157.3167056	65.06352918
4.73	157.3086335	65.14816942
4.74	157.3005535	65.23278401
4.75	157.2924632	65.31736724
4.76	157.2843651	65.40192483
4.77	157.2762566	65.48645107
4.78	157.2681404	65.57095166
4.79	157.2600139	65.6554209
4.8	157.2518796	65.7398645
4.81	157.243735	65.82427675
4.82	157.2355826	65.90866337
4.83	157.2274199	65.99301864
4.84	157.2192495	66.07734827
4.85	157.2110689	66.16164656
4.86	157.2028805	66.24591923
4.87	157.1946818	66.33016055
4.88	157.1864754	66.41437624
4.89	157.1782588	66.4985606
4.9	157.1700345	66.58271933
4.91	157.1617999	66.66684673
4.92	157.1535577	66.75094851
4.93	157.1453053	66.83501896

4.94	157.1370452	66.91906378
4.95	157.1287748	67.00307729
4.96	157.1204969	67.08706517
4.97	157.1122087	67.17102173
4.98	157.1039129	67.25495267
4.99	157.0956069	67.33885231
5	157.0872933	67.42272632
5.01	157.0789695	67.50656902
5.02	157.0706381	67.59038611
5.03	157.0622966	67.67417189
5.04	157.0539475	67.75793206
5.05	157.0455882	67.84166093
5.06	157.0372214	67.92536418
5.07	157.0288444	68.00903614
5.08	157.0204599	68.09268249
5.09	157.0120652	68.17629755
5.1	157.0036631	68.259887
5.11	156.9952508	68.34344517
5.12	156.986831	68.42697772
5.13	156.978401	68.510479
5.14	156.9699636	68.59395467
5.15	156.9615161	68.67739907
5.16	156.9530612	68.76081786
5.17	156.9445961	68.84420538
5.18	156.9361236	68.92756729
5.19	156.927641	69.01089795
5.2	156.919151	69.094203
5.21	156.9106509	69.17747679
5.22	156.9021434	69.26072498
5.23	156.8936258	69.34394192
5.24	156.8851008	69.42713325
5.25	156.8765658	69.51029334
5.26	156.8680234	69.59342783
5.27	156.859471	69.67653108
5.28	156.8509112	69.75960873
5.29	156.8423414	69.84265515
5.3	156.8337642	69.92567597
5.31	156.8251771	70.00866555
5.32	156.8165826	70.09162955
5.33	156.8079781	70.17456231
5.34	156.7993663	70.25746949
5.35	156.7907445	70.34034544
5.36	156.7821154	70.42319581
5.37	156.7734763	70.50601496
5.38	156.76483	70.58880852
5.39	156.7561737	70.67157087

5.4	156.7475101	70.75430763
5.41	156.7388366	70.83701319
5.42	156.7301558	70.91969316
5.43	156.7214651	71.00234193
5.44	156.7127672	71.08496513
5.45	156.7040593	71.16755712
5.46	156.6953443	71.25012354
5.47	156.6866193	71.33265877
5.48	156.6778871	71.41516842
5.49	156.669145	71.49764688
5.5	156.6603958	71.58009977
5.51	156.6516367	71.66252148
5.52	156.6428704	71.74491761
5.53	156.6340942	71.82728257
5.54	156.6253109	71.90962197
5.55	156.6165177	71.99193019
5.56	156.6077174	72.07421284
5.57	156.5989072	72.15646433
5.58	156.59009	72.23869025
5.59	156.5812628	72.32088502
5.6	156.5724286	72.40305422
5.61	156.5635846	72.48519227
5.62	156.5547335	72.56730475
5.63	156.5458726	72.64938609
5.64	156.5370046	72.73144187
5.65	156.5281268	72.8134665
5.66	156.519242	72.89546558
5.67	156.5103474	72.97743353
5.68	156.5014458	73.05937592
5.69	156.4925344	73.14128717
5.7	156.4836159	73.22317288
5.71	156.4746878	73.30502745
5.72	156.4657526	73.38685648
5.73	156.4568077	73.46865439
5.74	156.4478558	73.55042675
5.75	156.4388941	73.632168
5.76	156.4299255	73.7138837
5.77	156.4209472	73.79556829
5.78	156.4119619	73.87722734
5.79	156.402967	73.95885529
5.8	156.3939651	74.04045769
5.81	156.3849535	74.122029
5.82	156.3759349	74.20357477
5.83	156.3669067	74.28508945
5.84	156.3578717	74.36657859
5.85	156.3488269	74.44803665

5.86	156.3397753	74.52946917
5.87	156.330714	74.61087061
5.88	156.3216458	74.69224653
5.89	156.312568	74.77359136
5.9	156.3034834	74.85491068
5.91	156.2943891	74.93619892
5.92	156.285288	75.01746163
5.93	156.2761772	75.09869329
5.94	156.2670597	75.17989942
5.95	156.2579325	75.26107449
5.96	156.2487986	75.34222404
5.97	156.2396551	75.42334254
5.98	156.2305048	75.50443553
5.99	156.2213449	75.58549747
6	156.2121782	75.66653389
6.01	156.203002	75.74753928
6.02	156.193819	75.82851915
6.03	156.1846265	75.90946799
6.04	156.1754273	75.99039132
6.05	156.1662185	76.07128362
6.06	156.157003	76.15215042
6.07	156.147778	76.23298619
6.08	156.1385462	76.31379646
6.09	156.129305	76.39457572
6.1	156.1200571	76.47532947
6.11	156.1107997	76.55605221
6.12	156.1015356	76.63674946
6.13	156.092262	76.7174157
6.14	156.0829818	76.79805645
6.15	156.0736921	76.8786662
6.16	156.0643958	76.95925046
6.17	156.05509	77.03980372
6.18	156.0457777	77.1203315
6.19	156.0364558	77.20082829
6.2	156.0271274	77.28129959
6.21	156.0177895	77.36173991
6.22	156.0084451	77.44215476
6.23	155.9990912	77.52253862
6.24	155.9897308	77.60289701
6.25	155.9803609	77.68322443
6.26	155.9709846	77.76352637
6.27	155.9615988	77.84379735
6.28	155.9522065	77.92404286
6.29	155.9428047	78.00425741
6.3	155.9333966	78.08444649
6.31	155.923979	78.16460462

6.32	155.9145549	78.24473728
6.33	155.9051215	78.324839
6.34	155.8956816	78.40491526
6.35	155.8862323	78.48496058
6.36	155.8767766	78.56498043
6.37	155.8673116	78.64496936
6.38	155.8578401	78.72493283
6.39	155.8483593	78.80486537
6.4	155.8388721	78.88477246
6.41	155.8293755	78.96464863
6.42	155.8198726	79.04449935
6.43	155.8103604	79.12431916
6.44	155.8008418	79.20411352
6.45	155.7913138	79.28387697
6.46	155.7817796	79.36361498
6.47	155.772236	79.44332209
6.48	155.7626861	79.52300375
6.49	155.7531269	79.60265453
6.5	155.7435615	79.68227986
6.51	155.7339867	79.76187431
6.52	155.7244057	79.84144333
6.53	155.7148153	79.92098146
6.54	155.7052188	80.00049416
6.55	155.6956129	80.07997599
6.56	155.6860009	80.15943239
6.57	155.6763795	80.23885792
6.58	155.666752	80.31825803
6.59	155.6571152	80.39762727
6.6	155.6474722	80.4769711
6.61	155.63782	80.55628407
6.62	155.6281615	80.63557163
6.63	155.6184939	80.71482833
6.64	155.6088201	80.79405962
6.65	155.5991371	80.87326007
6.66	155.589448	80.95243511
6.67	155.5797496	81.03157931
6.68	155.5700452	81.11069811
6.69	155.5603315	81.18978608
6.7	155.5506117	81.26884864
6.71	155.5408828	81.34788039
6.72	155.5311478	81.42688673
6.73	155.5214036	81.50586226
6.74	155.5116533	81.58481239
6.75	155.5018939	81.66373171
6.76	155.4921285	81.74262564
6.77	155.4823539	81.82148877

6.78	155.4725732	81.90032651
6.79	155.4627835	81.97913345
6.8	155.4529877	82.05791501
6.81	155.4431828	82.13666578
6.82	155.4333719	82.21539117
6.83	155.4235519	82.29408578
6.84	155.4137259	82.37275501
6.85	155.4038909	82.45139346
6.86	155.3940498	82.53000654
6.87	155.3841997	82.60858885
6.88	155.3743437	82.6871458
6.89	155.3644786	82.76567198
6.9	155.3546075	82.84417279
6.91	155.3447275	82.92264285
6.92	155.3348414	83.00108755
6.93	155.3249464	83.07950149
6.94	155.3150455	83.15789008
6.95	155.3051355	83.23624793
6.96	155.2952197	83.31458043
6.97	155.2852948	83.39288218
6.98	155.2753641	83.4711586
6.99	155.2654244	83.54940427
7	155.2554788	83.62762461
7.01	155.2455243	83.70581422
7.02	155.2355639	83.7839785
7.03	155.2255946	83.86211205
7.04	155.2156195	83.94022027
7.05	155.2056354	84.01829778
7.06	155.1956455	84.09634996
7.07	155.1856466	84.17437144
7.08	155.175642	84.25236758
7.09	155.1656285	84.33033304
7.1	155.1556091	84.40827317
7.11	155.1455809	84.48618261
7.12	155.1355469	84.56406673
7.13	155.1255041	84.64192016
7.14	155.1154555	84.71974829
7.15	155.105398	84.79754574
7.16	155.0953348	84.87531787
7.17	155.0852627	84.95305934
7.18	155.0751849	85.0307755
7.19	155.0650983	85.10846101
7.2	155.055006	85.1861212
7.21	155.0449048	85.26375075
7.22	155.034798	85.341355
7.23	155.0246824	85.4189286

7.24	155.0145611	85.4964769
7.25	155.0044309	85.57399457
7.26	154.9942952	85.65148694
7.27	154.9841506	85.72894869
7.28	154.9740005	85.80638514
7.29	154.9638415	85.88379098
7.3	154.953677	85.96117153
7.31	154.9435036	86.03852146
7.32	154.9333247	86.11584612
7.33	154.923137	86.19314017
7.34	154.9129438	86.27040894
7.35	154.9027418	86.34764711
7.36	154.8925343	86.42486001
7.37	154.882318	86.50204232
7.38	154.8720962	86.57919936
7.39	154.8618656	86.65632581
7.4	154.8516296	86.733427
7.41	154.8413848	86.81049761
7.42	154.8311346	86.88754297
7.43	154.8208756	86.96455775
7.44	154.8106112	87.04154728
7.45	154.8003381	87.11850625
7.46	154.7900595	87.19543997
7.47	154.7797723	87.27234313
7.48	154.7694796	87.34922104
7.49	154.7591782	87.42606841
7.5	154.7488715	87.50289054
7.51	154.738556	87.57968212
7.52	154.7282352	87.65644847
7.53	154.7179057	87.73318429
7.54	154.7075709	87.80989487
7.55	154.6972274	87.88657493
7.56	154.6868786	87.96322976
7.57	154.6765211	88.03985407
7.58	154.6661583	88.11645317
7.59	154.6557869	88.19302174
7.6	154.6454101	88.26956511
7.61	154.6350248	88.34607796
7.62	154.6246341	88.42256561
7.63	154.6142349	88.49902276
7.64	154.6038304	88.5754547
7.65	154.5934173	88.65185615
7.66	154.5829989	88.7282324
7.67	154.572572	88.80457817
7.68	154.5621398	88.88089874
7.69	154.5516991	88.95718883

7.7	154.5412531	89.03345374
7.71	154.5307986	89.10968817
7.72	154.5203389	89.18589742
7.73	154.5098707	89.26207621
7.74	154.4993972	89.33822981
7.75	154.4889153	89.41435296
7.76	154.4784281	89.49045094
7.77	154.4679325	89.56651847
7.78	154.4574317	89.64256083
7.79	154.4469225	89.71857275
7.8	154.436408	89.7945595
7.81	154.4258851	89.87051583
7.82	154.4153571	89.94644699
7.83	154.4048206	90.02234773
7.84	154.394279	90.09822331
7.85	154.383729	90.17406848
7.86	154.3731738	90.24988849
7.87	154.3626103	90.3256781
7.88	154.3520416	90.40144256
7.89	154.3414645	90.47717663
7.9	154.3308824	90.55288555
7.91	154.3202919	90.62856408
7.92	154.3096963	90.70421747
7.93	154.2990923	90.77984048
7.94	154.2884833	90.85543835
7.95	154.2778659	90.93100586
7.96	154.2672435	91.00654823
7.97	154.2566127	91.08206024
7.98	154.245977	91.15754712
7.99	154.2353329	91.23300365
8	154.2246838	91.30843505
8.01	154.2140263	91.38383611
8.02	154.203364	91.45921206
8.03	154.1926932	91.53455766
8.04	154.1820176	91.60987815
8.05	154.1713336	91.68516831
8.06	154.1606447	91.76043337
8.07	154.1499475	91.8356681
8.08	154.1392454	91.91087773
8.09	154.128535	91.98605705
8.1	154.1178197	92.06121127
8.11	154.1070961	92.13633518
8.12	154.0963677	92.21143401
8.13	154.085631	92.28650253
8.14	154.0748894	92.36154597
8.15	154.0641396	92.43655912

8.16	154.053385	92.51154719
8.17	154.0426221	92.58650498
8.18	154.0318544	92.66143769
8.19	154.0210784	92.73634013
8.2	154.0102977	92.8112175
8.21	153.9995088	92.8860646
8.22	153.988715	92.96088664
8.23	153.9779131	93.03567841
8.24	153.9671064	93.11044514
8.25	153.9562915	93.18518161
8.26	153.9454718	93.25989303
8.27	153.934644	93.3345742
8.28	153.9238115	93.40923033
8.29	153.9129708	93.48385622
8.3	153.9021253	93.55845708
8.31	153.8912717	93.6330277
8.32	153.8804135	93.7075733
8.33	153.869547	93.78208867
8.34	153.8586759	93.85657901
8.35	153.8477967	93.93103914
8.36	153.8369128	94.00547425
8.37	153.8260208	94.07987916
8.38	153.8151242	94.15425905
8.39	153.8042194	94.22860874
8.4	153.7933101	94.30293342
8.41	153.7823926	94.37722792
8.42	153.7714705	94.45149741
8.43	153.7605404	94.52573672
8.44	153.7496056	94.59995103
8.45	153.7386628	94.67413517
8.46	153.7277155	94.74829431
8.47	153.71676	94.8224233
8.48	153.7058	94.89652729
8.49	153.694832	94.97060113
8.5	153.6838594	95.04464999
8.51	153.6728788	95.1186687
8.52	153.6618937	95.19266244
8.53	153.6509006	95.26662604
8.54	153.639903	95.34056467
8.55	153.6288973	95.41447316
8.56	153.6178872	95.4883567
8.57	153.6068691	95.56221011
8.58	153.5958465	95.63603856
8.59	153.5848159	95.7098369
8.6	153.5737809	95.78361029
8.61	153.5627379	95.85735358

8.62	153.5516905	95.93107191
8.63	153.5406352	96.00476015
8.64	153.5295754	96.07842345
8.65	153.5185077	96.15205667
8.66	153.5074355	96.22566494
8.67	153.4963555	96.29924314
8.68	153.4852711	96.37279641
8.69	153.4741787	96.44631961
8.7	153.463082	96.51981789
8.71	153.4519774	96.5932861
8.72	153.4408684	96.6667294
8.73	153.4297516	96.74014265
8.74	153.4186304	96.81353098
8.75	153.4075013	96.88688927
8.76	153.396368	96.96022265
8.77	153.3852267	97.033526
8.78	153.3740812	97.10680445
8.79	153.3629278	97.18005287
8.8	153.3517701	97.2532764
8.81	153.3406046	97.32646991
8.82	153.3294349	97.39963853
8.83	153.3182573	97.47277714
8.84	153.3070754	97.54589087
8.85	153.2958858	97.61897461
8.86	153.2846919	97.69203346
8.87	153.2734902	97.76506233
8.88	153.2622843	97.83806632
8.89	153.2510707	97.91104034
8.9	153.2398528	97.98398948
8.91	153.2286271	98.05690866
8.92	153.2173973	98.12980298
8.93	153.2061597	98.20266733
8.94	153.194918	98.27550683
8.95	153.1836685	98.34831638
8.96	153.1724148	98.42110108
8.97	153.1611535	98.49385584
8.98	153.149888	98.56658575
8.99	153.1386147	98.63928573
9	153.1273374	98.71196087
9.01	153.1160523	98.78460609
9.02	153.1047632	98.85722648
9.03	153.0934664	98.92981695
9.04	153.0821654	99.00238259
9.05	153.0708568	99.07491833
9.06	153.0595442	99.14742926
9.07	153.0482238	99.21991028

9.08	153.0368994	99.29236649
9.09	153.0255674	99.36479281
9.1	153.0142313	99.43719433
9.11	153.0028876	99.50956597
9.12	152.9915399	99.58191281
9.13	152.9801845	99.65422977
9.14	152.9688252	99.72652195
9.15	152.9574582	99.79878426
9.16	152.9460873	99.87102179
9.17	152.9347087	99.94322946
9.18	152.9233262	100.0154124
9.19	152.9119361	100.0875654
9.2	152.900542	100.1596937
9.21	152.8891404	100.2317921
9.22	152.8777348	100.3038658
9.23	152.8663217	100.3759096
9.24	152.8549047	100.4479287
9.25	152.8434801	100.519918
9.26	152.8320516	100.5918825
9.27	152.8206155	100.6638172
9.28	152.8091756	100.7357272
9.29	152.7977282	100.8076074
9.3	152.7862769	100.8794628
9.31	152.7748181	100.9512884
9.32	152.7633554	101.0230893
9.33	152.7518852	101.0948605
9.34	152.7404112	101.1666069
9.35	152.7289297	101.2383235
9.36	152.7174444	101.3100154
9.37	152.7059516	101.3816775
9.38	152.6944551	101.453315
9.39	152.682951	101.5249226
9.4	152.6714432	101.5965056
9.41	152.6599279	101.6680588
9.42	152.6484089	101.7395874
9.43	152.6368824	101.8110861
9.44	152.6253522	101.8825602
9.45	152.6138145	101.9540046
9.46	152.6022731	102.0254243
9.47	152.5907243	102.0968143
9.48	152.5791718	102.1681796
9.49	152.5676119	102.2395152
9.5	152.5560483	102.3108261
9.51	152.5444773	102.3821073
9.52	152.5329027	102.4533638
9.53	152.5213206	102.5245907

9.54	152.5097349	102.5957929
9.55	152.4981418	102.6669654
9.56	152.4865451	102.7381133
9.57	152.474941	102.8092315
9.58	152.4633333	102.8803251
9.59	152.4517183	102.951389
9.6	152.4400996	103.0224282
9.61	152.4284736	103.0934378
9.62	152.416844	103.1644228
9.63	152.4052071	103.2353782
9.64	152.3935667	103.3063089
9.65	152.3819189	103.3772099
9.66	152.3702675	103.4480864
9.67	152.3586089	103.5189333
9.68	152.3469467	103.5897555
9.69	152.3352773	103.6605481
9.7	152.3236043	103.7313161
9.71	152.311924	103.8020545
9.72	152.3002403	103.8727684
9.73	152.2885493	103.9434526
9.74	152.2768547	104.0141122
9.75	152.265153	104.0847423
9.76	152.2534478	104.1553477
9.77	152.2417353	104.2259236
9.78	152.2300194	104.296475
9.79	152.2182962	104.3669967
9.8	152.2065697	104.4374939
9.81	152.1948359	104.5079616
9.82	152.1830987	104.5784046
9.83	152.1713542	104.6488182
9.84	152.1596064	104.7192071
9.85	152.1478514	104.7895666
9.86	152.136093	104.8599015
9.87	152.1243275	104.9302068
9.88	152.1125585	105.0004877
9.89	152.1007824	105.070739
9.9	152.089003	105.1409657
9.91	152.0772164	105.211163
9.92	152.0654264	105.2813358
9.93	152.0536293	105.351479
9.94	152.0418289	105.4215978
9.95	152.0300214	105.491687
9.96	152.0182105	105.5617517
9.97	152.0063926	105.631787
9.98	151.9945714	105.7017978
9.99	151.982743	105.7717791

10	151.9709114	105.8417358

Appendix 5-14: Gas and Solid Phase Velocity along the Flash tube

Distance (m)	Solid velocity (m/s)	Gas velocity (m/s)
0.01000000000000	0.00100000000000	24
0.02000000000000	1.27240940500000	24.00280396297973
0.03000000000000	1.26077847800000	24.00270526615227
0.04000000000000	1.26077847900000	24.00555022196630
0.05000000000000	1.27240940500000	24.00547043883386
0.06000000000000	1.27240940453666	24.00832810381794
0.07000000000000	1.26077847940345	24.00825826530561
0.08000000000000	1.25631132365822	24.01112542145545
0.09000000000000	1.25460808935188	24.01106431061465
0.10000000000000	1.25397481653046	24.01394049139170
0.11000000000000	1.25375631646870	24.01388792446287
0.12000000000000	1.25369873370424	24.01677305996258
0.13000000000000	1.25370364035212	24.01672900679019
0.14000000000000	1.25373286927055	24.01962308678247
0.15000000000000	1.25377161400954	24.01958754042330
0.16000000000000	1.25381413605832	24.02249056370703
0.17000000000000	1.25385820589693	24.02246352072773
0.18000000000000	1.25390296286542	24.02537548746289
0.19000000000000	1.25394806919787	24.02535694495490
0.20000000000000	1.25399339792293	24.02827785550049
0.21000000000000	1.25403889577408	24.02826781062766
0.22000000000000	1.25408454613592	24.03119766536566
0.23000000000000	1.25413033850599	24.03119611529570
0.24000000000000	1.25417627288059	24.03413491460440
0.25000000000000	1.25422234516898	24.03414185649849
0.26000000000000	1.25426855788289	24.03708960074846
0.27000000000000	1.25431490787738	24.03710503175973
0.28000000000000	1.25436139806031	24.04006172131322
0.29000000000000	1.25440802541085	24.04008563858649
0.30000000000000	1.25445479291436	24.04305127379732
0.31000000000000	1.25450169755061	24.04308367446910
0.32000000000000	1.25454874233462	24.04605825568272
0.33000000000000	1.25459592422817	24.04609913688120
0.34000000000000	1.25464324626872	24.04908266443464
0.35000000000000	1.25469070539730	24.04913202327971
0.36000000000000	1.25473830467275	24.05212449750164
0.37000000000000	1.25478604101487	24.05218233110489
0.38000000000000	1.25483391750375	24.05518375231559
0.39000000000000	1.25488193103792	24.05525005778033
0.40000000000000	1.25493008471867	24.05826042629174
0.41000000000000	1.25497837542324	24.05833520071303
0.42000000000000	1.25502680627414	24.06135451682872
0.43000000000000	1.25507537412732	24.06143775729337
0.44000000000000	1.25512408212649	24.06446602130859
0.45000000000000	1.25517292710631	24.06455772489515
0.46000000000000	1.25522191223172	24.06759493709685
0.47000000000000	1.25527103431605	24.06769510087564
0.48000000000000	1.25532029654548	24.07074126154246
0.49000000000000	1.25536969571205	24.07084988257558
0.50000000000000	1.25541923502313	24.07390499197785
0.51000000000000	1.25546891124947	24.07402206731923
0.52000000000000	1.25551872761969	24.07708612571900
0.53000000000000	1.25556868088320	24.07721165241434
0.54000000000000	1.25561877428986	24.08028466006541
0.55000000000000	1.25566900456776	24.08041863515227
0.56000000000000	1.25571937498801	24.08350059230017
0.57000000000000	1.25576988225737	24.08364301280791
0.58000000000000	1.25582052966820	24.08673391968994
0.59000000000000	1.25587131390592	24.08688478263980
0.60000000000000	1.25592223828415	24.08998463948504
0.61000000000000	1.25597329946697	24.09014394189008

0.62000000000000	1.25602450078927	24.09325274891939
0.63000000000000	1.25607583889377	24.09342048778459
0.64000000000000	1.25612731713664	24.09653824521063
0.65000000000000	1.25617893213925	24.09671441753283
0.66000000000000	1.25623068727904	24.09984112556007
0.67000000000000	1.25628257915601	24.10002572832801
0.68000000000000	1.25633461116890	24.10316138715275
0.69000000000000	1.25638677989633	24.10335441734711
0.70000000000000	1.25643908875834	24.10649902715750
0.71000000000000	1.25649153431218	24.10670048175086
0.72000000000000	1.25654411999916	24.10985404272688
0.73000000000000	1.25659684235519	24.11006391868378
0.74000000000000	1.25664970484285	24.11322643099732
0.75000000000000	1.25670270397668	24.11344472527424
0.76000000000000	1.25675584324057	24.11661618908903
0.77000000000000	1.25680911912765	24.11684289863443
0.78000000000000	1.25686253514315	24.12002331410612
0.79000000000000	1.25691608775880	24.12025843586044
0.80000000000000	1.25696978050113	24.12344780313659
0.81000000000000	1.25702360982047	24.12369133403226
0.82000000000000	1.25707757926470	24.12688965325235
0.83000000000000	1.25713168526272	24.12714159021380
0.84000000000000	1.25718593138375	24.13034886150925
0.85000000000000	1.25724031403528	24.13060920145296
0.86000000000000	1.25729483680785	24.13382542494715
0.87000000000000	1.25734949608755	24.13409416478162
0.88000000000000	1.25740429548625	24.13731934058987
0.89000000000000	1.25745923136862	24.13759647721566
0.90000000000000	1.25751430736788	24.14083060544531
0.91000000000000	1.25756951982726	24.14111613575503
0.92000000000000	1.25762487240136	24.14435921650538
0.93000000000000	1.25768036141195	24.14465313738374
0.94000000000000	1.25773599053499	24.14790517074612
0.95000000000000	1.25779175607082	24.14820747906991
0.96000000000000	1.25784766171675	24.15146846512768
0.97000000000000	1.25790370375169	24.15177915776579
0.98000000000000	1.25795988589431	24.15504909659435
0.99000000000000	1.25801620440207	24.15536817040780
1	1.25807266301503	24.15864706207459
1.01000000000000	1.25812925796917	24.15897451391655
1.02000000000000	1.25818599302595	24.16226235848108
1.03000000000000	1.25824286439987	24.16259818519685
1.04000000000000	1.25829987587378	24.16589498271072
1.05000000000000	1.25835702364072	24.16623918113777
1.06000000000000	1.25841431150494	24.16954493164469
1.07000000000000	1.25847173563799	24.16989749861267
1.08000000000000	1.25852929986552	24.17321220214844
1.09000000000000	1.25858700033761	24.17357313447921
1.10000000000000	1.25864484090132	24.17689679107176
1.11000000000000	1.25870281768522	24.17726608557937
1.12000000000000	1.25876093455779	24.18059869524879
1.13000000000000	1.25881918762612	24.18097634873950
1.14000000000000	1.25887758078010	24.18431791149804
1.15000000000000	1.25893611010531	24.18470392077038
1.16000000000000	1.25899477951310	24.18805443662244
1.17000000000000	1.25905358506750	24.18844879846718
1.18000000000000	1.25911253070131	24.19180826740936
1.19000000000000	1.25917161245705	24.19221097860954
1.20000000000000	1.25923083428897	24.19557940063065
1.21000000000000	1.25929019221804	24.19599045796159
1.22000000000000	1.25934969021998	24.19936783304264
1.23000000000000	1.25940932429423	24.19978723327195
1.24000000000000	1.25946909843794	24.20317356138622
1.25000000000000	1.25952900862905	24.20360130127383
1.26000000000000	1.25958905888616	24.20699658238681
1.27000000000000	1.25964924516565	24.20743265868498
1.28000000000000	1.25970957150761	24.21083689275445
1.29000000000000	1.25977003384685	24.21128130220777
1.30000000000000	1.25983063624496	24.21469448918379
1.31000000000000	1.25989137461518	24.21514722852921
1.32000000000000	1.25995225304059	24.21856936835413

1.33000000000000	1.26001326741285	24.21903043432099
1.34000000000000	1.26007442183654	24.22246152692946
1.35000000000000	1.26013571218176	24.22293091623948
1.36000000000000	1.26019714257457	24.22637096155849
1.37000000000000	1.26025870886350	24.22684867092579
1.38000000000000	1.26032041519612	24.23029766887468
1.39000000000000	1.26038225739937	24.23078369500580
1.40000000000000	1.26044423964233	24.23424164549625
1.41000000000000	1.26050635773034	24.23473598509016
1.42000000000000	1.26056861585402	24.23820288802625
1.43000000000000	1.26063100979709	24.23870553777437
1.44000000000000	1.26069354377171	24.24218139305255
1.45000000000000	1.26075621354000	24.24269234963878
1.46000000000000	1.26081902333563	24.24617715714792
1.47000000000000	1.26088196889911	24.24669641724863
1.48000000000000	1.26094505448568	24.25019017686999
1.49000000000000	1.26100827581420	24.25071773715405
1.50000000000000	1.26107163716146	24.25422044876138
1.51000000000000	1.26113513422471	24.25475630589017
1.52000000000000	1.26119877130229	24.25826796934963
1.53000000000000	1.26126254406981	24.25881211997705
1.54000000000000	1.26132645684716	24.26233273514731
1.55000000000000	1.26139050528832	24.26288517591982
1.56000000000000	1.26145469373477	24.26641474265200
1.57000000000000	1.26151901781881	24.26697547020861
1.58000000000000	1.26158348190350	24.27051398834636
1.59000000000000	1.26164808159950	24.27108299931865
1.60000000000000	1.26171282129145	24.27463046869813
1.61000000000000	1.26177769656834	24.27520775971030
1.62000000000000	1.26184271183641	24.27876418016020
1.63000000000000	1.26190786266296	24.27934974782902
1.64000000000000	1.26197315347585	24.28291511917060
1.65000000000000	1.26203857982070	24.28350896010548
1.66000000000000	1.26210414614697	24.28708328215255
1.67000000000000	1.26216984797859	24.28768539295555
1.68000000000000	1.26223568978665	24.29126866551452
1.69000000000000	1.26230166707337	24.29187904278034
1.70000000000000	1.26236778433147	24.29547126565021
1.71000000000000	1.26243403704147	24.29608990596623
1.72000000000000	1.26250042971772	24.29969107893864
1.73000000000000	1.26256695781902	24.30031797888492
1.74000000000000	1.26263362588138	24.30392810174412
1.75000000000000	1.26270042934186	24.30456325789344
1.76000000000000	1.26276737275814	24.30818233041634
1.77000000000000	1.26283445154553	24.30882573933420
1.78000000000000	1.26290167028337	24.31245376129037
1.79000000000000	1.26296902436526	24.31310541953500
1.80000000000000	1.26303651839219	24.31674239068673
1.81000000000000	1.26310414773600	24.31740229480910
1.82000000000000	1.26317191701936	24.32104821491135
1.83000000000000	1.26323982159238	24.32171636145523
1.84000000000000	1.26330786609940	24.32537123025569
1.85000000000000	1.26337604586876	24.32604761575762
1.86000000000000	1.26344436556649	24.32971143299670
1.87000000000000	1.26351282049918	24.33039605398603
1.88000000000000	1.26358141535455	24.33406881939693
1.89000000000000	1.26365014541740	24.33476167239582
1.90000000000000	1.26371901539717	24.33844338570449
1.91000000000000	1.26378802055687	24.33914446722794
1.92000000000000	1.26385716562767	24.34283512815311
1.93000000000000	1.26392644585077	24.34354443470898
1.94000000000000	1.26399586597907	24.34724404296219
1.95000000000000	1.26406542123196	24.34796157105122
1.96000000000000	1.26413511638408	24.35167012633683
1.97000000000000	1.26420494663302	24.35239587245264
1.98000000000000	1.26427491677514	24.35611337446786
1.99000000000000	1.26434502198623	24.35684733509694
2	1.26441526708439	24.36057378353184
2.01000000000000	1.26448564722358	24.36131595515365
2.02000000000000	1.26455616724366	24.36505134969115
2.03000000000000	1.26462682227676	24.36580172877807

2.04000000000000	1.26469761718451	24.36954606909400
2.05000000000000	1.26476854707719	24.37030465211136
2.06000000000000	1.26483961683820	24.37405793787445
2.07000000000000	1.26491082155598	24.37482472128056
2.08000000000000	1.26498216613570	24.37858695215248
2.09000000000000	1.26505364564394	24.37936193239862
2.10000000000000	1.26512526500768	24.38313310803398
2.11000000000000	1.26519701927161	24.38391628156446
2.12000000000000	1.26526891338453	24.38769640161081
2.13000000000000	1.26534094236924	24.38848776486296
2.14000000000000	1.26541311119635	24.39227682896085
2.15000000000000	1.26548541486678	24.39307637836503
2.16000000000000	1.26555785837294	24.39687438614800
2.17000000000000	1.26563043669389	24.39768211812763
2.18000000000000	1.26570315484384	24.40148906922225
2.19000000000000	1.26577600777994	24.40230498019383
2.20000000000000	1.26584900053826	24.40612087421967
2.21000000000000	1.26592212805403	24.40694496059280
2.22000000000000	1.26599539538516	24.41076979716250
2.23000000000000	1.26606879744496	24.41160205533987
2.24000000000000	1.26614233931318	24.41543583405915
2.25000000000000	1.26621601588123	24.41627626043658
2.26000000000000	1.26628983225071	24.42011898090422
2.27000000000000	1.26636378329108	24.42096757187069
2.28000000000000	1.26643787412581	24.42481923367859
2.29000000000000	1.26651209960244	24.42567598561624
2.30000000000000	1.26658646486630	24.42953658834941
2.31000000000000	1.26666096474297	24.43040149763355
2.32000000000000	1.26673560439968	24.43427104087015
2.33000000000000	1.26681037864004	24.43514410386929
2.34000000000000	1.26688529265319	24.43902258718064
2.35000000000000	1.26696034122075	24.43990380025651
2.36000000000000	1.26703552955376	24.44379122320709
2.37000000000000	1.26711085241188	24.44468058271465
2.38000000000000	1.26718631502806	24.44857694486213
2.39000000000000	1.26726191213996	24.44947444714960
2.40000000000000	1.26733764900246	24.45337974804488
2.41000000000000	1.26741352033123	24.45428538945373
2.42000000000000	1.26748953140306	24.45819962864094
2.43000000000000	1.26756567691163	24.45911340550593
2.44000000000000	1.26764196215568	24.46303658252245
2.45000000000000	1.26771838180685	24.46395849117165
2.46000000000000	1.26779494118583	24.46789060554810
2.47000000000000	1.26787163494227	24.46882064230290
2.48000000000000	1.26794846841879	24.47276169356321
2.49000000000000	1.26802543624300	24.47369985473834
2.50000000000000	1.26810254377950	24.47764984239974
2.51000000000000	1.26817978563387	24.47859612430329
2.52000000000000	1.26825716719267	24.48255504787632
2.53000000000000	1.26833468303943	24.48350944680975
2.54000000000000	1.26841233858271	24.48747730579831
2.55000000000000	1.26849012838396	24.48843981805646
2.56000000000000	1.26856805787373	24.49241661195779
2.57000000000000	1.26864612159144	24.49338723382894
2.58000000000000	1.26872432498961	24.49737296213366
2.59000000000000	1.26880266258558	24.49835168989951
2.60000000000000	1.26888113985392	24.50234635209164
2.61000000000000	1.26895975128984	24.50333318202732
2.62000000000000	1.26903850238994	24.50733677758429
2.63000000000000	1.26911738762736	24.50833170595841
2.64000000000000	1.26919641252071	24.51234423435110
2.65000000000000	1.26927557152103	24.51334725742575
2.66000000000000	1.26935487016897	24.51736871811847
2.67000000000000	1.26943430289346	24.51837983214924
2.68000000000000	1.26951387525719	24.52241022459977
2.69000000000000	1.26959358166697	24.52342942583578
2.70000000000000	1.26967342770756	24.52746874949540
2.71000000000000	1.26975340776363	24.52849603417931
2.72000000000000	1.26983352744201	24.53254428849280
2.73000000000000	1.26991378110522	24.53357965286080
2.74000000000000	1.26999417438217	24.53763683726648

2.75000000000000	1.27007470161324	24.53868027754837
2.76000000000000	1.27015536844942	24.54274639147808
2.77000000000000	1.27023616920894	24.54379790389723
2.78000000000000	1.27031710956487	24.54787294677639
2.79000000000000	1.27039818381327	24.54893252754979
2.80000000000000	1.27047939764933	24.55301649879740
2.81000000000000	1.27056074534693	24.55408414413568
2.82000000000000	1.27064223262337	24.55817704316435
2.83000000000000	1.27072385373033	24.55925274927177
2.84000000000000	1.27080561440726	24.56335457548771
2.85000000000000	1.27088750888363	24.56443833856220
2.86000000000000	1.27096954292102	24.56854909136528
2.87000000000000	1.27105171072671	24.56964090759847
2.88000000000000	1.27113401808440	24.57376058638221
2.89000000000000	1.27121645917916	24.57486045195942
2.90000000000000	1.27129903981686	24.57898905611102
2.91000000000000	1.27138175416033	24.58009696721130
2.92000000000000	1.27146460803761	24.58423449611166
2.93000000000000	1.27154759558929	24.58535044890779
2.94000000000000	1.27163072266559	24.58949690193151
2.95000000000000	1.27171398338485	24.59062089259005
2.96000000000000	1.27179738361947	24.59477626910548
2.97000000000000	1.27188091746553	24.59590829378676
2.98000000000000	1.27196459081763	24.60007259315601
2.99000000000000	1.27204839774960	24.60121264801414
3	1.27213234417823	24.60538586959309
3.01000000000000	1.27221642415507	24.60653395077602
3.02000000000000	1.27230064361912	24.61071609391432
3.03000000000000	1.27238499659966	24.61187219756382
3.04000000000000	1.27246948905791	24.61606326160496
3.05000000000000	1.27255411500085	24.61722738385667
3.06000000000000	1.27263888041194	24.62142736813795
3.07000000000000	1.27272377927584	24.62259950512138
3.08000000000000	1.27280881759827	24.62680840897395
3.09000000000000	1.27289398934157	24.62798855681249
3.10000000000000	1.27297930053371	24.63220637956140
3.11000000000000	1.27306474511472	24.63339453437235
3.12000000000000	1.27315032913482	24.63762127533650
3.13000000000000	1.27323604651169	24.63881743323110
3.14000000000000	1.27332190331786	24.64305309172333
3.15000000000000	1.27340789344865	24.64425724880676
3.16000000000000	1.27349402299887	24.64850182413382
3.17000000000000	1.27358028584148	24.64971397650523
3.18000000000000	1.27366668809359	24.65396746796783
3.19000000000000	1.27375322360581	24.65518761172034
3.20000000000000	1.27383989851753	24.65945001861315
3.21000000000000	1.27392670665700	24.66067814983391
3.22000000000000	1.27401365418593	24.66494947144558
3.23000000000000	1.27410073491016	24.66618558621575
3.24000000000000	1.27418795501375	24.67046582182896
3.25000000000000	1.27427530828014	24.67170991622374
3.26000000000000	1.27436280091572	24.67599906511517
3.27000000000000	1.27445042668152	24.67725113520384
3.28000000000000	1.27453819180629	24.68154919664422
3.29000000000000	1.27462609002864	24.68280923849013
3.30000000000000	1.27471412759966	24.68711621174426
3.31000000000000	1.27480229823556	24.68838422140485
3.32000000000000	1.27489060820978	24.69270010573161
3.33000000000000	1.27497905121610	24.69397607925846
3.34000000000000	1.27506763355034	24.69830087391084
3.35000000000000	1.27515634888382	24.69958480734965
3.36000000000000	1.27524520353475	24.70391851157476
3.37000000000000	1.27533419115201	24.70521040096541
3.38000000000000	1.27542331807620	24.70955301400450
3.39000000000000	1.27551257793372	24.71085285538101
3.40000000000000	1.27560197708760	24.71520437646951
3.41000000000000	1.27569150914175	24.71651216586014
3.42000000000000	1.27578118048162	24.72087259422764
3.43000000000000	1.27587098468863	24.72218832765483
3.44000000000000	1.27596092817066	24.72655766252514
3.45000000000000	1.27605100448664	24.72788133600559

3.46000000000000	1.27614122006688	24.73225957659674
3.47000000000000	1.27623156844781	24.73359118614138
3.48000000000000	1.27632205608219	24.73797833166563
3.49000000000000	1.27641267648392	24.73931787327969
3.50000000000000	1.27650343612823	24.74371392294357
3.51000000000000	1.27659432850649	24.74506139262656
3.52000000000000	1.27668536011640	24.74946634563088
3.53000000000000	1.27677652442679	24.75082173937662
3.54000000000000	1.27686782795785	24.75523559491651
3.55000000000000	1.27695926415585	24.75659890871314
3.56000000000000	1.27705083956349	24.76102166597803
3.57000000000000	1.27714254760445	24.76239289580807
3.58000000000000	1.27723439484394	24.76682455398174
3.59000000000000	1.27732637468309	24.76820369582206
3.60000000000000	1.27741849370962	24.77264425408264
3.61000000000000	1.27751074530207	24.77403130390450
3.62000000000000	1.27760313607068	24.77848076142454
3.63000000000000	1.27769565937139	24.77987571519361
3.64000000000000	1.27778832183701	24.78433407114002
3.65000000000000	1.27788111680085	24.78573692481641
3.66000000000000	1.27797405091826	24.79020417835053
3.67000000000000	1.27806711749997	24.79161492788879
3.68000000000000	1.27816032322386	24.79609107816642
3.69000000000000	1.27825366137803	24.79750971951556
3.70000000000000	1.27834713866295	24.80199476568695
3.71000000000000	1.27844074834407	24.80342129479047
3.72000000000000	1.27853449714445	24.80791523600037
3.73000000000000	1.27862837830688	24.80934964879629
3.74000000000000	1.27872239857703	24.81385248418390
3.75000000000000	1.27881655117502	24.81529477660476
3.76000000000000	1.27891084286912	24.81980650530387
3.77000000000000	1.27900526685679	24.82125667327674
3.78000000000000	1.27909982992890	24.82577729441564
3.79000000000000	1.27919452526024	24.82723533386218
3.80000000000000	1.27928935966431	24.83176484656374
3.81000000000000	1.27938432629320	24.83323075340018
3.82000000000000	1.27947943198305	24.83776915678183
3.83000000000000	1.27957466986323	24.83924292691901
3.84000000000000	1.27967004679256	24.84379022009281
3.85000000000000	1.27976555587768	24.84527184943620
3.86000000000000	1.27986120400006	24.84982803150882
3.87000000000000	1.27995698424363	24.85131751595852
3.88000000000000	1.28005290351253	24.85588258603128
3.89000000000000	1.28014895486794	24.85737992148205
3.90000000000000	1.28024514523670	24.86195387865094
3.91000000000000	1.28034146765722	24.86345906099224
3.92000000000000	1.28043792907905	24.86804190434791
3.93000000000000	1.28053452251784	24.86955492946390
3.94000000000000	1.28063125494584	24.87414665809173
3.95000000000000	1.28072811935594	24.87566752186128
3.96000000000000	1.28082512274309	24.88026813484136
3.97000000000000	1.28092225807741	24.88179683313810
3.98000000000000	1.28101953237658	24.88640632954526
3.99000000000000	1.28111693858791	24.88794285823758
4	1.28121448375184	24.89256123714142
4.01000000000000	1.28131216079287	24.89410559209248
4.02000000000000	1.28140997677418	24.89873285255740
4.03000000000000	1.28150792459747	24.90028502962517
4.04000000000000	1.28160601134868	24.90492117071036
4.05000000000000	1.28170422990666	24.90648116574762
4.06000000000000	1.28180258738015	24.91112618650710
4.07000000000000	1.28190107662516	24.91269399536150
4.08000000000000	1.28199970477321	24.91734789484413
4.09000000000000	1.28209846465745	24.91892351335815
4.10000000000000	1.28219736343221	24.92358629060768
4.11000000000000	1.28229639390777	24.92516971461869
4.12000000000000	1.28239556326129	24.92984136867373
4.13000000000000	1.28249486428016	24.93143259401401
4.14000000000000	1.28259430416435	24.93611312390809
4.15000000000000	1.28269387567838	24.93771214640482
4.16000000000000	1.28279358604505	24.94240155116641

4.17000000000000	1.28289342800599	24.94400836664174
4.18000000000000	1.28299340880684	24.94870664529423
4.19000000000000	1.28309352116631	24.95032124956525
4.20000000000000	1.28319377235291	24.95502840112703
4.21000000000000	1.28329415506243	24.95665079000580
4.22000000000000	1.28339467658625	24.96136681349023
4.23000000000000	1.28349532959721	24.96299698278384
4.24000000000000	1.28359612140959	24.96772187719929
4.25000000000000	1.28369704467328	24.96935982270983
4.26000000000000	1.28379810672546	24.97409358705971
4.27000000000000	1.28389930019305	24.97573930458432
4.28000000000000	1.28400063243615	24.98048193786708
4.29000000000000	1.28410209605869	24.98213542319795
4.30000000000000	1.28420369844370	24.98688692440713
4.31000000000000	1.28430543217214	24.98854817333153
4.32000000000000	1.28440730464997	24.99330854145574
4.33000000000000	1.28450930843514	24.99497754975604
4.34000000000000	1.28461145095656	24.99974678377902
4.35000000000000	1.28471372474917	25.00142354723272
4.36000000000000	1.28481613726484	25.00620164613333
4.37000000000000	1.28491868101550	25.00788616051306
4.38000000000000	1.28502136347599	25.01267312326533
4.39000000000000	1.28512417713519	25.01436538433888
4.40000000000000	1.28522712949093	25.01916120991199
4.41000000000000	1.28533021300905	25.02086121344233
4.42000000000000	1.28543343521036	25.02566590080067
4.43000000000000	1.28553678853767	25.02737364254598
4.44000000000000	1.28564028053479	25.03218719064916
4.45000000000000	1.28574390362144	25.03390266636282
4.46000000000000	1.28584766536447	25.03872507416567
4.47000000000000	1.28595155816051	25.04044827959630
4.48000000000000	1.28605558959945	25.04527954604893
4.49000000000000	1.28615975205482	25.04701047694043
4.50000000000000	1.28626405313954	25.05185060098820
4.51000000000000	1.28636848520406	25.05358925307973
4.52000000000000	1.28647305588435	25.05843823366331
4.53000000000000	1.28657775750773	25.06018460268934
4.54000000000000	1.28668259773326	25.06504243874473
4.55000000000000	1.28678756886511	25.06679652043504
4.56000000000000	1.28689267858543	25.07166321089356
4.57000000000000	1.28699791917525	25.07342500097328
4.58000000000000	1.28710329833980	25.07830054476161
4.59000000000000	1.28720880833698	25.08007003895122
4.60000000000000	1.28731445689511	25.08495443499143
4.61000000000000	1.28742023624892	25.08673162900680
4.62000000000000	1.28752615414986	25.09162487621636
4.63000000000000	1.28763220280947	25.09340976576874
4.64000000000000	1.28773839000234	25.09831186306053
4.65000000000000	1.28784470791681	25.10010444385660
4.66000000000000	1.28795116435062	25.10501539013897
4.67000000000000	1.28805775146891	25.10681565788085
4.68000000000000	1.28816447709258	25.11173545205758
4.69000000000000	1.28827133336354	25.11354340244285
4.70000000000000	1.28837832812585	25.11847204341322
4.71000000000000	1.28848545349821	25.12028767213494
4.72000000000000	1.28859271734787	25.12522515879372
4.73000000000000	1.28870011177027	25.12704846154045
4.74000000000000	1.28880764465585	25.13199479277795
4.75000000000000	1.28891530807682	25.13382576523377
4.76000000000000	1.28902310994682	25.13878093993583
4.77000000000000	1.28913104231477	25.14061957778035
4.78000000000000	1.28923911311755	25.14558359482841
4.79000000000000	1.28934731438080	25.14742989373679
4.80000000000000	1.28945565406463	25.15240275200783
4.81000000000000	1.28956412417139	25.15425670765084
4.82000000000000	1.28967273268443	25.15923840601749
4.83000000000000	1.28978147158281	25.16110001406148
4.84000000000000	1.28989034887313	25.16609055139196
4.85000000000000	1.28999935651112	25.16795980749890
4.86000000000000	1.29010850252667	25.17295918265710
4.87000000000000	1.29021777885217	25.17483608248460

4.88000000000000	1.29032719354079	25.17984429433008
4.89000000000000	1.29043673850159	25.18172883353142
4.90000000000000	1.29054642181104	25.18674588091941
4.91000000000000	1.29065623535483	25.18863805514354
4.92000000000000	1.29076618723275	25.19366393692501
4.93000000000000	1.29087626930711	25.19556374181656
4.94000000000000	1.29098648970103	25.20059845683820
4.95000000000000	1.29109684025344	25.20250588803756
4.96000000000000	1.29120732911080	25.20754943514179
4.97000000000000	1.29131794808864	25.20946448828506
4.98000000000000	1.29142870535678	25.21451686631011
4.99000000000000	1.29153959270733	25.21643953702916
5	1.29165061833347	25.22150074480902
5.01000000000000	1.29176177400390	25.22343102873151
5.02000000000000	1.29187306793518	25.22850106509600
5.03000000000000	1.29198449187256	25.23043895784536
5.04000000000000	1.29209605405600	25.23551782162014
5.05000000000000	1.29220774620731	25.23746331881564
5.06000000000000	1.29231957658984	25.24255100882221
5.07000000000000	1.29243153690194	25.24450410607896
5.08000000000000	1.29254363543039	25.24960062113471
5.09000000000000	1.29265586385005	25.25156131406368
5.10000000000000	1.29276823047113	25.25666665298189
5.11000000000000	1.29288072694503	25.25863493718992
5.12000000000000	1.29299336160537	25.26374909877978
5.13000000000000	1.29310612608007	25.26572496986962
5.14000000000000	1.29321902872620	25.27084795293626
5.15000000000000	1.29333206114816	25.27283140650658
5.16000000000000	1.29344523172652	25.27796320985111
5.17000000000000	1.29355853204211	25.27995424149650
5.18000000000000	1.29367197049901	25.28509486391599
5.19000000000000	1.29378553865451	25.28709346922703
5.20000000000000	1.29389924493617	25.29224290951455
5.21000000000000	1.29401308087775	25.29424908407777
5.22000000000000	1.29412705493031	25.29940734102242
5.23000000000000	1.29424115860404	25.30142108042037
5.24000000000000	1.29435540037353	25.30658815280727
5.25000000000000	1.29446977172539	25.30860945261852
5.26000000000000	1.29458428115774	25.31378533922888
5.27000000000000	1.29469892013359	25.31581419502802
5.28000000000000	1.29481369717464	25.32099889463912
5.29000000000000	1.29492860372028	25.32303530199682
5.30000000000000	1.29504364831576	25.32822881338204
5.31000000000000	1.29515882237686	25.33027276786504
5.32000000000000	1.29527413447242	25.33547508979388
5.33000000000000	1.29538957599457	25.33752658696503
5.34000000000000	1.29550515553575	25.34273771820315
5.35000000000000	1.29562086446444	25.34479675362141
5.36000000000000	1.29573671139669	25.35001669293062
5.37000000000000	1.29585268767731	25.35208326215108
5.38000000000000	1.29596880194598	25.35731200828938
5.39000000000000	1.29608504552383	25.35938610686331
5.40000000000000	1.29620142707418	25.36462365858491
5.41000000000000	1.29631793789446	25.36670528205975
5.42000000000000	1.29643458667165	25.37195163811509
5.43000000000000	1.29655136467948	25.37404078203447
5.44000000000000	1.29666828062857	25.37929594117023
5.45000000000000	1.29678532576895	25.38139260107401
5.46000000000000	1.29690250883492	25.38665656203315
5.47000000000000	1.29701982105277	25.38876073345742
5.48000000000000	1.29713727118050	25.39403349497918
5.49000000000000	1.29725485042065	25.39614517345630
5.50000000000000	1.29737256755492	25.40142673427622
5.51000000000000	1.29749041376210	25.40354591533483
5.52000000000000	1.29760839784760	25.40883627418479
5.53000000000000	1.29772651096644	25.41096295334982
5.54000000000000	1.29784476194777	25.41626210895805
5.55000000000000	1.29796314192282	25.41839628175076
5.56000000000000	1.29808165974449	25.42370423284185
5.57000000000000	1.29820030652020	25.42584589477983
5.58000000000000	1.29831909112661	25.43116264007479

5.59000000000000	1.29843800464735	25.43331178667198
5.60000000000000	1.29855705598283	25.43863732488820
5.61000000000000	1.29867623619285	25.44079395165493
5.62000000000000	1.29879555420163	25.44612828150627
5.63000000000000	1.29891500104511	25.44829238394926
5.64000000000000	1.29903458567133	25.45363550414599
5.65000000000000	1.29915429909236	25.45580707776839
5.66000000000000	1.29927415028005	25.46115898701729
5.67000000000000	1.29939413022263	25.46333802731868
5.68000000000000	1.29951424791576	25.46869872432300
5.69000000000000	1.29963449432378	25.47088522679942
5.70000000000000	1.29975487846621	25.47625471025894
5.71000000000000	1.29987539128348	25.47844867040290
5.72000000000000	1.29999604181899	25.48382693901393
5.73000000000000	1.30011682098925	25.48602835231445
5.74000000000000	1.30023773786151	25.49141540476985
5.75000000000000	1.30035878332838	25.49362426671245
5.76000000000000	1.30047996648101	25.49902010170167
5.77000000000000	1.30060127818803	25.50123640776842
5.78000000000000	1.30072272756452	25.50664102397750
5.79000000000000	1.30084430545516	25.50886476964703
5.80000000000000	1.30096602099893	25.51427816575862
5.81000000000000	1.30108786501655	25.51650934650612
5.82000000000000	1.30120984667093	25.52193152119952
5.83000000000000	1.30133195675881	25.52417013249679
5.84000000000000	1.30145420446704	25.52960108444795
5.85000000000000	1.30157658056837	25.53184712176340
5.86000000000000	1.30169909427360	25.53728684964496
5.87000000000000	1.30182173633148	25.53954030844363
5.88000000000000	1.30194451597679	25.54498881092491
5.89000000000000	1.30206742393424	25.54724968666851
5.90000000000000	1.30219046946260	25.55270696241556
5.91000000000000	1.30231364326255	25.55497525056246
5.92000000000000	1.30243695461686	25.56044129823809
5.93000000000000	1.30256039420214	25.56271699424336
5.94000000000000	1.30268397132520	25.56819181250710
5.95000000000000	1.30280767663858	25.57047491182253
5.96000000000000	1.30293151947311	25.57595849933071
5.97000000000000	1.30305549045726	25.57824899740482
5.98000000000000	1.30317959894590	25.58374135281058
5.99000000000000	1.30330383554340	25.58603924508864
6	1.30342820962870	25.59154036704193
6.01000000000000	1.30355271178204	25.59384564896599
6.02000000000000	1.30367735140647	25.59935553611361
6.03000000000000	1.30380211905808	25.60166820312250
6.04000000000000	1.30392702416401	25.60718685410811
6.05000000000000	1.30405205725622	25.60950690163747
6.06000000000000	1.30417722778594	25.61503431510161
6.07000000000000	1.30430252626100	25.61736173858394
6.08000000000000	1.30442796215673	25.62289791316405
6.09000000000000	1.30455352595680	25.62523270802867
6.10000000000000	1.30467922716067	25.63077764235912
6.11000000000000	1.30480505622782	25.63311980403224
6.12000000000000	1.30493102268189	25.63867349674434
6.13000000000000	1.30505711695812	25.64102302064905
6.14000000000000	1.30518334860433	25.64658547037107
6.15000000000000	1.30530970803156	25.64894235192738
6.16000000000000	1.30543620481180	25.65451355728458
6.17000000000000	1.30556282933185	25.65687779190942
6.18000000000000	1.30568959118792	25.66245775152406
6.19000000000000	1.30581648074255	25.66482933463131
6.20000000000000	1.30594350761616	25.67041804712267
6.21000000000000	1.30607066214704	25.67279697412318
6.22000000000000	1.30619795397983	25.67839443810761
6.23000000000000	1.30632537342854	25.68078070440921
6.24000000000000	1.30645293016205	25.68638691850009
6.25000000000000	1.30658061447010	25.68878051950764
6.26000000000000	1.30670843604582	25.69439548231545
6.27000000000000	1.30683638515464	25.69679641343081
6.28000000000000	1.30696447151395	25.70242012356314
6.29000000000000	1.30709268536487	25.70482838018524

6.30000000000000	1.30722103644909	25.71046083624680
6.31000000000000	1.30734951498338	25.71287641377162
6.32000000000000	1.30747813073374	25.71851761436425
6.33000000000000	1.30760687389259	25.72094050818486
6.34000000000000	1.30773575425024	25.72659045190759
6.35000000000000	1.30786476197475	25.72902065741416
6.36000000000000	1.30799390688077	25.73467934286320
6.37000000000000	1.30812317911197	25.73711685544303
6.38000000000000	1.30825258850735	25.74278428121178
6.39000000000000	1.30838212518619	25.74522909624931
6.40000000000000	1.30851179901185	25.75090526092842
6.41000000000000	1.30864160007919	25.75335737380524
6.42000000000000	1.30877153827597	25.75904227598259
6.43000000000000	1.30890160367261	25.76150168207750
6.44000000000000	1.30903180618127	25.76719532033824
6.45000000000000	1.30916213584793	25.76966201502719
6.46000000000000	1.30929260260914	25.77536438795376
6.47000000000000	1.30942319648646	25.77783836660998
6.48000000000000	1.30955392744084	25.78354947278211
6.49000000000000	1.30968478546937	25.78603073077603
6.50000000000000	1.30981578055745	25.79175056877079
6.51000000000000	1.30994690267767	25.79423910147012
6.52000000000000	1.31007816183991	25.79996766986191
6.53000000000000	1.31020954799224	25.80246347263163
6.54000000000000	1.31034107116900	25.80820076999223
6.55000000000000	1.31047272129377	25.81070383819461
6.56000000000000	1.31060450842536	25.81644986309319
6.57000000000000	1.31073642246282	25.81896019208780
6.58000000000000	1.31086847348948	25.82471494309094
6.59000000000000	1.31100065137982	25.82723252823472
6.60000000000000	1.31113296624168	25.83299600390639
6.61000000000000	1.31126540792500	25.83552084055363
6.62000000000000	1.31139798656216	25.84129303945528
6.63000000000000	1.31153069197850	25.84382512295761
6.64000000000000	1.31166353433094	25.84960604364814
6.65000000000000	1.31179650342025	25.85214536935461
6.66000000000000	1.31192960942792	25.85793501039041
6.67000000000000	1.31206284213009	25.86048157364747
6.68000000000000	1.31219621173284	25.86627993358243
6.69000000000000	1.31232970798768	25.86883372973396
6.70000000000000	1.31246334112529	25.87464080711950
6.71000000000000	1.31259710087253	25.87720183150686
6.72000000000000	1.31273099748471	25.88301762489193
6.73000000000000	1.31286502066403	25.88558587285389
6.74000000000000	1.31299918069042	25.89141038078504
6.75000000000000	1.31313346724141	25.89398584765790
6.76000000000000	1.31326789062156	25.89981906867921
6.77000000000000	1.31340244048374	25.90240174979677
6.78000000000000	1.31353712715716	25.90824368244997
6.79000000000000	1.31367194026998	25.91083357314355
6.80000000000000	1.31380689017609	25.91668421596795
6.81000000000000	1.31394196647893	25.91928131156641
6.82000000000000	1.31407717955707	25.92514066309901
6.83000000000000	1.31421251898923	25.92774495892876
6.84000000000000	1.31434799517870	25.93361301770420
6.85000000000000	1.31448359767942	25.93622450908926
6.86000000000000	1.31461933691942	25.94210127363985
6.87000000000000	1.31475520242787	25.94471995590183
6.88000000000000	1.31489120465753	25.95060542475759
6.89000000000000	1.31502733311280	25.95323129321571
6.90000000000000	1.31516359827120	25.95912546490439
6.91000000000000	1.31529998961233	25.96175851487551
6.92000000000000	1.31543651763846	25.96766138792260
6.93000000000000	1.31557317180440	25.97030161472124
6.94000000000000	1.31570996263721	25.97621318764998
6.95000000000000	1.31584687956684	25.97886058658833
6.96000000000000	1.31598393314518	25.98478085791974
6.97000000000000	1.31612111277734	25.98743542430771
6.98000000000000	1.31625842904000	25.99336439256061
6.99000000000000	1.31639587131343	25.99602612170577
7	1.31653345019915	26.00196378539681

7.01000000000000	1.31667115505253	26.00463267260452
7.02000000000000	1.31680899649996	26.01057903024817
7.03000000000000	1.31694696387191	26.01325507082150
7.04000000000000	1.31708506781965	26.01921012093010
7.05000000000000	1.31722329764873	26.02189331016990
7.06000000000000	1.31736166403529	26.02785705125367
7.07000000000000	1.31750015625997	26.03054738445858
7.08000000000000	1.31763878502382	26.03651981502562
7.09000000000000	1.31777753958252	26.03921728749208
7.10000000000000	1.31791643066205	26.04519840604842
7.11000000000000	1.31805544749313	26.04790301307069
7.12000000000000	1.31819460082665	26.05389281812030
7.13000000000000	1.31833387986839	26.05660455499050
7.14000000000000	1.31847329539418	26.06260304503528
7.15000000000000	1.31861283658479	26.06532190704338
7.16000000000000	1.31875251424104	26.07132908058322
7.17000000000000	1.31889231751869	26.07405506301706
7.18000000000000	1.31903225724352	26.08007091854984
7.19000000000000	1.31917232254628	26.08280401669518
7.20000000000000	1.31931252427777	26.08882855271679
7.21000000000000	1.31945285154368	26.09156876185729
7.22000000000000	1.31959331521982	26.09760197686165
7.23000000000000	1.31973390438684	26.10034929227890
7.24000000000000	1.31987462994557	26.10639118475800
7.25000000000000	1.32001548095160	26.10914560173155
7.26000000000000	1.32015646833079	26.11519617017543
7.27000000000000	1.32029758111365	26.11795768398281
7.28000000000000	1.32043883025112	26.12401692687958
7.29000000000000	1.32058020474860	26.12678553279630
7.30000000000000	1.32072171558209	26.13285344863223
7.31000000000000	1.32086335173188	26.13562914193179
7.32000000000000	1.32100512419908	26.14170572919123
7.33000000000000	1.32114702193884	26.14448850514520
7.34000000000000	1.32128905597737	26.15057376231066
7.35000000000000	1.32143121524467	26.15336361618862
7.36000000000000	1.32157351079210	26.15945754174078
7.37000000000000	1.32171593152447	26.16225446881038
7.38000000000000	1.32185848851830	26.16835706122810
7.39000000000000	1.32200117065320	26.17116105675507
7.40000000000000	1.32214398903085	26.17727231451541
7.41000000000000	1.32228693250569	26.18008337376359
7.42000000000000	1.32243001220455	26.18620329534183
7.43000000000000	1.32257321695666	26.18902141357317
7.44000000000000	1.32271655791405	26.19514999744283
7.45000000000000	1.32286002388070	26.19797516991740
7.46000000000000	1.32300362603388	26.20411241455028
7.47000000000000	1.32314735315231	26.20694463652632
7.48000000000000	1.32329121643847	26.21309054039247
7.49000000000000	1.32343520464582	26.21592980712639
7.50000000000000	1.32357932900211	26.22208436869417
7.51000000000000	1.32372357823549	26.22493067544056
7.52000000000000	1.32386796359898	26.23109389317665
7.53000000000000	1.32401247379543	26.23394723518831
7.54000000000000	1.32415712010314	26.24011910755773
7.55000000000000	1.32430189119965	26.24297948008569
7.56000000000000	1.32444679838855	26.24916000555178
7.57000000000000	1.32459183032204	26.25202740384531
7.58000000000000	1.32473699832902	26.25821658086982
7.59000000000000	1.32488229103636	26.26109100017645
7.60000000000000	1.32502771979828	26.26728882721951
7.61000000000000	1.32517327321627	26.27017026278504
7.62000000000000	1.32531896266991	26.27637673830517
7.63000000000000	1.32546477673532	26.27926518537372
7.64000000000000	1.32561072681742	26.28548030782790
7.65000000000000	1.32575680146693	26.28837576164187
7.66000000000000	1.32590301211416	26.29459952948550
7.67000000000000	1.32604934728441	26.29750198528565
7.68000000000000	1.32619581843341	26.30373439697261
7.69000000000000	1.32634241406098	26.30664384999804
7.70000000000000	1.32648914564829	26.31288490398069
7.71000000000000	1.32663600166972	26.31580134946886

7.72000000000000	1.32678299363185	26.32205104419807
7.73000000000000	1.32693010998361	26.32497447738483
7.74000000000000	1.32707736225702	26.33123281130997
7.75000000000000	1.32722473887552	26.33416322742958
7.76000000000000	1.32737225139660	26.34043019899858
7.77000000000000	1.32751988821821	26.34336759328371
7.78000000000000	1.32766766092331	26.34964320094305
7.79000000000000	1.32781555788432	26.35258756862481
7.80000000000000	1.32796359070973	26.35887181081955
7.81000000000000	1.32811174774641	26.36182314712751
7.82000000000000	1.32826004062836	26.36811602230129
7.83000000000000	1.32840845767690	26.37107432246348
7.84000000000000	1.32855701055158	26.37737582905858
7.85000000000000	1.32870568754813	26.38034108830153
7.86000000000000	1.32885450035166	26.38665122475884
7.87000000000000	1.32900343723231	26.38962343830758
7.88000000000000	1.32915250990077	26.39594220306665
7.89000000000000	1.32930170660157	26.39892136614475
7.90000000000000	1.32945103907097	26.40524875764379
7.91000000000000	1.32960049552790	26.40823486547335
7.92000000000000	1.32975008773422	26.41457088214926
7.93000000000000	1.32989980388322	26.41756392995093
7.94000000000000	1.33004965576238	26.42390857023932
7.95000000000000	1.33019963153933	26.42690855323235
7.96000000000000	1.33034974302720	26.43326181556754
7.97000000000000	1.33049997836793	26.43626872896976
7.98000000000000	1.33065034940032	26.44263061178482
7.99000000000000	1.33080084424062	26.44564445081268
8	1.33095147475329	26.45201495253943
8.01000000000000	1.33110222902889	26.45503571240800
8.02000000000000	1.33125311895756	26.46141483147705
8.03000000000000	1.33140413260414	26.46444250740005
8.04000000000000	1.33155528188448	26.47083024224079
8.05000000000000	1.33170655483766	26.47386482943060
8.06000000000000	1.33185796340528	26.48026117847126
8.07000000000000	1.33200949560065	26.48330267213894
8.08000000000000	1.33216116339111	26.48970763380655
8.09000000000000	1.33231295476420	26.49275602916186
8.10000000000000	1.33246488171303	26.49916960188230
8.11000000000000	1.33261693219932	26.50222489413372
8.12000000000000	1.33276911824197	26.50864707633176
8.13000000000000	1.33292142777690	26.51170926068649
8.14000000000000	1.33307387284880	26.51814005078577
8.15000000000000	1.33322644136775	26.52120912244977
8.16000000000000	1.33337914540427	26.52764851887284
8.17000000000000	1.33353197284258	26.53072447305081
8.18000000000000	1.33368493577904	26.53717247421913
8.19000000000000	1.33383802207200	26.54025530611459
8.20000000000000	1.33399124384366	26.54671191044856
8.21000000000000	1.33414458892652	26.54980161526381
8.22000000000000	1.33429806946863	26.55626682118278
8.23000000000000	1.33445167327657	26.55936339411894
8.24000000000000	1.33460541252430	26.56583720004125
8.25000000000000	1.33475927499248	26.56894063629826
8.26000000000000	1.33491327288097	26.57542304064124
8.27000000000000	1.33506739394449	26.57853333541790
8.28000000000000	1.33522165040883	26.58502433659788
8.29000000000000	1.33537603000274	26.58814148509185
8.30000000000000	1.33553054497797	26.59464108152420
8.31000000000000	1.33568518303729	26.59776507893203
8.32000000000000	1.33583995645840	26.60427326903114
8.33000000000000	1.33599485291810	26.60740411054829
8.34000000000000	1.33614988472004	26.61392089272763
8.35000000000000	1.33630503951503	26.61705857354845
8.36000000000000	1.33646032963272	26.62358394622057
8.37000000000000	1.33661574269788	26.62672846153836
8.38000000000000	1.33677129106618	26.63326242311490
8.39000000000000	1.33692696233635	26.63641376812191
8.40000000000000	1.33708276889007	26.64295631701362
8.41000000000000	1.33723869830002	26.64611448690107
8.42000000000000	1.33739476297395	26.65266562151784

8.43000000000000	1.33755095045843	26.65583061147593
8.44000000000000	1.33770727318729	26.66239033022680
8.45000000000000	1.33786371868101	26.66556213544471
8.46000000000000	1.33802029939949	26.67213043673789
8.47000000000000	1.33817700283710	26.67530905240384
8.48000000000000	1.33833384147985	26.68188593464670
8.49000000000000	1.33849080279597	26.68507135594794
8.50000000000000	1.33864789929759	26.69165681754709
8.51000000000000	1.33880511842679	26.69484903966990
8.52000000000000	1.33896247272183	26.70144307903114
8.53000000000000	1.33911994959864	26.70464209716089
8.54000000000000	1.33927756162164	26.71124471268926
8.55000000000000	1.33943529618055	26.71445052201038
8.56000000000000	1.33959316586597	26.72106171211019
8.57000000000000	1.33975115804143	26.72427430780622
8.58000000000000	1.33990928532372	26.73089407088102
8.59000000000000	1.34006753505014	26.73411344813460
8.60000000000000	1.34022591986368	26.74074178258725
8.61000000000000	1.34038442707542	26.74396793658018
8.62000000000000	1.34054306935458	26.75060484081284
8.63000000000000	1.34070183398597	26.75383776672603
8.64000000000000	1.34086073366506	26.76048323914018
8.65000000000000	1.34101975565038	26.76372293215372
8.66000000000000	1.34117891266367	26.77037697115017
8.67000000000000	1.34133819193717	26.77362342644333
8.68000000000000	1.34149760621891	26.78028603042227
8.69000000000000	1.34165714271480	26.78353924317351
8.70000000000000	1.34181681419917	26.79021041053448
8.71000000000000	1.34197660785162	26.79347037592147
8.72000000000000	1.34213653647278	26.80015010506341
8.73000000000000	1.34229658721591	26.80341681826305
8.74000000000000	1.34245677290800	26.81010510758429
8.75000000000000	1.34261708067590	26.81337856377272
8.76000000000000	1.34277752337298	26.82007541167103
8.77000000000000	1.34293808809971	26.82335560602366
8.78000000000000	1.34309878773583	26.83006101089625
8.79000000000000	1.34325960935541	26.83334793858774
8.80000000000000	1.34342056586457	26.84006189883126
8.81000000000000	1.34358164431097	26.84335555503558
8.82000000000000	1.34374285762715	26.85007806904618
8.83000000000000	1.34390419283431	26.85337844893660
8.84000000000000	1.34406566289143	26.86010951510989
8.85000000000000	1.34422725479326	26.86341661385900
8.86000000000000	1.34438898152523	26.87015623059012
8.87000000000000	1.34455083005559	26.87347004336986
8.88000000000000	1.34471281339626	26.88021820905346
8.89000000000000	1.34487491848899	26.88353873103511
8.90000000000000	1.34503715837217	26.89029544406539
8.91000000000000	1.34519951996107	26.89362267041959
8.92000000000000	1.34536201632057	26.90038792919031
8.93000000000000	1.34552463433939	26.90372185508710
8.94000000000000	1.34568738710895	26.91049565799158
8.95000000000000	1.34585026149142	26.91383627860039
8.96000000000000	1.34601327060476	26.92061862403155
8.97000000000000	1.34617640128457	26.92396593452124
8.98000000000000	1.34633966667537	26.93075682087160
8.99000000000000	1.34650305358618	26.93411081641045
9	1.34666657518809	26.94091024207215
9.01000000000000	1.34683021826352	26.94427091782790
9.02000000000000	1.34699399601016	26.95107888119273
9.03000000000000	1.34715789518380	26.95444623233256
9.04000000000000	1.34732192900875	26.96126273179197
9.05000000000000	1.34748608421415	26.96463675348255
9.06000000000000	1.34765037405095	26.97146178742763
9.07000000000000	1.34781478522164	26.97484247483513
9.08000000000000	1.34797933100381	26.98167604165669
9.09000000000000	1.34814399807327	26.98506338994678
9.10000000000000	1.34830879973430	26.99190548803533
9.11000000000000	1.34847372263599	26.99529949237319
9.12000000000000	1.34863878010933	27.00215012011895
9.13000000000000	1.34880395877667	27.00555077566933

9.14000000000000	1.34896927199573	27.01240993146226
9.15000000000000	1.34913470636212	27.01581723338944
9.16000000000000	1.34930027526029	27.02268491561926
9.17000000000000	1.34946596525909	27.02609885908709
9.18000000000000	1.34963178976972	27.03297506614329
9.19000000000000	1.34979773533426	27.03639564631522
9.20000000000000	1.34996381539068	27.04328037658705
9.21000000000000	1.35013001645426	27.04670758862612
9.22000000000000	1.35029635198975	27.05360084050267
9.23000000000000	1.35046280848564	27.05703467957153
9.24000000000000	1.35062939943348	27.06393645144167
9.25000000000000	1.35079611129492	27.06737691270261
9.26000000000000	1.35096295758834	27.07428720295507
9.27000000000000	1.35112992474853	27.07773428157002
9.28000000000000	1.35129702632072	27.08465308859337
9.29000000000000	1.35146424871284	27.08810677972392
9.30000000000000	1.35163160549699	27.09503410190659
9.31000000000000	1.35179908305420	27.09849440071401
9.32000000000000	1.35196669498345	27.10543023644431
9.33000000000000	1.35213442763886	27.10889713808955
9.34000000000000	1.35230229464632	27.11584148575570
9.35000000000000	1.35247028233303	27.11931498539941
9.36000000000000	1.35263840435179	27.12626784338954
9.37000000000000	1.35280664700286	27.12974793619210
9.38000000000000	1.35297502396598	27.13670930289425
9.39000000000000	1.35314352151444	27.14019598401577
9.40000000000000	1.35331215335496	27.14716585781795
9.41000000000000	1.35348090573383	27.15065912241828
9.42000000000000	1.35364979238474	27.15763750170845
9.43000000000000	1.35381879952699	27.16113734494722
9.44000000000000	1.35398794092127	27.16812422811330
9.45000000000000	1.35415720275986	27.17163064514992
9.46000000000000	1.35432659883047	27.17862603057983
9.47000000000000	1.35449611529832	27.18213901657349
9.48000000000000	1.35466576597817	27.18914290265516
9.49000000000000	1.35483553700819	27.19266245276485
9.50000000000000	1.35500544223019	27.19967483788623
9.51000000000000	1.35517546775525	27.20320094727079
9.52000000000000	1.35534562745226	27.21022182981987
9.53000000000000	1.35551590740521	27.21375449363795
9.54000000000000	1.35568632151008	27.22078387200277
9.55000000000000	1.35585685582374	27.22432308541288
9.56000000000000	1.35602752426929	27.23136095798154
9.57000000000000	1.35619831287646	27.23490671614206
9.58000000000000	1.35636923559548	27.24195308130276
9.59000000000000	1.35654027842893	27.24550537937193
9.60000000000000	1.35671145535421	27.25256023551296
9.61000000000000	1.35688275234669	27.25611906864894
9.62000000000000	1.35705418341095	27.26318241415871
9.63000000000000	1.35722573449519	27.26674777751955
9.64000000000000	1.35739741963117	27.27381961078658
9.65000000000000	1.35756922473987	27.27739149953027
9.66000000000000	1.35774116388026	27.28447181894324
9.67000000000000	1.35791322294609	27.28805022822769
9.68000000000000	1.35808541602356	27.29513903217545
9.69000000000000	1.35825772897918	27.29872395715852
9.70000000000000	1.35843017592640	27.30582124403007
9.71000000000000	1.35860274270443	27.30941267986961
9.72000000000000	1.35877544345402	27.31651844805416
9.73000000000000	1.35894826398708	27.32011638990797
9.74000000000000	1.35912121847164	27.32723063779492
9.75000000000000	1.35929429269231	27.33083508082080
9.76000000000000	1.35946750084443	27.33795780679980
9.77000000000000	1.35964082868527	27.34156874615556
9.78000000000000	1.35981429043751	27.34869994861646
9.79000000000000	1.35998787183108	27.35231737945993
9.80000000000000	1.36016158711598	27.35945705679285
9.81000000000000	1.36033542199478	27.36308097428191
9.82000000000000	1.36050939074487	27.37022912487722
9.83000000000000	1.36068347904141	27.37385952416978
9.84000000000000	1.36085770118917	27.38101614641814

9.85000000000000	1.36103204283593	27.38465302267218
9.86000000000000	1.36120651831385	27.39181811496456
9.87000000000000	1.36138111324328	27.39546146333813
9.88000000000000	1.36155584198382	27.40263502406578
9.89000000000000	1.36173069012836	27.40628483971703
9.90000000000000	1.36190567206396	27.41346686727153
9.91000000000000	1.36208077335603	27.41712314535873
9.92000000000000	1.36225600841909	27.42431363813202
9.93000000000000	1.36243136279109	27.42797637381352
9.94000000000000	1.36260685091403	27.43517533019787
9.95000000000000	1.36278245829833	27.43884451863218
9.96000000000000	1.36295819941352	27.44605193702024
9.97000000000000	1.36313405974249	27.44972757336600
9.98000000000000	1.36331005378229	27.45694345215081
9.99000000000000	1.36348616698827	27.46062553156684
10	1.36366241388503	27.46784986914180